The Dissertation Committee for Erin Camille Overstreet Certifies that this is the approved version of the following dissertation:

The role of epsins in *Drosophila* eye development

Committee:

Janice Ann Fischer, Supervisor

David Stein

Jon Huibregste

Theresa O'Halloran

John Sisson

Bing Zhang

The role of epsins in *Drosophila* eye development

by

Erin Camille Overstreet, B.S.

Dissertation

Presented to the Faculty of the Graduate School of

The University of Texas at Austin

in Partial Fulfillment

of the Requirements

for the Degree of

Doctor of Philosophy

The University of Texas at Austin

May, 2005

Dedication

To myself and family and friends, especially Roz Sweeney

Acknowledgements

Thank you Janice, for everything. You gave me everything I needed to succeed including your time, encouragement, guidance and patience. I will forever be grateful and indebted to you. I am also grateful to the members of my committee for their constructive criticism and insightful discussions. Especially Dave – I'm sure I wouldn't have published my first paper without his excellent comments. Thanks to everyone who wrote fantastic recommendations for me when I applied for fellowships and post-doctoral positions. Big thanks to Erin Fitch who did a lot of great work for me and made me laugh. I am especially appreciative of all the kindness and friendship I have received from the members of the Fischer, Macdonald, Stein and Sisson labs. Finally , I would like to thank my partner, Roz Sweeney, and the rest of my family and friends who saw me through all the stressful and tough times during graduate school. I acknowledge monetary support from the University of Texas for three years of fellowship support.

I would also like to acknowledge, for posterity, exactly how I felt in the days heading toward my defense. The following quote was written by a person

named Matt Welch, whom I've never met, but I ran across his website which contained the following:

"All your insecurity demons come out of the closet when you write a dissertation. Every sentence, every phrase, is a chance to become more convinced of your inadequacy. Somehow -- hypnosis, therapy, fear of disappointing your parents, a stout glass of wine at noon and another one at 5 o'clock every day -- you get it done. But that's all it is: done. It's not good, and it's not worth reading and it's nowhere near the project you hoped you'd have when you started. You can barely stand to look at it. That's what makes the last days before the defense so painful: You're sitting around waiting for the committee to ask you what the hell you thought you were doing when you tried to put this flimsy, illogical piece of sham scholarship over on them."

Everything turned out okay in the end. It was probably one of the best days of my life – I will never forget it. Thanks to everyone who helped it happen.

The role of epsins in *Drosophila* eye development

Publication No._____

Erin Camille Overstreet, Ph.D.

The University of Texas at Austin, 2005

Supervisor: Janice Ann Fischer

The goal of my doctoral work is to understand how proteins involved in vesicle trafficking contribute to proper animal development. To understand aspects of this process, I studied how two vesicle trafficking proteins, Liquid facets(Lqf)/epsin1 and D-Epsin-Related, affect *Drosophila* eye development.

I determined that Lqf, an endocytosis protein, together with Fat facets (Faf), a deubiquitinating enzyme, regulate the Notch and Delta signaling in the developing *Drosophila* eye. Notch signaling pathway is used in most developmental processes and is dependent on its ligand Delta. Faf deubiquitinates Lqf in the signaling cells, thereby increasing Lqf protein levels and also levels of Delta endocytosis. This event is necessary for Notch activation in neighboring cells. Lqf probably works in concert with the E3 ubiquitin ligase Neuralized (Neur), which ubiquitinates Delta. These conclusions are consistent with a

relatively new model describing an obligate role for endocytosis in the signaling cells to effect activation in neighboring cells.

To understand how Lqf functions mechanistically in this process, I performed a structure/function analysis of the Lqf protein. Lqf proteins with strategic deletions of certain functional domains were tested for their ability to function *in vivo*. The major result of these experiments is that the N-terminal ENTH domain of Lqf and a protein without the ENTH domain each retain significant activity. This suggests that Lqf has two functions: the ENTH domain function and the ENTH-less function. These data are in contrast with the most popular model suggesting that ENTH-less epsins are non-functional proteins. I present possible models for how ENTH-less epsins may retain function.

The final part of my thesis focuses on D-Epsin-Related (D-Epsin-R) protein. I showed that D-Epsin-R is a Golgi protein, like its homologs. Surprisingly, D-Epsin-R ENTH domain is not required for function because an ENTH-less D-Epsin-R can substitute for endogenous D-Epsin-R. Also, D-Epsin-R has essential and probably specific developmental roles in the eye as *D-Epsin-R* mutants exhibit impaired cell growth. This work suggests that epsins are specific components of certain developmental pathways.

Table of Contents

List of Figures

Chapter 1. General Introduction

INTRACELLULAR VESICLE TRAFFICKING

Many molecules are transported inside cells in tiny membrane bound structures called vesicles. These vesicles must be trafficked to specific regions of the cell with temporal precision. Thus, vesicle trafficking regulates the spatial and temporal availability of certain molecules within a cell, profoundly impacting a vast array of cellular functions.

Vesicle trafficking pathways in the cell

There are numerous pathways by which molecules are trafficked in vesicles in the cell and they serve different purposes. These include the biosynthetic pathway, endocytosis and exocytosis pathways, and retrograde transport pathway (Fig.1).

The biosynthetic pathway regulates the biosynthesis and trafficking of transmembrane and secreted proteins, including signaling receptors (i.e. receptor tyrosine kinases and G-protein coupled receptors), signaling molecules (i.e. diffusible receptor ligands), extracellular matrix proteins and lysosomal hydrolases. These proteins are all produced by ribosomes located in the endoplasmic reticulum (ER). They are transported then in membrane bound

vesicles to the *cis* face of the Golgi apparatus. In Golgi compartments, enzymes modify these proteins post-translationally.

Proteins exiting the Golgi do so at the *trans* face of the Golgi (the *trans*-Golgi network). These proteins are transported then to specific cellular locations. Lysosomal proteins are packaged in vesicles destined to fuse with the lysosome. These vesicles can either travel directly to the lysosome from the Golgi or can travel to an intermediate endosome before transport to the lysosome. By contrast, proteins such as signaling receptors or secreted signaling molecules are delivered to the cell surface in vesicular packages that fuse with the plasma membrane in a process called exocytosis. These vesicles may also pass first through and intermediate endosomal compartment. The molecular guidance cues for delivering these proteins are only now beginning to be understood. However, it is clear that the biosynthetic secretory pathway is used to produce proteins that will function in specific membrane regions of the cell. These processes can affect the signaling activities of certain proteins (see below).

Endocytosis is the internalization of material from the cell surface into membrane-bound vesicles. Cells internalize materials for a multitude of purposes including eating, and modulation of signaling activity. Materials internalized from the cell surface are incorporated into vesicles that bud and pinch off into the cytosol. The contents of the vesicle are then trafficked to appropriate cellular destinations. Some of these vesicles fuse with the lysosome where their contents are degraded and the remnants may be utilized as energy or food by the cell.

These vesicles travel through intermediate endosomal compartments first. Finally, some vesicles bypass the degradation route and are recycled back to the surface to re-use their protein contents. These processes also modulate the signaling activities of certain receptors (see below).

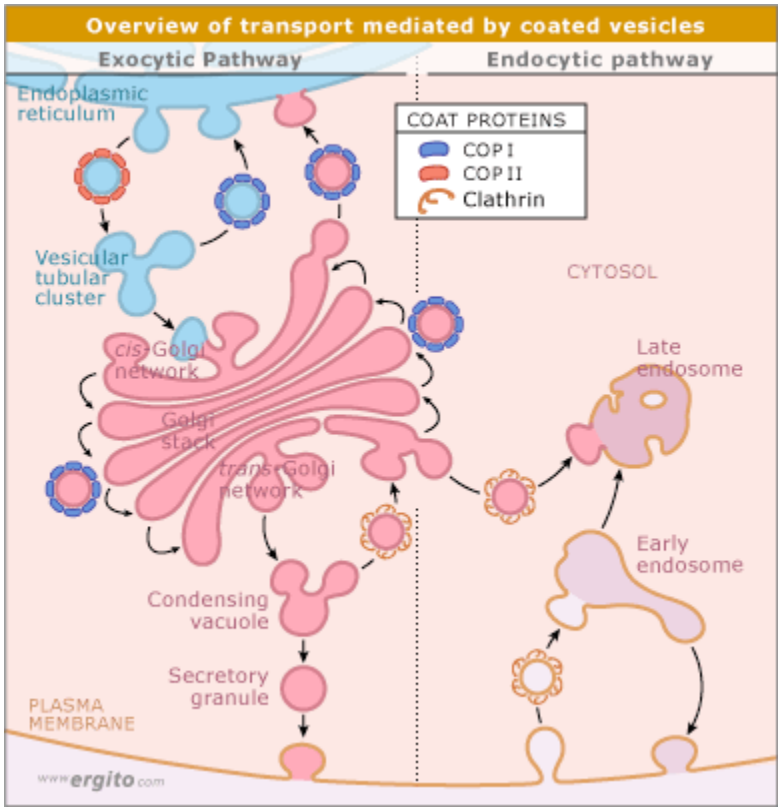

Fig. 1. Some vesicle trafficking pathways within a cell. Pathways requiring a coated vesicle formation are highlighted in this figure. COPI coated vesicles are formed on the Golgi apparatus to deliver material between Golgi stacks or in retrograde transport to the ER. COPII vesicles are formed at the ER containing materials destined for the Golgi. Clathrin coated vesicles are utilized in several pathways including transport from the Golgi to endosomes and endocytosis and retrograde transport. See text for details.

The forward trafficking of vesicles and proteins from the Golgi apparatus to other parts of the cell must be counterbalanced by retrograde trafficking back to the Golgi and ER. One of the major functions of retrograde trafficking is to recycle lipids and membrane proteins that function in sorting of secretory cargo. For example, retrograde trafficking within the Golgi complex functions to retrieve resident Golgi proteins to their proper Golgi stack. Another retrograde traffic route retrieves material from endosomes to be sent back to the Golgi. Such materials might include sorting proteins that originated at the Golgi and were transported to endosomes.

Trafficking of molecules in intracellular vesicles requires the coordination of numerous proteins that have specialized functions. Generating and transporting vesicles involves several distinct steps: budding and coating of vesicles from donor membrane, fission of the vesicle, vesicle uncoating, and docking and fusion with target membrane. Hence, the following section will consist of an overview of the general protein architecture of these pathways as well as a description of the mechanism of these proteins' functions.

Principles of coat formation

Vesicles are formed at most cellular membranes such as the Golgi complex, the endoplasmic reticulum, endosomes, lysosomes and the plasma membrane. Most of these vesicles are covered with a protein coat, although there are modes of vesicle formation that do not require a coat (i.e. caveolar

endocytosis). Three major classes of coated vesicles have been identified: COPI (coatomer), COPII, and clathrin-coated vesicles. The protein components of these coats have several functions: generation of membrane curvature, recruitment of cargo, fission of vesicles, and uncoating of vesicles (McMahon et al 2004). This review will focus on clathrin coated vesicle formation and transport because it is the most extensively studied and thus provides a good basis for understanding how vesicles form. Additionally, clathrin-dependent processes are a major focus of this thesis.

Most transport vesicles originate from coated regions of membranes. They bud off as coated vesicles that have a characteristic cage of proteins on the outer surface. The vesicle protein coat is thought to have at least two functions. First, several coat proteins help to select the membrane proteins by concentrating them into membrane domains rich in protein and lipid components that facilitate membrane invagination, or budding. Second, one protein component, clathrin, can polymerize into basket-like structures *in vivo* and *in vitro*. This self assembling activity is thought to provide some of the force required for membrane deformation or invagination during budding (McMahon *et al*. 2004; Owen *et al*. 2004). However, other proteins that may not be part of the coat may participate in membrane deformation as well (see below).

Budding and cargo selection via coat components

Electron micrographs of clathrin coats indicate that there are two layers, an inner and outer shell. The inner shell is composed of adaptor proteins that contact the vesicle membrane (see below). The outer shell is composed of clathrin lattices. Clathrin is a trimer of 192 kDa polypeptides (heavy chains) and each are associated with 22-25 kDa light chains. The heavy chain is called a triskelion because it appears with three legs extending from a central hub. The trimers are linked by their C-terminus and the N-terminals are free to bind to other clathrin triskelia with a well-defined geometry of polyhedral lattices (see Fig. 2). The light chains are thought to regulate assembly of triskelions. The globular N-terminal domain binds to a number of endocytic proteins that possess conserved clathrin box motifs (LLNLD or Løxø(D/E) (Owen et al. 2004; McMahon et al. 2004; Mousavi et al. 2004). The mechanisms and forces that govern triskelion lattice formation are beyond the scope of this review.

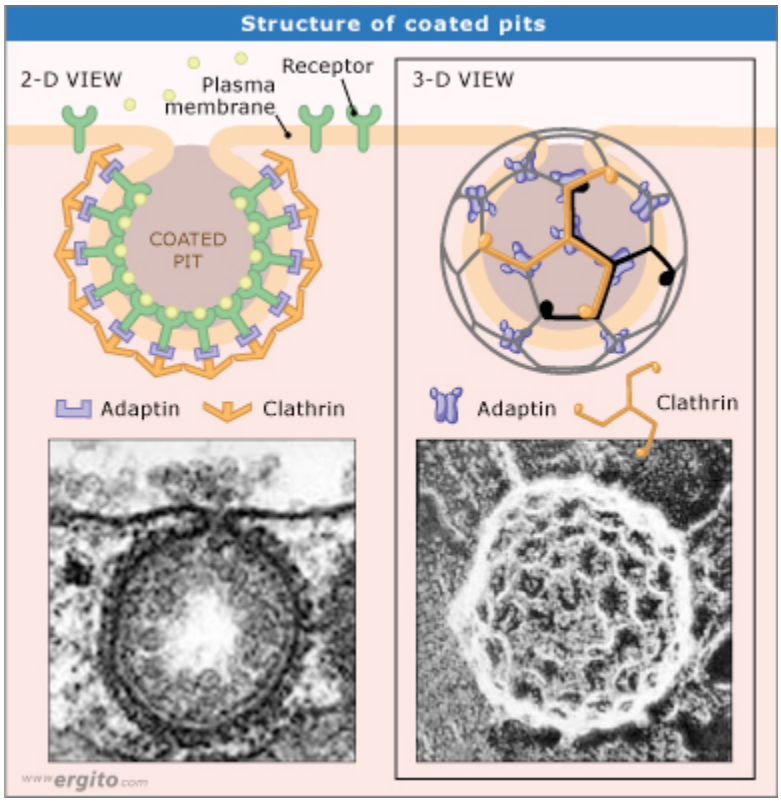

Fig. 2. Structure of coated pits. Coated pits typically have an inner shell composed of adaptor proteins such as AP-2 and an outer protein shell formed by the clathrin lattice. Clathrin lattices polymerize to form a regular polyhedral structure. Polymerization is speculated to generate part of the force to invaginate the membrane into the forming bud.

The inner shell of clathrin coats contains heterotetrameric adaptor protein (AP) complexes (AP-1, AP-2, AP-3, and AP-4). These proteins have two functions in vesicle formation: They mediate the recruitment of clathrin to membranes and they recognize transmembrane cargo via certain motifs in their cytosolic tails (di-leucine or tyrosine based) to facilitate cargo incorporation into a coated vesicle (Fig. 2 and 3). AP-2 works at the plasma membrane during clathrin mediated endocytosis, while AP-1 is involved in formation of CCVs at the trans-

Golgi network (TGN) that are sorted to endosomes or to the plasma membrane (Fig. 1). AP-1 also has roles in retrograde traffic from endosomes to TGN. AP-3 may have roles in forming CCVs at the Golgi that are sorted to the lysosome. Finally, AP-4 was recently identified and is found only in mammals and plants. Its function is unknown, but it may mediate CCV formation at late endosomes or lysosomes. The function of AP-2 is most well known, but the other adaptor complexes are similarly constructed and thought to function analogously in the CCV forming process (Boehm et al. 2002).

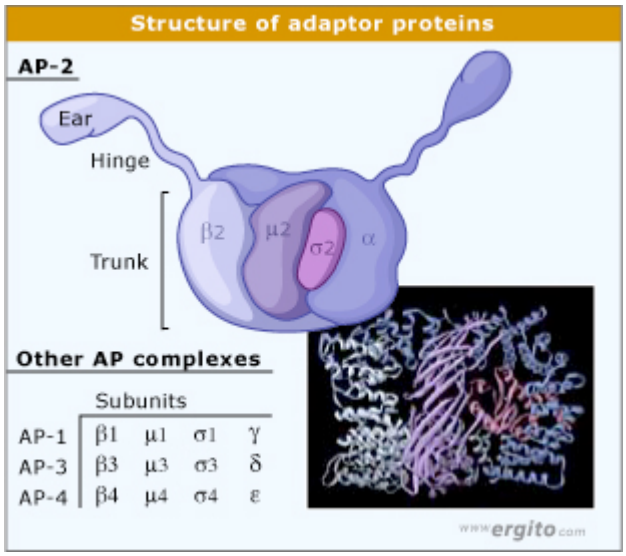

Fig. 3. Structure of adaptin protein, AP-2. See text for details.

All AP complexes are composed of four subunits similar to the construction of AP-2 (Fig. 3). The AP-2 complex has two large subunits (alpha 2and ß2), one medium (μ2) and one small (gamma2). The alpha subunit binds to membranes and interacts with other endocytic proteins containing DPF or DPW

motifs. The beta subunit binds to clathrin and cargo carrying di-leucine motif (D/E)xxx(L/I) and can bind to some endocytic proteins. The μ2 domain recognizes cargo containing tyrosine based motifs (YXXø) (Mousavi et al 2004, Traub 2003). AP-2 binds only to the YXXø motif and only at the plasma membrane. AP-2 does not bind proteins with this motif in the cytosol because of regulation by phosphorylation. When AP-2 is in the cytosol, the μ2 binding site is inaccessible, but when AP-2 is at the membrane the μ2 subunit is phosphorylated and can now bind to its cargo (Traub 2003).

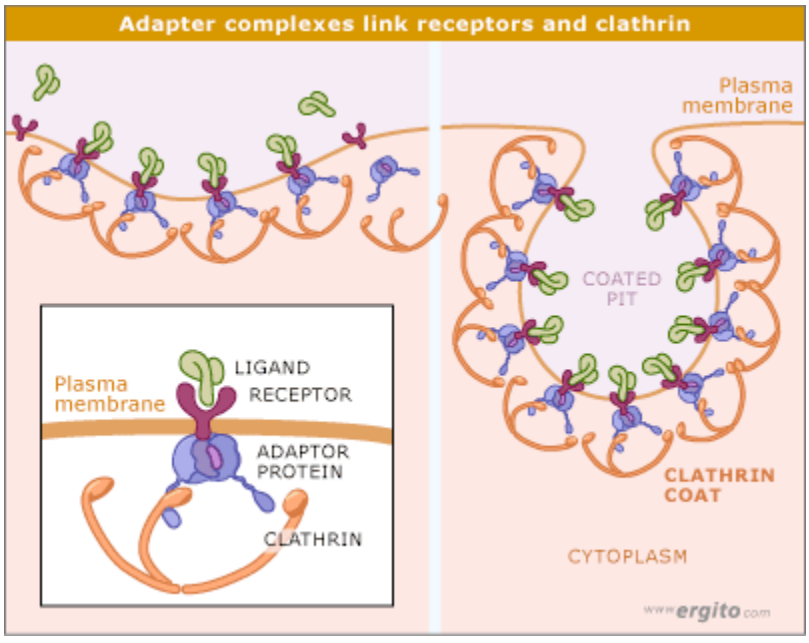

Fig. 4. Two dimensional view of the recruitment of clathrin by adaptor complexes. AP-2 physically links the transmembrane cargo to the assembly of clathrin in invaginating pits.

The formation of a clathrin coated pit is driven by the forces generated by the assembly of adaptins at membranes and the successive recruitment of clathrin. The most popular model suggests that AP-2 first binds to inositol phospholipids, PI(4,5)P2, at the plasma membrane where AP-2 localizes. This localization enables AP-2 to recruit clathrin to the cortex while simultaneously concentrating cargo proteins at the membrane. Once clathrin is concentrated, clathrin can then self polymerize into a lattice around the cargo. The polymerization may facilitate invagination of the membrane or somehow act to stabilize newly forming membrane buds (Mousavi et al. 2004, Szymkiewics et al. 2004). However, several other coating complex proteins are recruited to pits that may share functions in both cargo concentration and invagination (see below).

This view of coat assembly is somewhat outdated because it is clear now that not all clathrin coats require AP-2 to assemble them**.** When *AP-2* expression is knocked-down in HeLa cells using RNAi, internalization of the transferrin receptor is inhibited, but not of epidermal growth factor receptor or low density lipoprotein receptors**.** Also, clathrin coated pits still form in the absence of *AP-2*, although to a lesser extent (Motley et al 2003). These results suggest that some cargo molecules do not require AP-2 recognition to be incorporated into CCVs.

If AP-2 does not recruit all cargo into coated pits, then other adaptor molecules probably fill this role. These alternative adaptor proteins must be able to recognize cargo molecules and recruit the coating complex. How do these alternative adaptors recognize cargo? An emerging principle concerning cargo

packaging into coated pits is that signals in the cytoplasmic domain regulate incorporation into vesicles. Recognition of these signals by chaperone proteins, or adaptor proteins, can mediate their incorporation into membrane domains enriched for vesicle coat components.

AP-2 adaptors interact directly with cargo molecules containing tyrosine-based motifs. Perhaps the alternative adaptors also recognize this motif. However, not all transmembrane cargo molecules have this sequence in their cytoplasmic tails. Hence, other clathrin adaptors may recognize different short peptide motifs. Also, it is well documented that cargo molecules are often modified post-translationally for example by phosphorylation or mono-ubiquitination. These post-translational modifications are probably not recognized directly by AP proteins, but rather by alternative clathrin adaptors.

Alternative clathrin adaptors

In the past decade, numerous other clathrin adaptors have been identified. They differ from the AP complexes in that they are all monomeric. Unlike AP-2, most are not incorporated into the coat. Most clathrin adaptors have domains that bind to membranes, cargo, and coat components. Thus, it is thought that they function in cargo recognition, linking the recruitment of coat components for subsequent internalization. Their precise roles are largely unclear, though some may operate at distinct steps in internalization and sorting (see below) (Traub 2003; Mousavi et al. 2004; Szymkiewics et al. 2004).

All alternative clathrin adaptors share certain structural and functional features. (Fig. 5) They all have a modular design with motifs that interact simultaneously with numerous endocytosis complex components. Most have a folded domain that binds to phospholipid membrane components. They all possess an unfolded region with a modular design containing motifs that bind endocytic proteins like clathrin, AP-2 and accessory coat components (Mousavi et al. 2004 and Fig. 5).

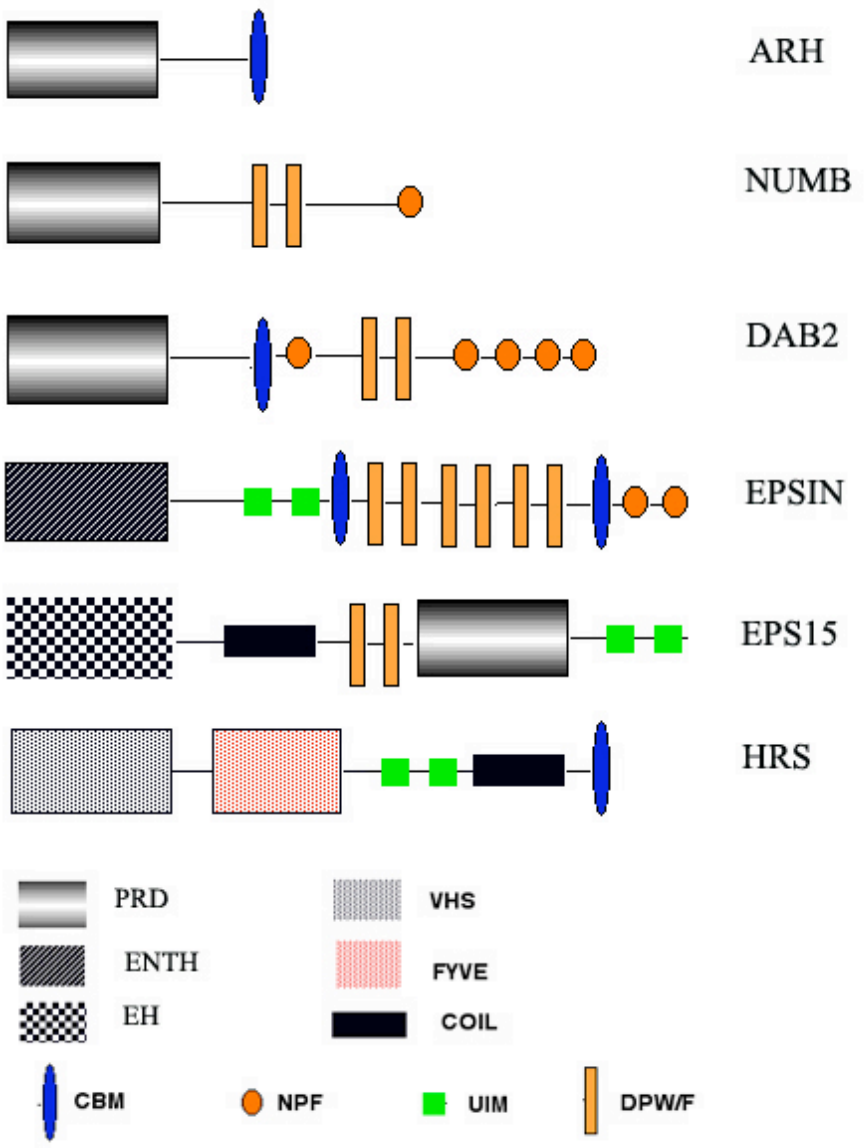

Fig. 5. Structure of some alternative endocytic clathrin adaptors. Not drawn to scale. Most clathrin adaptors contain multiple motifs that interact with components of the endocytic machinery. They also have motifs that bind cargo and some bind to specific intracellular membranes. Thus, these adaptors link cargo carrying specific internalization motifs to the clathrin coating machinery at membranes (Mousavi et al. 2004). NPF motifs bind to EH domains in proteins such as Eps15. DPW/F motifs bind to the alpha-adaptin ear of AP-2 (Wendland et al. 1999). PRD binds to tyrosine-based motifs in certain cargo and can also bind to PI(4,5)P2. VHS domain helps to recognize proteins with an acidic-

cluster–dileucine motif. FYVE domain binds to PI(3,5)P2 on endosomes. UIM binds to ubiquitin (Lohi et al. 2002). See text and chapter 5 for more details.

One purpose of a modular design is to regulate the dynamic association with the coat. Coat complex proteins must interact with each other at the right place and time for a vesicle to form and then they must disassociate for the next phases, that include uncoating and vesicle transport (see below). Dynamic or transient interactions can be achieved only if binding of proteins is not too tight. Weak binding is achieved when folded domains recognize motifs that are 3-8 amino acids in length. Binding affinities can be increased by increasing the number of motifs present. Thus, differences in the number of motifs present partially determine the relative strength with which they bind. For example, several CCV complex proteins contain different numbers of DPW/F motifs and therefore bind to the AP-2 with different strengths (Mousavi et al. 2004; Szymkiewics et al. 2004; Wendland 2002).

Another purpose of a modular design with multiple short amino acid motifs may be to establish a cooperative network between multivalent binding interactions. This type of network could result in a synergy of binding between the components, such that when coat components are concentrated, coat formation can drive itself. In other words, where affinity of binding between components is low, enhanced avidity of binding is what drives complex formation. It follows then that once some interactions are abolished, the network can propagate its own

disassembly (Mousavi et al. 2004, Szymkiewics et al. 2004; Wendland 2002 and see below).

Most clathrin adaptors are regulated by post-translational modifications such as phosphorylation or ubiquitination (Chen and De Camilli et al. 1999; Polo et al. 2002; Watson et al. 2001; Shenoy et al. 2003; Mousavi et al. 2004; and Chen et al. 2002). These modifications can have activating or inhibitory effects depending on the adaptor and in many cases, the effect of the modification is unknown (see below). In any case, this type of regulation offers a higher degree of control over the vesicle trafficking processes.

Beta Arrestin

Beta arrestins mediate the clathrin-dependent internalization of seven-membrane spanning receptors (7MSR). They contain domains that bind to PI(4,5)P2, phosphorylated cargo, AP-2 and clathrin. Beta-arrestins bind to the beta-hinge of AP-2 through an unknown region (Santolini et al. 2002; Scott et al. 2002). Thus, arrestins link their cargo to the core endocytic machinery. The precise mode of action is far from completely understood, however, ubiquitination plays a central role (Mousavi et al. 2004). In some cases, when a certain 7MSR is stimulated, it recruits beta arrestin. This triggers ubiquitination of beta arrestin by a ubiquitin ligase called Mdm2 (Hicke et al. 2003). This ubiquitination step is required to activate the beta arrestin clathrin adaptor function which leads to internalization.

Receptors that are internalized in a beta-arrestin dependent pathway are sorted differentially depending on how tightly they bind to beta arrestin. The strength of binding may be determined by the ubiquitination state of beta arrestin. For example, deubiquitination of beta-arrestin is thought to mediate receptor dissociation (Shenoy et al. 2003). The receptors that bind transiently are recycled to the plasma membrane rapidly. The receptors that associate tightly with beta arrestin are not recycled but traffic to endosomes and will eventually be degraded (Martin et al. 2002; Tulipano et al. 2004; Mousavi et al. 2004). Receptors may associate tightly only with ubiquitinated beta-arrestin. In support of this idea, beta-arrestin fused to ubiquitin remains associated with the receptor and associates with it in endosomes (Shenoy et al. 2003; Hicke et al. 2003). Beta arrestins also have other roles in regulation of signaling apart from their roles in endocytosis and vesicle trafficking.

PTB domain proteins

Phosphotyrosine binding domains (PTB) are found in several proteins that act as alternative cargo adaptors, for example ARH (autosomal recessive hypercholesterolemia), Dab-2 (Disabled), and Numb. PTB domains bind to the consensus sequence FXNPXY (where tyrosine is either phosphorylated or unphosphorylated). PTB domains also bind to phosphoinositides enriched at the plasma membrane. PTB domain adaptors bind to AP-2 either at the alpha or beta appendages. Thus, these adaptor proteins are thought to facilitate internalization

by coupling specific cargo to the AP-2 internalization complex (Szymkiewicz et al. 2004).

ARH and Dab2 are two adaptor proteins that are responsible for the internalization of low density lipoprotein (LDL) receptor and other receptors. Transmembrane nutrient receptors like LDL receptor, deliver extracellular macromolecules to the interior of the cell via endocytosis (see below). ARH and Dab2 may function redundantly in LDL receptor endocytosis in some contexts (Mishra et.al. 2002; Szymkiewicz et.al. 2004).

Dab2 and ARH interact with LDL receptors and endocytic proteins in a similar way. Dab2 binds to unphosphorylated LDL receptors via its PTB domain. The PTB domain of Dab2 also binds to PI(4,5)P2 at the plasma membrane. Dab2 binds to AP-2 via its DPF motif and to other endocytic proteins via its NPF motifs and clathrin via its clathrin binding motif. ARH utilizes its PTB domain in a similar way as does Dab2, except it preferentially binds to phosphorylated LDL receptors. ARH binds to the beta-appendage of AP-2, not the alpha, and associates with clathrin via a conserved clathrin motif (Mishra et.al. 2002; Szymkiewicz et.al. 2004).

Neither Dab2 nor ARH are purified from CCVs suggesting they are only associated transiently with the coat complex at the plasma membrane, at the beginning stages of bud formation. Therefore, Dab2 and ARH may function in cargo sorting only and may not remain associated with the coat machinery after the vesicle buds. One popular model poses that Dab2 and ARH might act to

gather cytoplasmic domains efficiently with the appropriate recognition signal (FXNPXY) and package the cargo into the vesicle faithfully while recruiting clathrin. Once the cargo is incorporated at sites of budding, the cargo can then be passed along to AP-2, which has a weak affinity for FXNPXY motifs, for further processing into coated vesicles (Mishra et al. 2002; Traub 2003). Currently, the exact mode of function of these two proteins is highly debated and under much investigation.

The cargo adaptor Numb may specifically mediate the internalization of the receptor Notch. Notch is a signaling receptor that regulates gene expression in a multitude of developmental events (see below). Numb differs from other PTB domain adaptors because it does not directly bind to clathrin, but primarily serves as an adaptor between cargo and AP-2. Numb may recognize Notch specifically via its PTB domain. Numb binds to AP-2 via DPF motifs. It is thought that Numb mediates Notch internalization via coupling its subcellular localization to the clathrin polymerizing agent, AP-2. The action of Numb is subject to much post-translational modification, such as ubiquitination and phosphorylation, which negatively regulates its activity (Szymkiewicz et al. 2004). Numb activity is needed in certain developmental situations where Notch receptor signaling needs to be down-regulated, i.e. in dividing neuroblasts of sensory organ precursor cells in *Drosophila* (Le Borgne et al. 2003; Berdnik et al. 2002 and see below).

UIM-containing adaptors

UIM containing clathrin adaptors are hypothesized to bind to ubiquitinated cargo and link them to internalization and/or sorting machinery by virtue of their other binding motifs to accessory proteins, clathrin, AP-2 and phospholipids (Szymkiewics et al. 2004; Mousavi et al. 2004; Traub 2003). The candidate ubiquitin adaptors are Eps15, epsins and Hrs. All of these proteins contain multiple copies of a ubiquitin interacting motif (UIM) which was discovered based on sequence homology with a region of the S5a subunit of the proteasome that binds ubiquitin (Hofmann et al. 2001). Subsequently, the UIMs of epsin, Eps15 and Hrs were shown to bind non-covalently to mono-ubiquitin (and poly-ubiquitin chains) *in vitro* (Polo et al. 2002; Shih et al. 2002; Schnell et al. 2003). Because UIMs bind ubiquitin, one major function of the UIM domain might be to recognize ubiquitinated transmembrane proteins along the endocytic pathway (see below).

In the past few years it has come to light that ubiquitination of cargo facilitates internalization and sorting in endosomal compartments. In fact, ubiquitination is the major internalization signal in yeast. In higher organisms, ubiquination serves mainly as a sorting signal for internalized proteins that are routed toward the degradative pathway (Hicke et al. 2002). Membrane proteins that are ubiquitinated are internalized into early endocytic vesicles. At the early endosome, a monoubiquitin signal can route the protein into late endosomes that will mature into MVBs.

The UIM proteins epsin and Eps15 are speculated to function at the internalization step to recognize ubiquitinated receptors to be internalized. Consistent with this idea, some ubiquitinated transmembrane proteins fail to be internalized in yeast when the UIM domain of the epsin homolog is absent (Shih et al. 2002). Also, the *Drosophila* homolog of epsin, Liquid facets (Lqf), mediates internalization of a transmembrane protein called Delta. The internalization event is thought to be dependent upon ubiquitination of Delta because Lqf mutants show strong genetic interactions with Neuralized, the E3 ligase that ubiquitinates Delta (Overstreet et al. 2004 and see chapter 2).

Hrs is a UIM containing protein thought to mediate sorting of ubiquitinated cargo to late endosomes. At late endosomes, Hrs recognizes ubiquitinated cargo and recruits sorting machinery responsible for delivery into the lumen of multivesicular bodies (MVBs) (Lloyd et al. 2002). MVBs form by invagination of membrane at the endosome to form intralumenal vesicles. Monoubiquitinated proteins are sorted into these intralumenal vesicles that are destined to fuse with the lysosome. Several pieces of evidence support this model. First, the UIM domain of Hrs is required for sorting certain ubiquitinated cargo into multivesicular bodies. Second, Hrs co-localizes and associates physically with a Ub-protein fusion *in vivo* (Hicke et al. 2002). Finally, Hrs co-localizes with endosomal and MVB markers.

Recently, new data has surfaced that suggests that UIM proteins, epsin and Eps15, mediate the decision between clathrin-dependent and clathrin-independent

internalization routes of receptors based on the ubiquitination state of the receptors. In support of this idea, a Ub-EGFR fusion protein is internalized only into caveoli (clathrin-independent vesicles) and co-localizes in caveoli with epsin (Sigismund et al. 2005). Interestingly, Chen et al. (2005) find that clathrin binding and Ub binding of epsins are mutually exclusive. Perhaps epsin is prevented from forming clathrin coated vesicles when it interacts with ubiquitinated cargo, although other ideas are of course possible.

The choice of internalization route may affect the subcellular destination of the cargo protein. In support of this idea, Sigismund et al. (2005) find that EGFR follows different routes depending on ligand concentration. At low ligand concentration, EGFR is internalized only via clathrin-dependent pathway. However, at high EGF concentrations, EGFR internalization is partitioned equally between clathrin-independent and clathrin-dependent pathways. Interestingly, EGFR is ubiquitinated only at high EGF dose and at this dosage of ligand, EGFR levels decrease. Thus, there is a correlation between ubiquitination state and degradation, possibly via lysosomes. Taken together with the data above, this led to a model where epsin and other UIM proteins might function as cargo adaptors by recognizing ubiquitinated receptors and internalizing them via a clathrin-independent pathway toward a degradative route.

Despite the above data, it is likely that UIM proteins also function in clathrin-dependent pathway. Both epsin and eps15 contain clathrin binding motifs and bind to clathrin *in vivo*. Both epsin and eps15 co-localize with clathrin

positive vesicles *in vivo* (Chen et al. 1998; Chen et al. 2005). Additionally, in *Drosophila, lqf* mutations genetically interact with *clathrin heavy chain* gene mutants (Cadavid et al. 2000). How might these data be reconciled? It is possible that receptors entering the clathrin-dependent pathway are not ubiquitinated. In this scenario, UIM proteins would participate as accessory factors possibly to help recruit clathrin, but may not bind directly to cargo. This and other possible models are under investigation (see chapter 2).

In addition to binding ubiquitin on receptor proteins, UIMs may have another function in facilitating intramolecular ubiquitination of some UIM containing proteins. Eps15 and Epsin become ubiquitinated upon stimulation by growth factor signaling in vertebrate cell culture assays. Currently, the effect of ubiquitination on protein function is unknown (Hicke et al. 2003). It is speculated that the UIMs mediate this process by recruiting ubiquitin ligases to ubiquitinate the protein at a site other than the UIM. This raises the possibility for intramolecular interactions that may serve to regulate protein activity in any number of ways. For example, one idea is that intramolecular binding of UIM and a Ub moiety elsewhere on the same protein might affect protein conformation and activity. Currently, this issue is under much investigation (DiFiore et al. 2003; Polo et al. 2002; Hicke et al. 2003; Shih et al. 2003).

The next sections concentrate on the clathrin adaptor proteins containing an ENTH domains and ANTH domains, as they are the major focus of this thesis.

ENTH domain proteins

ENTH (Epsin-N-terminal Homology) domain proteins are a family of proteins which mediate clathrin coated vesicle formation and vesicle trafficking at various cell membranes. These proteins are present in genomes from yeast to mammals. Presently, two types of ENTH domain proteins have been characterized: epsins and Epsin-Related (Epsin-R) proteins. Mechanistically, both are thought to mediate the formation of clathrin coated vesicles, but they do so at different subcellular locations. Epsins function at the plasma membrane during clathrin-mediated endocytosis, while Epsin-R works at the Golgi membranes (Legendre-Guillemin et al. 2004).

The ENTH domain is a stretch of about 150 highly conserved amino acids at the N-terminus of epsin and Epsin-R. ENTH domains bind to specific types of inositol phospholipids enriched at certain membranes. The ENTH domain of rat epsin-1 preferentially binds to $PI(4,5)P_2$ (Itoh et al. 2001) while the ENTH domain of Epsin-R preferentially binds to PI(4)P and PI(5)P in some assays (Mills et al. 2003). These types of inositol phospholipids are enriched at different cellular membranes: $PI(4,5)P_2$ at the plasma membrane and PI(4)P and PI(5)P are enriched at Golgi or endosomal membranes. Therefore, it is speculated that epsin and Epsin-R localize to distinct subcellular compartments by selective binding of the ENTH domain to certain inositol phospholipids. In support of this idea, most

ENTH domain proteins fail to localize correctly without their ENTH domain (Legendre-Guillemin et al. 2004 and see chapter 5).

The secondary structure of ENTH domains consists of 8 alpha-helices of which the first four helices bind to particular phosphoinositol (PIP) molecules. Crystal structures of the ENTH domain of rat epsin-1 have pinpointed the amino acids responsible for recognition of the distinct inositol phospholipids. Eight conserved amino acid residues, mostly positively charged, are responsible for binding to PI(4,5)P2, which is enriched at the plasma membrane (R7, R8, K11, R25, N30, R63, K69, H73) However, some of the positively charged amino acids are not conserved in the ENTH domain of Epsin-R (see chapter 4 Fig 1). The ENTH domain of Epsin-R is less positively charged and therefore preferentially excludes highly phosphorylated PIPs and instead binds less phosphorylated PIPs, such as PI(4)P and PI(5)P (Itoh et. al 2001; Mills et al. 2003; Ford et al. 2002). This may not be true for the putative yeast homolog of Epsin-R, Ent3p. Ent3p binds to PI(3,5)P2 which is enriched on yeast multi-vesicular bodies (Friant et al. 2003, and see chapter 5).

The ENTH domain was first identified in epsin proteins. Epsins (Eps15 Interactor) regulate clathrin-coated vesicle formation at the plasma membrane and maybe trafficking of vesicles through endocytic compartments (De Camilli et al. 2001 and Wang et al. 2004). All epsins possess an N-terminal ENTH domain that binds to PI(4,5)P2 (De Camilli 2001). They also have ubiquitin interacting motifs that bind ubiquitin non-covalently. These motifs may have two abilities: to

recognize ubiquitinated cargo and regulate the ubiquitination of epsin (Hofmann et al. 2001; Polo et al. 2002). The C-terminal part of the protein contains clathrin binding motifs (CBM) and DPW motifs that bind to the AP-2 clathrin adaptor. Finally, NPF motifs bind to EH domain present in accessory endocytic factors, namely Eps15 (De Camilli 2001). Yeast epsin homologs, Ent1p and Ent2p have a similar structure, but they do not possess DPW motifs (Wendland et. al 1999).

Epsin-Related was identified recently as another ENTH domain protein. Like endocytic epsins, it possesses an ENTH domain at the N-terminus, but its ENTH domain binds less phosphorylated PIPs. Epsin-R also lacks UIMs. At the C-terminus, Epsin-R contains protein interaction motifs important for binding vesicle-making proteins present at the Golgi complex, i.e. clathrin and AP-1 binding regions (Mills et. al 2003; Hirst et. al 2003; Wasiak et al. 2002 and see chapter 4).

How ENTH domain containing proteins function mechanistically in forming clathrin coats around particular cargo molecules is the subject of much research. Most of the research has focused on epsin1, however other ENTH domain proteins are speculated to work somewhat analogously. The ENTH domain binds to the phospholipids, and so is thought to localize the protein to specific membranes. At this early step, the ENTH domain of epsin1 might induce membrane curvature at the edges of the forming bud. Recently, the ENTH domain of rat epsin1 was shown to tubularize lipids (Ford et al. 2002). At these edges, epsin1 can recruit coat components (such as AP-2, clathrin and accessory

factors) to stimulate clathrin cage assembly (Szymkiewics et al. 2004; Mousavi et. al 2004). As epsin1 cannot be isolated from CCVs, it might associate only with the pit at the edges, not deep into the invaginating bud. Thus, epsin1 is thought to work only at the earliest stages of vesicle formation. This model may not reflect the function of Epsin-R entirely, because Epsin-R is purified easily from CCVs. Thus, Epsin-R might remain associated with the coat even after scission (Mills et al. 2003; Hirst et al. 2003; Wasiak et al. 2003 and see chapter 4).

Epsins are also the subject of post-translational regulation as they undergo both phosphorylation and ubiquitination. Phosphorylation of epsin is thought to inhibit its activity by preventing epsin binding to its partners in mammals and in yeast (Chen et al. 1999; Watson et al. 2001). The function of epsin ubiquitination is less clear. Studies in *Drosophila* indicate that epsin function may be negatively regulated by ubiquitination possibly by leading to its degradation (see below). In support of this idea, deubiquitination of *Drosophila* epsin positively regulates epsin activity, possibly by increasing epsin protein levels or activity (Chen and Fischer 2002; Cadavid et al. 2000).

In the future, it will be important to establish more precisely epsin's function in ubiquitin-mediated endocytosis. We must also determine the extent of functional overlap epsins have with other ubiquitin adaptors like eps15. Finally, it will be important to understand the regulatory mechanisms that govern epsin function. Answers to these questions could be facilitated by studies in

multicellular organisms in specialized cellular contexts that rely on endocytosis for intercellular communication.

ANTH domain proteins

ANTH domain proteins such as AP180/CALM and Hip1 (Huntingtin interacting protein) contain a region that is structurally similar to the ENTH domain. The ANTH domain of AP180/CALM binds to PI(4,5)P2 and the ANTH domain of Hip1 binds to other types of inositol phospholipids such as PI(3,5)P2. Unlike the ENTH domain, the ANTH domains do not appear to be able to deform lipids (Legendre-Guillemen et al. 2004).

Outside of the ANTH domain, these proteins are similar to ENTH domain proteins in that they have motifs that interact with clathrin, ubiquitin, EH domains and AP-2. This region is thought to participate in clathrin lattice assembly much like the C-terminal domains of ENTH proteins. Indeed, *in vitro*, both epsin1 and AP180 recruit clathrin to membranes, but the epsin1 lattices are invaginated whereas AP180 lattices are flat (Ford et al. 2002).

The function the ANTH domain may not be to control membrane invagination during coat assembly, but rather to control coat size. Clathrin lattices assembled *in vitro* by AP180 are more uniform in size than those assembled by epsin1 (Ford et. al 2002). In addition, a *Drosophila* mutant for AP180 results in clathrin coated vesicles of abnormal size (Zhang et al. 1998).

ANTH domain proteins may also have roles in packaging specific cargo in to coated pits. Hip1 has been implicated in the endocytosis of several receptors such as growth factor receptors. However, it remains to be determined if Hip1 is specific for these receptors or is a general component of endocytosis machinery (Legendre-Guillemen 2004).

AP-2 interactions with specialized clathrin adaptors

The term adaptor defines a class of proteins that can connect cargo physically to the clathrin coat. Therefore, adaptors are responsible for the selectivity and fidelity of cargo incorporation into vesicles. AP-2 was the first adaptor protein identified, but since then the monomeric adaptors have been recognized as alternate clathrin adaptors for specific types of cargo. Do these proteins function with AP-2 in coat formation? A number of studies suggest that the answer is likely to be yes. First, the density of clathrin coated pits in cell culture in absence of AP-2 is only 10% that of normal. This might mean that most endocytic events depend on AP-2, but there is only a small subset that can function without it. *In vitro* most of the alternative clathrin adaptors can assemble clathrin coats, but their coating abilities are enhanced in the presence of AP-2 (Ford et al. 2001; Mishra et al. 2002). Finally, many of these adaptors are associated *in vivo* with AP-2 either by direct binding to AP-2 or indirectly associated through a complex of proteins. Still, it is possible adaptor proteins

work with AP-2 sometimes and other times, they function independently. Nevertheless, this remains an interesting question for future research.

Adaptor proteins and their regulation of vesicle trafficking are diverse and rich with subtlety and complexity that is only in the beginning stages of understanding. In the future, it will be important to understand more about the spatial and temporal relationships between cargo, cargo adaptors and coat components. Also, we must understand in what circumstances the cell regulates and utilizes various modes of cargo incorporation into vesicles.

Fission

As the vesicle budding process nears completion and the bud is fully matured, the next step is to pinch off the vesicle into the cytoplasm. One of the major goals is to constrict the neck sufficiently to bring the opposing membranes close enough together to fuse them and set the vesicle free into the cytoplasm. Several cytosolic proteins are responsible for these events including dynamin and endophilin (Mousavi et al. 2004; Alberts et al. 2002).

The physical problem that must be overcome is that chemical energy must be converted to mechanical energy to pinch off the forming vesicles. Dynamin is a candidate protein to perform this function. The GTPase Dynamin localizes to necks of buds via its PH (pleckstrin homology) domain which binds to PI(4,5)P2. Dynamin oligomerizes around the neck via self association through its GED

domain. Dynamin then recruits other cytosolic proteins such endophilin via interaction with its PRD (proline rich domain) (Mousavi et al. 2004; Reutens et al. 2002).

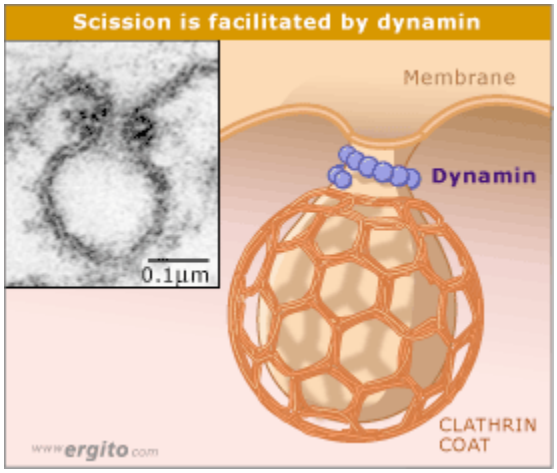

Fig. 6. Dynamin is absolutely required for vesicle scission. Dynamin forms oligomers around the neck of an invaginated membrane. The GTPase activity of dynamin might directly contribute to membrane sission or dynamin might recruit other proteins that mediate this event.

Exactly how dynamin mediates the fission event is the subject of much research. Currently there are several working models. One model suggests that dynamin itself provides the mechanical energy to pinch off the vesicle. Dynamin self-assembles around the neck of a bud. Then GTP energy causes a conformational change equivalent to some sort of mechanical force that can be applied to constrict the membrane. The mode of mechanical force dynamin applies is controversial (Mousavi et al. 2004; Alberts et al. 2002 and Fig. 6).

Alternatively, the main function of dynamin may be to recruit accessory proteins that mediate fission. Dynamin binds to Endophilin which is an enzyme

with acyltransferase activity. Endophilin may modify the lipid composition of the neck by condensing lysophosphatidic acid to phosphatidic acid. Thus, it converts an inverted cone shaped lipid to a cone shaped lipid. This might induce negative curvature in the neck which could support fission by promoting the conversion from a shallow to a deeply invaginated pit (Reutens et al. 2002).

Uncoating

Upon fission of the vesicle from the membrane, the coat components must be recycled, rendering the naked membrane-bound vesicle able to fuse with target membranes. To accomplish this, coat components must rapidly dissociate from each other and from the lipid membrane of the vesicle. The mechanisms regulating uncoating are only now being discovered, however, dissociation of protein components may be controlled in part by ATPase and phosphatase activity (Alberts et al. 2002).

Major players in the uncoating process are the DnaJ family protein Auxilin and Hsc70 (See Fig 7). According to the most recent models, auxilin binds to assembled clathrin. Next, auxilin recruits Hsc70 by binding via its J domain. Hsc70 then uses its ATPase activity to disrupt clathrin interactions. Once the clathrin lattice is disassembled, the inner shell of adaptors must be removed. Phosphatase activity of a synaptojanin (or similarly functioning proteins) may mediate this event. Synaptojanin dephosphorylates PI(4,5)P2

thereby decreasing the affinity of clathrin adaptors for the membrane (Brodsky 2001; Lemmon 2001).

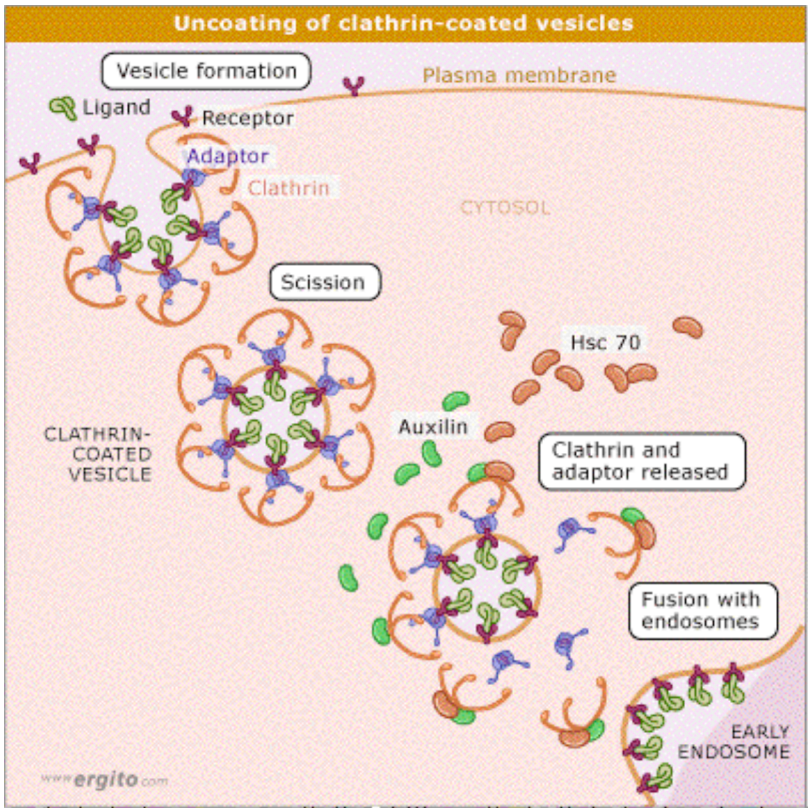

Fig. 7. Uncoating of vesicles begins rapidly after scission. Uncoating is mediated by the ATPase activity of Hsc70 in coordination with the kinase Auxilin. Uncoating of vesicles is prerequisite to vesicle fusion with target membrane and is also necessary for the recycling of clathrin monomers.

Questions for the future will be directed at uncovering how these proteins regulate the timing of uncoating. How are the uncoating actions of these proteins restricted to polymerized clathrin of vesicle only after the fission reaction has occurred and not before? (Alberts et al. 2002).

Targeting and sorting

To ensure that molecules arrive in their membrane bound packages at their appropriate destinations, vesicles must be able to select the correct membrane with which to fuse. There are several different types of membranes within the cell. Each is identifiable by distinct concentrations of molecular markers. Vesicles display surface markers identifying their origins and type of cargo. Target membranes display molecules that recognize vesicle markers.

The targeting is thought to be controlled by two classes of proteins: Rabs (targeting GTPases) and SNARES. Rabs function in recognition and docking while SNARES provide specificity and mediate fusion.

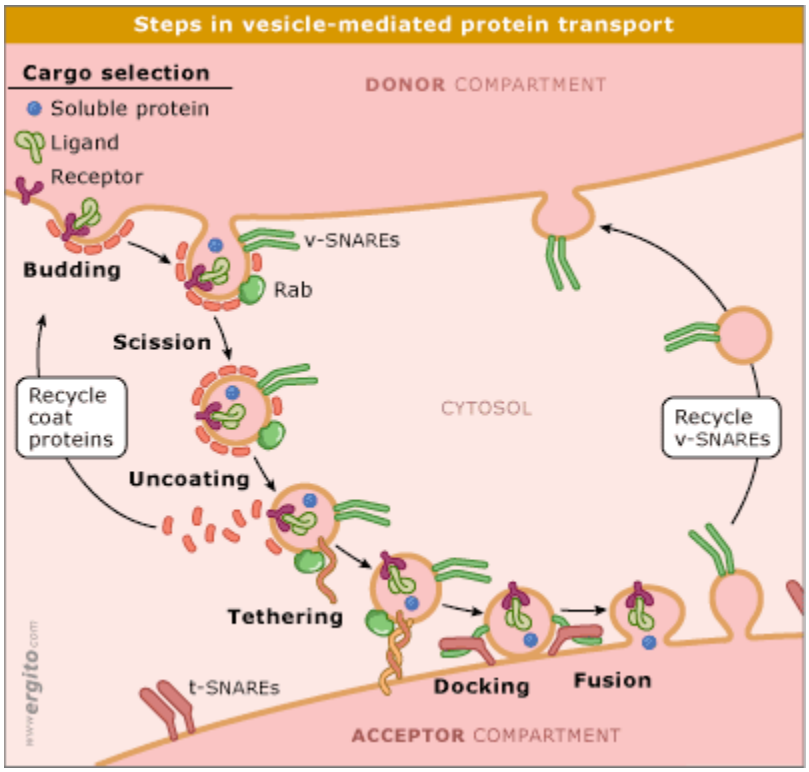

Fig. 8. SNARE proteins function as molecular address tags. Thus, they participate in the specificity of vesicle recognition to donor membrane. They also actively mediate fusion of the vesicle to target membrane. Once the vesicle is fused with the target, SNAREs must be recycled back to vesicle membranes. See text for more detail.

SNARES ensure that vesicles are targeted to the correct membrane location. Individual classes of SNARES are associated with distinct membrane-bound organelles. They are transmembrane proteins that exist as complementary sets called v-SNARES (vesicle) and t-SNARES (target). When these two recognize and bind to one another, their characteristic helical domains wrap around one another and form complexes that stabilize the membrane interaction. This interaction also contributes directly to fusion of these two membranes (Alberts et al. 2002; Jahn 2004 and Fig. 8)

Rab proteins regulate SNARE mediated vesicle recognition. Rab GTPases are the largest subfamily of monomeric GTPases. Rabs act as "molecular switches". They cycle between active GTP-bound and inactive states, GDP-bound. These changes in state are coupled to reversible membrane association at distinct membranes. Activated GTP-bound Rabs, which are membrane associated, recruit specific downstream effector molecules that facilitate SNARE interactions. Because Rabs coordinate the assembly of specific components to membranes, their function also participates in regulating membrane identity.

Because Rabs function as molecular switches, they are a focal point for regulation of fusion. Regulators of Rab GTPases determine when and where Rabs can bind to GTP (Seabra et al. 2004 and see Fig. 9). Rab proteins have

diverse functions in vesicle trafficking as they also regulate aspects of vesicle budding and transport that are beyond the scope of this review.

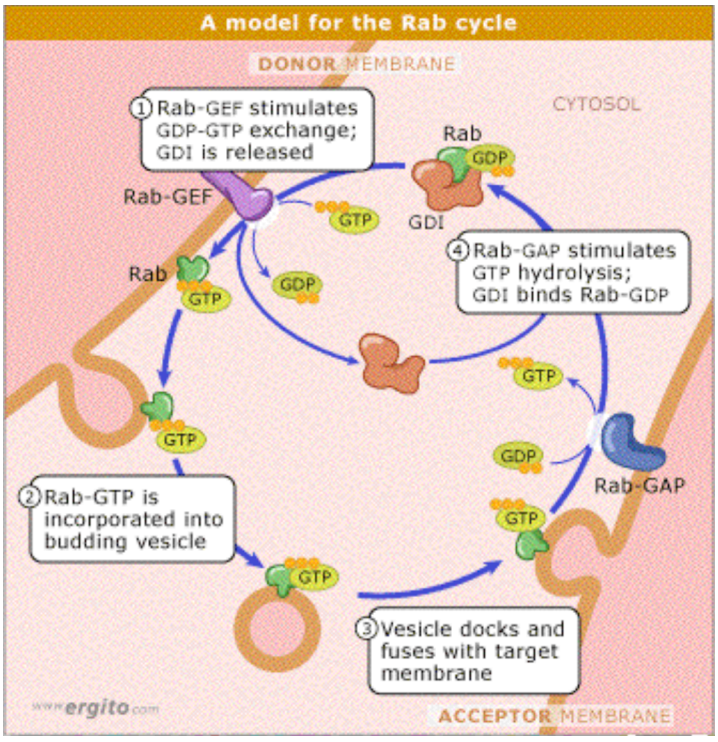

Fig. 9. Rab GTPases function as molecular switches. Active GTP bound Rabs are associated with membranes and can recruit effector molecules that facilitate SNARE interactions. Rab activity is turned off upon hydrolysis of GTP to GDP. GDP bound Rabs are cytosolic. Rab activity is regulated by several effector proteins including guanine nucleotide exchange factors (GEFs) and GTP-activating proteins (GAP)s that ensure the proper timing of Rab function (Alberts et al. 2002).

Future work will most likely focus on determining how Rabs are regulated and how they regulate membrane identity. Also, it will be important to understand the molecular SNARE code that determines compartmental addresses. This code is not readily obvious because at least *in vitro*, SNARE association is promiscuous (Wendler and Tooze 2001).

Fusion and cargo unloading

Once the vesicle membrane and the target membrane are close enough, SNARE proteins can mediate their fusion and cargo can be unloaded. Fusion requires that the membranes come within 1.5nm of each other, close enough so that they can join. Therefore, water must be displaced from the hydophilic surface between the vesicles, which is energetically unfavorable**.** It is thought that SNARE proteins have the job of overcoming this energy barrier. When SNARE helices bind to one another in *trans*, energy is freed that can be used to pull the membranes together. When lipids are close enough, lipids can flow from one membrane to the other and somehow fuse. After fusion, SNARE complexes are in the *cis*-configuration. SNARE activity can be recycled by the activity of N-ethylmaleimide sensitive factor (NSF). NSF mediates SNARE dissociation by using its ATPase activity to disassemble the coiled-coil association (Jan et al. 2003; Jahn 2004, and Alberts et. al; 2002 and Fig 10).

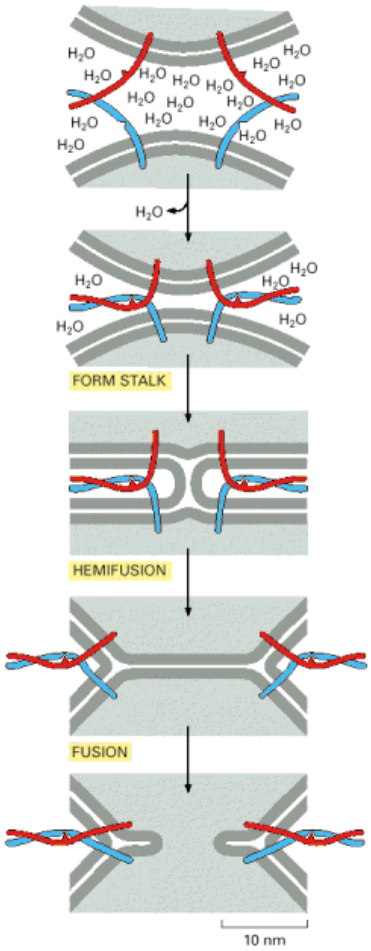

Fig. 10. SNARE mediated membrane fusion. Figure from Alberts et al. (2002). See text for details.

There has been much progress in the field of cell biology in identifying proteins that regulate all aspects of vesicle trafficking and in understanding their cellular functions. The challenge for the future demands that we also understand how their cellular roles impact the development of multicellular organisms.

VESICLE TRAFFICKING AND DEVELOPMENTAL REGULATION

The study of vesicle trafficking in developmental contexts in higher organisms is rapidly becoming a field unto itself. Research in the past decade has shown clearly that proteins at all stages of the vesicle trafficking process are involved in the development of multicellular organisms. Vesicle trafficking pathways regulate developmental processes such as morphogen gradient formation, intercellular signal attenuation and potentiation, and morphogenesis. This next section will focus on reviewing recent advances in the field of regulation of signal dispersal and morphogenesis via vesicle trafficking in during the development of a multicellular organism.

Morphogen gradients

Morphogen gradients are used in all organisms to allow cells to interpret their position in a field of otherwise equivalent cells. The morphogen gradient model suggests that certain cells in the field act as a source of dispersible signal. The signal is somehow distributed over long distances and its concentration decreases as the distance from the source increases. Thus, cells interpret the concentration of morphogen to "know" their position relative to source. By this method, cells can distinguish themselves from one another, which is the root of pattern formation.

The mechanisms of morphogen gradient formation have long been an intense area of focus in developmental biology. To account for gradient formation, a simple diffusion model was originally proposed where morphogens

moved cell distances by pure diffusion in the extracellular space (Gonzalez-Gaitan 2003a). To understand how morphogens travel long distance over several cell diameters to set up a gradient, researchers constructed functional GFP or HRP fusion molecules to monitor morphogen movement *in vivo* (Entchev et al. 2000; Lin et al. 2004; Belenkaya et al. 2004; Dubois et.al. 2001; Pfeffer et al. 2002). Using these technologies, researchers suggest that the movement of morphogens, Dpp (Decapentaplegic) and Wg (Wingless) may be controlled by the balance between planar transcytosis (multiple rounds of endocytosis and resecretion) and lysosomal degradation.

Decapentaplegic

Decapentaplegic is the *Drosophila* TGF-beta (transforming growth factor) homolog that acts as a long-range morphogen in developing tissues such as the *Drosophila* wing. Formation of a Dpp gradient is critical for proper wing formation. Entchev et al. (2000) speculate that Dpp movement and gradient formation is dependent on the endocystosis pathway. They propose that Dpp moves across cell space by transcytosis, rounds of endocytosis and resecretion on the other side. The gradient is formed by intracellular degradation of Dpp.

To test explore these ideas, they used a GFP-Dpp reporter construct. They find that most of the GFP-Dpp forms a long-range concentration gradient. Interestingly, they find that most of GFP-Dpp is intracellular in wing discs, although they do detect some extracellular GFP-Dpp. Thus, they propose that the

gradient is formed intracellularly. In support of this idea, a secreted form of GFP-Dpp is unable to form a concentration gradient.

They find that GFP-Dpp intracellular morphogen gradient formation in the developing wing is impaired when endocytosis is blocked in receiving cells expressing a dominant negative form of dynamin. GFP-Dpp is not internalized in the receiving cells and the intracellullar GFP-Dpp gradient is reduced. Also, in a population of cells with a long-range Dpp gradient formed, a patch of endocytosis defective cells fails to propagate the intracellular gradient; Dpp cannot cross this patch, and is found at reduced levels in vesicles behind the mutant patch. The authors conclude that endocytosis of Dpp facilitates gradient formation or movement across cells. Exactly how endocytosis facilitates movement of Dpp across cells is unclear. Perhaps once Dpp is endocytosed in the receiving cells, it can be resecreted, in a process called transcytosis, to send to neighboring cells. Direct evidence of transcytosis has yet to be observed.

Another possibility is that endocytosis does not directly influence morphogen movement, but only indirectly affects the movement of extracellular Dpp. For example, endocytosis could facilitate the removal of another protein that affects Dpp movement in extracellular space, i.e. the Dpp receptor Thickveins (Tkv). If too much receptor is present due to a block in endocytosis, Dpp may be trapped by receptors at the cell surface and would be unable to diffuse across the ECM. Another interpretation is that a block in Tkv receptor internalization could prevent Dpp movement by preventing transcytosis. Either way, both of these

ideas suggest that Dpp requires its receptor to get endocytosed. Supporting this idea, in *tkv*- clones, Dpp accumulates on cell membranes near to the source, failing to diffuse any farther, possibly because Dpp cannot get internalized in a Tkv-dependent way (Entchev et al. 2000; Gonzalez-Gaitan 2003a).

The role of endocytosis in movement of morphogens is still controversial as new experiments from Lin and colleagues (2004) suggest that Dpp movement is independent of dynamin function but instead regulated by the glypicans Dally and dally-like. In this study, the same GFP-Dpp reporter is used to monitor Dpp localization in wing discs, similar to Entchev et al. (2000). However, Lin and colleagues perform their analyses under conditions more sensitive in detecting extracellular GFP-Dpp. The gradient of extracellular GFP-Dpp visualized by Entchev et al. (2000) does not extend over cell distances that the full range of Dpp function. Therefore, some GFP-Dpp signal must be undetected. To detect the full range of extracellular GFP-Dpp, Belenkaya et al. (2004) used different tissue preparation conditions which allowed visualization of a gradient that coincided with the Dpp activity gradient.

Using these conditions, Belenkaya et al. (2004) assess the movement of extracellular GFP-Dpp in various genetic backgrounds. They find that signal transduction is impaired in dynamin deficient clones in the wing disc. However, cells behind these clones and farther away from the source of Dpp can still receive Dpp signal. This suggests that Dpp can move over the endocytosis-defective patch of cells to activate signaling far away from the source. Entchev et al. (2000)

observed the same thing, but thought that the cells behind the clone were receiving signal laterally from neighboring wild-type cells.

Extracellular movement of GFP-Dpp is not impaired in dynamin-deficient patch of cells. In fact, they find that GFP-Dpp accumulates at higher than normal levels on the surface of dynamin-deficient cells inside mutant clones. Since GFP-Dpp is found deep inside the clones, this also suggests that GFP-Dpp can move over these cells. Since GFP-Dpp accumulates at higher than normal levels in dynamin deficient cells, this suggests that endocytosis may be required to downregulate GFP-Dpp levels, possibly via receptor-mediated endocytosis. Consistent with this idea, they find that Tkv levels are upregulated in these clones. Therefore, a block in endocytosis does not affect the spread of extracellular GFP-Dpp. However, a block in endocytosis does affect the gradient formation of intracellular GFP-Dpp as described in Entchev et al. (2000), likely reflecting an impairment only in GFP-Dpp internalization.

If endocytosis is not required for extracellular movement of Dpp, what is? Dpp movement (and signaling) is impaired in clones of cells deficient for Dally and Dally-like as well as in wild-type cells behind them. Dally and Dally-like are glypican members of heparin sulfate proteoglycan family, part of the ECM. How do these molecules contribute to movement? The authors propose that Dpp is secreted from source cells and captured by proteoglycans Dally and Dally-like on the receiving cells. The initial differential concentration of Dpp on the signaling cells versus the receiving cells drives the displacement of Dpp from the

proteoglycans on the signaling cells to another on more distant receiving cells by a process they call "restricted diffusion". Dpp would then be presented to its receptor on receiving cells where it would be endocytosed to activate signal transduction via endocytosis. They also propose that endocytosis also shapes the Dpp gradient. Endocytosis influences the shape of the gradient by downregulating Dpp levels via receptor mediated endocytosis (Lin et al. 2004; Belenkaya et al. 2004). Thus, endocytosis does not participate in movement of Dpp, but regulates the shape of the gradient and mediates signaling.

Mammalian TGF-beta

Like *Drosophila* Dpp, results from studies of mammalian TGF-beta suggest that subcellular trafficking also regulates signaling activity. Specifically, TGF-beta signaling is potentiated by trafficking to endosomes. An endosomal protein called SARA binds to activated receptors on endosomes that have been endocytosed in a clathrin-dependent way. At endosomes, SARA binds to downstream effectors of TGF-beta, called Smads 2 and 3, allowing the receptor to phosphorylate and activate the Smads. It is not clear why endosomes are the platform for signal transduction. It could be that effectors are concentrated at endosomes. However, internalization of the receptors is prerequisite for activation because phosphorylation of downstream Smad effectors does not occur in the absence of endocytosis (Belenkaya et. al 2004; Gonzalez-Gaitan 2003).

Wingless

Wingless (Wg) is a member of the Wnt family of secreted proteins that act as morphogens over a short range. Wg signaling is integrated with several other pathways in the embryo to pattern the embryonic cuticle. Wg morphogen gradients may be influenced by endocytosis during embryonic development. Rounds of endocytosis and differential rates of Wg degradation may set up the asymmetric Wg gradient that exists in the early embryo

The Wg gradient in the embryo is distributed symmetrically at both sides of its source at the beginning of embryogenesis. Later, its spreading is restricted posteriorly. Dubois et al (2001) proposed that Wg spreading is limited by increased lysosomal degradation posteriorly. An HRP-Wg fusion reporter construct was used to monitor the fate of Wg protein because HRP is stable in lysosomes even after Wg protein has been degraded. Using this approach, HRP was found in degradative subcellular compartments at higher levels posterior to the Wg source than anteriorly (Dubois et.al. 2001; Gonzalez-Gaitan 2003).

How does Wg travel over cell distances? Several pieces of evidence support the idea that Wg moves intracellularly via planar transcytosis, endocytosis on one side of the cell and resecretion to another side. Bejsovec et al (1995) showed that Wg is internalized into vesicles into receiving cells. Also, endocytosis is necessary to spread the Wg signal because dynamin-defective cells could not transduce the signal. Recently, Pfeiffer et al. (2002) showed that GFP-

Wg could be recycled by a mechanism of planar transcytosis. Also, they showed that Wg vesicles could move inside cells from one cell to the next.

The planar transcytosis model is subject of much debate as newer models suggest that Dally and Dally-like proteins shape the Wg gradient in the wing disc similarly to Dpp gradient formation (Han et al. 2005; Baeg et al. 2004; Kirkpatrick et al. 2004; Giraldez et al. 2004). It is possible that Wg and Dpp gradients are established differently in various tissues or both transcytosis and restricted diffusion mechanisms are used to form gradients.

Signal attenuation and potentiation

Signaling from receptors at the plasma membrane entails binding of ligand and subsequent recruitment of cytosolic effectors to propagate a downstream response, which may involve changes in gene expression. Vesicle trafficking pathways are used in diverse ways to modulate the cellular responses to these receptors.

Epidermal Growth Factor Receptor Signaling

EGFR is a receptor tyrosine kinase responsible for a profound array of developmental decisions including cell proliferation, survival and differentiation. EGF binding induces dimerization of the receptor which then autophosphorylates its cytoplasmic tails in *trans*. Once the receptors are activated by phosphorylation, downstream effector proteins can be recruited. Signal transduction is modulated

in several ways by trafficking of the receptor in vesicles. Signal transduction can be attenuated by receptor degradation in lysosomes or potentiated by trafficking through endosomes.

One of the first pieces of genetic evidence for signal attenuation via lysosomal degradation came from a study of *Drosophila* Hrs (Lloyd et al. 2002 and see above). This study demonstrated that Hrs is responsible for trafficking of proteins from the early endosome to lysosome. In the absence of Hrs, activated EGFR gets recycled back to the plasma membrane in the embryo. As a result, EGFR signaling is upregulated. This suggests that delivery to the lysosome attenuates signaling.

Even though receptor internalization can down-regulate signaling, in some cases, internalization of receptors is required to potentiate signaling. Dynamin-dependent endocystosis is required to potentiate signaling because in dynamin-defective cells, signaling of EGFR is attenuated (Vieira et al. 1996). Why would internalization be necessary to enhance signaling? One possibility is that signaling effectors are efficiently recruited at endosomes, similar to TGF-beta signaling (see above). In support of this, EGFR associates with some of its downstream effectors on endosomes. Perhaps there are different types of effectors at the plasma membrane and another set away from the cortex at endosomes. This could be a mechanism to access different types of effectors and so vary the magnitude or type of response to the same activated receptor (Mousavi et al. 2004).

Hedgehog

Hedgehog (Hh) proteins are a family of secreted signaling molecules that mediate many developmental processes. Its two receptors, Patched (Ptc) and Smoothened (Smo), mediate the responses to Hh proteins. When Hh is absent, Ptc binds to Smo at the cell surface and Smo activity is repressed. When Hh is present, repression of Smo by Ptc is relieved and Smo is free to signal.

Smo signaling activity is modulated by the endocytic pathway. Smo inhibition is relieved by Hh binding to Ptc because Hh binding induces internalization of both Ptc and Smo. Following this, the Hh/Patched complex is then routed to degradative lysosomal compartment, while Smo is recycled in activated form at the cell surface (Denef et al. 2000; Incardona et al. 2002)

Notch signaling

The Notch pathway also plays profound roles in most developmental decisions. This pathway is regulated in numerous ways by vesicle trafficking proteins in both the signaling and the receiving cells. Vesicle trafficking events in this pathway are vitally connected to the ubiquitin pathway via the activity of several E3 ligases and also the activity of at least one known deubiquitinating enzyme (see below).

In the signaling cells, endocytosis of the Notch ligands Delta and Serrate is required for activation of the receptor Notch in the receiving cells (Le Borgne et

al. 2005b). Several lines of evidence support this notion. Using clonal analysis Seugnet et al. (1997) demonstrated that dynamin-mediated endocytosis was required not only in the receiving cells, but also in the signaling cells for activation. Recently, it was demonstrated that two E3 ligases, mind bomb (mib) and Neuralized (Neur), are required for the ubiquitination of Delta in signaling cells in Zebrafish and flies, respectively. Furthermore, in the absence of their E3 ligase activity, endocytosis of DSL ligands fails resulting in impaired N activation (Itoh et al. 2003; Pavlopoulos et al. 2001; Deblandre et al. 2001; Lai et al. 2001). The homolog of mib in *Drosophila,* D-mib, was studied recently. And found to ubiquitinate Serrate and Delta. Thus, Neur and D-mib may have similar, but complementary functions in DSL ligand signaling in *Drosophila* (Le Borgne et al. 2005a). The function of ubiquitination of DSL ligands appears to be to route these ligands to the lysosome, consistent with most studies of receptor ubiquitination (Lai et al. 2001; Lai et al. 2005; Deblandre et al. 2001). While endocytosis of DSL ligands is necessary for signaling, it is not understood if and how trafficking downstream of internalization may influence signaling.

The mechanism by which endocytosis is required for ligand activation is controversial (Fig 11). One model proposes that trans-endocytosis of Delta bound to the extracellular domain of Notch provides mechanical force necessary to unmask a cleavage site in the N extracellular domain, called the S2 cleavage site (Fig 11 (2)). Cleavage of this site allows for subsequent cleavage of the N intracellular domain, called the S3 cleavage, and its translocation to the nucleus

where it acts to influence gene expression (see chapter 2). In support of the trans-endocytosis model, the N extracellular domain is endocytosed with DSL ligands in the signaling cells. When endocytosis of ligands is impaired, trans-endocytosis is reduced along with signaling activity (Parks et al. 2000).

Another recent model proposes that endocytosis is only necessary to traffic the ligands through a recycling endosomal compartment (Fig 11(3)). This is required to activate the ligand, possibly via a proteolytic cleavage in the low pH endosomal compartment. This activated form of Delta is recycled to the cell surface where it is now competent to signal and activate N (Wang et al. 2004 and see chapter 2). Interestingly, the recycling of Delta may be dependent on the endocytic ENTH domain protein epsin, or Liquid facets (Lqf) in *Drosophila*. The authors propose that Lqf is responsible for a subset of endocytic events important for routing Delta into a select endocytic pathway. They determined that Lqf probably recognizes an ubiquitinated form of Delta, probably via a UIM interaction. As ubiquitination directs trafficking toward degradative pathway (Hicke et al. 2003), they speculate that Lqf may protect a portion of ubiquitinated Delta from this route (for more details, see chapter 2).

Alternatively, clustering of ligands in membrane microdomains in signaling cells may promote clustering of N receptors in the receiving cells (Fig 11(1)). Clustering may somehow facilitate robust signaling perhaps by restricting diffusion of N receptors and concentrating their ability to be cleaved. In support of this idea, a membrane-bound N receptor fused to Torso dimerization sequences

is able to signal independently of ligand binding and endocytosis in *Drosophila* (Seugnet et al. 1997; Le Borgne et al. 2005b). In a vertebrate cell culture assay, antibody-induced oligomerization of a secreted Delta protein was able to bind to N receptors and activate signaling. In contrast, unclustered Delta protein could not bind N. However, whether or not N was activated depended on the degree of clustering, as high amounts of clustering (induced by high concentrations of antibody) inhibited N activation (Hicks et al. 2002).

Ligand endocytosis may not be required for signaling in *C. elegans*. One of the major reasons for thinking this is that three of the five Notch/Lin-12 ligands are secreted. Also, an engineered secreted form of a membrane-bound Notch/LIN-12 ligand can activate signaling normally (Fitzgerald and Greenwald 1995). However, Henderson et al. (1997) found that the TM domain of the same DSL ligand was required for Notch/LIN-12 signaling, suggesting that membrane tethering is required. Interestingly, the *C. elegans* epsin homolog is required for N activation in the gonad, suggesting that endocytosis is required (Tian et al. 2004). These two pieces of data might be reconciled if endocytosis promotes trafficking of ligand through and endosomal compartment where it can be activated and/or processed into secreted forms. However, it is entirely likely that DSL signaling in *C. elegans* occurs differently from DSL signaling in higher organisms. In support of this idea, secreted forms of DSL ligands in *Drosophila* act as antagonists (Hukriede and Flemming 1997; Sun and Artavanis-Tsakonis 1997).

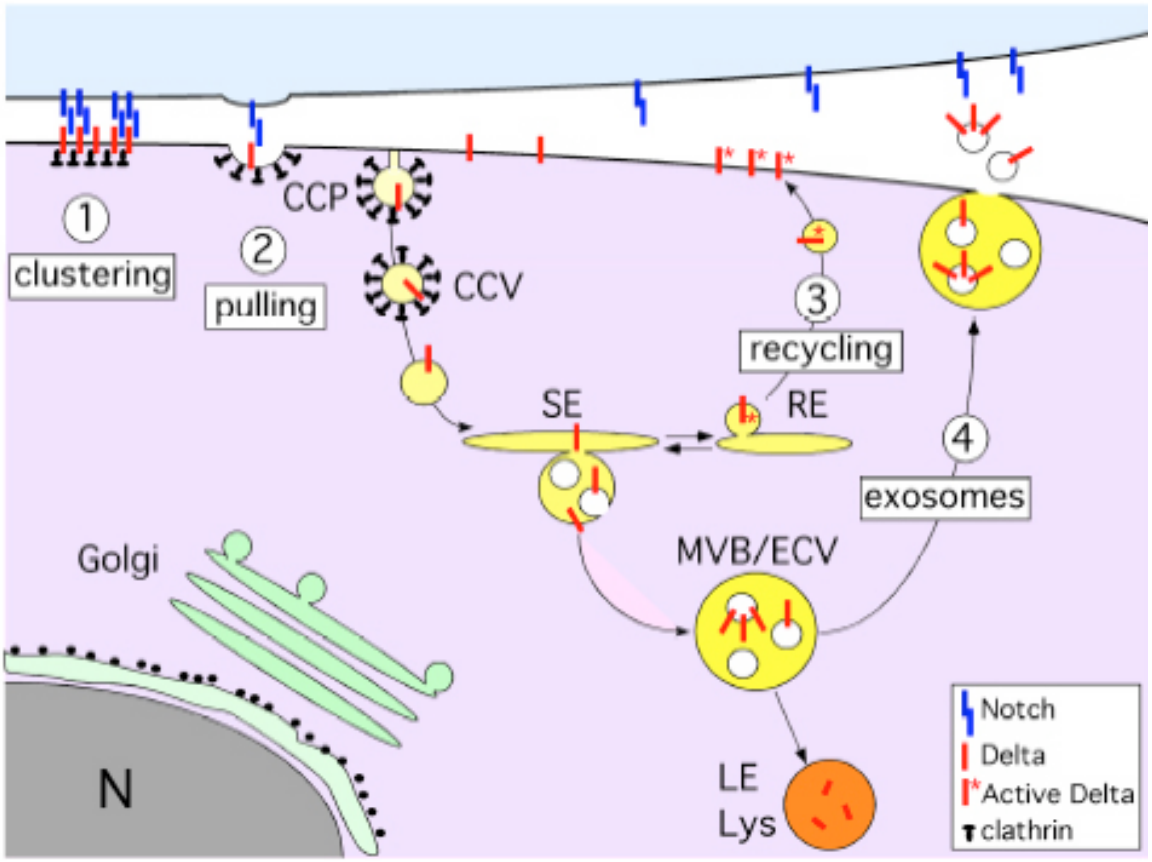

Fig. 11. Models of how ligand endocytosis promotes N signaling.
(1) The clustering of DSL ligands (in red) may be required to promote clustering of N (in blue) in signal receiving cell. Clustering may facilitate proteolytic cleavage of N - see text. (2) Endocytosis of DSL ligands provides the mechanical force necessary to expose cleavage site in NECD. (3 and 4) Recycling ligands post-internalization at either recycling endosomes or the multi-vesicular body might produce activated forms of ligand. In the first case, trafficking through recycling endosome might result in activating chemical changes. In case 4, signaling exosomes may be produced on MVBs. The black spikes represent the clathrin-coated membranes. The pH gradient seen in the endocytic pathway is color-coded, from neutral (pale yellow) to pH±5 (orange). Figure and legend adapted from Le Borgne et al. (2005b).

This story is further complicated because endocytosis of Notch in receiving cells is also required for signaling. As mentioned before, Seugnet et al. (1997) found that endocytosis was required in the signaling cells. In support of

this, a recent report suggests that endocytosis of N following S2 cleavage is required for S3 cleavage of intracellular domain of Notch by gamma secretase. A block in endocytosis of an S2-cleaved form of N, prevents S3 cleavage. Interestingly, this engineered form of N was found to be mono-ubiquitinated and blocking mono-ubiquitination resulted in decreased endocytosis and S3 cleavage. The authors suggest that gamma secretase-dependent S3 cleavage relies on endocytosis of the receptor. Endocytosis may transport N receptors away from the plasma membrane to an intracellular site enriched in gamma-secretase activity (Gupta-Rossi et al. 2004).

These new results may be in contrast with those observed by Seugnet et al. (1997): a membrane-tethered and dimerized form of N no longer needs dynamin-dependent endocytosis to signal. There are a few ways to reconcile these two studies. The dimerized form of Notch may be endocytosed in a dynamin-independent way to arrive at sites where gamma secretase is present. Alternatively, the dimerize form of Notch may mimic the function of endocytosis which may be to cluster the receptors in such a way that S3 cleavage site is exposed.

Endocytosis may have other roles in modulation of signaling. Two E3 ubiquitin ligases, Su(dx)/Itch and Nedd4, appear to act in concert to ubiquitinate Notch and thus target Notch for internalization and degradation in lysosomes. Downregulation of the Notch receptor may be one way attenuate signaling (Le Borgne et al. 2005b). Consistent with this idea, the cargo adaptor Numb binds to

the intracellular domain of Notch and links it to the clathrin adaptor AP-2. This interaction mediates the internalization of Notch to prevent Notch activation cell autonomously in *Drosophila* SOP cells. However, it is not clear if Numb activity leads to degradation of Notch (Le Borgne et al. 2003).

Low density lipoprotein receptors

Low density lipoprotein (LDL) receptors regulate the uptake of cholesterol in animal cells. Most cholesterol is transported in blood in the form of lipid-protein particles called low density lipoproteins (LDL). When a cell needs cholesterol for membrane synthesis, it makes LDLR and inserts them into the plasma membrane where they can bind to LDL. LDLR are constitutively endocytosed into clathrin coated vesicles where they are routed to early endosomes. This compartment's pH is low enough to facilitate the dissociation of LDL from the receptor. At this point the receptor is efficiently recycled to the plasma membrane. The LDL particle is routed to the degradative lysosomal compartment to be digested to free cholesterol and utilized by the cell (Alberts et al. 2002). When this process is impaired, cholesterol accumulates in the blood vessels resulting in atherosclerosis.

LDL receptors have recently been shown to participate in signaling important during the development of mammalian nervous system. Besides LDL proteins, LDL receptors have other ligands in the nervous system. One ligand is a protein called Reelin (Reln). Mice deficient for Reln, display nervous system

defects where several regions of CNS are displaced. Interestingly, this phenotype is similar to loss of function in the clathrin adaptor Dab-1 (see above). One hypothesis is that Dab-1 mediates the internalization of LDL receptor internalization bound to Reln. Internalization may facilitate activation of downstream effectors important for proper nervous system development. However, the exact sequence of events is still being investigated (Cooper and Howell 1999; Howell et al. 2001; Herz 2001).

E-cadherin

E-cadherin is a cell adhesion molecule that has many roles in development including cell polarity determination and cell adhesion. E-Cadherin (E-Cad) is a major component of adherens junctions where it promotes cell-cell adhesion. E-cadherin also localizes to intracellular vesicles indicating that cadherin-based adhesion is regulated in part by vesicle trafficking.

After synthesis, E-cad must be delivered to the lateral cell surface where it functions to maintain cell polarity and/or influence cell morphogenesis. Therefore, proper vesicular sorting to the correct cellular location is vital. This aspect of E-cad regulation occurs at the TGN. The di-leucine motifs in the cytoplasmic tail ensure E-cad is delivered to the right membrane domain (possibly via AP-1 regulation) after synthesis. There are a variety of proteins implicated in regulation of this step of E-cad vesicle sorting including several GTPases.

Endocytosis of E-cad is used to modify the adhesive properties of cells. Downregulation of E-cad occurs as a result of lysosomal degradation and leads to permanent loss of cell adhesion. Alternatively, certain amounts of E-cad could be recycled back to the basolateral surface. In this way, cell adhesion could be modulated to varied degrees and can thus affect morphogenesis during development.

Regulation via the biosynthetic pathway

Commissureless and Roundabout

The balance between attraction and repulsion mediates certain aspects of axon pathfinding in CNS development. Commissureless (Comm) and Roundabout (Robo) are two proteins that participate in attraction and repulsion in axon guidance during the development of the *Drosophila* central nervous system. Comm is a transmembrane protein that negatively regulates Robo, the transmembrane receptor for Slits. The Slit/Robo interaction results in repulsion of axons at the CNS midline. Comm activity overcomes the repulsive action of Robo. Therefore, Comm and Robo modulate the levels of repulsion and attraction of certain axons to allow for correct pathfinding. The molecular mechanism involves regulated vesicle trafficking (Keleman et al. 2002; Myat et al. 2002).

One model proposes that Comm influences the subcellular trafficking of Robo by preventing Robo from reaching the cell surface. Comm has been shown

definitively to regulate surface expression of Robo. When Comm is overexpressed, Robo levels at the surface are decreased. Keleman et al. (2005) propose that Comm activity routes Robo to late endosomes before it reaches the surface. Consistent with this idea, these two proteins co-localize in endosomes when both are coexpressed in cell culture (Keleman et al. 2002). Also, a GFP-tagged Robo is normally transported to the cell surface in transport vesicles which display a characteristic movement. However, when co-expressed with Comm, GFP-Robo discontinues its transport to the surface, but is readily seen in motionless endosomes (Keleman et al. 2005). This model is in dispute as another group proposes that Comm mediates the downregulation of Robo via endocytosis and degradation (Georgiou et al. 2003).

Drosophila cellularization

The main goal of cellularization in the *Drosophila* embryo is to generate a polarized epithelium that can then undergo dramatic morphological rearrangements during gastrulation. Cellularization in *Drosophila* begins after the nuclear syncytial stage or stage 13. After 13 rounds of nuclear divisions, some 5000 nuclei rise apically and plasma membrane forms between each nucleus. Membranes invaginate in a furrow between nuclei in process that resembles cytokinesis. This process requires considerable membrane addition to the furrow (LeCuit et al. 2003).

Membrane trafficking through several pathways, including the biosynthetic pathway, plays a major role during cellularization. In support of this idea, interference with proteins known to function in the secretory pathway at the Golgi and in exocytosis abrogates cellularization. Mutations in a SNARE protein, syntaxin 1 and injection of antibodies against Golgin Lava Lamp result in cellularization defects (Burgess et al. 1997; Sisson et al. 2000). Also, Sisson et al. (2000) showed that treatment with Brefeldin A, which interferes with ER to Golgi transport, abrogates cellularization. This supports the notion that membrane addition via the secretory pathway is necessary for furrow growth. Other vesicle trafficking pathways also participate in cellularization. For example, it was recently shown that trafficking from Rab11 recycling endosomes also participates in membrane addition at the furrow (Pelissier et al. 2003).

Drosophila eye color pathway

Pigmentation of the *Drosophila* compound eye occurs as a result of pigment granule deposition into structures that are related biogenically to lysosomes. Pigmentation of the eye is required to isolate optically the individual eyes or facets from one another. Pigment granule deposition is regulated by a group of proteins, called ABC (ATP-binding cassette) transporters, that mediates movement of pigment granule precursors across membranes. ABC transporters are delivered to pigment granule organelles in vesicles from the Golgi complex.

The proteins that regulate this vesicle trafficking pathway are conserved in other organisms and function in lysosomal biogenesis (Lloyd et al. 1998).

Mutations in components of lysosomal delivery machinery in *Drosophila* result in defects in pigment granule biogenesis. The phenotypic result is that eye color is altered and therefore the genes in this pathways are named for the color of eye their mutant phenotypes cause. *deep-orange* and *light* encode homologs of yeast proteins Vps18p and Vps41p, respectively. These genes regulate delivery of vesicles to the vacuole in yeast. Mutations in the AP-3 adaptor complex encoded by a gene called *garnet*. As mentioned before, the AP-3 adaptor is required for delivery to lysosomes from the Golgi (Lloyd et al. 1998).

STUDYING VESICLE TRAFFICKING USING THE DROSOPHILA EYE

One way to gain insight into the functions of mammalian vesicle trafficking proteins is to study their homolog's function in genetically tractable organisms, such as the fruit fly *Drosophila melanogaster*. Many mammalian vesicle trafficking proteins are not only conserved at the protein level in insects, but their function is also conserved in many cases. *Drosophila* has many obvious advantages over vertebrate model organisms such as the mouse or frog. Foremost, flies are relatively simple to manipulate genetically. Compared to other model systems, it is simple to make transgenic animals, generate knock-out mutations, and perform genetic screens. Also, overwhelming amounts of diagnostic tools exist such as antibodies and enhancer traps, and transgene

constructs. Finally, there are a number of tissues in *Drosophila* amenable to scientific study mainly because some of these tissues are not required for flies to live and breed in the laboratory. This quality enables scientists to perform simple and fast genetic screens to obtain mutants in genes that would otherwise be lethal at early stages of fly development. These mutants can then be analyzed for their function in specialized developmental contexts. One of these tissues is the *Drosophila* eye.

Ommatidial assembly

The adult fly eye is a compound eye consisting of about ~800 ommatidia or facets. Each ommatidium contains 19 individual cell types including 8 photoreceptor cells, 4 cone cells, 6 pigment cells, and a mechanosensory bristle cell. Most of these cell types in the facet are determined in the larval eye disc, after the disc primordium has been specified. In the third instar disc, a wave of morphogenesis passes through the disc from posterior to anterior. This wave, termed the morphogenetic furrow, sweeps across the disc leaving in its wake rows of differentiating clusters of cells, which will become the individual ommatidia in the adult eye. Cells join the clusters sequentially and are induced to form distinct cell types in a stereotypical fashion starting with the photoreceptor cells (see Fig. 12) (Pappu and Mardon 2002; Wolff and Ready 1993).

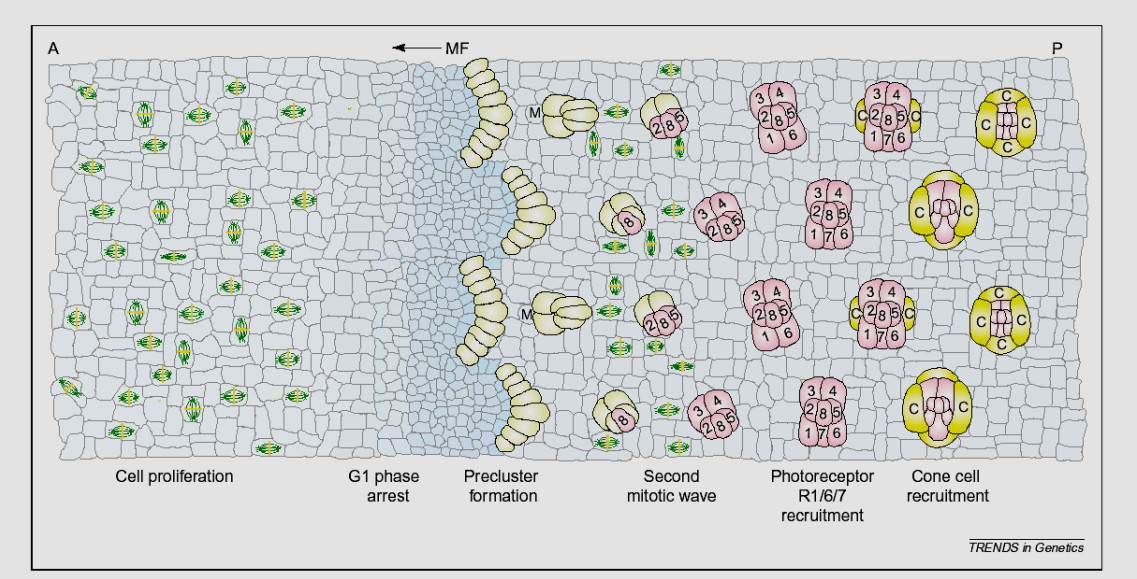

Fig. 12. Ommatidial assembly in the *Drosophila* eye disc. Anterior is to the lefte, posterior to the right. MF marks the morphogenetic furrow. See text for details. Figure from Ou et al. (2003).

Every aspect of eye development is controlled by cell-cell signaling. These signaling events are universal as they are not only employed during eye development, but are also used in other developmental settings. Furthermore, many of the cell signaling pathways (morphogens, EGFR, and Notch) may be controlled by vesicle trafficking at some level (see above). This next part will review the signaling events that govern furrow initiation and movement and cell determination.

Differentiation in the eye disc requires signaling pathways that rely on vesicle trafficking

Furrow initiation

In the 3rd larval instar eye disc, the initiation of the morphogenetic furrow depends upon the establishment of the D-V axis. A complex interplay of signaling pathways, including Wingless and Hedgehog, establish the expression of *Iro-C* complex genes in the dorsal compartment (Fig. 13). These genes repress the expression of *Fringe* in the dorsal compartment, thus *Fringe* is only expressed ventrally. Fringe is a glycosyltransferase whose substrate is the Notch receptor. Fringe modifies Notch by adding N-acetylglucosamine to O-linked fucose residues. This modification renders Notch more responsive to its ligand Delta than its other ligand Serrate. Because Delta expression is limited to the dorsal side of the disc and Serrate to the ventral side, Notch is selectively activated at the midline, boundary of Fringe expression. This region marks the D-V boundary. The furrow initiates at the intersection of the D-V and A-P axes (Lee and Treisman 2002; Cho and Choi 1998).

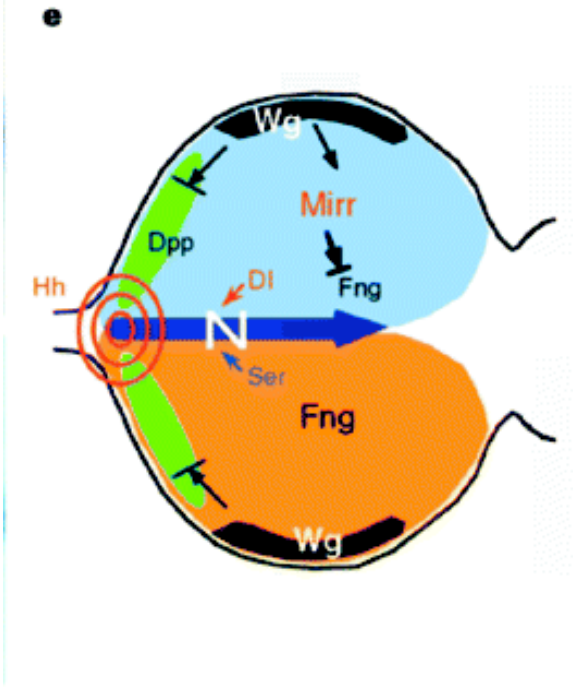

Fig. 13. N activation defines the furrow initiation point. In this figure top is dorsal and bottom is ventral. See text for further details. Figure is from Cho and Choi (1998).

Furrow progression

Once the furrow is formed, signaling via the secreted protein, Hh, mediates its anterior progression by promoting cell differentiation (Fig. 14). When the furrow initiates its progression anteriorly into the field of undifferentiated cells, clusters of maturing cells immediately posterior to the furrow secrete Hh, which in turn induces furrow expression of Dpp, a long-range signaling molecule. Dpp induces undifferentiated cells ahead of the furrow to acquire a "pre-proneural" state. This state is associated with upregulation proneural activating genes. These cells can then transition into the proneural state that coincides with the upregulation of proneural gene Atonal by Notch. Ato,

which is a bHLH transcription factor, is then restricted by Scabrous signaling to clusters of about 10-15 cells, called intermediate groups (see below). Lateral inhibitory signaling by Notch then mediates the resolution of Ato to a single cell within the intermediate groups. The Ato expressing cells become R8 cells, which subsequently begin recruitment of R1-R7. These cells begin secreting Hh, which begins the process again thus driving progression of the furrow. Without Hh, cells will not be able to adopt the pre-proneural state and furrow movement ceases (Lee and Treisman 2002; Greenwood and Struhl 1999).

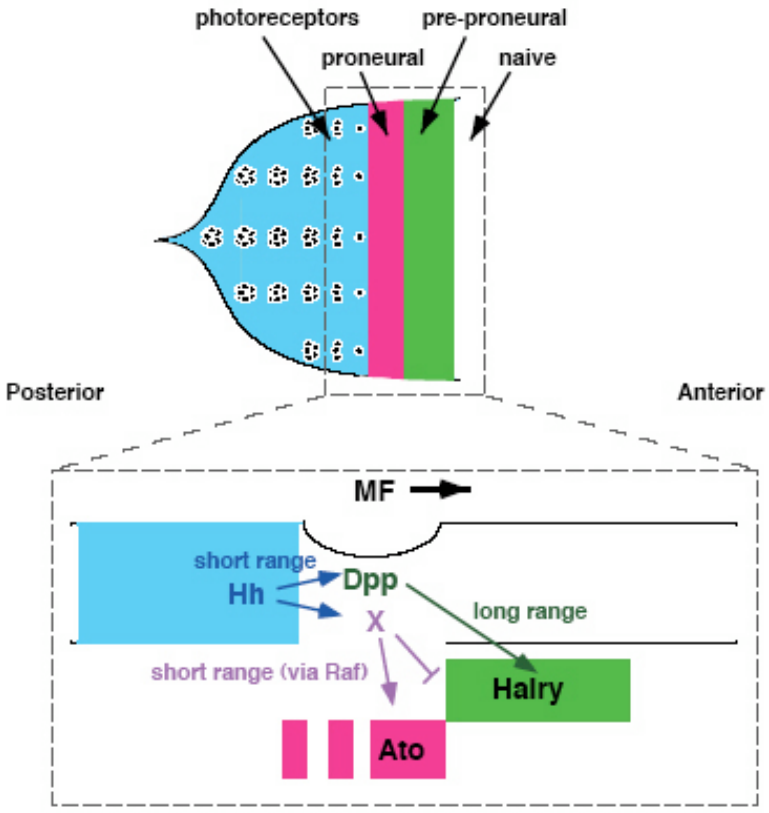

Fig. 14. Several signaling pathways control furrow progression. Maturing photoreceptors secrete Hh, which induces a long-range signal, Dpp, and an unidentified short-range signal, X. Dpp induces undifferentiated cells to become

'pre-proneural', a state that correlates with the upregulation of both proneural activators, such as Daughterless, and pro-neural repressors, such as Hairy, which hold the activators in check. The presumed short-range signal, X, activates the Raf signal transduction pathway, inducing the subsequent transition to the proneural state. Acquisition of the proneural state correlates with the downregulation of Hairy and expression of Ato. Figure and legend from Greenwood and Struhl (1999).

Patterning

Following progression of the furrow, patterning of ommatidial cells depends on the proper specification of the founder cell, R8. R8 specification is dependent on complex regulation of Ato expression by the Notch pathway (Fig 15). Repression of Ato expression is relieved by Hh anterior to the furrow resulting in a stripe of low level of Ato expression ahead of the furrow. Notch activation in all cells at the furrow results in a dramatic increase in Ato expression resulting in the proneural state. Next, Ato expression is reduced to clusters of about 10-15 cells (see below). Finally, Ato is repressed in all but a single cell from each of these groups. This is mediated by lateral inhibitory activity of Notch pathway. The cell retaining Ato expression is destined to become the R8 (Baker 2002).

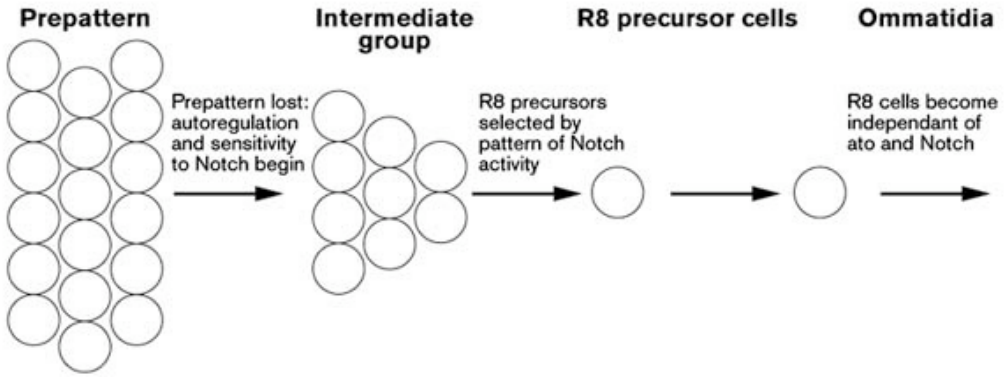

Fig. 15. Atonal resolution. Ato is initially expressed in all cells at the furrow. Through action of Scabrous and Notch, Ato expression is limited to intermediate group of 10-15 cells. Notch lateral inhibition then restricts Ato expression to a single cell within this group, which will become the R8. Figure adapted from Baker et al. (1996).

Spacing between the intermediate groups is accomplished by the interplay between Scabrous and Notch lateral inhibition. Scabrous is secreted from intermediate group cells. Scabrous (Sca) reduces Ato expression in intermediate groups. When Sca function is eliminated in the background of reduced N function, a continuous stripe of R8s differentiates. This suggests that Sca inhibits Ato expression between intermediate groups to complement the role of lateral inhibition within them (Baker 2002). The molecular mechanism of Sca function is unknown.

Recently it was shown that Sca and an endosomal protein called Gp150, associate with Notch on endosomes. Sca is thought to be internalized into cells and routed to Gp150 positive endosomes. It may be that action of Sca and Gp150 on endosomes sustains N activation by antagonizing Notch inactivation.

The mechanism is unclear. One idea is that in the absence of Sca and Gp150 proteins, N signaling might be downregulated via an endosomal pathway. Thus, Sca and Gp150 might antagonize this activity and act to recycle the N receptor back to the plasma membrane. Many other models are of course possible and are currently being investigated (Li et al. 2003).

After R8 is specified, other cells are then recruited to join the facet in a stereotyped fashion (R2 and R5 first, then R3 and R4, then R6, R1 and R7 and later the cone cells). However, if the R8 is not properly determined, subsequent recruitment steps cannot occur and no eye will form. The R8 cell is thought to recruit other cells via Ato mediated activation of Spitz secretion. Spitz secreted from the R8 activates EGFR in neighboring cells. EGFR activation in cells renders them competent to differentiate (Kumar 2002).

How EGFR can be used to specify the unique identities of the cells that join the facet remain unclear. It is thought that within each cell a combinatorial set of transcription factors could dictate the identities of the cells. Also, several signaling pathways could be integrated in parallel with EGFR to produce different types of signals. One prime example of this is R7 determination. Tomlinson and Struhl (2001) showed that proper determination of R7 cells require inputs from three different signaling molecules: two RTKs that activate the Ras pathway (Sevenless and EGFR) and Notch. R7 is the only cell in the eye that requires Sev RTK. Therefore, it is speculated that Sev signals in combination with EGFR to increase the levels of Ras signaling. The role of N activation in R7 is less clear.

However, Notch may be used to drive expression of genes that distinguish this cell from R1/6, which also receive low levels of Sev activation. One possibility is that N functions to increase the levels of *Sev* expression in R7 cells, although the exact roles of N in this process are unclear (Tomlinson et al. 2001; Kumar 2002; Nagaraj et al. (2002).

Because conserved signaling pathways are used in the eye, it is an excellent system to study mechanisms of vesicle trafficking. All they pathways have been exhaustively dissected and therefore, the tools and reagents available are unmatched by any other system.

LIQUID FACETS AND FAT FACETS

Faf is a deubiquitinating enzyme with essential roles in eye development

The *lqf* gene encodes the *Drosophila* homolog of endocytic epsin1. Epsins belong to a family of ENTH domain proteins that regulate aspects of the endocytosis pathway. *lqf* was identified on the basis of its involvement in a cell communication pathway in the developing *Drosophila* eye that is regulated by Fat facets (Faf), a deubiquitinating enzyme. Thus, Lqf and Faf are important protein that regulate both vesicle trafficking and developmental decisions (Fischer-Vize et al. 1992; Cadavid et al. 2000).

Flies carrying null mutations in the *faf* gene are viable but have two characterized phenotypes. *faf* mutant mothers are sterile because the somatic nuclei of their fertilized embryos do not cellularize completely. In wild-type embryos, after the nuclear divisions in the synctial blastoderm, cellularization occurs where cell membranes form and separate the nuclei. In *faf*- embryos, this does not occur. However, some of the pole cells do appear to develop membranes in *faf*- mutants.

faf mutant eyes also develop abnormally with too many photoreceptors in each facet. This improper patterning decision occurs early in eye development, during events near the furrow. Cells that would normally remain undifferentiated are incorporated as neurons into the preclusters in *faf* mutant discs. The extra cells are outer photoreceptors of the R3/R4 type (Fischer-Vize et al. 1992). A series of genetic experiments suggest that Faf's function in this pathway is non-autonomous or outside the extra photoreceptors. In facets mosaic for *faf*- and *faf*+ photoreceptors, the ectopic photoreceptors could be *faf*+ when they neighbor *faf*- R-cells. Therefore, the extra R-cells are failing to receive a signal from the neighboring *faf*- cells. Faf's critical function is in the R-cells 2/3/4/5 because expression of *faf* cDNAs with a promoter called *rough* rescues completely *faf* phenotypes. These data support a model whereby Faf regulates a cell-cell signaling pathway that prevents extra R-cells from prematurely joining the facet as neurons (Fischer-Vize et al. 1992; Huang and Fischer Vize 1996; Overstreet et al. 2004).

Faf is a deubiquitinating enzyme (DUB). DUBs cleave peptide or isopeptide bonds between ubiquitin residues or between ubiquitin and other proteins. These enzymes have numerous roles within the cell. Most DUBs have housekeeping roles whereby they function to generate Ub monomers by recycling of Ub chains or processing of polymeric Ub precursors. Other DUBs regulate the process of substrate ubiquitination. They recognize specific substrate proteins and antagonize their ubiquitination and therefore their proteolysis. There are five subfamilies of DUBs, two I'll mention here: the ubiquitin-specific processing proteases (UBPs) and the ubiquitin carboxy terminal hydrolases (UCHs). UBPs are identifiable by the conserved structure of their catalytic domains and they also have conserved Cys and His residues in catalytic domains that are responsible for hydrolyzing ubiquitin. The UBP subfamily contains the largest number of DUBs. The UCH subfamily of proteins generally consists of smaller proteins (Amerik et al. 2004).

Faf is most similar in sequence to the UBP family of DUBs. Genetic experiments indicated that Faf might be the type of UBP that recognizes polyubiquitin chains of substrate proteins and cleaves these chains to save the substrate from recognition by the proteasome (Huang et al. 1995). The catalytic domain of Faf can cleave a Ub-protein fusion in *E. coli* and mutation of the Cys residue abolishes this activity (Huang et al. 1995). Second, the function of Faf antagonizes the proteolysis pathway because mutations in genes that facilitate proteolysis suppress *faf* mutants. Mutations in *UbcD1*, which encodes an

ubiquitin conjugating enzyme, and *Pros26*, which encodes a subunit of the proteasome, suppress *faf*. This indicates that Faf function antagonizes both ubiquitination and proteolysis (Huang et al. 1995; Wu et al. 1999).

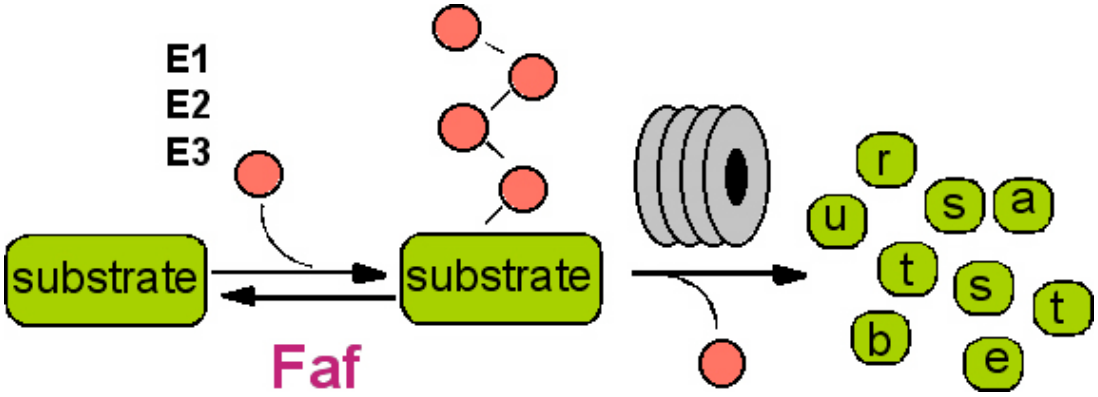

Fig. 16. Model of faf function in the eye. Faf saves its substrate from degradation by the proteasome via deubiquitination of poly-ubiquitin chains from the substrate.

Lqf is the substrate of Faf in the eye

This genetic evidence led to a model proposing that Faf deubiquitinates a specific substrate protein thus saving it from proteolysis (Fig. 16). To test this hypothesis a genetic screen was performed for modifiers of the mutant eye phenotype of *faf* hypomorphs. In *faf* hypomorphs, the level of the substrate is lower than normal (but not as low as in *faf* nulls). Hence, a mutation in one copy of the substrate gene should make the hypomorphic *faf* phenotype worse (similar to *faf* null phenotype), or should dominantly enhance the *faf* mutant eye. In this

screen, *lqf* was identified as a very strong enhancer of *faf* mutants (Fischer et al. 1997; Cadavid et al. 2000).

Before Lqf could be considered a candidate substrate of Faf in the eye it must meet a few criteria. First, *lqf* mutant phenotype should be similar to *faf* because both will have lower levels of Lqf protein. If Faf normally functions to protect Lqf from being degraded, then reduction in Lqf should phenocopy *faf* null phenotype. This is indeed the case in the eye as *lqf* weak loss-of-function mutants have eyes with extra outer photoreceptors (Cadavid et al. 2000).

Second, Lqf and Faf should function in the same set of cells. This is also true because expression of *lqf* cDNAs with *rough* rescues *lqf* phenotypes. Therefore, both Faf and Lqf function in R-cells 2/3/4/5. Finally, if Faf is needed only to increase the level of its substrate then expression of lqf^{+} should overcome the need for faf^{+}. Slight overexpression of lqf^{+} with either of two transgenes obviates the need for Faf's deubiquitinating activity (Cadavid et al. 2000).

This genetic evidence strongly indicates that Lqf might be the substrate of Faf, however, biochemical experiments offer a more direct way to test the hypothesis. If this hypothesis is true, then Lqf and Faf might be associated *in vivo*. These two proteins do associate *in vivo* because they can be co-immunoprecipitated together from tissue extracts. If Faf saves Lqf from degradation, then Lqf should be ubiquitinated in the absence of Faf and the levels of Lqf should be lower than normal. Western blots of eye disc extracts from *faf* mutants indicate that the level of Lqf is more than two times lower than wild-type.

Furthermore, immunostaining with Lqf antibody of eye discs with clones of *faf* mutant cells show that cells within the *faf-* clone have lower levels of Lqf protein compared to neighboring wild-type cells. Finally, ubiquitinated forms of Lqf can be detected on Western blots of tissue from *faf* mutants, but not in wild-type discs. This effect depends on the critical cysteine residue in Faf's catalytic domain that mediates deubiquitination. This indicates two things: Lqf can be ubiquitinated and, in the absence of Faf, fails to be deubiquitinated and is degraded (Chen et al. 2002). Based on these genetic and biochemical data, it was concluded that Lqf is the substrate of Faf in the eye (Fig. 17). Recently, the mouse homolog of Lqf, epsin1, was found to be the substrate of Fam, the mouse homolog of Faf (Chen et al. 2003).

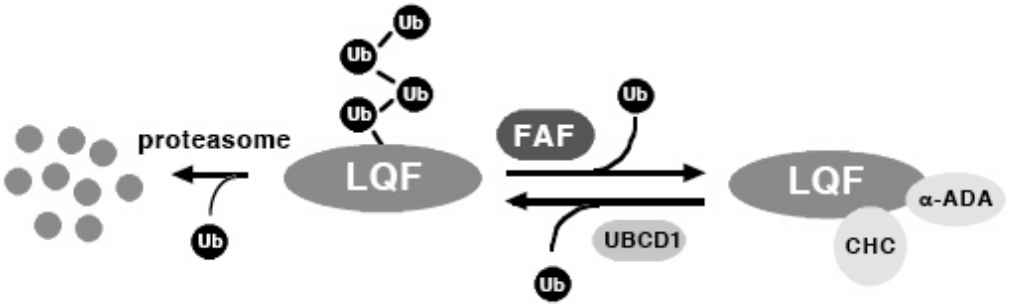

Fig. 17. Model for Faf and Lqf relationship in the eye. Faf recognizes poly-ubiquitinated forms of Lqf. Faf deubiquitinates Lqf saving it from recognition and proteolysis by the proteasome.

The homologs of Lqf are endocytosis proteins and it is likely that *Drosophila* epsin functions similarly. A mutant in the endocytosis pathway

encoding the *clathrin heavy chain* gene genetically interacts strongly with *lqf* mutants. Also, Lqf protein localizes subcellularly to the plasma membrane in developing eye discs where endocytosis occurs. Therefore, Lqf and Faf probably regulate endocytosis during eye development. Since both regulate a cell signaling pathway, this raises the exciting possibility that Faf and Lqf regulate trafficking of a certain signaling molecule(s) to ensure that photoreceptors are properly determined. The signaling molecules affected by Faf and Lqf remain to be identified (Cadavid et al. 2000; Chen et al. 2002).

Other Deubiquitinating enzymes regulate vesicle trafficking

Only a few other deubiquitinating enzymes have been linked functionally to vesicle sorting machinery. As mentioned above, beta-arrestin-dependent vesicle trafficking activity is regulated by deubiquitination via an unknown DUB (Shenoy et al. 2003). Yeast Ubp1 is speculated to control the steady state levels of the ATP-binding cassette-transporter Ste6p by stabilizing it at the plasma membrane. Overexpression of Ubp1 results in stabilization of Ste6p at the membrane, but does not change the ubiquitination of state of Ste6p. This implicates Ubp1 either in mediation of internalization and/or recycling of Ste6p (Schmitz et al. 2005).

Yeast Doa4 is another DUB implicated in recycling of ubiquitin monomers from proteins recognized by the proteasome. Its activity is theorized to facilitate proteolysis. Interestingly, Doa4 was recently found to interact

genetically with several vacuolar sorting proteins, which direct endosomal maturation and fusion with the lysosome. The details of the physical interactions between Doa4 and Vps proteins are unclear. One hypothesis is that Doa4 recycles ubiquitin by removing Ub from proteins that will be degraded in the vacuole (Amerik 2000).

Finally, a mouse DUB called UBPY associates physically with the SH3 domain of Hrs binding protein (Hbp). Hbp is required in concert with Hrs for its role in late endosomal fusion. The functional significance of the interaction between UBPY and Hbp is unknown (Kato 2000).

Because the relationship between deubiquitination and vesicle trafficking is only now being discovered, a detailed study of the Faf and Lqf pathway may facilitate our understanding of the roles of deubiquitination in vesicle transport. In addition, understanding the developmental roles of Lqf will increase our knowledge of how epsins regulate endocytosis of certain membrane molecules.

GOALS OF MY DOCTORAL WORK

The main goal of my doctoral work is to understand how proteins involved in vesicle trafficking contribute to proper animal development. To understand aspects of this process, I studied two types of epsin proteins and their roles in *Drosophila* eye development. The first part of my thesis focuses on how *Drosophila* Liquid facets/epsin1 regulates cell fate determination via the Notch and Delta signaling pathway. The second part of my thesis is concerned with the

role of *Drosophila* Epsin-Related protein and its potential involvement with signaling pathways that regulate cell growth.

Analyze the cellular roles of Faf and Lqf in eye patterning

In the second chapter of my thesis I describe how I determined that Faf and Lqf regulate the Notch and Delta signaling in the developing *Drosophila* eye. Specifically, Faf and Lqf work in signaling cells in the eye to endocytose Delta, thereby facilitating Notch activation in neighboring cells. Also, Lqf probably works in concert with the E3 ubiquitin ligase Neuralized (Neur), which ubiquitinates Delta thus modulating the endocytosis and signaling of Delta. Perhaps Lqf recognizes ubiquitinated Dl via its UIMs. These conclusions are consistent with a relatively new model describing an obligate role for endocytosis in the signaling cells to effect activation in neighboring cells. This work also sets the stage for future experiments that may elucidate the molecular reasoning behind why endocytosis is required for Delta signaling.

Structural and functional analysis of Lqf

To understand how Lqf functions mechanistically in this process, I performed a detailed structure/function analysis of the Lqf protein, described in chapter three. Lqf proteins with strategic deletions of certain functional domains were tested for their ability to function *in vivo*. The assay I used was a complementation test for rescue the *lqf* eye phenotypes: ectopic neuronal

differentiation and failure to internalize the protein Delta. The major result of these experiments is that the ENTH domain of Lqf and a Lqf protein without the ENTH domain each retain significant Lqf activity. These data suggest that Lqf protein has two functions: the ENTH domain function and the ENTH-less function. As they do not interact with the same endocytosis components, these two fragments must be performing independent functions. These results suggest that either function is required and, when one is absent, other proteins in the endocytosis complex may supply it redundantly. These results also challenge the current model for epsin function that poses that the ENTH domain is critical for epsin function and epsin localization at the plasma membrane. The ENTH-less protein still retains function thus, this protein might localize to the endocytosis complex via protein-protein interactions**.** Therefore, epsins may be recruited to sites of endocytosis through multiple independent interactions i.e. lipid binding and binding to endocytosis complex proteins. We propose this may be a general strategy of recruitment for many other vesicle forming proteins. This strategy may help to ensure vesicle complexes are formed even if challenged with multiple mutations in the system. This work contributed to understanding how epsin proteins, and possibly other proteins, are recruited onto the coat complex.

Analyze the role of D-Epsin-R in eye development

The final part of my thesis focuses on D-Epsin-Related protein, a previously unstudied locus in *Drosophila*. I showed that D-Epsin-R, like its mammalian

homolog, is a Golgi protein. Like its cousin, Lqf, D-Epsin-R has essential and maybe even specific developmental roles, not only in the eye, but also in other tissues. Also, in a similar structure function analysis, I found that the D-Epsin-R ENTH domain is also not required for function. Taken in total, my thesis work demonstrates the importance of vesicle trafficking by ENTH domain proteins during development.

Chapter 2. Fat facets and Liquid facets Promote Delta Endocytosis and Delta Signaling in the Signaling Cells

The data described in this chapter has been published in *Development* (see Overstreet et al. 2004).

INTRODUCTION

Endocytosis controls cell signaling through a variety of different mechanisms (Seto et al., 2002; Gonzalez-Gaitan and Stenmark, 2003). For example, signaling by the epidermal growth factor receptor following ligand binding is attenuated by receptor endocytosis and lysosomal degradation. Endocytosis of epidermal growth factor receptor also enhances signaling by transporting activated receptor to its targets. In addition, endocytosis plays a variety of roles in establishing gradients of morphogens like Hedgehog, Decapentaplegic and Wingless. Moreover, several different aspects of Notch pathway function rely on endocytosis.

Two proteins required for pattern formation in the *Drosophila* eye, the deubiquitinating enzyme Fat facets (Faf) and its substrate Liquid facets (Lqf), are linked to both cell signaling and clathrin-mediated endocytosis (Fischer-Vize et al., 1992; Huang et al., 1995; Cadavid et al., 2000; Chen et al., 2002; Overstreet et

al., 2003). Lqf protein levels in the *Drosophila* eye are controlled by the balance between ubiquitination, which targets the protein for proteasomal degradation, and deubiquitination by Faf, which prevents Lqf degradation (Huang et al., 1995; Wu et al., 1999; Chen et al., 2002). Faf and Lqf mediate a cell communication event that prevents overneuralization of the compound eye. Accordingly, *faf* or *lqf* mutant eyes contain more than the normal complement of eight photoreceptors in each facet (or ommatidium) of the eye. As mosaic experiments demonstrate that faf^{+} and lqf^{+} function outside of the ectopic photoreceptors, the extra photoreceptors must result from a failure of cell signaling (Fischer-Vize et al., 1992; Cadavid et al., 2000). Several observations suggest that Faf and Lqf facilitate endocytosis. First, Lqf is the *Drosophila* homolog of epsin, a multi-modular protein that binds phosphoinisitol lipids at the cell membrane, the adapter complex AP-2, clathrin, ubiquitin, and other endocytic accessory factors (Kay et al., 1998; De Camilli et al., 2001; Wendland 2002). Epsin is required for endocytosis in yeast and in mammalian cells (Wendland et al., 1999; Itoh et al., 2001; Shih et al., 2002). In addition, *faf* and *lqf* mutations show dramatic genetic interactions with mutations in the *clathrin heavy chain* gene which indicate that all three genes function in the same direction in a pathway (Cadavid et al., 2000). Finally, the Notch ligand Delta fails to be internalized normally in *lqf* mutant eye discs (Overstreet et al., 2003).

The overneuralization phenotype in *faf* and *lqf* mutants and the altered Delta localization in *lqf* mutants suggest a role for Faf and Lqf in Notch/Delta

signaling. The Notch pathway is highly conserved in metazoans and participates in a wide range of cell communication events that determine cell fate. Mutants in the Notch receptor and in other genes in the signaling pathway ("neurogenic" genes) were first isolated on the basis of their role in inhibiting neural cell fate determination in *Drosophila* embryos (Lehmann et al., 1981). It is now apparent that Notch receptor activation, in different cellular contexts, can result in either inhibition or promotion of a variety of cell fates (Artavanis-Tsakonas et al., 1999). The mechanism of Notch signaling is unusual in that upon ligand binding, a fragment of the Notch intracellular domain is cleaved, travels into the nucleus, and acts a transcriptional regulator (Artavanis-Tsakonas et al., 1999). Although details of the events that lead to nuclear translocation of the Notch intracellular domain are contentious, there is a consensus model where binding of ligand to the Notch extracellular domain induces two cleavages of Notch. The first cleavage (called S2) detaches the extracellular domain from the remainder of the Notch protein, and is prerequisite for the second cleavage (S3) that releases the transcription factor domain (Baron, 2003).

Endocytosis controls Notch signaling in both the signaling and receiving cells. The first evidence for this idea came from analysis of *Drosophila shibire* mutants. *shibire* encodes the *Drosophila* homolog of dynamin, a GTPase required for scission of endocytic vesicles (Chen et al., 1991). *shibire* mutant phenotypes resemble *Notch* loss-of-function phenotypes, and the results of mosaic experiments suggest that *shibire* is required in both the signaling and receiving

cells (Poodry, 1990; Seugnet et al., 1997). A model for the dual function of *shibire* was formulated for Notch signaling during lateral inhibition, where both the signalers and receivers express both Notch and Delta. In this case, selective internalization of either Notch or Delta could bias cells to become either the signaler or the receiver. Recent experiments with *Drosophila* sensory organ precursors support the idea that Notch internalization may bias a cell to become the signaler. The Numb protein, which binds Notch and the endocytic protein a-adaptin, is asymmetrically distributed between two daughter cells and the Numb-containing cell becomes the signaler (Rhyu et al., 1994; Lu et al., 1998; Santolini et al., 2000; Berdnik et al., 2002; Le Borgne and Schweisguth, 2003). Thus by stimulating Notch internalization, Numb may bias one sensory organ precursor cells to become the signaler.

In addition to preventing a cell from displaying either Notch or Delta at the cell membrane, endocytosis has also been proposed to play a positive role in Notch receptor activation (Parks et al., 2000). The idea is that the Notch extracellular domain, bound to Delta, is *trans*-endocytosed into the Delta-expressing (signaling) cell. This *trans*-endocytosis event is prerequisite for S2 cleavage, and therefore for S3 cleavage and activation of Notch in the receiving cell. Evidence for this model comes from experiments in the developing *Drosophila* eye using two non-neural cell types: cone cells and pigment cells (Parks et al., 1995; Parks et al., 2000). *Delta* is transcribed in cone cells, and *Notch* is transcribed in pigment cells. Yet, the extracellular domain of Notch

(N^{ECD}) is detected with Delta in endosomes inside the cone cells. Moreover, in *shibire* mutants, Notch and Delta both accumulate at cone cell plasma membranes. In addition, in *Delta* mutants, there are significantly fewer N^{ECD}-containing vesicles in cone cells. Also, in temperature-sensitive *Delta* loss-of-function mutants, Delta accumulates on cone cell membranes. Finally, in cell culture, cells expressing *Delta* alleles that encode endocytosis-defective ligands do not *trans*-endocytose N^{ECD}.

Consistent with the trans-endocytosis model, the ubiquitin-ligases Neuralized (in *Drosophila* and *Xenopus*) and Mindbomb (in zebrafish) modulate Delta endocytosis and Delta signaling. Neuralized (Neur) and Mindbomb ubiquitinate Delta thereby stimulating Delta internalization (Itoh et al., 2003; Yeh et al., 2001; Deblandre et al., 2001; Lai et al., 2001; Pavlopoulos et al., 2001). The results of several studies suggest that Neur and Mindbomb are required in the Delta signaling cells to promote Notch activation in the receiving cells (Pavlopoulos et al., 2001; Itoh et al., 2003; Le Borgne and Schweisguth, 2003; Li and Baker, 2004). However, the role of Neur is unclear, as two reports suggest that Neur is required for Delta internalization in the receiving cells, perhaps to bias those cells to become the receivers (Yeh et al., 2000; Lai et al, 2001).

Here, we report a unique mechanism for regulating Notch/Delta signaling. We show that the deubiquitinating enzyme Faf, through its substrate Lqf, promotes Delta internalization and Delta signaling by the signaling cells. The signaling cells, photoreceptor precursors R2/3/4/5, thus activate Notch in

surrounding undifferentiated cells, preventing recruitment of ectopic photoreceptors (R-cells). We call this event R-cell restriction. In addition, we show that while Faf is required only for R-cell restriction, Lqf is needed also for two earlier events in the eye that require Notch/Delta signaling: proneural enhancement and lateral inhibition. We also provide evidence that Neur functions with Faf and Lqf in R-cell restriction. There are three main conclusions of this work. First, the results provide strong support for the model where Delta internalization by the signaling cell is required for Notch activation in the receiving cell. Second, the results support a model where Neur stimulates Delta internalization in the signaling cells rather than in the receiving cells. Finally, we demonstrate that deubiquitination by Faf of the endocytic factor Lqf is a novel mechanism for regulating Delta signaling. We propose that by elevating Lqf activity, Faf enhances the efficiency of Delta endocytosis and promotes Delta signaling.

RESULTS

faf^{+} and *lqf*$^{+}$ are required for Delta endocytosis in R-cell preclusters

Drosophila eye development is controlled by a complex network of cell signaling pathways which includes many roles for Notch/Delta signaling. The *Drosophila* compound eye is composed of hundreds of identical ommatidia. The eye develops in larval and pupal stages from a cellular monolayer called the eye disc (Wolff and Ready, 1993). In third instar larvae, a wave of morphogenesis,

initiated at the posterior of the disc by the morphogenetic furrow, moves anteriorly through the monolayer of undifferentiated cells. A column of organized preclusters emerges from the furrow (column 0) (Fig. 1G). A few cells are excluded from the initial preclusters and the remainder differentiate into five of the eight photoreceptors (R-cells; R8/2/3/4/5). These clusters then recruit R167, then four cone cells, and finally the pigment and bristle cells. As the furrow moves forward by one column approximately every 2 hours, each more posterior column is one step more mature and the sequence of ommatidial assembly can be observed in a single disc.

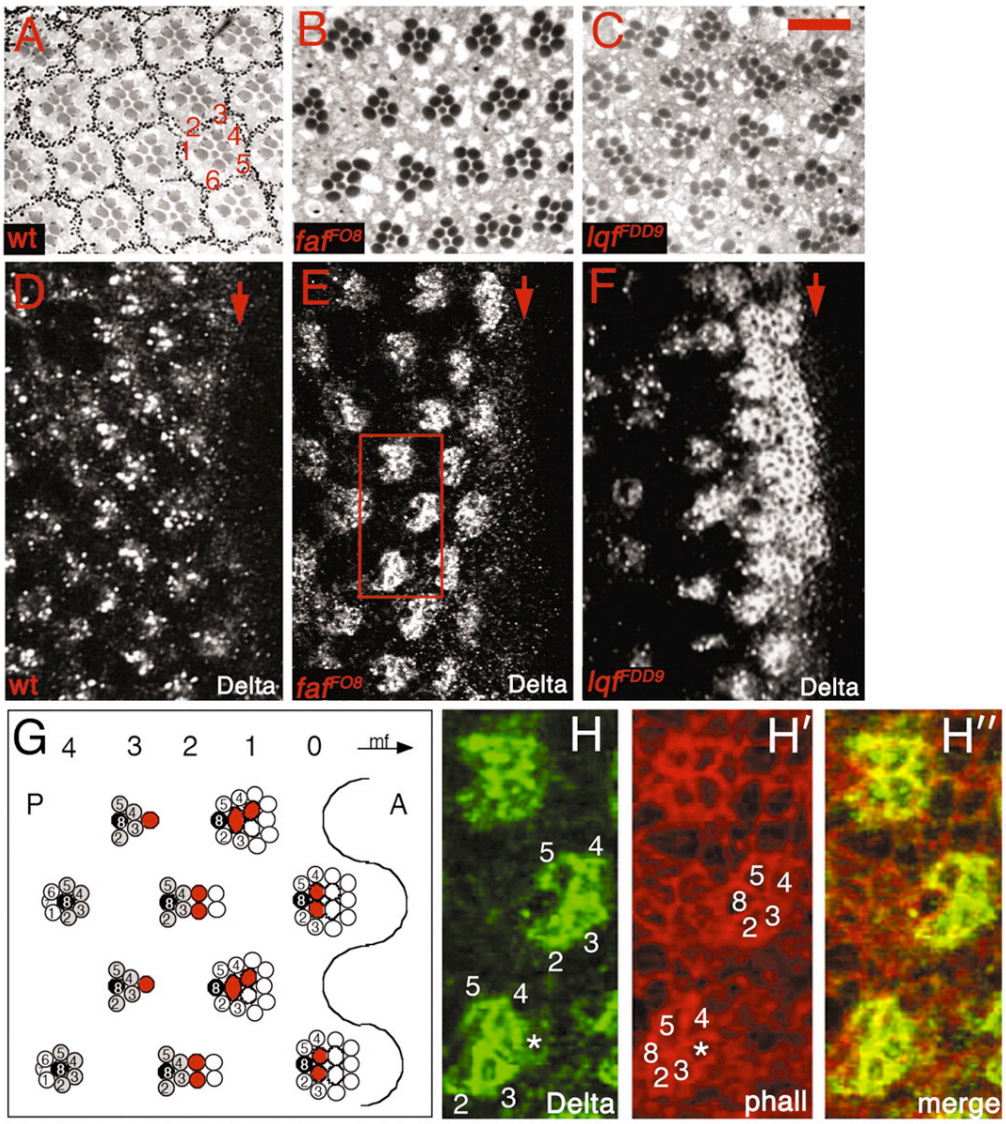

Fig. 1. Delta localization in eye discs. (A-C) Tangential sections through adult eyes are shown. The numbers in A refer to the outer R-cells, R1-R6. (D-F) Confocal images of eye discs labeled with anti-Delta are shown. Anterior is towards the right and the arrows indicate the position of the furrow. (G) A diagram of the early stages of ommatidial assembly. A is anterior, P is posterior; 0-4 at the top indicate columns emerging from the furrow (mf). R-cell identities are indicated by the numbers inside the circles. The red cells may be those that become ectopic R-cells in *faf* mutants. (H-H') Enlargement of the boxed region in E. Numbers indicate R-cells and asterisks indicate an ectopic R-cell. In H", both membrane-bound Delta (yellow) and vesicular Delta (green) are present. Scale bar: 20 μm in A-C; 10 μm in D-F; 5 μm in H-H".

The pattern of *Delta* expression in wild-type eye discs has been well-characterized. *Delta* transcription is ubiquitous in the morphogenetic furrow, and then resolves to the R-cell preclusters as they emerge from the furrow (Parks et al., 1995). Delta protein is detected in a similar pattern of cells and its subcellular localization is intriguing. Although Delta is expected to function at the membrane, an antibody to the Delta extracellular domain detects most of the protein in endosomal vesicles posterior to the furrow (Fig. 1D) (Parks et al., 1995). Delta-containing vesicles first accumulate in preclusters emerging from the furrow, then in R-cells as they differentiate, and remain detectable in some R-cells until at least column 14 (Parks et al., 1995). Using unusual tissue preparation conditions (no detergent), low levels of membrane-bound Delta are observed in the same pattern as Dl transcripts (Baker and Yu, 1998). These observations suggest that in some cells, most of the Delta at the cell surface is internalized and that endosomal Delta is not degraded rapidly.

In lqf^{FDD9} eye discs, which produce low levels of wild-type Lqf protein, Delta accumulates on cell membranes in columns 0-3 posterior to the furrow (Fig. 1F) (Overstreet et al., 2003). Like lqf^{FDD9}, *faf* mutant discs have decreased levels of Lqf protein (Chen et al., 2002). In order to determine if Delta internalization is defective in *faf* mutant discs and in which cells, we double-labeled faf^{FO8} third instar larval eye discs (faf^{FO8} is a strong mutant allele (Fischer-Vize et al., 1992; Chen and Fischer, 2000)) with antibodies to the Delta extracellular domain and with phalloidin to outline the apical membranes of the ommatidial cluster cells.

We find that Delta is present on the membranes of R2/3/4/5 and the ectopic R-cells in columns 0-3 of *faf*^{FO8} discs (Fig. 1E,H-H"). Some vesicular Delta is also observed (Fig. 1H"). We conclude that both *faf*$^{+}$ and *lqf*$^{+}$ are required for Delta endocytosis in R-cell clusters in columns 0-3.

The observation that similar Delta internalization defects occur in *faf* and *lqf* mutant discs supports the idea that the *faf* mutant phenotype results from a decrease in the level of Lqf protein. However, more Delta-expressing cells emerge posterior to the furrow in *lqf*^{FDD9} discs than in wild-type or *faf* discs. The difference in *Delta* expression between *faf* and *lqf*^{FDD9} discs reflects a broader requirement for *lqf*$^{+}$ in early developmental decisions (see below).

faf^{+} and *lqf*$^{+}$ function in R2/3/4/5 precursors

In *faf* mutants, the R2/3/4/5 precursors display Delta endocytosis defects. In order to determine if *faf*$^{+}$ and *lqf*$^{+}$ function in these cells, we investigated the expression pattern of the vector pRO (Huang and Fischer-Vize, 1996). pRO transgenes that drive expression of a *faf* cDNA (*RO-faf*) can substitute for the endogenous *faf* gene (Huang and Fischer-Vize, 1996). Likewise, a *RO-lqf* transgene rescues to wild-type the mutant eye phenotype of *lqf*^{FDD9} or *faf* (Cadavid et al., 2000). We generated a *RO-GFP* transgene and observed the pattern of GFP expression in eye discs from 3 independent transformant lines. We find that GFP is expressed in R2/3/4/5 beginning in column1 (Fig. 2A,B). The same results were obtained with a *RO-GFP-lqf* transgene which also complements the *faf* and

lqf^{FDD9} mutant phenotypes (data not shown). We conclude that expression of *faf*$^{+}$ or *lqf*$^{+}$ in R2/3/4/5 is sufficient to substitute for the endogenous *faf* gene or to compensate for the lower levels of Lqf protein in *lqf*^{FDD9}.

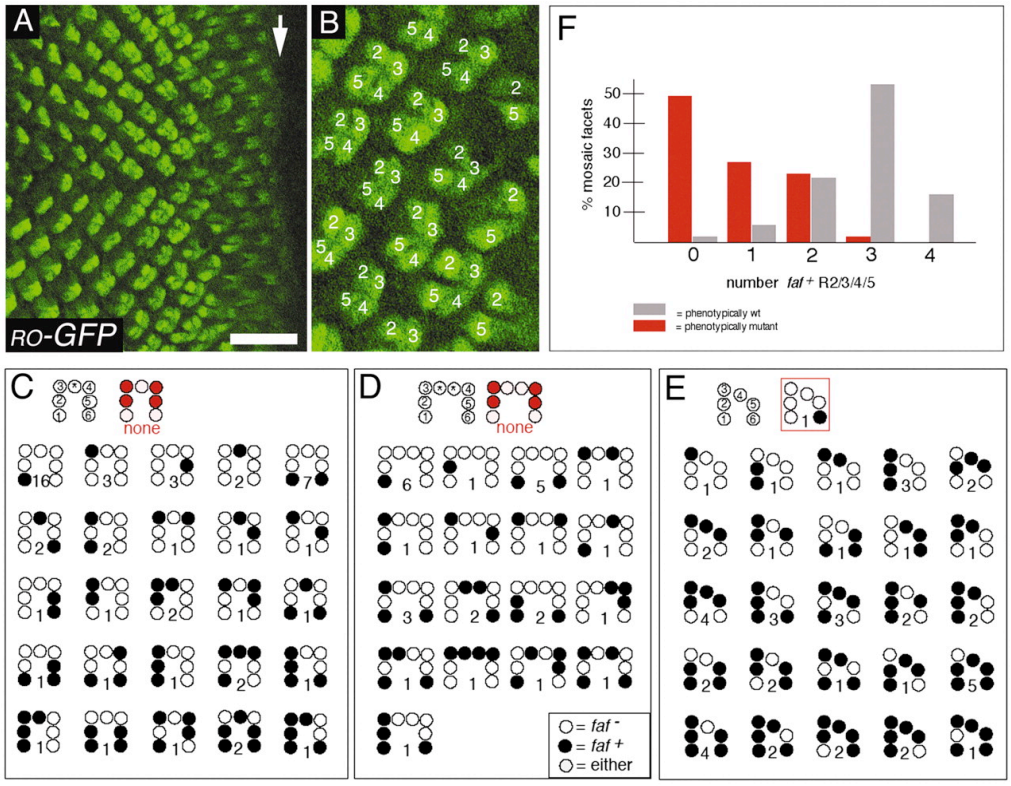

Fig. 2. *faf* +functions in R2/3/4/5. (A,B) Confocal images of GFP expression from a *RO-GFP* transgene in an eye disc. In A, anterior is towards the right and the arrow indicates the position of the furrow. (B) An enlargement of part of A is shown, the numbers indicating R-cells R2/3/4/5. (C,D) Tabulation of the different phenotypically mutant *faf* +/*faf FO8* mosaic facets with one (C) or two (D) ectopic R-cells are shown. (E) Tabulation of the different phenotypically wild-type *faf* +/*faf BX4* mosaic ommatidia are shown. Numbers beneath each diagram refer to the number of facets with that particular mosaic pattern observed. The *faf* +R-cells are *white* +(have pigment granules) and the *faf* -R-cells are *white* -(do not have pigment granules). (F) Aspects of the data in C-E are displayed graphically. Scale bar: 20 μm in A; 10 μm in B. Experiments presented in panels C-F were performed by Janice Fischer.

To investigate further the requirement for *faf*$^{+}$ in R2/3/4/5, we analyzed adult ommatidia mosaic for marked *faf*$^{+}$ and *faf* $^{-}$ cells generated by mitotic recombination. Two types of genetically mosaic facets were observed and analyzed: phenotypically mutant ommatidia with more than 6 outer (R1-6) R-cells, and phenotypically wild-type ommatidia. The genotype of each outer R-cell (including ectopic cells) was scored in both types of mosaic facets (Fig.2C-E). In assigning R-cell identities, we assumed that the ectopic R-cells arise between R3 and R4. If *faf*$^{+}$ is required in all or a subset of R2/3/4/5, then we would expect to find no phenotypically mutant facets where R2/3/4/5 are all *faf*$^{+}$. As expected, in not one of 86 mosaic facets at the borders of 30 different *faf*^{FO8} clones were R2/3/4/5 all *faf*$^{+}$(Fig. 2C,D). Moreover, in nearly half of the mutant mosaic ommatidia (42/86), none of the R2/3/4/5 group are *faf*$^{+}$ and in only 2/88 mutant mosaics are 3 of the R2/3/4/5 group *faf*$^{+}$ (Fig. 2C,D,F). Conversely, we expected that R2/3/4/5 would not all be *faf* $^{-}$ in phenotypically wild-type facets. For this analysis, we used *faf*^{BX4} which is a null allele (Fischer-Vize et al., 1992). In only 1/51 phenotypically wild-type mosaic facets in 13 different clones were R2/3/4/5 all *faf* $^{-}$ (Fig. 2E). Moreover, while no particular R-cells in the R2/3/4/5 cell group were always *faf*$^{+}$, at least three of them were *faf*$^{+}$ in 36/51 mosaic facets, and at least two of them were *faf*$^{+}$ in 47/51 of the mosaic facets (Fig. 2E,F). The wild-type mosaic ommatidia where not one R-cell (1/51) or only one R-cell (3/51) of the R2/3/4/5 group is *faf*$^{+}$ can be explained by the observation that in *faf*^{BX4} homozygtoes, ~10% of the facets are phenotypically wild-type. These results

show that as more of the R-cells in the R2/3/4/5 group are *faf*$^{+}$, there is an increasing tendency for the ectopic R-cells to be excluded.

Endocytosis is required in R2/3/4/5 precursors to prevent ectopic R-cell recruitment

faf^{+} and *lqf*$^{+}$ activities are linked to endocytosis and Delta endocytosis fails in precluster cells with decreased *lqf*$^{+}$ activity (*faf*^{FO8} or *lqf*^{FDD9}). Is a failure of endocytosis the cause of the *faf* and *lqf*^{FDD9} mutant eye phenotypes? If so, then disrupting endocytosis in R2/3/4/5 through a mechanism other than blocking *faf*$^{+}$ or *lqf*$^{+}$ gene activity should result in an eye phenotype similar to that of *faf* or *lqf*^{FDD9}. We interfered with endocytosis in R2/3/4/5 by expressing a dominant negative form of Shibire (Moline et al., 1999) using the pRO vector (*RO-shi*^{DN}). We find that otherwise wild-type flies expressing *RO-shi*^{DN} display adult retinal defects similar to those in *faf* or *lqf*^{FDD9} mutants (Fig. 3A, Fig. 1A-C). The ectopic R-cells in *RO-shi*^{DN} join the clusters in columns 0-3 as in *faf* or *lqf*^{FDD9} discs (Fig. 3B-D). Moreover, Delta internalization defects similar to those in *faf* or *lqf*^{FDD9} are observed in *RO-shi*^{DN} eye discs (Fig. 3B–D, Fig. 1E,F). We conclude that R2/3/4/5 precursors require endocytosis to prevent inappropriate recruitment of neighboring precluster cells as R-cells.

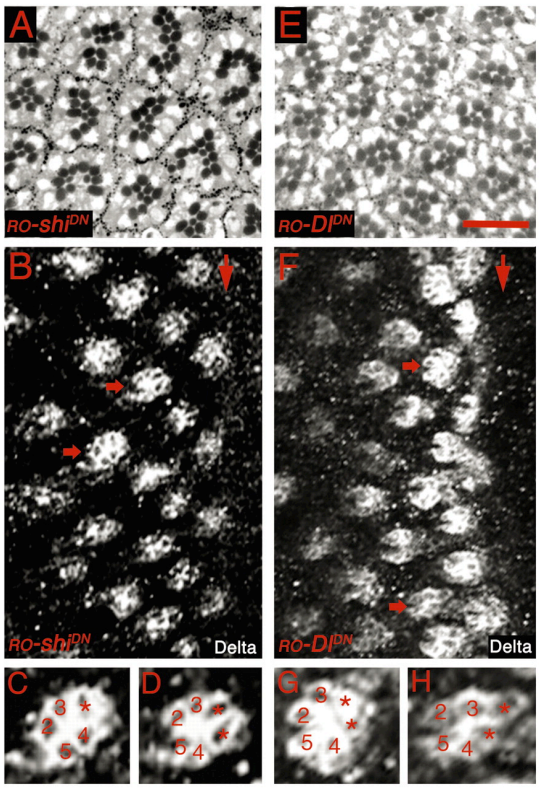

Fig. 3. *RO-shi DN* (A-D) or *RO-Dl DN* (E-H) phenocopy *faf* mutant eyes. (A,E) Shown are tangential sections through adult eyes of flies expressing the indicated transgenes. (B,F) Confocal images of eye discs labeled with anti-Delta are shown. Anterior is towards the right and large arrows indicate the position of the furrow. (C,D) Enlargements of clusters in B indicated by small arrows. (G,H) Enlargements of clusters in F indicated by small arrows. In C,D,G,H, numbers refer to R-cells and asterisks are ectopic R-cells. Scale bar: 20 μm in A,B,E,F; 10 μm in C,D,G,H.

Delta signaling and endocytosis in R2/3/4/5 precursors is required to prevent ectopic R-cell recruitment

Does the failure of Delta signaling in R2/3/4/5 cause the *faf* and lqf^{FDD9} mutant phenotypes? If so, then specifically interfering with Delta endocytosis and signaling in R2/3/4/5 should phenocopy *faf* and lqf^{FDD9} mutants. To test this we used the pRO vector to express in R2/3/4/5 a dominant negative form of Delta

(Dl^{DN}) (Sun and Artavanis-Tsakonas, 1996). In *RO-Dl^{DN}* transformant eye discs, ectopic R-cells join the clusters in columns 0-3 (Fig. 3F-H) and are present in adult eyes (Fig. 3E). In addition, Delta protein accumulates on R-cell membranes near the furrow (Fig. 3F). The Dl^{DN} protein has a truncated intracellular domain and if Delta endocytosis is required for Delta signaling, the dominant negative activity of Dl^{DN} is likely due to its failure to be internalized. Thus, the membrane-associated Delta protein observed in *RO-Dl^{DN}* discs may be a mixture of Dl^{DN} protein and wild-type Delta that is prevented by Dl^{DN} from interacting with Notch. We conclude that specific disruption of Delta signaling and endocytosis in R2/3/4/5 results in the same developmental consequences as interfering with *faf* or *lqf* function.

lqf$^+$ is required in the signaling cells for two _faf_$^+$-independent Delta signaling events at the morphogenetic furrow

We have shown that in order to prevent recruitment of ectopic R-cells into the ommatidia, *faf*$^+$ and *lqf*$^+$ are required for Delta signaling by R-cell precursors just posterior to the furrow. *faf*$^+$ appears to be essential only for this one Delta signaling event: in *faf^{FO8}* (strong) mutants, Delta is on the membrane in R-cell preclusters, ectopic R-cells are recruited just posterior to the furrow and the adult eye phenotype (ectopic R-cells) reflects these events. By contrast, *lqf*$^+$ appears necessary also for earlier patterning processes. In *lqf* mutant eye discs (*lqf^{FDD9}* or discs with small *lqf^{ARI}* (null) clones), all cells emerging from the furrow express

Delta (Fig. 1F) (Overstreet et al., 2003; also see below) whereas in wild-type discs Delta is expressed in distinct clusters (Fig. 1D) (Parks et al., 1995). Also, in the adult eye, the phenotype of *lqf*^{ARI} clones is much more severe than that of *faf* mutants (Fischer et al., 1997).

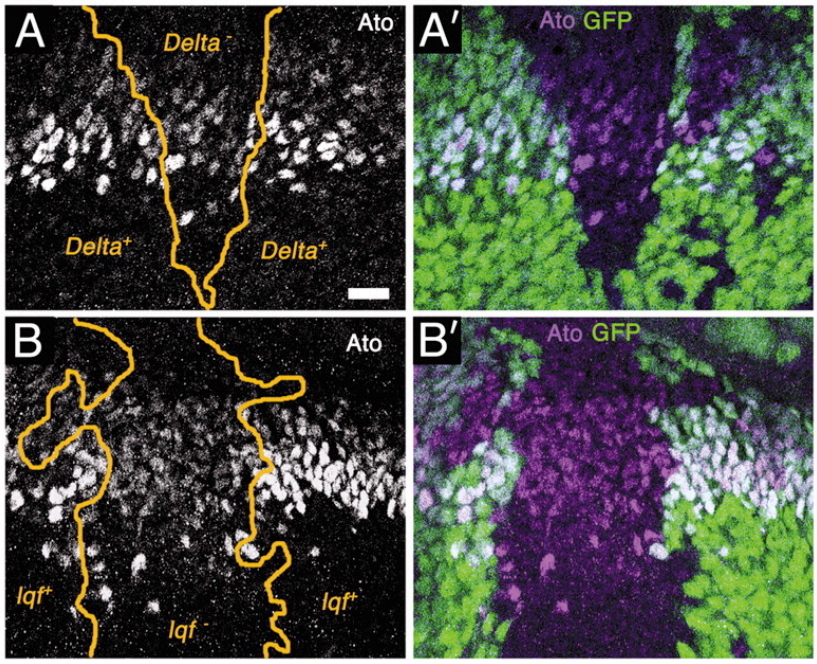

Fig. 4. Atonal expression in *Delta* and *lqf* -null eye disc clones. Eye discs labeled with anti-Atonal are shown. Anterior is upwards. (A,A) A clone of *Delta rev10* cells marked by the absence of GFP. (B,B) A clone *lqf ARI* cells marked by the absence of GFP. Clone borders are outlined in A and B. Scale bar: 10 μm.

Prior to the *faf*$^{+}$-dependent signaling event, two discrete Notch/Delta signaling processes are required for the evolution of expression of the proneural protein Atonal (Baker and Yu, 1996; Baker, 2002). First, Notch activation in groups of cells anterior to the furrow up-regulates Atonal expression; this event is referred to as proneural enhancement. Elevated Atonal levels are necessary for neural determination of these cells. Second, Notch/Delta signaling is essential for

lateral inhibitory interactions that resolve Atonal expression to one cell by column 0. The one Atonal-expressing cell becomes R8, the founder R-cell of each ommatidium (Baker and Yu, 1998).

In order to determine whether *lqf*$^{+}$ is required for Delta-signaling during proneural enhancement and/or lateral inhibition, we analyzed the phenotypes of large *lqf*^{ARI} (null) clones using a number of different antibodies and compared them to the phenotypes of large *Dl*^{rev10} (null) clones. We find that the *lqf*^{ARI} clone phenotypes closely resemble those of *Dl*^{rev10} clones originally described by Baker and Yu, 1996. Up-regulation of *atonal* (proneural enhancement) does not occur in the *Dl*^{rev10} or *lqf*^{ARI} clone centers (Fig. 4); although the cells in the middle of the clone are *Notch*$^{+}$, there are no *Delta*$^{+}$ cells adjacent to them to activate Notch. As would be expected, *Dl*^{rev10} or *lqf*^{ARI} mutant cells at the clone borders adjacent to *Delta*$^{+}$ cells do up-regulate *atonal* (Fig. 4). In the absence of proneural enhancement, no R-cells are expected to be determined posterior to the furrow. Consistent with this, R-cells are absent from the centers of *Dl*^{rev10} or *lqf*^{ARI} clones (Fig. 5A,A',C,C). By contrast, at the clone borders where mutant cells undergo proneural enhancement, R-cells are present (Fig. 5A,A',C,C). Lateral inhibition also fails in *Dl*^{rev10} and *lqf*^{ARI} clones. The R-cells at the *Dl*^{rev10} or *lqf*^{ARI} clone borders are not organized into discrete ommatidia; instead, it appears that all of the mutant border cells are R-cells (Fig. 5A,A',C,C). As these cells cannot send Delta signals, lateral inhibition fails. Consistent with this idea, there are clusters of R8s at the borders of the clones (Fig. 5B,B',D,D). We conclude that *lqf*$^{+}$ is

required in the Delta signaling cells for proneural enhancement and lateral inhibition.

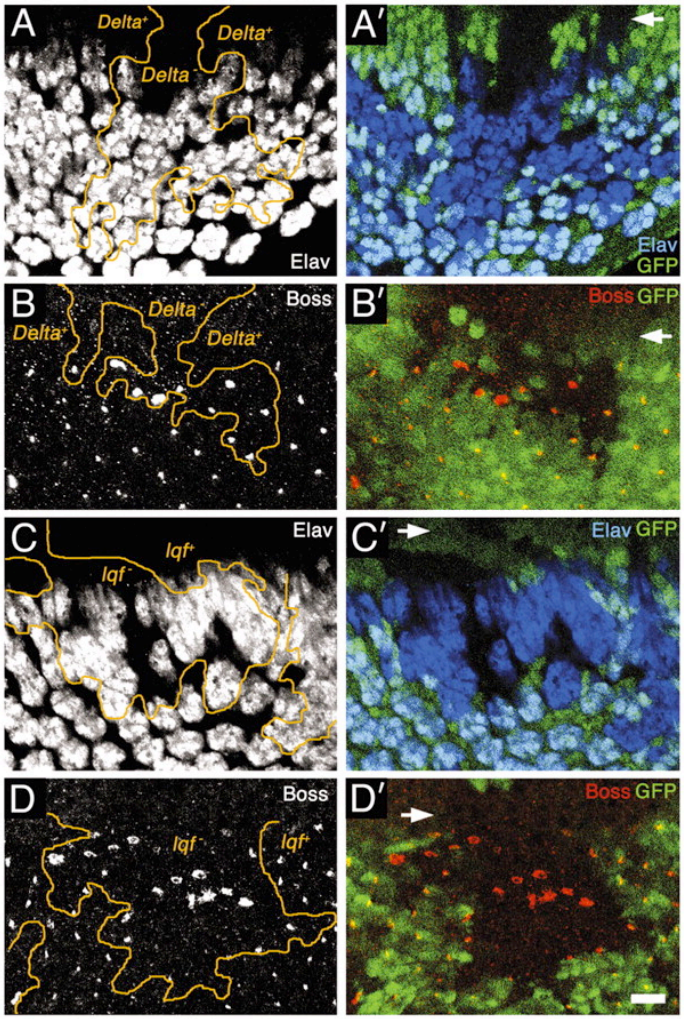

Fig. 5. R-cell determination in *Delta* and *lqf* -null eye disc clones. Confocal images of eye discs are shown. Anterior is upwards in all panels and the arrows indicate the position of the furrow. The discs contain *Delta rev10* clones (A,A',B,B) or *lqf ARI* clones (C,C',D,D) marked by the absence of GFP. The discs are labeled with anti-Elav in (A,A',C,C) and with anti-Boss in (B,B',D,D). In A-D, the clone borders are outlined. The Elav and Boss-expressing cells can be seen several cell distances in from the edge of the clone. This is probably due to long-range Delta signaling, a phenomenon that is not well understood (De Joussineau et al., 2003). Scale bar: 10 μm.

***lqf* null mutant cells can function as receivers but not as signalers**

The results so far suggest that faf^{+} and lqf^{+} are required for Delta internalization and Delta signaling. One prediction of this model is that faf^{+} and lqf^{+} should function non-autonomously; faf^{+} or lqf^{+} cells adjacent to mutant cells should fail to have their Notch pathways activated and should be misdetermined as R-cells. Ectopic R-cells present in faf^{+}/faf^{-} mosaic ommatidia in adult eyes are often faf^{+}(Fig. 2C, D) (Fischer-Vize et al., 1992). The same phenomenon was observed in lqf^{+}/lqf^{-} mosaic facets (Cadavid et al., 2000). Thus, faf^{+} and lqf^{+} function non-autonomously. Conversely, if lqf^{+} functions in the Delta-signaling cells as opposed to the receiving cells, it should be possible to activate Notch in *lqf* null mutant cells that are adjacent to lqf^{+} cells. To test this, we generated lqf^{ARI} clones and Dl^{rev10} (null) clones as a control in eye discs and labeled them with mAb323, which recognizes several different Enhancer of split (E(spl)) proteins expressed in response to Notch activation (Jennings et al., 1994). There is little Notch activation in the middle of the Dl^{rev10} clones (Fig. 6A, A) or the lqf^{ARI} clones (Fig. 6B, B) (see also legend). Thus like $Delta^{+}$, lqf^{+} is required for Notch activation in neighboring cells. At the borders of the Dl^{rev10} clones near the furrow, $Delta^{+}$ $Notch^{+}$ cells outside the clone can signal the Dl^{rev10} $Notch^{+}$ cells inside the clone. Thus, E(spl) protein is detected in many Dl^{rev10} cells at the clone borders (Fig. 6A,A). The same phenomenon is observed the borders of lqf^{ARI} clones (Fig. 6B,B). Thus, the Notch signaling pathway may be activated in lqf^{-} cells. We

conclude that cells lacking *lqf*$^{+}$ activity can activate their own Notch pathway in response to signals from neighboring cells, but cannot signal to activate Notch in their neighbors.

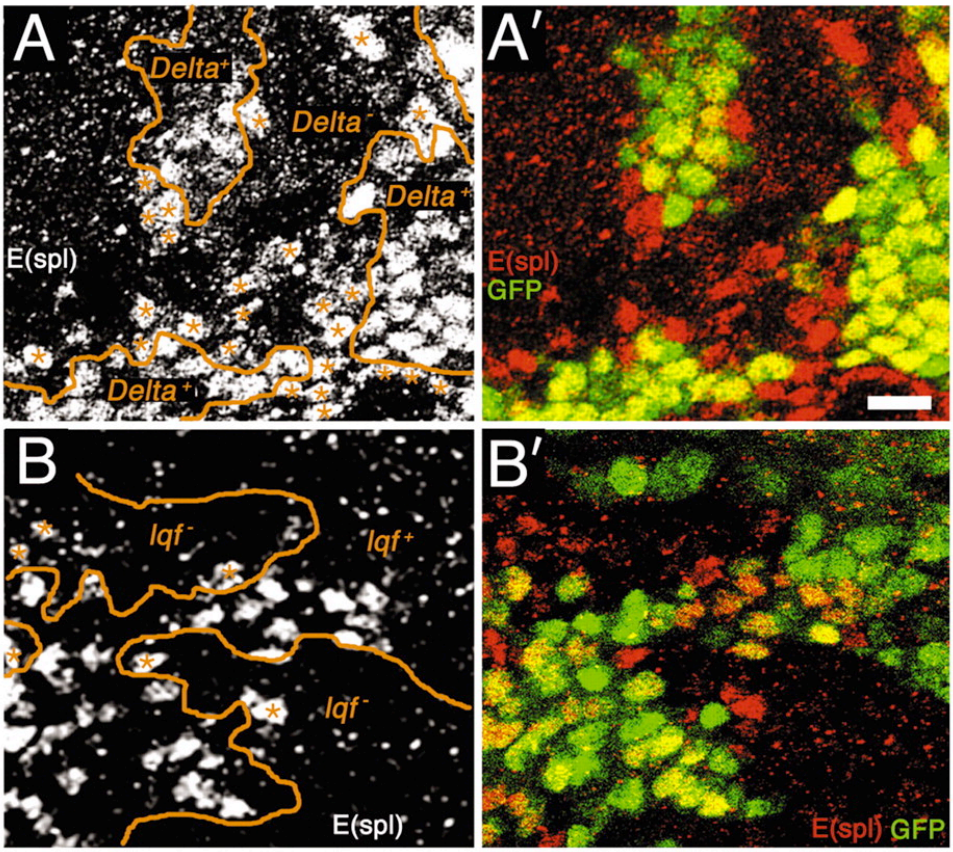

Fig. 6**.** Notch activation in *Delta* and *lqf* -null eye disc clones. Confocal images of eye discs in the region of the furrow are shown. Anterior is upwards in all panels. Eye discs are labeled with mAb323, which recognizes E(spl) proteins. (A,A) An eye disc containing a *Delta rev10* clone marked by the absence of GFP is shown. In A, the clone is outlined and the asterisks indicate *Delta rev10* cells that express E(spl). (B,B) An eye disc containing a *lqf ARI* clone marked by the absence of GFP is shown. In B, the clone is outlined and the asterisks indicate *lqf ARI* cells that express E(spl). The clones were examined throughout the depth of the eye disc and most E(spl)-expressing cells are adjacent to clone borders at all levels. Some E(spl)-positive cells are several distances from the clone border (as in A,A). This may be evidence for long-range Delta signaling, a process that is not well understood (De Joussineau et al., 2003). Scale bar: 10 μm.

Membrane accumulation of Delta is cell autonomous in *lqf* null mutant cell clones

If the effect of *lqf*$^{+}$ on Delta endocytosis is direct, then when *lqf*$^{+}$ and *lqf*$^{-}$ cells are juxtaposed, Delta should accumulate only on the membranes of *lqf*$^{-}$ mutant cells. In small *lqf*^{ARI} (null) clones in eye discs, Delta accumulates on the membranes of all cells emerging from the furrow (Fig. 7) (Overstreet et al., 2003). At the clone borders, high levels of membrane-bound Delta are observed only in the *lqf*^{ARI} mutant cells (Fig. 7). We conclude that the effect of Lqf on Delta internalization is cell autonomous.

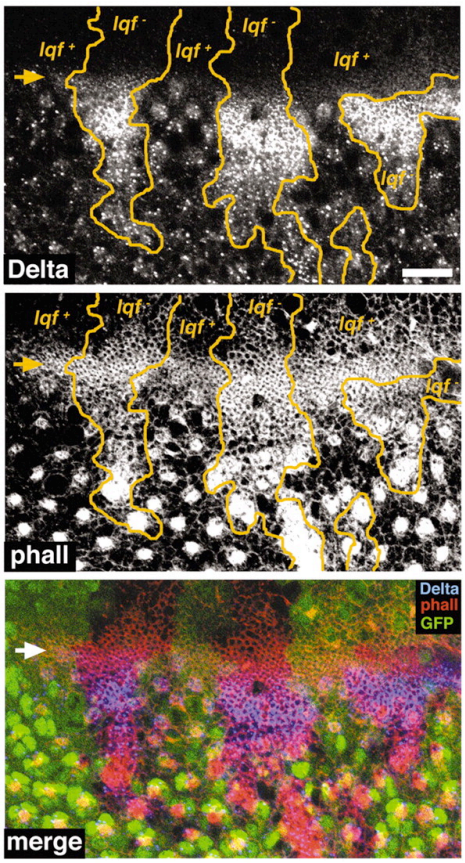

Fig. 7. Cell autonomy of Delta mislocalization in *lqf* null eye disc clones. Confocal images of an eye disc (anterior upwards) containing *lqf ARI* clones, marked by the absence of GFP, is labeled with anti-Delta and with phalloidin, which marks f-actin at cell membranes. The top panel shows Delta localization, the middle panel shows phalloidin, and the bottom panel is a merge of Delta, phalloidin and GFP. Arrows indicate the position of the furrow. Scale bar: 20 μm.

neur^{+} functions with *faf*$^{+}$ and *lqf*$^{+}$ in R2/3/4/5

Neur is required for Delta internalization in wing and eye discs (Lai et al., 2001; Pavlopoulos et al., 2001). However, the only specific functions demonstrated for *neur*$^{+}$ in the eye are a weak requirement in proneural enhancement and lateral inhibition (Lai and Rubin, 2001; Baker and Yu, 1996; Li and Baker, 2004). The observation that the *neur* adult eye mutant phenotype resembles that of *faf* and *lqf*^{FDD9} mutants (Fig. 8A) (Lai and Rubin, 2001) and that *neur*$^{+}$ is expressed specifically in R-cells that emerge from the furrow (Pavlopoulos et al., 2001; Lai and Rubin, 2001) led us to test whether *neur*$^{+}$ is also required for *faf*$^{+}$-dependent Delta signaling by R2/3/4/5 precursors.

In order to determine if *neur*$^{+}$ is required in R2/3/4/5 precursors for Delta internalization and signaling, we performed three experiments. We first tested *neur* for genetic interactions with *faf* and *lqf*. We find that two strong mutant *neur* alleles (*neur*^{1} and *neur*^{11}) are powerful dominant enhancers of *lqf*^{FDD9}. *neur*^{1} *lqf*^{FDD9}/*lqf*^{FDD9} animals die as larvae. *neur*^{11} *lqf*^{FDD9}/*lqf*^{FDD9} are viable and their retinal defects are more severe than *lqf*^{FDD9}/*lqf*^{FDD9} (compare Fig. 8B and Fig. 1C). In eye discs *neur* enhances the lateral inhibition defects in *lqf*^{FDD9}; the clusters of Delta-expressing cells are larger in *lqf*^{FDD9} *neur*^{1} /*lqf*^{FDD9} discs (Fig. 8C, C) than in

lqf^{FDD9} (Fig. 1F) and Delta is on the cell membrane. *neur* mutants enhance the *faf* mutant phenotype weakly (data not shown). The genetic interactions are consistent with the idea that *neur*$^{+}$, *lqf*$^{+}$, and *faf*$^{+}$ function in the same direction in a pathway. Second, we monitored the distribution of Delta in *neur* eye discs. In *neur*^{11} eye discs that express *RO-GFP* we find that, similar to *faf* mutants, Delta accumulates on membranes of the R-cell clusters (Fig. 8D,D). The Delta mislocalization phenotype of *neur*^{1} eye discs is stronger than *neur*^{11} and similar to *lqf*^{FDD9} (Fig. 8E,E). Finally, we asked what effect *neur* mutant cells have on Notch activation near the furrow. We find that *neur* $^{-}$ cells behave similarly to *lqf*$^{-}$ cells; Notch is activated in *neur*^{1} cells at clone borders that are adjacent to *neur*$^{+}$ cells, but not in *neur*^{1} cells in the center of mutant clones (Fig. 8F, F). These results suggest that an important function of *neur*$^{+}$ in the eye is in R-cell restriction and that *neur*$^{+}$ functions with *faf*$^{+}$ and *lqf*$^{+}$ in the Delta signaling cells.

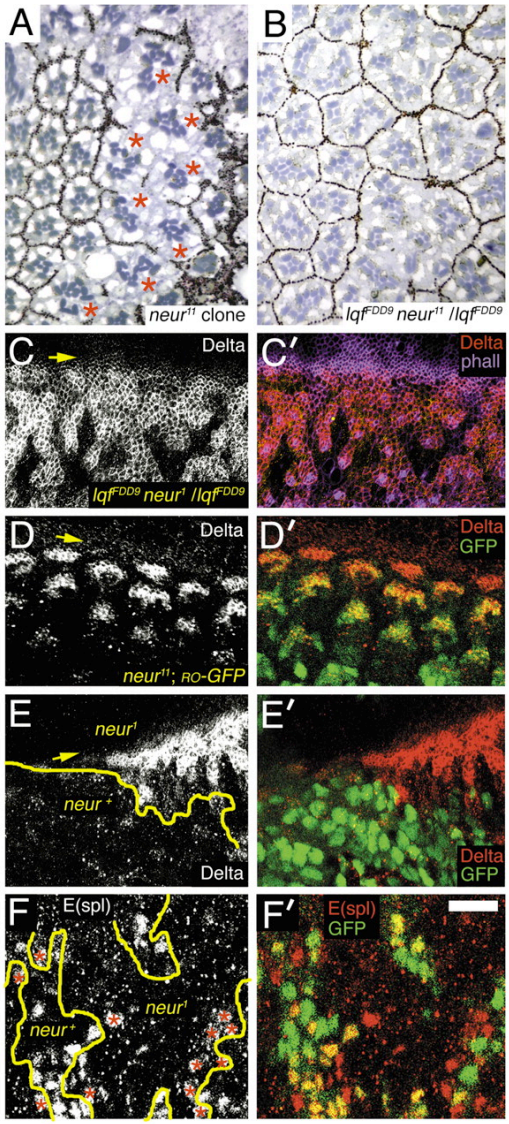

Fig. 8. Role of *neur* +in eye patterning. (A,B) Tangential sections of adult eyes are shown. In A, ommatidia with ectopic R-cells (indicated by asterisks) within a clone of *neur 11* cells. In B, the entire eye is the genotype indicated. (C,C) Eye discs labeled with anti-Delta and phalloidin. (D,D) Eye disc expressing a *RO-GFP* transgene and labeled with anti-Delta. (E,E) Eye disc containing a clone of *neur 1*cells marked by the absence of GFP. In E, the clone border is outlined. The arrows in C-E indicate the position of the furrow. (F,F) An eye disc labeled with mAb323 [recognizes E(spl) proteins] containing *neur 1*clones near the furrow, which are marked by the absence of GFP. In F, the clone borders are outlined and *neur 1*cells that express E(spl) are marked with asterisks. Discs were observed at depths throughout the apical/basal plane and a few E(spl)-positive cells were

found at a distance from the clone borders. Scale bar: 20 μm in A-C'; 15 μm in D-F'.

DISCUSSION

Delta signaling requires Lqf-dependent endocytosis of Delta

Cells with decreased *lqf*$^{+}$ activity accumulate Delta on apical membranes and fail to signal to neighboring cells. We examined three Notch/Delta signaling events in the eye: proneural enhancement, lateral inhibition and R-cell restriction (Fig. 9A). We find that loss of *lqf*$^{+}$-dependent endocytosis during all three events has identical consequences to loss of Delta function in the signaling cells. We conclude that *lqf*$^{+}$-dependent endocytosis of Delta is required for signaling, supporting the notion that endocytosis in the signaling cells activates Notch in the receiving cells. However, Lqf is not required absolutely for all Delta internalization in the eye. Even in *lqf* null cells, which are incapable of Delta signaling, some vesicular Delta is present (see Fig. 7). Perhaps not all of the vesicular Delta present in wild-type discs results from signaling.

Deubiquitination of Lqf by Faf increases Lqf activity

Genetic studies in *Drosophila* indicate clearly that deubiquitination of Lqf by Faf activates Lqf activity (Wu et al., 1999; Cadavid et al., 2000). Moreover, genetic and biochemical evidence in *Drosophila* suggests that Faf prevents proteasomal degradation of Lqf (Huang et al., 1995; Chen et al., 2002). In

vertebrates, however, it is thought that epsin is mono-ubiquitinated to modulate its activity rather than poly-ubiquitinated to target it for degradation (Oldham et al., 2002; Polo et al., 2002). If Lqf regulation by ubiquitin also occurs this way in the *Drosophila* eye, the removal of mono-ubiquitin from Lqf by Faf would activate Lqf activity.

Whatever the precise mechanism, given that both Faf and Lqf are expressed ubiquitously in the eye (Fischer-Vize et al., 1992; Chen et al., 2002), two related questions arise. First, why is Lqf ubiquitinated at all if Faf simply deubiquitinates it everywhere? One possibility is that Faf is one of many deubiquitinating enzymes that regulate Lqf, and expression of the others is restricted spatially. This could also explain why Faf is required only for R-cell restriction (see below). Another possibility is that Faf activity is itself regulated in a spatial-specific manner in the eye disc. Alternatively, Lqf ubiquitination may be so efficient that Faf is needed to provide a pool of non-ubiquitinated, active Lqf. Similarly, Faf could be part of a subtle mechanism for timing Lqf activation. Second, why is Faf essential only for R-cell restriction? One possibility is that there is a graded requirement for Lqf in the eye disc, such that proneural enhancement requires the least Lqf, lateral inhibition somewhat more, and neural inhibitory signaling by R2/3/4/5 the most. The mutant phenotype of homozygotes for the weak allele lqf^{FDD9} supports this idea, as R-cell restriction is most severely affected. Alternatively, Lqf may be expressed or ubiquitinated with dissimilar efficiencies in different regions of the eye disc. More experiments are needed to

understand the precise mechanism by which the Faf/Lqf interaction enhances Delta signaling.

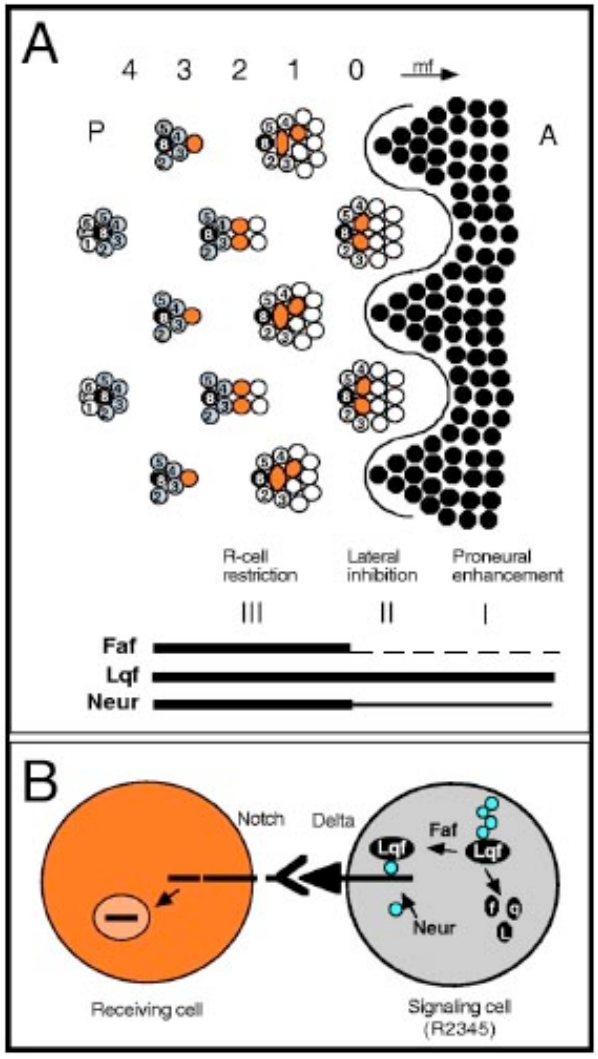

Fig. 9. Model for Faf, Lqf and Neur function. (A) Early events in ommatidial assembly (see Wolff and Ready, 1993). The morphogenetic furrow (mf) moves in the direction of the arrow. A is anterior and P is posterior. The first several columns (0-4) of developing ommatidia are shown. Atonal-expressing cells are black. R1-R8 are indicated. Three processes (I, II, III) that require Notch/Delta signaling are shown. (I) Proneural enhancement: Atonal expression is upregulated. (II) Lateral inhibition: Atonal expression is limited to groups of 10 cells and ultimately to R8s in column 0. (III) R-cell restriction: R2/3/4/5 precursors signal their neighbors to prevent excessive neural determination. As the ectopic cells in *faf* mutants appear to arise between R3/4, they may be the

orange cells. As depicted by the black bars, Faf is essential only for event III, Lqf is essential for events I, II and III, and Neur is essential for event III but is required to a lesser extent for the events I and II. Faf is required redundantly during events I and II (B) A model showing how Faf/Lqf may function with Neur in the Delta signaling cells is shown. The blue circles are ubiquitin. Lqf is deubiquitinated by Faf, which increases Lqf levels. Ubiquitination of Delta by Neur may stimulate interactions between Delta and Lqf and thereby facilitate Delta internalization.

Neur stimulates Delta internalization in the signaling cells

In *neur* mutants, Delta accumulates on the membranes of signaling cells and Notch activation in neighboring cells is reduced. These results support a role for Neur in endocytosis of Delta in the signaling cells to achieve Notch activation in the neighboring receiving cells, rather than in down-regulation of Delta in the receiving cells. Because *neur* shows strong genetic interactions with *lqf* and both function in R-cells, Neur and Lqf might work together to stimulate Delta endocytosis. Lqf has ubiquitin interaction motifs (UIMs) that bind ubiquitin (Polo et al., 2002; Oldham et al., 2002). One explanation for how Neur and Faf/Lqf could function together is that Lqf facilitates Delta endocytosis by binding to Delta after its ubiquitination by Neur (Fig. 9B). This is an attractive model that will stimulate further experiments.

Specificity of Lqf for Delta endocytosis

One exciting observation is that the endocytic adapter Lqf may be essential specifically for Delta internalization. Although we have not examined these signaling pathways directly, *hedgehog, decapentaplegic,* and *wingless*

signaling appear to be functioning in the absence of Lqf. These three signaling pathways regulate movement of the morphogenetic furrow (Lee and Treisman, 2002) and are thought to require endocytosis (Seto et al., 2002). The furrow moves through *lqf* null clones and at the same pace as the surrounding wild-type cells (Fig. 7) (Overstreet et al., 2003). Moreover, all mutant phenotypes of *lqf* null clones can be accounted for by loss of *Delta* function. Further experiments will clarify whether this apparent specificity means that Lqf functions only in internalization of Delta, or if the process of Delta endocytosis is particularly sensitive to the levels of Lqf.

Endocytic proteins as targets for regulation of signaling

Lqf expands the small repertoire of endocytic proteins that are known targets for regulation of cell signaling. In addition to Lqf, the endocytic proteins Numb and Eps15 (EGFR phosphorylated substrate 15) are objects of regulation. In vertebrates, asymmetrical distribution into daughter cells of the a-adaptin binding protein Numb may be achieved through ubiquitination of Numb by the ubiquitin-ligase LNX (Ligand of Numb-protein X) and subsequent Numb degradation (Nie et al., 2002). Also in vertebrate cells, Eps15 is phosphorylated and recruited to the membrane in response to EGFR activation and is required for ligand-induced EGFR internalization (Confalonieri et al., 2000). Given that endocytosis is so widely used in cell signaling, endocytic proteins are likely to provide an abundance of targets for its regulation.

CHAPTER 2 ADDENDUM – ADDITIONAL WORK IN PROGRESS

Activation of Notch in receiving cells is dependent on endocytosis of Notch ligands in signaling cells (see above). Recently, several models for how endocytosis of ligand facilitates signaling have been proposed (reviewed in chapter 1). Several labs, including ours, have found that Lqf promotes DSL endocytosis in the signaling cells, an event required for N activation in the receiving cells (see above, Overstreet et al. 2004; Wang et al. 2004; Tian et al. 2004). The precise molecular mechanism by which *lqf*-dependent endocytosis renders Delta able to signal is still under investigation. However, a detailed knowledge of Lqf function may be the key to understanding how endocytosis is required for signaling. In this work, I will explore two issues further to refine the model of Lqf function. In the first issue, I explore ways to precisely define the *lqf*-dependent Delta endocytosis and signaling events. Not all Delta endocytosis is *lqf*-dependent and is hard to visually isolate (see below). In the second issue, I directly test one proposed model for Lqf function. Wang and Struhl et al. (2004) proposed that Lqf-dependent recycling of endocytosed Delta ligands facilitates signaling (see below). To test this possibility, I will use a chimeric Delta protein that is synthetically engineered to be internalized and recycle independently of Lqf. I will perform one experiment to see if this protein can signal in the absence of Lqf.

ISSUE 1: GENETIC ISOLATION OF LQF-DEPENDENT ENDOCYTIC EVENTS

Lqf is likely to promote endocytosis of ubiquitinated forms of DSL ligands. Several observations support this idea. Ubiquination of DSL ligands by E3 ligases, Neuralized and Mind Bomb, is required in the signaling cells for endocytosis and signaling (Lai et al. 2001; Pavlopoulos et al. 2001; Le Borgne et al. 2005). Lqf and Neuralized function in the same cells in the developing eye disc and display very strong genetic interactions (Overstreet et al. 2004 and appendix IV). Struhl and colleagues (2004) demonstrated that ubiquitination of Dl is sufficient to drive endocytosis and is prerequisite for Lqf-mediated signaling. A chimeric protein composed of the Delta extracellular and transmembrane domains fused to an exogenous intracellular domain that is either a single ubiquitin monomer or a ubiquitinated peptide can activate Notch, but requires *lqf* to do so. Finally, a mammalian homolog of Lqf, epsin1, binds to ubiquitin via its ubiquitin interacting motifs (Polo et al. 2002).

Lqf is required absolutely to activate Notch via ubiquitin-dependent ligand endoctosis. We observe a failure of Delta internalization (and Notch activation) near the furrow in *lqf*-deficient cells in the eye. However, we note that a significant amount of Delta is internalized in the absence of *lqf*. We speculate that these internalization events do not represent signaling events (Overstreet et al. 2004). Thus, *lqf* is responsible only for a subset of Delta endocytic events which

are necessary for signaling. Struhl and colleagues (2004) obtained similar results in the wing disc (see below).

The subset of *lqf*-dependent Delta endocytic events is difficult to isolate because it is apparently a small fraction of the total Delta endocytic events. For this reason, it is difficult to monitor these events because they are eclipsed by the bulk of Delta endocytosis. For example, in the developing wing, Delta trafficking in *lqf* mutant cells appears essentially unaltered, supporting the idea that Lqf does not participate in the bulk of Delta endocytosis. To observe *lqf*-dependent processes in the wing, a sensitive genetic setting is required: the total amount of Delta on the membrane requiring Lqf-dependent internalization can be increased via simultaneous overexpression of Neuralized and Delta. Using this "sensitized" background, Wang and Struhl observed a persistence of Delta on the apical plasma membrane in *lqf*-deficient cells compared to wild-type cells. A similar situation occurs in the developing eye disc. *Delta* transcription is upregulated in *lqf*-deficient cells due to loss of Notch activation near the furrow (Wang et al. 2004). In this background it is easy to that see that in *lqf*- cells Delta persists at the membrane in all cells at the furrow and even posterior to the furrow. Nevertheless, because *Delta* transcription is upregulated in the absence of *lqf*, it is difficult to assess how much membrane accumulation is due to *Delta* transcriptional upregulation versus failure of *lqf*-dependent endocytosis of Delta.

In order to define more precisely the *lqf*-dependent endocytic events, we need to identify a genetic background that provides a clear view of those events.

Such a scenario would simplify future analyses of Lqf role in Delta signaling and endocytosis and might reveal novel insights into this process. The ideal genetic background would offer a genuine view of *lqf*-dependent Delta endocytic events without introducing an increase of *Delta* transcription or protein levels – either artificially as in Wang and Struhl (2004) or as a secondary phenotype (Overstreet et al. 2004).

Proposed experiments

Genetic isolation of *lqf*-dependent events in *lqf*-deficient cells

In *lqf-* cells, Delta accumulates strongly on the apical plasma membrane of all cells at the morphogenetic furrow. The protein accumulation persists on the apices of cells posterior to the furrow. Some of this accumulation is likely due to upregulation of *Delta* transcription because of impaired N activation at the furrow during lateral inhibition (Tsuda et al. 2002; Wang et al. 2004). In *lqf*-deficient cells, *Delta* transcription is upregulated as indicated by increased expression of *Dl-lacZ* (a *LacZ* reporter fusion to the endogenous *Delta* promoter). I obtained similar results to Wang et al. (2004) obtained using null alleles of *lqf* or a hypomorphic allele, FDD9 (data not shown).

Both alleles of *lqf* (null and FDD9) have been previously shown to accumulate high levels of Delta protein on apical cell membranes near the furrow (Overstreet et al. 2003). I want to distinguish between the Delta accumulation that is due failure of *lqf*-dependent endocytic events versus Delta protein upregulation due to loss of N activation. To do this, I plan to assess the level of

Delta protein accumulation and persistence on the membrane in eye discs where wild-type and *lqf*- cells are juxtaposed in the absence of N activity. In this way, the levels of Dl at the membrane due to transcriptional upregulation of Dl (at the furrow during lateral inhibition) are equalized in wild-type and mutant cells. As the removal of *lqf* can have no further effect on *Dl* upregulation (N is already inactive), the effect of Lqf on clearing Dl from the membrane is isolated and can be compared in wild-type and *lqf*- cells.

In eye discs mutant for a temperature sensitive allele of *N*, clones of *lqf* mutant alleles will be generated. These eye discs will be shifted to restrictive temperature for several hours in order to abolish N activity in the entire eye disc. Next, they will be fixed, and stained with an antibody to extracellular domain of Delta (DSHB and monoclonal from Kris Kleug).

When I examine the subcellular distribution of Delta in these discs, I expect that Delta protein will accumulate on all cells at the furrow because N-dependent lateral inhibition will be off in all cells, and *Dl* transcription will be maximally upregulated. In *lqf*- cells, Delta will persist on the membranes of all cells for approximately 4-5 rows posterior to the furrow as described in Overstreet et al. (2003 and 2004).

When I compare the Delta distribution in the wild-type cells (which are deficient for N) to neighboring *lqf*- cells, I expect one of two possible scenarios. In the first, the Delta accumulation in all wild-type cells at the furrow will not persist as far posterior to the furrow as the Delta in *lqf*- cells. If this is the case,

then the difference in Delta accumulation must reflect *lqf*-dependent Delta internalization. Alternately, Delta could persist equally as long posterior to the furrow in wild-type cells and in *lqf*- cells. In this case, I would conclude that isolation of *lqf*-dependent endocytic events is not possible using this genetic background.

Genetic isolation of lqf-dependent events in *faf*- clones

In *faf* eye discs, *lqf* levels or activity is lower than wild-type. Consequently, Delta protein accumulates on the surface of R-cells 2/3/4/5 posterior to the furrow (Overstreet et al. 2004). I want to know if any of this apical accumulation might be due to upregulation of *Dl* transcription. If so, then expression of *Dl-lacZ* should be elevated in *faf* mutant cells. To test this, I will examine *Dl-lacZ* expression in marked *faf* null clones and compare the levels of LacZ in R-cells 2/3/4/5 inside the clone (*faf*-) and outside the clone (*faf*+). I am currently constructing the chromosomes to generate the necessary flies (see materials and methods below).

If I find that *Dl* transcription is not noticeably altered in *faf* mutants, then I would conclude that the apical accumulation of Delta in *faf* mutants is not due to upregulation of *Delta* transcription, but rather reflects a failure of Delta internalization due to lower *lqf* activity. Therefore, this genetic background might offer a genuine view of the influence *lqf* has on Delta endocytic events.

I expect that this will be the case because *Delta* transcriptional levels are under the control of Epidermal Growth Factor Receptor (EGFR) signaling in R-cells posterior to the furrow. After the R8 cell has been specified via Notch-mediated lateral inhibition (see above), R8 cells recruit other R cells by activating EGFR in neighboring cells. In response to EGFR activation, the recruited cells begin expressing *Delta* in a Notch-independent way (Tsuda et al. 2002). Because *Delta* transcription is independent of N activity (and therefore also *lqf* activity) in R-cells 2/3/4/5, the Delta mislocalization in these cells in *faf* mutants probably reflects only a failure of internalization.

ISSUE 2: TESTING THE POSSIBILITY THAT LQF RECYCLES DELTA

What is the molecular reasoning behind why *lqf*-dependent endocytosis confers signaling ability? Recently, Wang and Struhl (2004) proposed that Lqf possesses the singular ability to route Delta protein through a select endocytic pathway where Delta can become an activated ligand. In support of this, an artificial Delta protein, which can traffic through endosomes and is subsequently recycled to the plasma membrane, can signal independently of Lqf activity. This led to a model where Lqf facilitates the recycling of Delta via routing through recycling endosomes. Passage through a recycling endosomal compartment might lead to chemical changes in Delta ligand (possibly due to acidic environment of endosomes) that transform Delta into an active ligand.

These experiments are some of the first to address how endocytosis is required for signaling and imparted interesting insights into Lqf function. However, this line of experimentation was performed using a gain-of-function assay for ectopic induction of N activation. Induction of ectopic N activation may not reflect the natural requirements of the signaling machinery. Therefore, a more germane genetic setting might be to perform similar analyses using a loss of function background to assay for restoration of normal N activity.

Proposed experiment

Test if overexpression of Dl-LDL chimera bypasses the need for Lqf activity

Wang and Struhl (2004) suggest that the essential function of Lqf is to recycle Delta protein to activate its signaling capabilities. A Delta chimera that enters the recycling pathway via LDL receptor cytosolic tail sequences, overcomes the need for Lqf activity in the wing. The assay was based on ectopic induction of N activation.

I want to use *lqf* loss of function genetic backgrounds to test this hypothesis. If this idea is correct, and this chimera can signal in the absence of *lqf*, it should be able to rescue *lqf* mutants by restoring N activation. To test this, I expressed the Delta (EC)-LDL chimera using *rough* promoter (see above). I will test to see if expression of this chimera in *lqf-* genetic backgrounds can rescue

patterning defects caused by *lqf* mutations. If this chimera does rescue, it will provide stronger support for the proposed recycling model because its activity was assessed in a loss-of-function background. In the case that I do not observe rescue, it may be because this chimera signals too weakly, as demonstrated in Wang et al. (2004). Nonetheless, in the future, this model will need to be tested rigorously using genetics. Perhaps a genetic screen for modifiers of hypomorphic *lqf* mutations will identify proteins that cooperate with Lqf in Delta signaling.

Materials and methods

To observe *Dl-lacZ* expression in *faf-* clones in eye discs, I will generate a fly of the following genotype: *Pw+[genomic faf fragment], Pw+[Ubi-GFP], FRT18A/FRT18A; EyGal4>UASFLP, faf/faf, Dl-lacZ.* To make this stock, I obtained the following chromosomes from the Bloomington stock center: *Pw+[Ubi-GFP], FRT18* and *FRT 18A* and *EGUF* on the third chromosome. *Dl-lacZ/TM3,Ser* was sent as a gift from Utpal Banerjee at UCLA. *Pw+[Genomic faf fragment]* and *fafFo8* stocks are maintained in the Fischer lab.

To observe *Dl-lacZ* expression in *lqf-* clones (null allele L71 or FDD9), I generated flies of the following genotype. *EyFlp/+; lqf-, FRT80B, Dl-lacZ/Pw+[Ubi-GFP], FRT80B*. To generate this fly, recombinants were recovered from standard fly crossing techniques and the following chromosomes:

lqf-, FRT80 (Overstreet et al. 2003) and *Dl-lacZ* (see above). EyFlp and Pw+[Ubi-GFP], FRT80B chromosome are those used in Overstreet et al. (2003). Discs generated from these crosses will be stained with anti-lacZ antibody available from the DSHB.

To generate mutant clones in a Nts genetic background, the following male flies will be produced using standard fly crossing: 1. *Nts2; EGUF/+;Pw+[Ubi-GFP], FRT80B/ lqf-, FRT80B*. 2. *Nts2; EGUF/+;FRT82B, Pw+[Ubi-GFP]/FRT82B, faf-,*. Chromosomes are as described in Overstreet et al. (2003). *Nts2* allele was obtained from Bloomington stock center. The larvae will be reared at 18 degrees celcius and shifted to restrictive temperature for 4-6 hours or longer as in Tsuda et al. (2002). The resultant discs will be stained with a monoclonal antibody to Delta extracellular domain available at the DSHB as in Overstreet et al. (2003).

Plasmid construction for RO-HS-Dl-LDL chimera can be found in plasmid construction section in Appendix IV. This construct was transformed into germline cells using standard procedures as in Overstreet et al. (2003).

Chapter 3. *In vivo* structure and function analysis of *Drosophila* Liquid facets

The data described in this chapter has been published in *Current Biology* (see Overstreet et al. 2003).

SUMMARY

Epsin is part of a protein complex that performs endocytosis in eukaryotes (Chen et al. 1998). *Drosophila* epsin, Liquid facets (Lqf), was identified because it is essential for patterning the eye and other imaginal disc derivatives (Cadavid et al. 2000). Previous work has provided only indirect evidence that Lqf is required for endocytosis in *Drosophila* (Cadavid et al. 2000, Chen et al. 2002). Epsins are modular, with an N -terminal ENTH (epsin N-terminal homology) domain that binds PIP_2 at the cell membrane (Kay et al. 1998, Itoh et al. 2001, Ford et al. 2002), and four different classes of protein-protein interaction motifs (Chen et al. 1998). The current model for epsin function is that epsin bridges the cell membrane, a transmembrane protein to be internalized, and the core endocytic complex (De Camilli et al. 2001). Here, we show directly that *Drosophila* epsin (Lqf) is required for endocytosis. Specifically, we find that Lqf is essential for internalization of the Delta (Dl) transmembrane ligand in the developing eye. Using this endocytic defect in *lqf* mutants, we develop a

transgene rescue assay and perform a structure/function analysis of Lqf. We find that when we divide Lqf into two pieces, an ENTH domain and an ENTH-less protein, each part retains significant ability to function in Dl internalization and eye patterning. These results challenge the current model for epsin function which requires an intact protein.

RESULTS AND DISCUSSION

lqf$^+$ is Required for Dl Internalization in the Eye Disc

To test for endocytosis defects in *lqf*$^-$ mutants, we monitored the localization of the transmembrane receptor Dl in developing eyes. Dl normally undergoes endocytosis in the eye, and as the internalized protein is not degraded rapidly, internalized Dl can be detected in vesicles (Parks et al. 1995, Baker et al. 1998).

The *Drosophila* eye, composed of ~800 identical 22-cell ommatidia, or facets, develops in the larval and pupal stages in a monolayer epithelium called the eye imaginal disc (Wolff et al. 1993). Eye development occurs as a wave, where the morphogenetic furrow forms at the posterior of the disc, and moves anteriorly into the monolayer of undifferentiated cells. Rows of ommatidia assemble stepwise posterior to the furrow, one or two cells at a time, starting with the eight photoreceptors (R1-R8).

In wild-type, we detect Dl exclusively as intracellular dots within developing ommatidial clusters throughout the eye disc (Figure 1A), as reported previously (Parks et al. 1995). In larval eye discs homozygous for *lqf*^{FDD9}, a weak,

viable mutant allele, Dl is detected mainly at the membranes of cells just posterior to the furrow (Figure 1C). In clones of cells homozygous for lqf^{ARI}, a strong, lethal mutant allele, similar membrane localization of Dl is observed (Figure 1F). We conclude that lqf^{+} is required for Dl internalization.

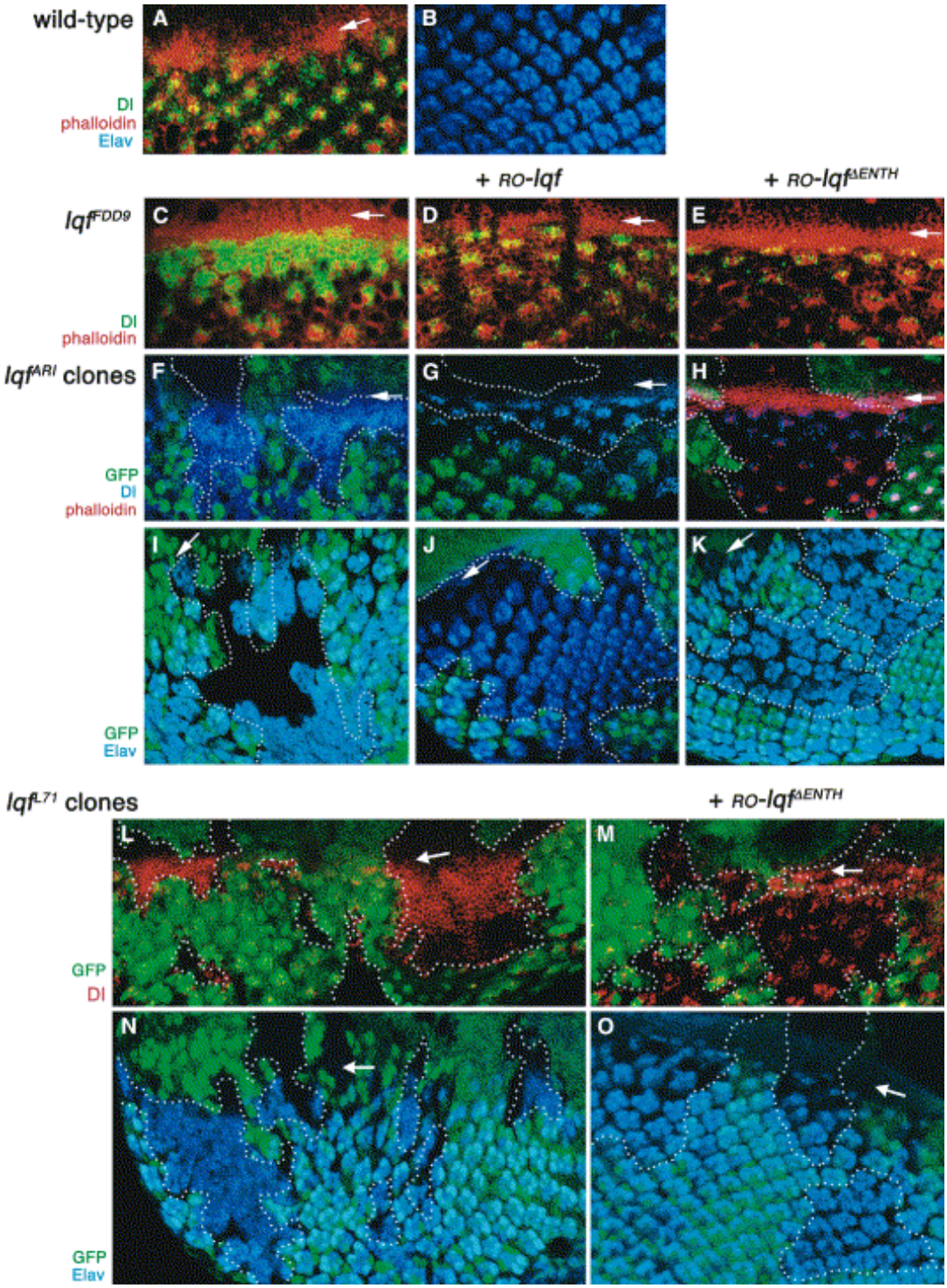

Fig. 1. Dl Internalization and Neural Patterning in *Drosophila* Eye Discs. Shown are apical views of third instar larval eye discs, oriented with anterior up. The arrows indicate the morphogenetic furrow, highlighted by

phalloidin staining, which is shown in some panels.(A) Intracellular Dl particles in wild-type ommatidial clusters.(B) Photoreceptor nuclei are labeled with anti-Elav (Robinow et al. 1991), which reveals regularly spaced rows of assembling ommatidia in wild-type.(C) Dl is mainly at the membrane just posterior to the furrow in *lqf* hypomorphs.(D and E) Dl internalization is restored to *lqf* hypomorphs by an *RO-lqf* or an *RO-lqf _ENTH* transgene.(F–K) Homozygous *lqf ARI* clones, marked by the absence of GFP, are contained within the dotted lines. (F) Dl is mainly at the membrane posterior to the furrow within *lqf ARI* clones. (G and H) Dl internalization is restored to *lqf ARI* clones by an *RO-lqf* or an *RO-lqf _ENTH* transgene. (I) Some *lqf ARI* clone edges are overneuralized, and there is no neural determination at all in the center of the clone. Smaller clones were overneuralized throughout (not shown). (J and K) Ommatidial patterning is largely restored within *lqf ARI* clones by an *RO-lqf* or an *RO-lqf _ENTH* transgene.(L–O) Homozygous *lqf L71* clones, marked by the absence of GFP, are contained within the dotted lines. (L) Dl is mainly at the membrane posterior to the furrow within *lqf L71* clones. (M) Dl internalization is restored to *lqf L71* clones by *RO-lqf _ENTH* . (N) *lqf L71* clones are overneuralized. (O) Ommatidial patterning is largely restored within *lqf L71* clones by *RO-lqf _ENTH* . Images of Delta expression alone, for all panels, are provided in Figure S1 in the Supplemental Data. Delta expression is not identical to wild-type in any of the rescued eye discs. For *RO-lqf _ENTH* , this is likely due to partial rescue. For *RO-lqf* , particularly in an *lqf FDD9* background, the Dl vesicles appear larger. Perhaps *RO-lqf* expression affects downstream events in the endosome. *lqf ARI* (or *lqf L71*) clones were induced in *lqf ARI* /*lqf* +larvae of the genotype w, P{ *ry* +;*ey-FLP.D* }2 (Newsome et al. 2000)/ +; *lqf ARI* P{ *ry* +;*hs-neo* ;*FRT* }80B (Xu et al. 1993)/ P{ *w*+;*Ubi-GFP(S65T)nls* } (Flybase 2003) P{ *ry* +;*hs-neo* ;*FRT* }80B. Eye disc staining was performed with PEMS/PBST (Fischer-Vize et al. 1992 a and b). The primary antibodies used were anti-Dl mAb 202 at 1:9 (Parks et al. 1995) and anti-Elav mAb 9F8A9 at 1:9 (DSHB). The secondary antibodies (Molecular Probes) used were Alexa 488 anti-mouse, Alexa 633 anti-mouse, or Cy3 anti-mouse at 1:600. After antibody treatment, some eye discs were incubated for 20 min in Alexa 568 -phalloidin (Molecular Probes), which had been dried and resuspended in 200 l PBST (0.1 U/ l), and then washed twice in PBST. Eye discs were mounted in VectaShield (Vector Laboratories). Images were produced with a Leica TCS SP2 confocal microscope.

Identification of Lqf modules required for function

All epsins have an amino-terminal ENTH domain (Kay et al. 1998)) which binds PIP_2 at the cell membrane (Itoh et al. 2001, Ford et al. 2002), and three or four types of protein-protein interaction motifs, whose copy numbers vary among different epsins (Figure 2). The UIMs bind ubiquitin (Ub) non-covalently (Hofmann et al. 2001, Polo et al. 2002, Shih et al. 2002, Oldham et al. 2002). There are also clathrin binding motifs (CBMs), DPW motifs that bind the core endocytic adaptor complex, AP-2, and NPF motifs that bind Eps15, another accessory factor (Chen et al. 1998, Salcini et al. 1997, Paoluzi et al. 1998, Owen et al. 1999).

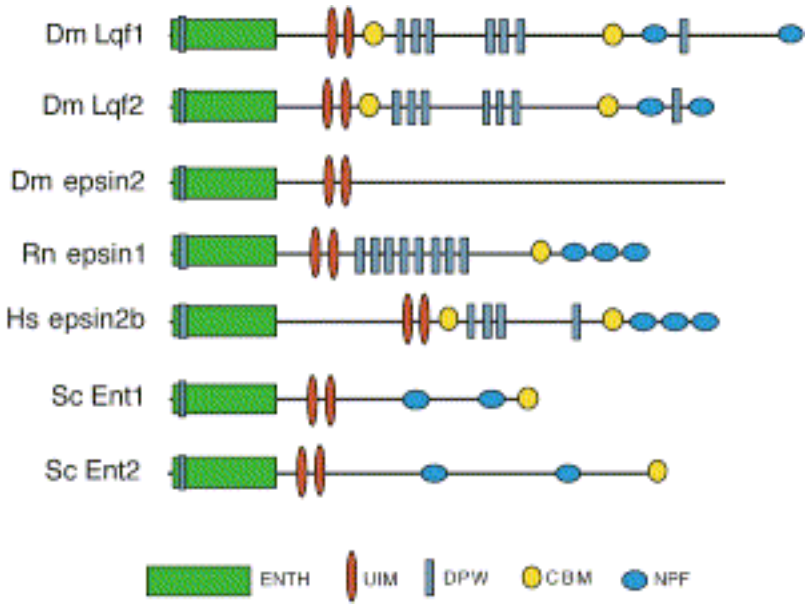

Fig. 2. Modular Structure of Epsins. The structures of epsin proteins from *Drosophila* (Dm), rat (Rn), human (Hs), and yeast (Sc) that are referred to in this work are diagrammed. Protein sequence accession numbers and references are: Dm Lqf1 and Lqf2, AAF05113 and AAF05114, respectively (Cadavid et al. 2000); Dm epsin2, AAF43421 (Lloyd et al. 2000, Flybase 2003); Rn epsin1, NM_057136 (1); Hs epsin 2b, AF062085 (Rosenthal et al. 1999); Sc Ent1 and Ent2, NP_010120 and NP_013307, respectively (Goffeau 1996). Dm Lqf1 and Dm Lqf2 are produced from a single alternatively spliced mRNA (Cadavid et al.

2000, Chen et al. 2002). Dm *epsin2* , also referred to as *epsin-like* , is an uncharacterized gene.

A step toward understanding the role of Lqf in endocytosis is the identification of the modules of Lqf protein that are required. In yeast, there are straightforward assays for the function of the two epsins (Ent1 and Ent2). Structure/function analyses have demonstrated that the ENTH domain of Ent1 is necessary and sufficient to rescue the lethality of *ent1*Δ*ent2*Δ double mutants (Wendland et al. 1999). Moreover, the ENTH domain and to a lesser extent the UIMs were shown to be required for endocytosis (Shih et al. 2002, Wendland et al. 1999). Because there are mechanistic differences between endocytosis in yeast and higher eukaryotes, the yeast epsins might function somewhat differently from vertebrate epsins and *Drosophila* Lqf. The major difference between these systems is that the AP-2 core adaptor complex in yeast has no known function in endocytosis (Huang et al. 1999), and accordingly, the yeast epsins lack DPW motifs (Figure 2). As in yeast, structure/ function analyses of epsins in vertebrate cell culture have pointed to the importance of the ENTH domain (Chen et al. 1998, Itoh et al. 2001, Nakashima et al. 1999). These assays, however, rely on dominant negative effects of mutant epsin proteins on endocytosis, and their interpretation is difficult.

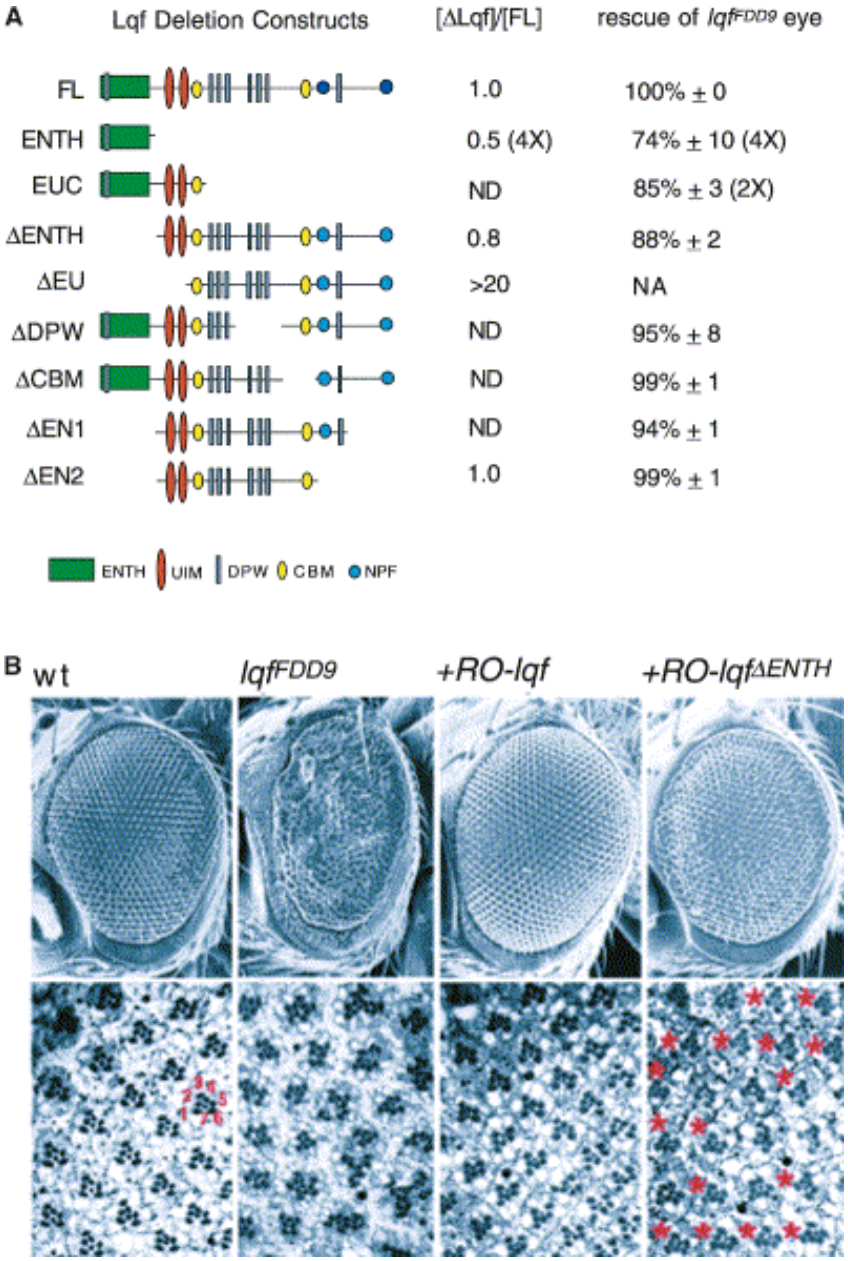

Fig. 3. Rescue of *lqf FDD9* Adult Eye Patterning Defects by *RO-lqf_* Transgenes(A) Full-length (FL) and eight different deleted versions of an *lqf1* cDNA, cloned into pRO, are shown; the construct name is shown at the left. One transformant line of each transgene was chosen for analysis based on preliminary assessment of how well it rescues *lqf FDD9* mutant eyes; the data shown are for one copy of the best rescuer for each construct. As single copies of *RO-lqf ENTH* and *RO-lqf EUC* rescue poorly (little Lqf ENTH or Lqf EUC protein accumulates), multiple copies were also tested; the data for four copies (4X) of *RO-lqf ENTH* and two copies (2X) of *RO-lqf EUC* are shown. In the second

column ((_lqf)/(FL)), the relative amounts of _Lqf proteins expressed by each transgene are shown, as determined in Western blot experiments; values are normalized to the level of full-length Lqf expressed by *RO-lqf* . In the third column (rescue of *lqf FDD9* eye), the fraction of wild-type facets in the eyes of *lqf FDD9* flies containing a transgene is tabulated. For each genotype, ~100 facets in each of three different eyes were analyzed. *lqf FDD9* eyes have 12% ± 2% wild-type facets. ND means not done, and NA means not applicable. We could not test *RO-lqf _EU* for its ability to substitute for the endogenous *lqf* +gene. Although wild-type *RO-lqf _EU* transformants appear normal, *lqf FDD9* mutants carrying one copy of the *RO-lqf _EU* transgene die as larvae. The lethality of the transgene is likely due to dominant-negative activity of Lqf _EU protein, which is highly overexpressed. The Lqf_ constructs were generated from a Flag-tagged full-length *lqf1* cDNA (Cadavid et al. 2000). All of the constructs were ligated as AscI fragments into the AscI site of the P element transformation vector pRO (Huang et al. 1996). P element transformation of *w1118* flies was performed as described previously (Fischer-Vize et. al 1992b). Quantitative Western blot experiments were performed as described previously (Chen et al. 2002). Expression of Lqf by the *RO-lqf* transgenes was detected by using anti-FlagM2 (Sigma) at 1:200 and HRP-conjugated anti-mouse (Santa Cruz Biochemicals) at 1:500.(B) Shown are scanning electron micrographs (top panels) and apical tangential sections (bottom panels) of eyes of the genotypes indicated. *RO-lqf* rescues *lqf FDD9* to wild-type, and *RO-lqf _ENTH* rescues significantly. Partial rescue by *RO-lqf _ENTH* as compared to complete rescue with *RO-lqf* is at least partly a reflection of the lower expression levels of *RO-lqf _ENTH* (see (A)). The numbers in the bottom left panel indicate R cells R1–R7. The red asterisks in the bottom right panel indicate wild-type ommatidia. Scanning electron micrographs and sections of adult eyes were produced as described previously (Huang et. al 1995).

In order to determine which parts of Lqf protein are required for Dl endocytosis, we generated the eight deleted lqf^{+} cDNAs shown in Figure 3A, and expressed them in transformed *Drosophila* using the eye-specific vector pRO (Huang et al. 1996). pRO transgenes that express full-length lqf^{+} (*RO-lqf*) rescue the Dl endocytosis defects defects in lqf^{FDD9} homozygous eye discs (Figure 1D), and in clones of homozygous lqf^{ARI} cells (Figure 1G). *RO-lqf* also rescues the

patterning defects (overneuralization) in adult eyes of lqf^{FDD9} homozygotes ((Cadavid et al. 2000) and Figure 3B) and in lqf^{ARI} clones (Figures 1B, 1I, and 1J).

We generated several transformant lines with each *RO-lqfD* transgene. Several different lines of each were tested for rescue of the defects in lqf^{FDD9} adult eyes. Rescuing activity was quantified by counting the fraction of wild-type facets in sectioned eyes. The results for the one line of each construct with the most rescuing activity is shown in Figure 3A. These particular lines were used in the remainder of the experiments. Seven of the eight deletion constructs rescue the lqf^{FDD9} mutant phenotype quite well (Figures 3A and 3B). Most notable is the observation that *RO-*$lqf^{\Delta ENTH}$, which expresses only the ENTH domain, and *RO-*$lqf^{\partial ENTH}$, which expresses an ENTH-less Lqf protein, each provide significant rescuing activity.

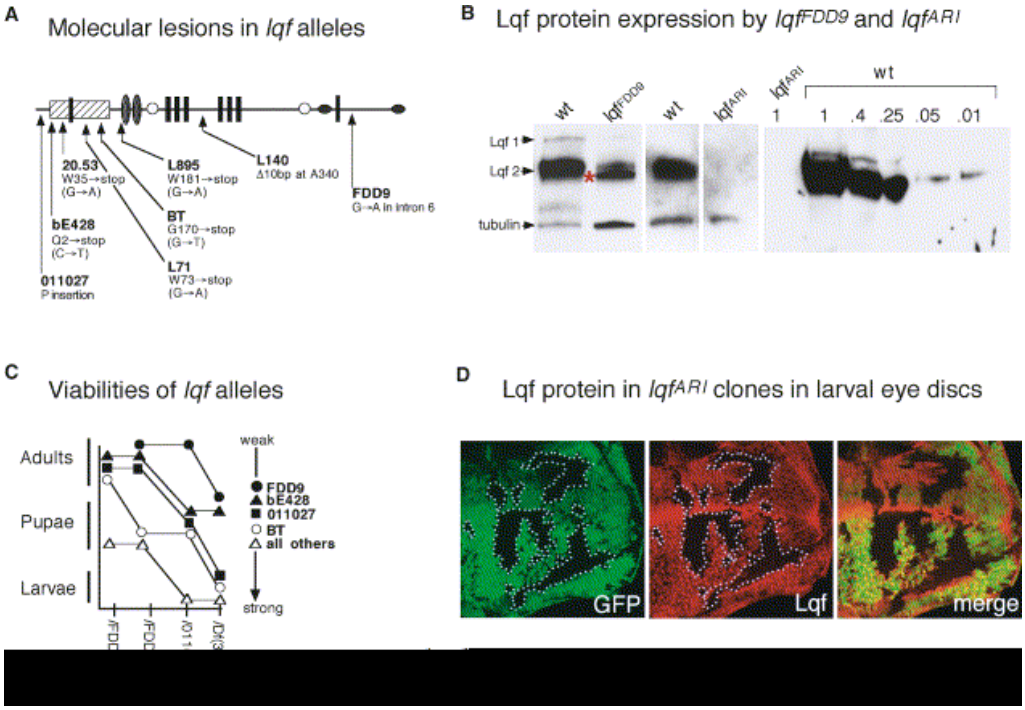

Fig. 4. Genetic and Molecular Analysis of *lqf* Mutant Alleles(A) Nucleotide and resulting amino acid changes in *lqf* mutant alleles are shown. DNA of each mutant allele was amplified by PCR using genomic DNA templates, and the products were subjected to automated flourimetric sequencing. The P element in *lqf 011027* is upstream of the coding region (Cadavid et al. 2000). In *lqf bE428* eye discs, an Lqf protein of a slightly smaller than normal size is produced at 1/10 the wild-type level (data not shown). This result is consistent with translation reinitiation downstream of the nonsense mutation. As the sequence of *lqf FDD9* reveals a single nucleotide change in intron 6 that could generate a cryptic splice acceptor site (AG), the *lqf* mRNA in *lqf FDD9* homozygotes was analyzed by RT-PCR. The presence of a cryptic splice acceptor was confirmed; *lqf FDD9* generates a mutant mRNA, in which the final 12 nt of intron 6 are not spliced out but are included in exon 7.(B) A Western blot of eye disc protein extracts from wild-type (wt) or *lqf FDD9* late third instar larvae grown at 25°C is shown at the left. *lqf FDD9* mutant mRNA (see above) would be expected to encode a truncated Lqf protein, as a stop codon is present 33 nt beyond the extra 12 nt in the mRNA. Consistent with this expectation, a protein smaller than Lqf2 is present in the *lqf FDD9* extracts (marked with a red asterisk). The small amount of normal Lqf2 protein also present presumably comes from low levels of correctly spliced mRNA. To the right, a Western blot of eye disc protein extracts from younger third instar larvae, wild-type, or *lqf ARI* homozygotes is shown. (The younger larvae do not produce Lqf1.) At the far right is a Western blot of protein extracts from whole second instar larvae. The lanes contain protein from 2.5 larvae, and dilutions of the wild-type extract are as indicated. Eye disc and

larval protein extracts were generated and analyzed on protein blots as described (Chen et al. 2002). Lqf was detected with guinea pig anti-Lqf (Chen et al. 2002) at 1:4000 and HRP-conjugated anti-guinea pig (Jackson) at 1:20,000. The antibody to tubulin was mAb E7 (DSHB) at 1:10. (C) The *lqf* alleles shown at the right are ranked as weak to strong on the basis of their viability as *trans* - heterozygotes with three different chromosomes: the temperature-sensitive allele *lqf FDD9* grown at either 18°C (permissive) or 25°C (restrictive), *lqf 011027* , and *Df(3L)pbl-X1* , which uncovers *lqf* . The developmental stage to which the animals survive is indicated. (D) Shown is a third instar larval eye disc with clones of *lqf ARI* cells (outlined), which are marked by the absence of GFP expression (green). The eye discs were labeled with anti-Lqf (red). No Lqf protein is detected in the clones.

The transgene that expresses only the ENTH domain (*RO-lqf*^{ENTH}), and three similar transgenes that express all or part of the C-terminal complement of the protein (*RO-lqf*$^{\Delta ENTH}$, *RO-lqf*$^{\Delta EN1}$, and *RO-lqf*$^{\Delta EN2}$) were also tested for rescue of the Dl endocytosis defect in *lqf*^{FDD9} eye discs. Dl is detected mainly in vesicles in *lqf*^{FDD9} eye discs expressing any one of these transgenes (Figure 1E and data not shown). Thus, either the ENTH domain alone, or an ENTH-less Lqf protein, rescues the patterning and Dl endocytosis defects in *lqf*^{FDD9} homozygous eyes. As experimental results in yeast and in vertebrates have emphasized the importance of the ENTH domain, the most remarkable result is that an ENTH-less Lqf protein can function.

In *lqf*^{FDD9}, a point mutation within an intron generates a cryptic splice acceptor site, resulting in an mRNA that encodes a C-terminally truncated protein (Figure 4A and legend). *lqf*^{FDD9} homozygotes produce low levels of a protein whose size is consistent with the predicted product of the mis-spliced message, and also a small amount of full-length Lqf protein (Figure 4B).

In order to determine whether the rescue results obtained were due to interaction between the partial Lqf proteins expressed by the transgenes and the full-length Lqf proteins present in a lqf^{FDD9} background, we tested the $RO\text{-}lqf^{\Delta ENTH}$ transgene for rescue of the Dl endocytosis and patterning defects in clones homozygous for three different strong mutant alleles: lqf^{L71}, lqf^{L895}, *and* lqf^{ARI}. All three of these alleles are in the strongest class in a genetic assay (Figure 4C). lqf^{L71} bears a nonsense mutation within the ENTH domain, and lqf^{L895} has a nonsense mutation just downstream of the ENTH domain (Figure 4A). lqf^{ARI} has a deletion close to the 3' end of the coding region (Cadavid et al. 2000), but no coding region mutations. $RO\text{-}lqf^{\Delta ENTH}$ rescues the Dl endocytosis and retinal patterning defects in clones homozgyous for each of these strong alleles (Figures 1H and 1K, and data not shown.)

Could there be sufficient full-length or ENTH domain-containing Lqf protein present in all of these backgrounds to influence the interpretation of our results? For example, is it possible that the rescuing activity of $RO\text{-}lqf^{\Delta ENTH}$ is due to titration of negative regulators from small amounts of ENTH-containing Lqf protein present in each of the three strong mutant backgrounds? We argue that this is unikely. First, lqf^{L71} has a nonsense mutation within the ENTH domain (Figure 4A); N-terminal protein fragments, if produced, would contain only a small part of the ENTH domain. Translation of the lqf^{L71} mRNA could reinitiate downstream of the nonsense mutation; the weak allele lqf^{pE428}, which bears a nonsense mutation in codon 2, produces a truncated protein at 1/10 wild-type

levels, consistent with reinitation of translation (Figures 4A, 4C and legend). However, if the mRNA of the strong allele *lqf*^{L71} were to reinitiate translation (the next Met is amino acid 198), the protein produced would be missing the ENTH domain. Second, Lqf protein levels are decreased drastically in all three of the strong alleles tested; in eye discs labeled with anti-Lqf , no Lqf protein is detectable in clones homozygous for any of these alleles (Figure 4D and data not shown.) In addition, for *lqf*^{ARI}, we approximated the maximal fraction of wild-type Lqf protein levels that homozygotes could contain. No Lqf is detected using anti-Lqf in Western blots of protein extracts from *lqf*^{ARI} homozygous larvae (Figure 4B). Moreover, experiments where wild-type and *lqf*^{ARI} eye disc protein extracts were serially diluted indicate that if *lqf*^{ARI} does produce protein, it would produce less than 1/100 of the wild-type amount (Figure 4B). Finally, if the Lqf$^{\Delta ENTH}$ protein is competing negative regulators off of ENTH-domain containing proteins, *RO-lqf*$^{\Delta ENTH}$ expression would be expected to result in a dominant mutant phenotype in an otherwise wild-type background, and it does not. We conclude that the simplest interpretation of the rescue results is that Lqf$^{\Delta ENTH}$ can function independently of the ENTH domain.

Epsins from different species are interchangeable

Transgenes that express Rat epsin1 or human epsin 2b (Figure 2) in *Drosophila* with pRO, each as full-length proteins or without the ENTH domain, rescue the eye defects in *lqf*^{FDD9} homozygotes (data not shown). Thus, there is unlikely to

be a significant functional difference between the *Drosophila* and vertebrate epsins in the region C-terminal to the ENTH domain. In addition, we find that the ENTH domains of Lqf and yeast epsin (Ent1; Figure 2) are functionally similar. It was shown previously that expression of the ENTH domain of Ent1, but not the complementary portion of the protein, restores viability to *ent1Dent2D* yeast (Wendland et al. 1999). Similarly, we find that expression of full-length Lqf or Lqf^{ENTH} rescues *ent1Dent2D* lethality, but Lqf$^{\Delta ENTH}$ expression does not (data not shown).

CONCLUSIONS

We have shown that *Drosophila* epsin, Lqf, is essential for endocytosis of Dl in the developing eye. Moreover, we find that the ENTH domain alone, or an ENTH-less Lqf protein, each retain significant function. The prevailing model in vertebrates is that epsin functions like a bridge, where the ENTH domain links the membrane to clathrin, a cell surface protein to be internalized, and AP-2. As this model requires an intact epsin protein, the results presented here suggest that it cannot be the whole story. Moreover, the observation that either the ENTH domain or the remainder of the protein, which are functionally distinct, can be deleted without destroying Lqf function completely, suggests that each fragment of Lqf may be partially redundant with another *Drosophila* endocytic protein. Candidates include the other ENTH-domain protein in *Drosophila*, Epsin-2 (Lloyd et al. 2000) (Figure 2), and Lap (Zhang et al. 1998), the *Drosophila*

homolog of AP180, which like the ENTH-less Lqf protein, binds clathrin and AP-2.

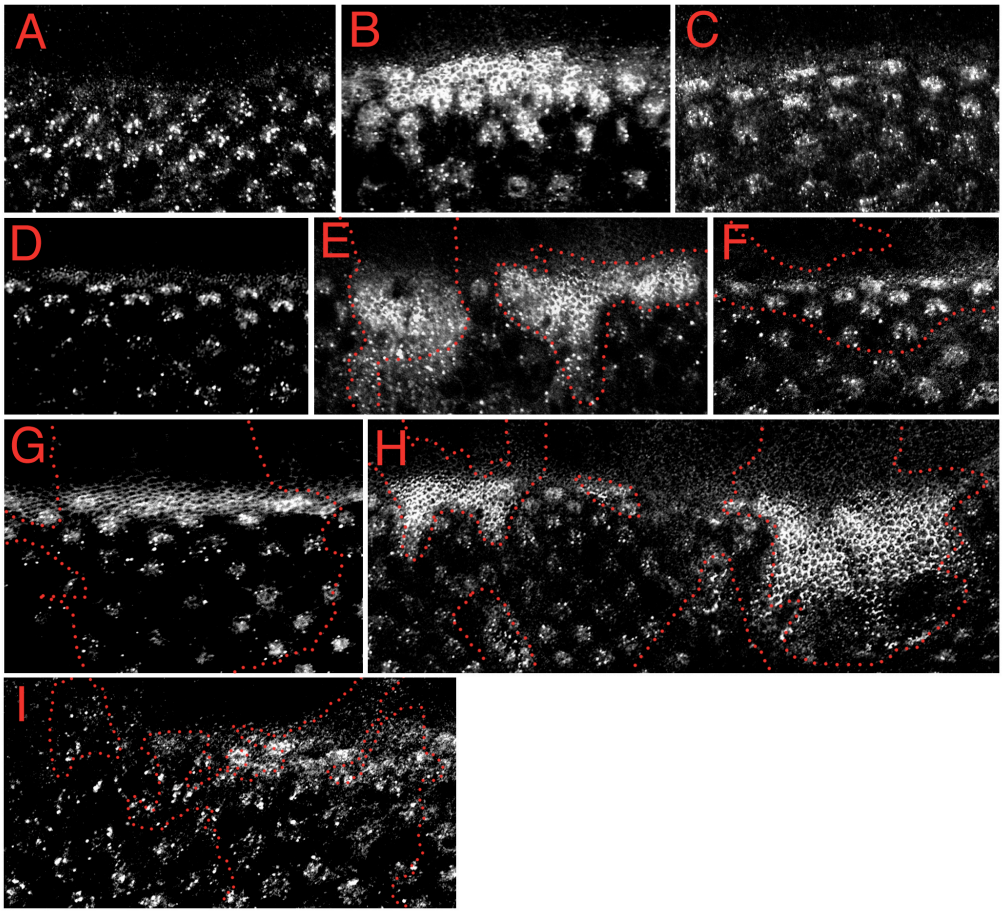

Fig. 5 (Supplemental). Delta expression in eye discs.
Delta expression alone in the panels of Figure 1 are shown here. The red lines mark the clone borders. (A) wild-type (Figure 1A). (B) lqf^{FDD9} (Figure 1C). (C) lqf^{FDD9} + *RO-lqf* (Figure 1D). (D) lqf^{FDD9} + *RO-*lqf^{DENTH} (Figure 1E). (E) lqf^{ARI} (Figure 1F). (F) lqf^{ARI} + *RO-lqf* (Figure 1G). (G) lqf^{ARI} + *RO-*lqf^{DENTH} (Figure 1H). (H) lqf^{L71} (Figure 1L). (I)) lqf^{L71} + *RO-*lqf^{DENTH}.

ADDENDUM TO CHAPTER 3

The ENTH domain of Lqf rescues lqf^{FDD9} quite well. Thus, this part of Lqf can function independently of the C-terminal part of Lqf. However, since this piece of Lqf was not tested for function in a null background, it is hard to say whether or not the ENTH domain function represents an essential function in Delta signaling. Since there is endogenous Lqf protein in lqf^{FDD9} background, it is possible the ENTH domain could be facilitating the function of the endogenous Lqf protein. In order to test if the ENTH domain can provide a function that is essential for Delta endocytosis and signaling, the activity of this protein should be tested in a null background. Since the C-terminal portion of Lqf rescues the null phenotypes of *lqf* loss of function, it seems likely that the C-terminal function of Lqf represents the essential function of Lqf in Delta signaling. These conclusions are discussed further in Chapter 5.

Chapter 4. Drosophila Epsin-R is a Golgi protein essential for development

INTRODUCTION

ENTH (Epsin-N-terminal Homology) domain proteins are a family of proteins thought to mediate packaging of cargo into clathrin coated vesicles at certain cell membranes. They function as clathrin adaptor proteins which link together membranes, cargo molecules and the clathrin coated vesicle machinery. Their function in this process is directly reflected by their modular structures. At their N-terminus, the ENTH domain binds to membranes, while their C-terminal region interacts with cargo, clathrin and coat components.

ENTH proteins are present in genomes from yeast to mammals. Presently, two types of ENTH domain proteins have been characterized: epsins and Epsin-Related (Epsin-R) proteins. Both are thought to mediate the formation of clathrin coated vesicles, but they do so at different subcellular locations. Epsins function at the plasma membrane during clathrin-mediated endocytosis, while Epsin-R works at Golgi membranes and endosomal membranes (Legendre-Guillemin et al. 2004 and see below).

Extensive functional analyses have been performed previously on epsin1 both in cell culture and in multicellular contexts. Cell culture studies have revealed that epsin1 has important roles in endocytosis of ubiquitinated cargo proteins (See chapter 1 for details). The *Drosophila* homolog of epsin1, Liquid facets (Lqf), functions to endocytose ubiquitinated Notch receptor ligands (DSL ligands). This role of epsins is critical for proper Notch signaling during developmental processes (Overstreet et al. 2004; Wang et al. 2004). Interestingly, Lqf potentially has a role in the recycling of ubiquitinated cargo to the plasma membrane (Wang et al. 2004 and see chapters 1 and 2). Importantly, these studies of Lqf in developmental contexts have revealed additional insights into the roles of this ENTH domain protein (i.e. their specificity for DSL ligands) that may have eluded cell biologists.

Epsin-Related was recently identified in mammals and so is only beginning to be characterized. However, it is quite likely that Epsin-R is a clathrin adaptor similar to epsins (Hirst et. al 2003; Wasiak et al. 2003; Mills et al. 2002). Structurally, Epsin-R is similar to epsin1 (Fig. 1). Epsin-R recognizes membranes via its ENTH domain. Epsin-R does not possess ubiquitin interacting motifs and therefore probably does not interact directly with ubiquitinated cargo like epsin1, but may interact with other types of cargo (Mills et. al 2003; Hirst et. al 2003; Wasiak et al. 2002 and see below). At its C-terminus, Epsin-R contains protein interaction motifs for binding coating proteins: clathrin binding motifs (CBM) which binds clathrin and a gamma ear binding region that interacts with

clathrin adaptors AP-1 or GGA (Golgi-localized gamma ear-containing ADP-ribosylation factor-binding) (Fig. 1). AP-1 and GGA mediate clathrin coated vesicle formation at the Golgi. AP-1 also has roles in retrograde traffic to the TGN from endosomes (see below).

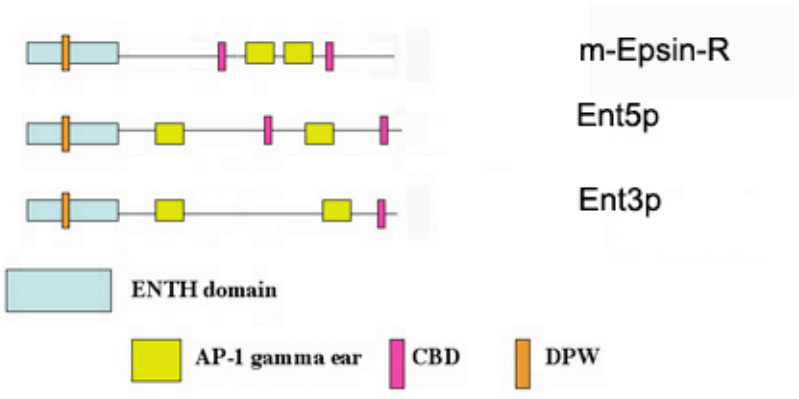

Fig. 1. Structure of mammalian-Epsin-R and potential yeast homologs, Ent5p and Ent3p. The C-terminals region of these proteins have similar protein interaction motifs. The ENTH domains of Ent3p and m-Epsin-R are the most similar to each other chemically. The ENTH domain of Ent5p resembles ANTH domains because it contains several basic residues which are not present in most ENTH domains (Duncan et al. 2003 and see chapter 1). Thus, it is thought that the most likely yeast homolog is Ent3p. However, the issue is not clear because Ent3p and Ent5p seem to have some redundant functions (Eugster et al. 2004).

Functional studies using mammalian cell culture systems also support the notion that Epsin-R normally functions as a clathrin adaptor. Wasiak et al. (2003) found that Epsin-R can stimulate clathrin assembly *in vitro*. Epsin-R co-localizes with a subset of clathrin-coated vesicles (CCVs) in cell culture and can be purified associated with CCVs (Hirst et al. 2003; Mills et al. 2003; Wasiak et al. 2003; Kalthoff et al. 2002). Also, Epsin-R binds to clathrin *in vivo* as Epsin-R

can pull down clathrin from cell extracts (Mills et al. 2003; Wasiak et al. 2003; Kalthoff et al. 2002)

Epsin-R is likely involved in making CCVs at the Golgi complex or endosomes. The ENTH domain of Epsin-R binds to inositol phospholipids, PI(4)P and PI(5)P, that are enriched at these membranes in mammals. Epsin-R also co-localizes with Golgi and endosome markers such as the clathrin adaptors AP-1 and GGA. Epsin-R has binding motifs that bind to GGA and AP-1 gamma ear and Epsin-R physically associates with AP-1 *in vivo* (Mills et al. 2003; Wasiak et al. 2003; Hirst et. al 2003; Kalthoff et al. 2002).

Mechanistically, Epsin-R is thought to function somewhat analogously to epsin1 (see chapters 1 and 4). The ENTH domain might localize the protein to Golgi and endosome compartments. Epsin-R might then recognize cargo proteins and facilitate their incorporation into CCVs by recruiting components of the clathrin machinery at these locations (i.e. AP-1, GGA and clathrin). Since Epsin-R is purified easily with CCVs, it is thought that Epsin-R stays associated with the vesicle after scission.

As described in chapter 1, CCVs formed at the Golgi are used to package cargo destined directly for the lysosome or for endosomes. CCVs formed on endosomes contain cargo destined for several locations including the lysosome, the plasma membrane, and back to the Golgi. Traffic from the endosome to the Golgi, termed retrograde traffic, contains proteins that need to be recycled to the Golgi. Because Epsin-R localizes to both the Golgi and endosomes, it could

function in any one or all of these processes. Indeed, several studies suggest that Epsin-R does have multiple roles in vesicle trafficking as discussed below (Fig. 2).

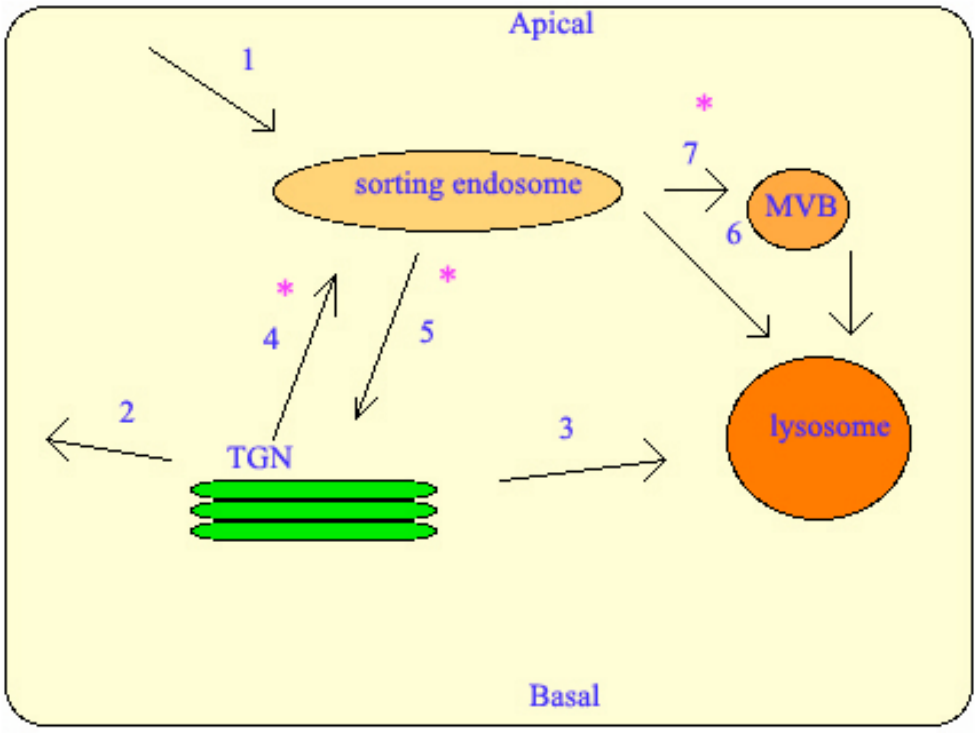

Fig. 2. Clathrin adaptor-dependent vesicle sorting in a polarized epithelial cell. Pathways marked with a purple asterisk indicate possible pathways Epsin-R and homologs may function (see below for details). (1) represents an endocytosis pathway that depends on clathrin adaptors such as epsin1 and AP-2 (see chapter 1). (2) Basolateral plasma membrane trafficking that depends on clathrin adaptor AP-1a (see discussion). (3) Direct trafficking route from Golgi to lysosome mediated by clathrin adaptors AP-3 and AP-4 (see chapter 1). (4) anterograde trafficking from TGN to sorting endosome that is AP-1 and GGA-dependent. (5) Retrograde traffic from endosome to TGN that is AP-1-dependent. (6) Direct trafficking pathway from the sorting endosome to lysosome or lysosome-related organelles mediated by AP-3. (7) Transport or maturation of endosomes into multivesicular bodies mediated by clathrin adaptor Hrs.

What type of cargo might Epsin-R help package into CCVs at the TGN and/or endosomes? Results from other labs suggest that Epsin-R might package cargo proteins at the TGN that will be delivered to late endosomes or lysosomes. Overexpression of *Epsin-R* in COS cells results in abnormal trafficking of CathepsinD to the outside of the cell instead of lysosomes. This result suggests that Epsin-R might have a role an essential role in making CCVs that will ultimately be trafficked to the lysosome (Mills et al. 2003). However, other data suggest that Epsin-R does not have a role in this process or might have a redundant role. Depletion of *D-Epsin-R* using RNAi in COS cells or HeLa cells resulted in no obvious defects in trafficking of CathepsinD to lysosomes (Hirst et. al 2003).

A study by Saint-Pol et al. (2004), suggests that Epsin-R is required for packaging cargo into vesicles that will be delivered to the TGN from early endosomal membranes in retrograde traffic. Overexpression of *Epsin-R* in cell culture impaired retrograde traffic from early endosomes to TGN of several proteins including mannose-6-phosphate receptor and Shiga toxin. Similar results were obtained in *Epsin-R* loss of function using RNAi.

Two recent studies implicate Epsin-R is somehow involved in the trafficking of a particular SNARE, Vti1b, a mammalian protein involved in endosomal fusion (Chidambaram et al. 2004; Hirst et al. 2003). Both studies observed that Epsin-R binds to Vti1b using *in vitro* pull-down assays. This interaction seems to occur through the Epsin-R ENTH domain in mammals as

well as in yeast homologs (Chidambaram et al. 2004). Hirst et al. (2003) demonstrated a functional link between these two proteins. They reported that in the absence of *Epsin-R*, Vti1b is mislocalized in the cell to the cell periphery from where it normally is found in the Golgi. Also, Vti1b is not efficiently incorporated into clathrin coated vesicles in the absence of *Epsin-R.* Exactly how Epsin-R normally traffics or sorts Vti1b is currently a mystery. Since Epsin-R was recently found to function in retrograde transport, the authors speculate that Epsin-R might be needed to sort Vti1b into budding vesicles at late endosomes to be transported back to earlier endosomal compartment where it functions.

A functional link was also observed in yeast. The Vti1b homolog in yeast is involved in trafficking of CCVs from the TGN to the pre-vacuole. Trafficking of carboxypeptidaseY to the prevacuole is reduced in *vti1-1* cells and mutations in the putative Epsin-R homolog, *ent3*Δ, worsen the effect considerably (Chidamdaram et al. 2004).

The putative yeast Epsin-R homologs, Ent3p and Ent5p, share some structural similarity (Fig. 1) with mammalian Epsin-R, but there may be some functional differences. Epsin-R and Ent3p/Ent5p have similar sequence structure consisting of an ENTH domain with characteristic chemical identity and conserved C-terminal binding motifs. However, the ENTH domain of Ent5p might be more similar to an ANTH domain (Duncan et al. 2003). Like Epsin-R, Ent3p and Ent5p bind to the ear appendages of yeast AP-1 and GGA. Ent3p and Ent5p also bind to clathrin and co-localizes with clathrin in vesicular structures.

Finally, Ent3p and Ent5p may also function redundantly in sorting proteins from the TGN to the prevacuolar endosomes. CarboxypeptidaseY is missorted to the plasma membrane instead of to prevacuole in *ent3*Δ*ent5*Δ mutants (Chidambaram et al. 2004; Duncan et. al 2003).

In contrast to Epsin-R, Ent3p and Ent5p bind to PI(3,5)P2 and PI(3)P which are localized to endosomes in yeast. At endosomes, these two proteins might function redundantly in sorting proteins into the lumen of the multivesicular body (MVB) (Eugster et al. 2004; Friant et al. 2003). *ent3*Δ, *ent5*Δ double mutants fail to sort some proteins into the MVB lumen. In one study, Ent3p was shown to form a complex with Ent5p and Vps27p/Hrs. It is speculated that these proteins work together to sort ubiquitinated cargo into lumen of MVBs (Eugster et al. 2004).

To date, Epsin-R analyses have been limited to cell culture experiments and therefore an *in vivo* study of this protein in multicellular context is lacking. Here, I present the first investigation of the Epsin-R homolog during the development of *Drosophila melanogaster*. I find that D-Epsin-R has similar domain structure and sequence identity to mammalian Epsin-R. D-Epsin-R localizes to the Golgi complex like m-Epsin-R. Finally, this protein has important developmental roles, as mutations in *D-Epsin-R* gene are lethal and cause eye development abnormalities. Specifically, clones of *D-Epsin-R* in the adult eye result in facets with smaller than normal photoreceptor cells. These phenotypes are similar to mutations in genes in pathways that regulate cell size or growth.

RESULTS

Drosophila Epsin-R is the homolog of mammalian Epsin-R

The Berkeley Drosophila Genome Project (BDGP) originally identified the *D-Epsin-R* locus (*CG31170)*, named *Epsin-2* or *Epsin-like* at the time. Since the identification of its homologs, most researchers have referred to this protein as *Epsin-R*, which is how I will refer to it from here on. One splice isoform of *D-Epsin-R* was identified by the BDGP, consisting of exons 1-5 and exon 7 (Fig. 3A). I refer to this isoform of *D-Epsin-Rb*. The BDGP isolated several ESTs of the *D-Epsin-Rb* isoform and I was easily able amplify this isoform from *Drosophila* tissue using RT-PCR. Upon closer examination of the genomic sequence, I identified another potential alternate exon (exon 6 in Fig. 3A) which contains a C-terminal stop codon. This exon was originally identified as a separate gene by the BDGP, called *CG31285*, possibly because there is a TATA-like box upstream of this exon. No ESTs from the BDGP were isolated for an isoform of *D-Epsin-R* that contains exon 6. However, Flybase reports that Genescan and Genie, two gene structure analysis programs, predict that exon 6 is a part of the *D-Epsin-R* gene. I confirmed the existence of this isoform, I call *D-Epsin-Ra*, with RT-PCR (data not shown, see materials and methods), and Western blot analyses (Fig. 3D).

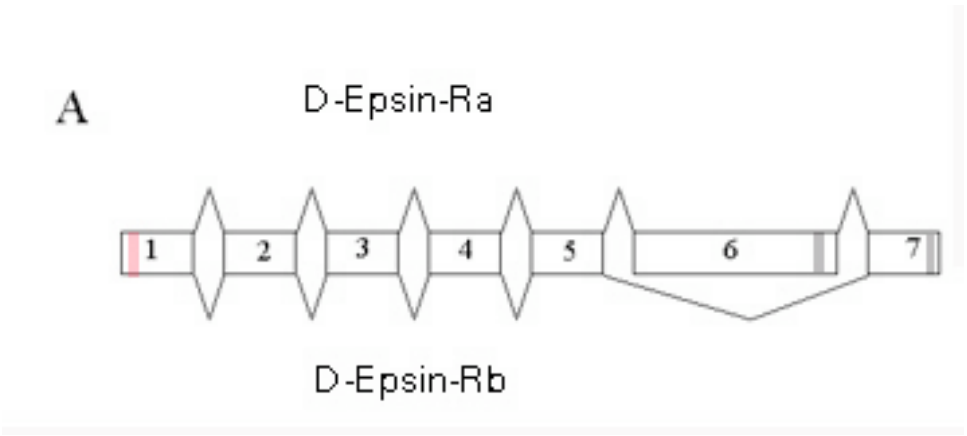
A
D-Epsin-Ra
1
2
3
4
5
6
7
D-Epsin-Rb

B

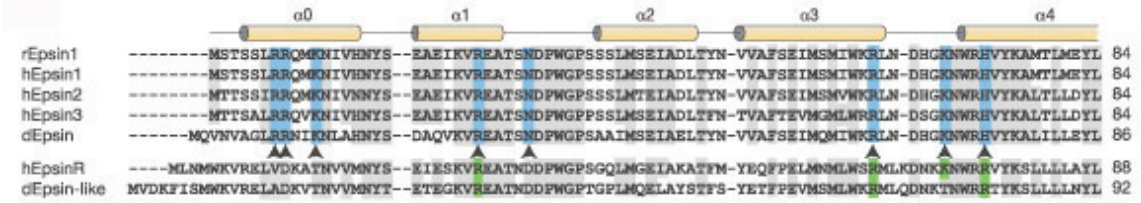
α0
α1
α2
α3
α4
rEpsin1 --------MSTSSLRRQMKNIVHNYS--EAEIKVREATSNDPWGPSSSLMSEIADLTYN-VVAFSEIMSMIWKRLN-DHGKNWRHVYKAMTLMEYL 84
hEpsin1 --------MSTSSLRRQMKNIVHNYS--EAEIKVREATSNDPWGPSSSLMSEIADLTYN-VVAFSEIMSMIWKRLN-DHGKNWRHVYKAMTLMEYL 84
hEpsin2 --------MTTSSIRRQMKNIVNNYS--EAEIKVREATSNDPWGPSSSLMTEIADLTYN-VVAFSEIMSMVWKRLN-DHGKNWRHVYKALTLLDYL 84
hEpsin3 --------MTTSALRRQVKNIVHNYS--EAEIKVREATSNDPWGPPSSLMSEIADLTFN-TVAFTEVMGMLWRRLN-DSGKNWRHVYKALTLLDYL 84
dEpsin ------MQVNVAGLRRNIKNLAHNYS--DAQVKVREATSNDPWGPSAAIMSEIAELTYN-VVAFSEIMQMIWKRLN-DHGKNWRHVYKALILLEYL 86
hEpsinR ----MLNMWKVRKLVDKATNVVMNYS--EIESKVREATNDDPWGPSGQLMGEIAKATFM-YEQFPKLMNMLWSRMLKDNKKNWRRVYKSLLLLAYL 88
dEpsin-like MVDKFISMWKVRELADKVTNVVMNYT--ETEGKVREATNDDPWGPTGPLMQELAYSTFS-YETFPEVMSMLWKRMLQDNKTNWRRTYKSLLLLNYL 92

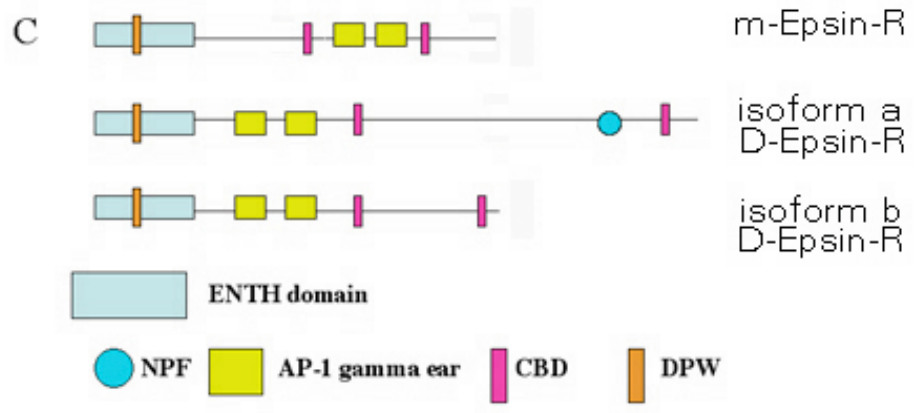
C
m-Epsin-R
isoform a
D-Epsin-R
isoform b
D-Epsin-R
ENTH domain
NPF
AP-1 gamma ear
CBD
DPW

D

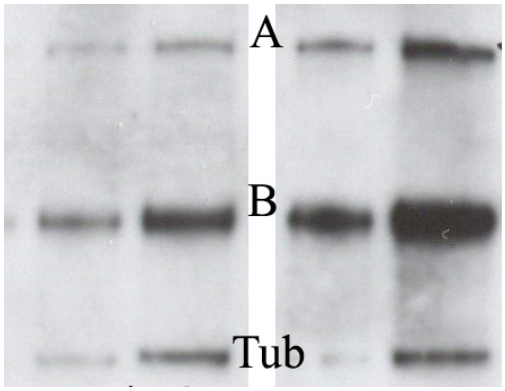

E

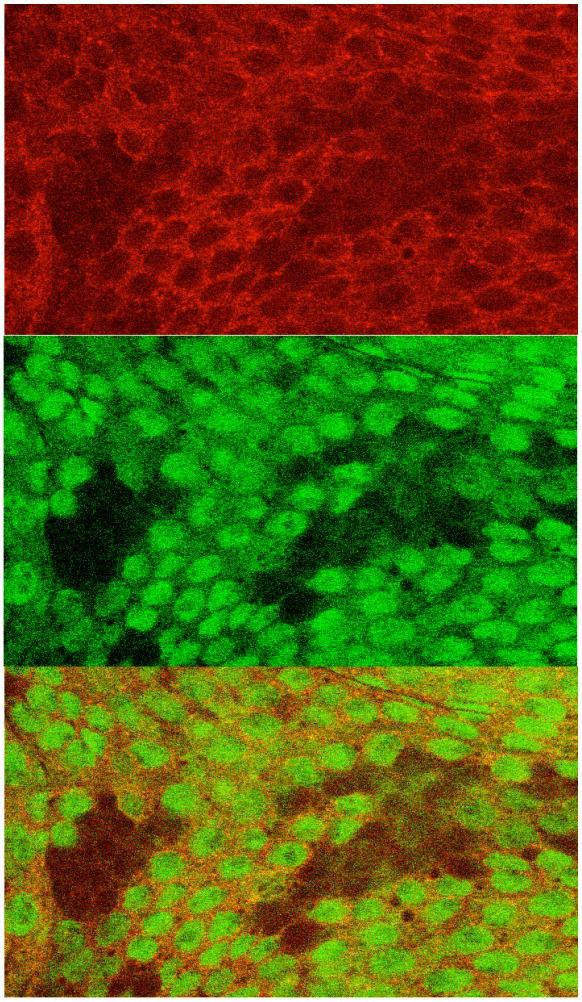

Fig. 3. Molecular analysis of the *D-Epsin-R* gene. (A). Splice isoforms of D-Epsin-Ra and D-Epsin-Rb isolated from *Drosophila* tissue. The red bar indicates the start codon. The gray bars indicate stop codons in exons 6 and 7. (see materials and methods). (B). Sequence alignment of the first part of the ENTH domains of all mammalian epsins , Lqf, human EpsinR and *Drosophila* EpsinR/Epsin-like. Amino acids important for phospholipid binding are colored in blue. Those conserved in EpsinR ENTH domains are colored in green. The positively charged residues R7, R8, K11 and N30 in epsins are not conserved in EpsinR ENTH domains (Figure from Ford et al. 2002) (C). A comparison of the structure of mammalian Epsin-R (Legendre-Guillemin et al. 2004) with the D-Epsin-R splice isoforms. The putative gamma ear binding motif in D-Epsin-R is (EFGDF and EFADF. The consensus is [D/E]FxD[F/W] Mills et al. 2003). Clathrin binding domains may be SFDLF(1) or AFDLF(2) in D-Epsin-Rb.

Clathrin binding domains in D-Epsin-Ra may be SFDLF (1) or LLVNLL(2). (D). Western blot (E). Clones of the *D-Epsin-R* null allele marked by the absence of GFP signal (green) generated in the peripodial epithelium of the eye disc. The disc is co-stained with the antibody to D-Epsin-R (red). For molecular details of the alleles, see below.

Drosophila Epsin-R has significant structural and sequence similarity to mammalian Epsin-R. Both isoforms of D-Epsin-R have an ENTH domain which is remarkably conserved in chemical properties and amino acid sequence to mammalian Epsin-R, but not epsin1 (Fig. 3B). Similar to mammalian Epsin-R, both isoforms of D-Epsin-R have a potential AP-1 gamma ear binding domain. The proposed binding motif responsible for this interaction is the consensus sequence [D/E]FxD[F/W] based on mutagenesis analysis, sequence homology with other gamma ear binding proteins, and sequence conservation in Epsin-R homologs (Mills et al. 2003; Wasiak et al. 2003b). Both isoforms also have putative CBMs. Mills et al. (2003) and Kalthoff et al. (2002) proposed that the sequences DLVDLF or DLFDLM might bind clathrin, based on mutagenesis analysis and the chemical similarity to conventional CBMs. D-Epsin-R isoforms contain two similar clathrin binding motifs. The D-Epsin-Ra isoform also contains an additional potential clathrin binding motif and one NPF motif, which are known to bind EH-domain containing proteins (e.g. Eps15 or gamma synergin both of which bind to AP-1) (Wendler and Tooze 2001) (Fig 3C).

Mammalian Epsin-R localizes to the Golgi complex and endosomes in mammalian cell culture. To test if D-Epsin-R has a similar subcellular

localization, an antibody was raised against the region of D-Epsin-R containing the first five exons (see materials and methods), the region common to both isoforms. The antibody was tested for specificity using mutant backgrounds (Fig 3D and E). *Drosophila* eye discs were stained with the D-Epsin-R antibody and co-stained with known Golgi markers such as p120 (Stanley et al. 1997) and Lava lamp (Lva) (Sisson et al. 2000). In eye discs extensively co-localizes with Golgi markers (Fig. 5 A and B). D-Epsin-R co-localizes very well with p120, which marks the TGN and to a lesser extent with Lva. D-Epsin-R does not localize to the plasma membrane in the disc proper like Lqf/epsin1 (data not shown). In the third instar eye disc, D-Epsin-R protein (and p120) is located only in the basal part of the disc where it colocalizes with Golgi markers. In contrast, Lva localizes evenly to all parts of the cell. D-Epsin-R is also highly expressed in the peripodial epithelium (Fig. 4).

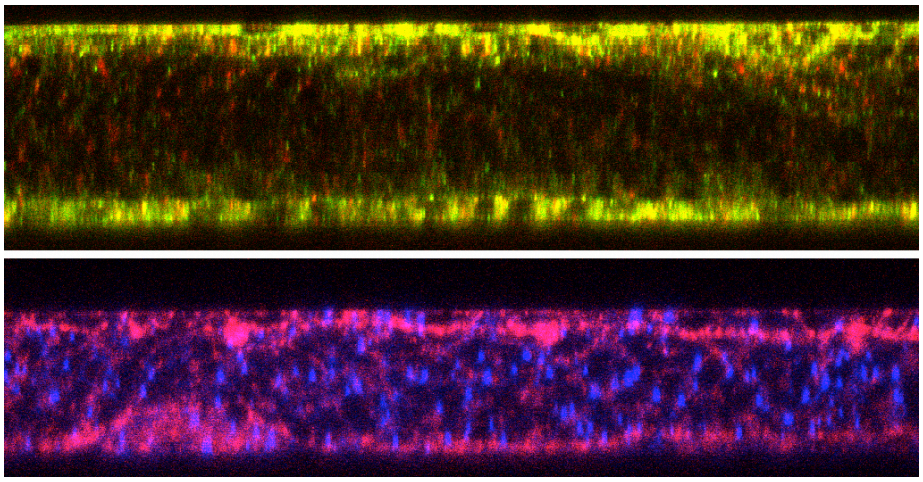

Fig. 4. Localization of Golgi proteins in eye discs. Shown are Z-sections of confocal images of eye discs labeled with antibodies to Golgi proteins. In each panel, the discs are oriented so that the peripodial epithelium is at the top and the basal part of the disc proper is at the bottom. In the top panel, the eye disc is labeled with p120 (red) and D-Epsin-R (green). Yellow indicates spatial overlap. The bottom panel the disc is labeled with phalloidin which marks actin (red) and Lva (blue).

D-Epsin-R is similar to mammalian Epsin-R both structurally and by amino acid sequence. D-Epsin-R also has a similar sub-cellular localization with mammalian Epsin-R. Thus, I conclude that D-Epsin-R is the homolog of mammalian-Epsin-R.

A

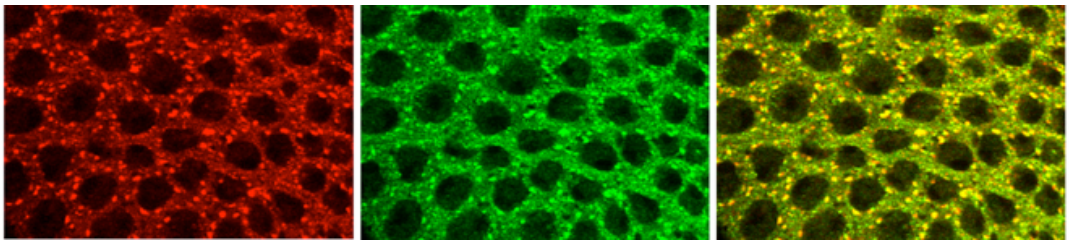

B

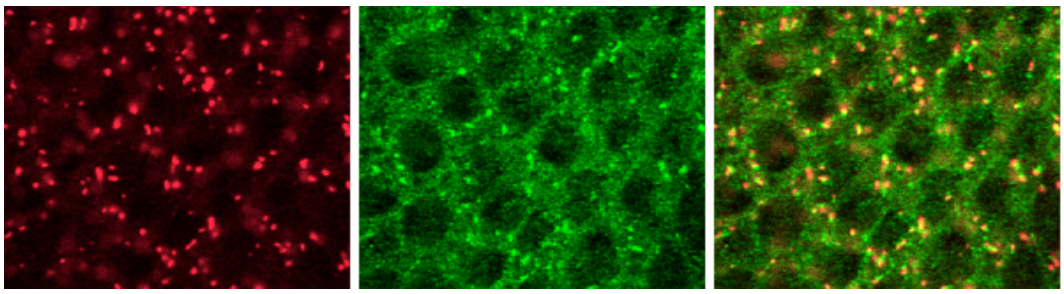

Fig. 5. D-Epsin-R co-localizes with Golgi markers (A and B) in the peripodial epithelium of the developing eye disc. (A). From left to right. TGN marker p120 in red and D-Epsin-R in green. In the merge, yellow indicates spatial overlap. (B). From left to right. Golgin Lava Lamp in red and D-Epsin-R in green. In the merge, yellow indicates overlap.

Drosophila Epsin-R is an essential protein

To understand the developmental and cellular roles of D-Epsin-R, I wanted to observe its mutant phenotypes. The BDGP generated a P-element insertion in the 5'UTR of *D-Epsin-R* gene (see materials and methods and Fig 3). This insertion is homozygous lethal at 25 degrees Celcius and the flies typically die fully formed in their pupal cases. The allele is temperature sensitive as homozygotes appear normal at 18 degrees Celcius. I determined that this allele retains residual D-Epsin-R protein activity because some endogenous full-length protein is still produced, though at much lower levels than normal (Fig. 3D). I hypothesize that this allele is hypomorphic, a simple partial-loss-of-function. The phenotypes associated with this insertion are caused by loss of *D-Epsin-R* activity because overexpression of a *D-Epsin-Ra* cDNA using UASt expression vector and an *Actin5C-Gal4* driver rescues the homozygotes to wild-type.

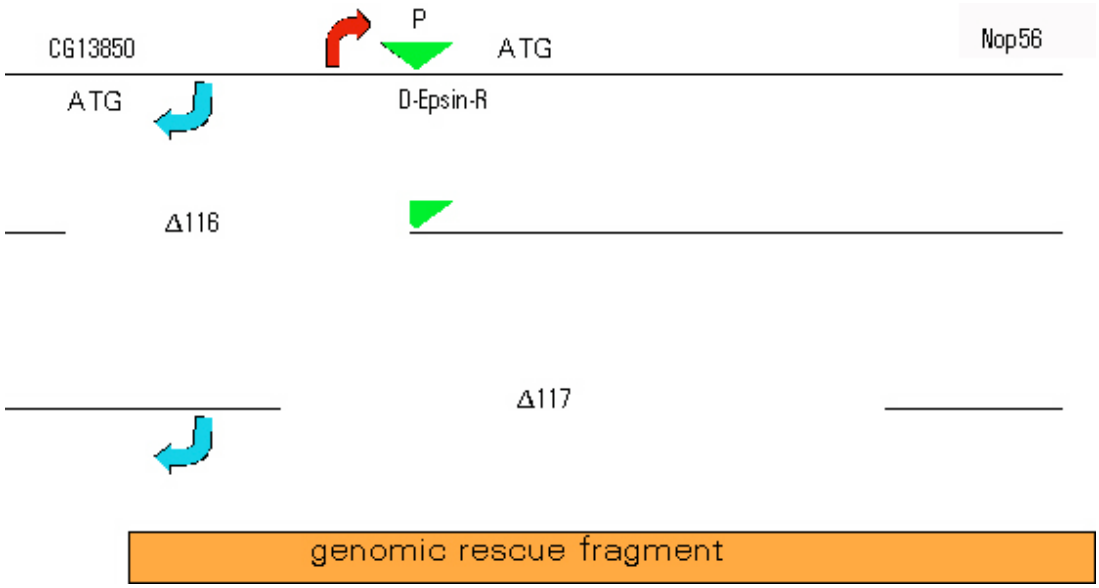

Fig. 6. Molecular characterization of *D-Epsin-R* mutant alleles and genomic rescue fragment. Not drawn to scale. The following is a description of positional information of molecular markers relative to the *D-Epsin-R* putative translation start arbitrarily chosen to be position 1. The final exon in *D-Epsin-R* ends at +7617 downstream. The original P-element is inserted at –94 bp upstream. *D-Epsin-R* TATA box begins at –255 upstream. *CG13850* putative translation start is positioned at –776. The allele Δ116 breakpoints are between –1171 to –94. This allele retains about 1000 bp of P-element sequences. The allele Δ117 breakpoints are-469 to +4081. The genomic rescue fragment breakpoints are –663 to 10905.

In order to generate a null allele, imprecise excisions at the *D-Epsin-R* locus were generated from "hopping out" the P-element using an *in vivo* transposase (see materials and methods). Two useful alleles, Δ116 and Δ117 (Fig 6) were obtained. Both of these alleles are genetically stronger than the original insertion as homozygotes die at the third instar larval stage. PCR analysis defined the breakpoints of these alleles. Both Δ116 and Δ117 delete the transcription start site of *D-Epsin-R*, which might account for their similar allelic strengths. Δ117 is the best candidate for a null allele because it deletes most of the *D-Epsin-R* gene.

Indeed, this allele produces no D-Epsin-R protein (Fig 3D). However, Δ117 also deletes near the 5' region of the neighboring gene, *CG13850,* and thus might affect the expression of *CG13850*. Therefore, the lethal phenotype might be due to a lesion in either *CG13850* or *D-Epsin-R* or both genes.

To distinguish among these possibilities, I performed two types of rescue experiments. First, I constructed a genomic fragment which contains *D-Epsin-R*, the 3' gene *Nop56*, and only a few base pairs of the putative 5' UTR of *CG13850* (see materials and methods and Fig 6). Flies containing two copies of this genomic fragment and homozygous for the Δ117 allele, live to adulthood and appear normal. Second, a *D-Epsin-Ra* cDNA expressed with UASt vector and an *Actin5C-Gal4* driver rescues homozygotes of the Δ117 allele to wild-type. Thus, this allele is a genuine null allele of *D-Epsin-R* and the lethality is due only to a loss of *D-Epsin-R* function.

D-Epsin-R is essential for normal eye development

The *Drosophila* compound eye is a useful system to study developmental processes (see chapter 1). Therefore, if *D-Epsin-R* has any roles in regulating eye development, this system would be advantageous to study the *D-Epsin-R* cellular function. To assess if *D-Epsin-R* is required in the developing eye, I used the GMR-hid technique to generate eye discs entirely mutant for the hypomorphic insertion allele, *D-Epsin-R*^{p} (Stowers et al. 1999 and see materials and methods). A fly of the genotype *EyGal4>UAS-Flp (referred to as EGUF)/+; FRT82B,*

GMR-hid, cl /FRT82B, D-Epsin-R^{P} resulted in adult flies whose outer eye appears very rough, with a characteristic "kidney-eye" phenotype; that is, an indention at the anterior edge (Fig. 7 C and D). Using the same technique, I generated eyes completely mutant for the null allele, D-Epsin-R$^{\Delta 117}$. Consistent with the idea that this allele is stronger than the P-allele, these fly eyes are much smaller and generate very few ommatidia (data not shown). Thus, *D-Epsin-R* does have important roles in regulating some aspect(s) of eye development.

As a first step toward understanding the phenotype, I generated clones of cells homozygous for the null allele, Δ117, in the eye disc during third larval instar stage using the FLP/FRT system (see materials and methods). The homozygous mutant tissue is marked by the absence of the *white* gene, which results in the elimination of pigment granules in the adult eye. In tangential sections of adult eyes, *D-Epsin-R* mutant photoreceptor cells are identifiable because they do not contain pigment granules associated with their rhabdomeres (Fig 7A and B). Examination of the rhabodomere morphology reveals that mutant cells appear considerably smaller than wild-type neighbors in mosaic facets, though they usually appear to be in the correct spatial position in the facet. However, I did not examine photoreceptorr cell body size directly. Sometimes, entirely mutant ommatidia are found that are several times smaller than normal facets, but otherwise normal in appearance. These data suggest that *D-Epsin-R* has a role in regulation of cell size or growth. Consistent with this idea, *D-Epsin-R* null mutant clones are relatively small in size.

In *D-Epsin-R* null mutant clones, I also observe two other interesting phenotypes. In mosaic facets, cells are often missing, therefore, it is also possible that *D-Epsin-R* might also have a role in cell survival. Additionally, all phenotypes observed appear cell autonomous. Wild-type cells did not rescue the cell size defects of their mutant neighbors.

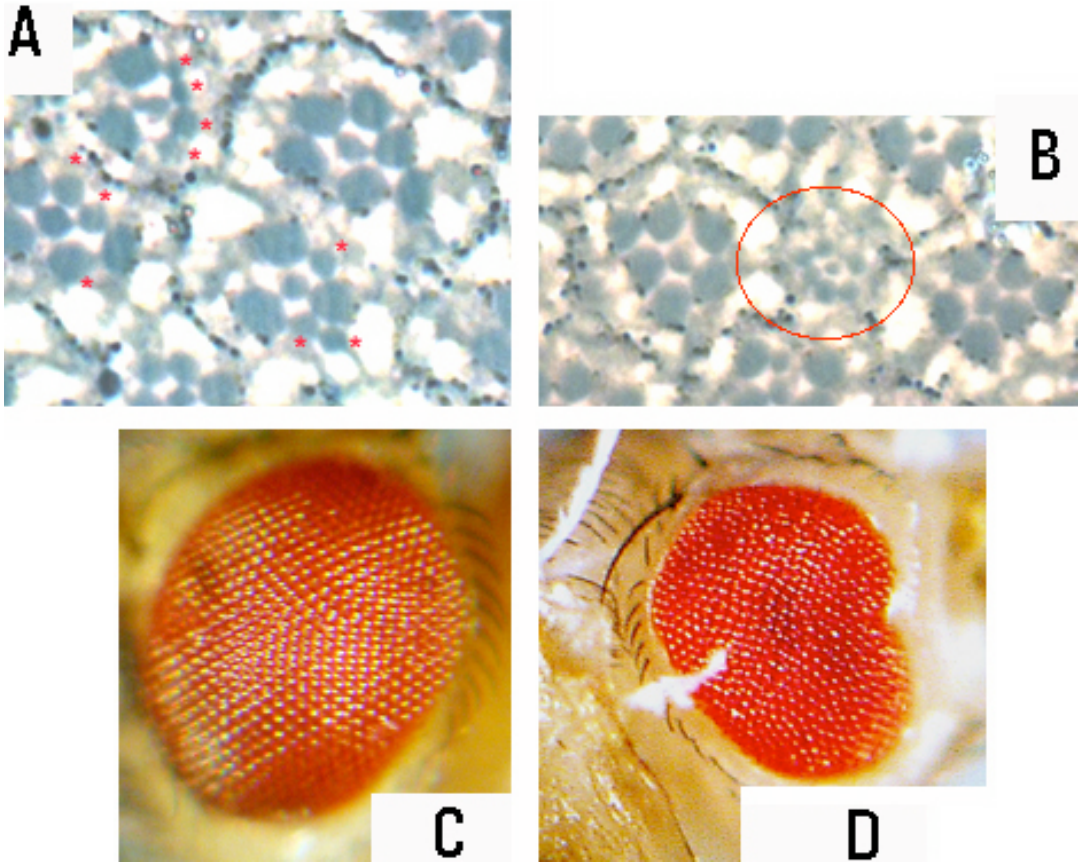

Fig. 7. Analysis of *D-Epsin-R* mutant eye phenotypes. A and B are tangential sections of adult eyes with homozygous mutant clones of *D-Epsin-R*$^{\Delta 117}$. The mutant cells, which have rhabdomeres without pigment granules are marked by a red asterisk (A). In (B), an entirely mutant ommatidium is circled in red. (C) Wild-type adult outer eye morphology. (D) Adult eye made entirely mutant for *D-Epsin-R*^{P} using GMR-hid technique. The outer eye morphology is rough and there is an anterior indentation which results in the kidney bean shape.

Clones of the hypomorphic allele generated in the developing eye disc result in adult eye phenotypes that are similar to the null allele. Tangential sections of adult eyes containing mutant clones of this genotype generate facets with some smaller rhabodomeres and some missing rhabodomeres. However, the phenotypes are far less penetrant than the null allele. Unlike the null clones, clones homozygous for the weak allele are relatively large. Interestingly, when clones of the hypomorphic allele are generated in this manner, they result in no obvious morphological defects or roughness on the outside of the eye (data not shown). In contrast, when the entire eye is made to be homozygous for the hypomorphic allele, (see above and Fig. 1D), the eye appears very rough. One possible interpretation of this data, is that D-Epsin-R has a function outside of the eye, perhaps in the peripodial epithelium (see discussion), though other interpretations are possible.

The spatial and temporal requirements of *D-Epsin-R* during eye development

Understanding when and where *D-Epsin-R* activity is needed during eye patterning will help to understand its developmental role. I wanted to figure out in what cells *D-Epsin*-R was required during eye development. To do this, several rescue assays were performed using *D-Epsin-Ra* cDNA expressed under the control of various promoters that drive expression at different times and places

during eye development. In this way, I hoped to pinpoint the developmental timepoint where *D-Epsin-R* activity is required.

First, I generated eyes completely mutant for the null allele, *D-Epsin-R*$^{\Delta 117}$ using the technique described above and flies of the following genotype: *EyGal4>UAS-Flp/+; FRT82B, GMR-hid, cl /FRT82B, D-Epsin-R*$^{\Delta 117}$. I observed complete rescue of the eye phenotype upon simultaneous expression of *D-EpsinRa-GFP* (and without GFP) cDNA with UASt and driven by the *EyGal4* promoter. The *Ey* promoter expresses in all cells in the first and second instar eye discs. In the third instar disc, it is expressed in the peripodial epithelium and in all undifferentiated cells ahead of the furrow. Therefore, I initially thought this result suggested that *D-Epsin-R* was not required posterior to the furrow in the differentiating cells. Consistent with this idea, expression of *D-Epsin-Ra-GFP* cDNA with UASt vector driven by *GMR-gal4* is unable to rescue the eye phenotype of *D-Epsin-R* null eyes (in this experiment, *Ey-Flp* was used to make the clones instead of EGUF). The *GMR* promoter expresses highly in all cells posterior to the furrow, except in the precluster cells in the first few rows near the furrow (our unpublished results).

Interestingly, I found that expression of *D-Epsin-Ra* cDNA using the RO-HS promoter (Huang and Fischer-Vize 1996; Cadavid et al. 2000; Overstreet et al. 2003) strongly suppresses the *D-Epsin-R* null eye phenotype. Expression with this vector is limited to R-cells 2/3/4/5 beginning in precluster cells near the

furrow (Overstreet et al. 2004). This result suggests there is a requirement for *D-Epsin-R* posterior to the furrow in photoreceptor cells.

This result seems in conflict with the previous result that *EyGal4* expression could give full rescue. I wondered if expression with the *EyGal4* driver ahead of the furrow might be perduring long enough to persist in cells behind the furrow. To test this idea, *D-epsin-Ra-GFP* was expressed with *Ey-Gal4*. I observed there was some persistence of expression well behind the furrow with this driver about 5-6 rows and there was low level persistence in all cells behind the furrow (Fig. 8). This could be due to stability of the D-Epsin-Ra-GFP protein or leaky expression of the *EyGal4* driver.

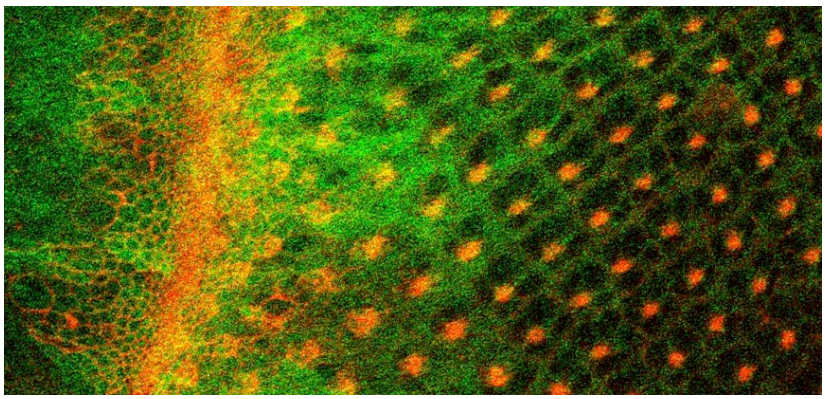

Fig. 8. D-Epsin-Ra-GFP protein persists past the furrow when expressed with *EyGal4*. Shown here is an eye disc stained with phalloidin in red to mark actin which labels the furrow. The eye disc is oriented anterior to the left and posterior to the right. D-Epsin-Ra-GFP is in green. There is a higher level of D-Epsin-Ra-GFP signal in the first 5-6 rows posterior to the furrow, though there is a low level of GFP signal in subsequent rows. *Ey* promoter seems to express highly in the peripodial epithelium but somewhat weaker in the undifferentiated cells anterior to the furrow (data not shown).

A *D-Epsin-Ra* cDNA also rescues the *D-Epsin-R* null eye phenotype when expressed with *EyGal4*. I did not observe the expression of this protein directly and thus there is a possibility its stability or expression is different from that observed with D-Epsin-Ra-GFP. In any case, from this data I cannot rule out the possibility that *D-Epsin-R* has roles in the differentiating cells behind the furrow. Given all these data, I think it is likely that the critical function of *D-Epsin-R* is at the morphogenetic furrow and/or in the precluster cells.

DISCUSSION

I have presented the first study of the homolog of mammalian-Epsin-R in a multicellular and developmental context. Several consclusions can be drawn from this work. First, I find that D-Epsin-R is the homolog of mammalian Epsin-R. These proteins are similar in sequence and structure and have similar subcellular localization at the Golgi complex. Thus, it is likely that D-Epsin-R participates in making CCVs at the Golgi complex and/or endosomes possibly to package specific cargo molecules. Second, D-Epsin-R is an essential protein as loss of *D-Epsin-R* results in developmental abnormalities and third larval instar lethality. Finally, the *D-epsin-R* null eye phenotypes are very specific and indicate that this protein may have specialized functions in the cell, as does the related ENTH domain protein, Liquid facets (Overstreet et al. 2004).

Establishing that D-Epsin-R is a homolog of mammalian Epsin-R is only the first step toward understanding this protein's function. The next step will be to exploit the powerful genetics of *Drosophila* to resolve precisely the cellular and developmental roles of this protein. In the mean-time, the *D-Epsin-R* mutant phenotypes might give important clues to its developmental functions. Loss of function in *D-Epsin-R* results in phenotypes reminiscent of cell growth defects, such as the Insulin receptor pathway (Oldham and Hafen 2003). Perhaps D-Epsin-R regulates trafficking of membrane components involved in regulating cell growth. Since the developmental eye phenotypes in null mutants is cell autonomous, I might expect that D-Epsin-R is regulating trafficking of proteins in signal receiving cells.

I am currently testing directly if *D-Epsin-R* regulates the Insulin pathway in two ways. First, I will see if the Insulin receptor (InR) protein localization is altered in *D-Epsin-R* mutant backgrounds. A commercially available antibody to human InR (Cell Signal) cross-reacts with the *Drosophila* protein. Thus, I may be able to use this antibody to monitor D-InR subcellular localization. Second, I will try to rescue *D-Epsin-R* mutant phenotypes by overexpressing the wild-type form of InR or a constitutively active form of InR. If trafficking of InR to the plasma membrane is not as efficient in backgrounds where *D-Epsin-R* function is impaired, then increasing the level of InR might overcome this problem. It is entirely possible that D-Epsin-R could affect membrane trafficking of many proteins in a general and non-specific way that would also result in impaired

growth. In the future, the best way to uncover the cellular role of D-Epsin-R may be to do a screen for genetic modifiers of the hypomorphic allele of *D-Epsin-R*.

Another way to gain insight into the developmental function of *D-Epsin-R* is to determine where in the eye its activity is required. From the mosaic rescue experiments, I pinpointed a critical requirement for *D-Epsin-R* function near the furrow and/or posterior to the furrow in precluster cells. Because expression of *D-EpsinRa* cDNA with *RO-HS* does not fully rescue, D-Epsin-R does have requirements in other parts of the eye. *Ey-Gal4* expression of *D-Epsin-Ra* fully rescues, but this might be because of D-Epsin-Ra persistence past the furrow. The persistence posterior to the furrow at high levels is only for about 5 to 6 rows. However, I do not know for sure if this reflects the activity of wild-type *D-EpsinRa* cDNA (without GFP), which also rescues. Nonetheless, given this data, I propose that the other requirements for *D-Epsin-R* in the eye are likely to be at the furrow or in the posterior rows near the furrow. Alternately it is possible that the other requirement for D-Epsin-R could be ahead of the furrow or in the peripodial epithelium, where *Ey* also expresses.

The *D-Epsin-R* hypomorphic mutant phenotype might also represent another function for *D-Epsin-R* and indicate where *D-Epsin-R* function is required. Unlike the null allele, the hypomorphic allele does not grossly perturb cell differentiation or cell size in the eye but, it does affect the general morphology of the eye. Adult eyes entirely mutant for this allele are rough and kidney-shaped. The “kidney-eye” phenotype is often associated with defects in

morphogenetic furrow movement (Thomas and Ingram 2003). Thus, *D-Epsin-R* would seem to regulate the movement of the furrow as indicated by the hypomorphic phenotype as well as cell size as revealed by the null phenotype.

I am performing experiments now to determine if the movement of the furrow is affected in *D-Epsin-R* mutant clones in the disc proper. Preliminary results suggest that the furrow movement is not affected in *D-Epsin-R* null clones in the disc proper that cross the furrow. If *D-Epsin-R* is controlling furrow movement, then it might be doing so at a location outside the disc proper, perhaps in the peripodial epithelium (PE). Interestingly, it was recently shown that signaling from the PE regulates growth and size of the eye (Gibson et al. 2000; Cho et al. 2000). If *D-Epsin-R* is regulating furrow movement from outside of the eye, this suggests that one important function of *D-Epsin-R* is in the PE, while another important function may be in cells near the furrow.

D-Epsin-R homologs mediate the formation of CCVs. It is likely that D-Epsin-R also functions as clathrin adaptor because it also has clathrin binding motifs and motifs that bind to other clathrin adaptors. However, I am currently working on a more direct way to test this possibility. First, I am testing if D-Epsin-R puncta co-localize with clathrin-light-chain (clc) positive puncta. I will express clc fused to GFP (Chang et al. 2002) in *Drosophila* tissues and co-stain with the antibody to D-Epsin-R. Second, I am testing if mutations in the *chc* gene genetically interact with *D-Epsin-R* mutants. If D-Epsin-R is in the clathrin

pathway, then a reduction in *chc* function should dominantly enhance *D-Epsin-R* hypomorphic allele phenotypes.

Finally, since D-Epsin-R has gamma ear binding domains, this protein probably interacts with the clathrin adaptor AP-1 and GGA *in vivo*. These adaptors are thought to have very general roles in the cells in making CCVs at Golgi and endosome. However, it was shown recently that a certain splice isoform of the mammalian AP-1 subunit mediates basolateral sorting in polarized epithelial cells (Folsch et al. 2003). AP-1a isoform localizes to the TGN and regulates the trafficking of membrane proteins to be transported to the basolateral surface in epithelial cells. D-Epsin-R localization in the eye disc is polarized to the basal part of the eye disc. Thus, it is an intriguing possibility that D-Epsin-R might regulate basolateral sorting of certain membrane proteins.

The *Drosophila* genome encodes two ENTH domain proteins, Lqf and D-Epsin-R. Lqf has been previously shown to have a rather specific role in regulating Notch and Delta signaling (Overstreet et al. 2004; Wang et al. 2004; Tian et al. 2004). Surprisingly, the phenotypes of *D-Epsin-R* in the eye also seem to be specific. Thus, this work raises the possibility that ENTH domain proteins are important components of specific signaling pathways. In conclusion, this work sets the stage for future experiments that will determine the precise cellular role of D-Epsin-R.

Chapter 5. Examination of the role of ENTH domains in localization and function

INTRODUCTION

Clathrin adaptors, epsin1 and Epsin-R, possess N-terminal ENTH domains that bind to membranes by recognizing certain types of inositol phospholipids. The most popular model suggests that ENTH domains bind to specific types of PIPs thereby localizing epsin1 and Epsin-R proteins to discrete subcellular membrane locations. The C-terminal portion of these proteins binds to clathrin coat components and probably cargo. Thus, ENTH domain proteins link membranes to the clathrin coating machinery and specific cargo. Currently, there is some debate in the literature about whether or not the ENTH domain is absolutely needed for localization and/or function (see below). In this chapter, I address this issue by investigating whether or not the ENTH domain of the *Drosophila* homolog of epsin1, Liquid facets (Lqf), is required for localization and if the ENTH domain of *Drosophila* Epsin-R is required for subcellular localization and function.

ENTH domain structure

The ENTH domain is a stretch of about 150 conserved amino acids at the N-terminus of epsin1 and Epsin-R. The ENTH domain of rat epsin-1

preferentially binds to $PI(4,5)P_2$ (Itoh et al. 2001) while the ENTH domain of Epsin-R preferentially binds to PI(4)P and PI(5)P in some assays (Hirst et. al 2003 and Mills et al. 2003). These types of inositol phospholipids are enriched at different cellular membranes: $PI(4,5)P_2$ at the plasma membrane and PI(4)P and PI(5)P are enriched at Golgi and endosomal membranes in mammals. It is not clear if the membrane concentrations of PIP are the same in *Drosophila*.

PIP binding and membrane curvature

The secondary structure of the ENTH domain consists of 8 alpha-helices of which the first four helices bind to particular phosphoinositol (PIP) molecules. Crystal structures of the ENTH domain of rat epsin-1 have pinpointed the amino acids responsible for recognition of the distinct inositol phospholipids. Eight highly conserved amino acid residues, mostly positively charged, are responsible for binding to PI(4,5)P2, which is enriched at the plasma membrane. (R7, R8, K11, R25, N30, R63, K69, H73 and see chapter 4 figure 1B). Upon binding to PIPs, another alpha-helix becomes ordered. It is speculated that this helix inserts into the membrane and induces curvature of the membrane (Ford et al. 2002).

Some of the positively charged amino acids are not conserved in the ENTH domain of Epsin-R. The ENTH domain of Epsin-R is less positively charged and therefore is theorized to preferentially exclude highly phosphorylated PIPs and instead bind less phosphorylated PIPs, such as PI(4)P and PI(5)P (Itoh et. al 2001, Mills et al. 2003, and Ford et al. 2002). However, this may not be true

in yeast, because the ENTH domain of the putative Epsin-R homolog, Ent3p, binds to PI(3,5)P2, which is enriched on prevacuolar endosomes (Friant et al. 2003).

ENTH domains as locators

There is some evidence that the ENTH domains of epsins and Epsin-R proteins are required for proper subcellular localization. Full-length Myc-tagged-epsin-1 normally localizes at the plasma membrane in punctate structures. These structures are thought to be clathrin coated pits that have not invaginated and pinched off into the cytoplasm. Similarly, the myc-tagged Epsin-1 ENTH domain localizes at the cortex in tubular structures. However, a myc-tagged ENTH-less version appears cytoplasmic in vertebrate cell culture (Ford et al. 2002). Thus, the ENTH domain of epsin1 is thought to localize the host protein to discrete puncta at the cortex.

Full-length Epsin-R (myc-tagged or GFP-tagged) locates to the Golgi and endosomal structures, as does the Epsin-R ENTH domain alone (Hirst et al. 2003; Mills et al. 2003; Wasiak et al. 2003). However, the localization of the ENTH-less version is not clear as a few studies observed different results. In two studies, a tagged ENTH-less Epsin-R does not localize to any distinct part of the cell and appears only to be cytoplasmic (Hirst et al. 2003; Mills et al. 2003). This result differs from another by Wasiak et al. (2003). They found that GFP-tagged ENTH-less Epsin-R still localizes to endosomal structures and concentrates to

clathrin enriched membrane fractions suggesting that C-terminal domain, downstream of the ENTH domain, contains localizing sequences as well. Therefore, the function of Epsin-R ENTH domain in localization remains to be determined.

Functional assays for ENTH domains

If the ENTH domain is required for proper subcellular localization, then, it must also be required for function. If the host protein is not localized to the correct membrane, the C-terminal will not be able to interact properly with clathrin coating complex. The ENTH domain of yeast epsin definitely is required for function (see below). However, whether or not the ENTH domain is required for function in vertebrates is unclear.

In yeast, ENTH domains have quite convincingly been shown to be required for yeast function in maintaining viability. Yeast cells doubly mutant for *ent1*Δ and *ent2*Δ , the yeast epsin1 homologs, die. Interestingly, the ENTH domain of Ent1p can rescue this lethal phenotype, but an ENTH-less version cannot (Wendland et al. 1999). Recently, Duncan et al. (2003) reported that the ENTH domain of yeast Epsin-R homolog, Ent3p was sufficient to rescue the viability of *ent3*Δ, *ent5*Δ double mutants, but the ENTH-less protein could not. Thus, in yeast, ENTH domains are not only necessary for function, they are sufficient.

To date, functional analyses of ENTH domain proteins in vertebrates have been limited to cell culture experiments using overexpression assays and dominant negative phenotypes which make interpretations difficult (Itoh et al. 2001; and see chapter 3). Itoh et al. 2001 showed that the full-length epsin1 when overexpressed does not interfere with clathrin-mediated endocytosis. However, an ENTH-less epsin1 or an epsin1 that cannot bind to the plasma membrane does interfere with endocytosis when overexpressed in cell culture. The authors speculate that these proteins are cytoplasmic and are titrating away core components of the endocytic machinery and preventing them from functioning. Ideally, functional and structural analysis of ENTH domain proteins should be performed in loss-of-function backgrounds where each domain of these proteins can be tested for activity by assaying for rescue of a specific phenotype or function.

One such functional analysis was developed by me in *Drosophila*. Using an *in vivo* rescue assay, I showed that that an ENTH-less epsin (Lqf) in *Drosophila* retains significant activity in the endocytosis and signaling of Delta (see chapter 3 and Overstreet et al. 2003). Thus, the ENTH-less protein can supply the essential Lqf function in Delta signaling.

Interestingly, the ENTH domain alone also retained function, suggesting this region of the protein has an independent function from the C-terminal region. However, the ENTH domain was not tested in a null background like the ENTH-less protein. Therefore, it is hard to say whether it can provide an essetial Lqf

function in Delta endocytosis/signaling in the absence of endogenous Lqf/epsin1. For example, the ENTH-domain function might facilitate the function of the endogenous Lqf in the hypomorpic background (see below).

Nevertheless, these results suggest that Lqf/epsin1 has two independent functions in endocytosis Delta: an ENTH domain function and an ENTH-less protein function. If the two parts of epsin have independent functions, then what are the functions? Biochemical analyses suggest that the C-terminal, ENTH-less region participates in coat formation. *In vitro*, the ENTH-less portion can stimulate clathrin assembly (Kalthoff et al. 2002b).

The ENTH domain may have several functions in addition to localizing the protein. Ford et al. (2002) showed that the ENTH domain can tubularize lipids, suggesting this region actively participates in invagination during budding assembly. Also, the ENTH domain may participate in protein-protein interactions as the ENTH domain of epsin1 has been shown to bind to two proteins including PLZF (a transcription factor) and tubulin (Hussain et al. 2003). Recently, the Epsin-R ENTH domain was shown to bind to the SNARE protein, Vti1b (Chidambaram et al. 2002). The significance of these ENTH-protein interactions is a mystery.

New assays for localization and function in *Drosophila*

Because of the differences in the literature regarding the requirements of the ENTH domain in localization and function, I decided to perform a series of

experiments to investigate this issue further. In the first part of this chapter, I analyze the role of the ENTH domain of Epsin-R in function and localization. I also perform experiments to address the question of whether or not ENTH domains are strong protein locators. Finally, I analyze the subcellular localization of the functional Lqf pieces, defined in chapter 3, in order to determine if their independent functions are in the same region of the cell. Some of the experiments described in this chapter are incomplete and so where needed, I have indicated what needs to be done in the near future to complete them.

RESULTS

The ENTH domain of D-Epsin-R is not required for function

To assess whether the ENTH domain of D-Epsin-R is required or is sufficient for function, I performed a structure/function analysis. The full-length D-Epsin-Ra (with or without a 3'GFP tag) rescues the null *D-Epsin-R* mutant when expressed in a UASt vector and driven by the *Actin5C-Gal4* promoter (see chapter 4). To test if the ENTH domain or D-Epsin-R or an ENTH-less version can also function, I constructed 3' GFP tagged versions of these proteins (Fig. 2). When expressed under the control of *Actin5CGal4*, I find that the ENTH-less D-Epsin-Ra rescues all phenotypes completely, while the ENTH domain alone retains no rescuing ability, even though it is expressed very well, as I can detect high levels of GFP signal (data not shown and Fig 1). It is possible that the GFP

tag is interfering with its ability of the ENTH domain to function. Thus, this experiment should be performed without a tag as well. Nonetheless, the ENTH-less version rescues, indicating that the ENTH domain of D-Epsin-R is not required for function of this protein *in vivo*.

Is the ENTH domain required for proper subcellular localization? To test this the GFP tagged pieces of D-Epsin-R were expressed using the *Actin5Cgal4* driver and assessed for subcellular localization relative to characterized markers in the developing eye disc (Fig. 2). I used the developing eye disc in this assay because I am most interested in the functions of this protein during eye development and thus its localization in the eye will have direct bearing on its function in the eye. However, it might be instructive to perform a similar analysis in other tissues and I plan to do this in the future.

The full-length 3' GFP tagged D-Epsin-R locates to the cytoplasm and p120 positive Golgi structures in the peripodial epithelium (Fig. 1) and in the disc proper of the developing eye disc (data not shown), similar to the antibody staining pattern (see chapter 4). In the disc proper, D-Epsin-R-GFP was distributed throughout the entire disc, not localized basally like the endogenous protein. This might be due to overexpression with a strong promoter. The ENTH domain alone, 3' GFP-tagged, locates to the nucleus, cytoplasm and p120 positive Golgi structures. The nuclear localization of the ENTH domain is an unexpected result. Currently, the significance of this localization if any is unknown. It is possible this protein diffuses into the nuclei of cells simply because it is relatively

small (about 35kDa). In the future, I will look at the subcellular localization of the ENTH-less version.

A

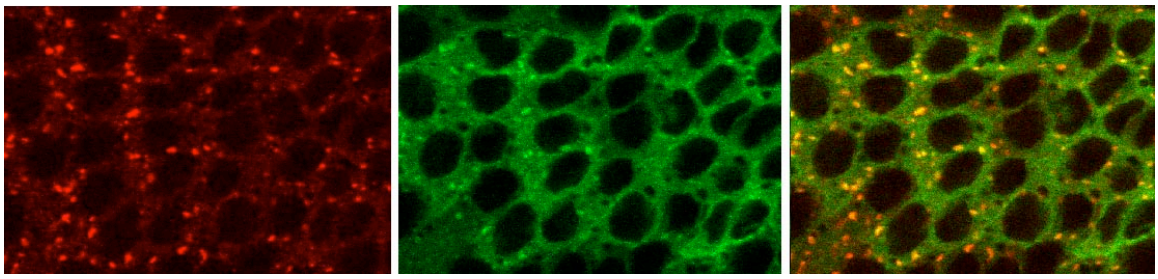

B

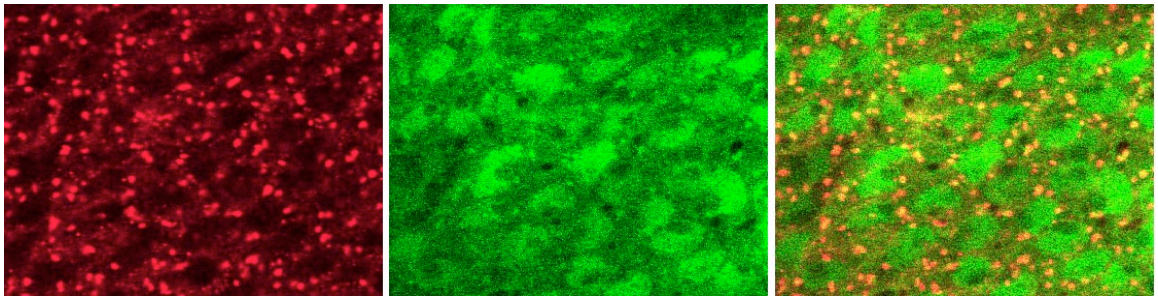

Fig. 1. Localization of GFP tagged D-Epsin-R pieces in the peripodial epithelium. (A). D-Epsin-Ra-GFP expressed with Actin5CGal4 driver (green), colocalizes with p120 (red) in puncta and in the cytoplasm. Far right panel is the merge and yellow indicates overlap. (B) D-Epsin-R-ENTH-GFP (green) localizes to the nuclei, cytoplasm and p120 (red) puncta. In the merge, yellow indicates overlap.

The ENTH domains are not strong locators

Do the ENTH domains of Lqf and D-Epsin-R act as strong locators? To test this idea, I engineered chimeric proteins in which the ENTH domains of Lqf and D-Epsin-R are interchanged (Fig. 2). If switching the ENTH domains of Lqf and D-Epsin-R profoundly alters subcellular localization, then function should be

affected too. To test if these chimeras retained any function, I performed an *in vivo* rescue assay. I found that the C-terminus of D-Epsin-R fused to the ENTH domain of Lqf expressed with UASt vector driven by *Act5Cgal4* promoter rescues the null phenotypes of *D-Epsin-R* mutants, but not lqf^{FDD9} mutants. Conversely, the chimera with Lqf C-terminus fused to the ENTH domain of D-Epsin-R rescues *lqf* phenotypes using the *rough* promoter (Overstreet et al. 2003 and see chapter 3). These data suggest that fusion of the C-terminal regions of these proteins to a heterologous ENTH domain does not alter their localization enough to interfere with their functions (data not shown).

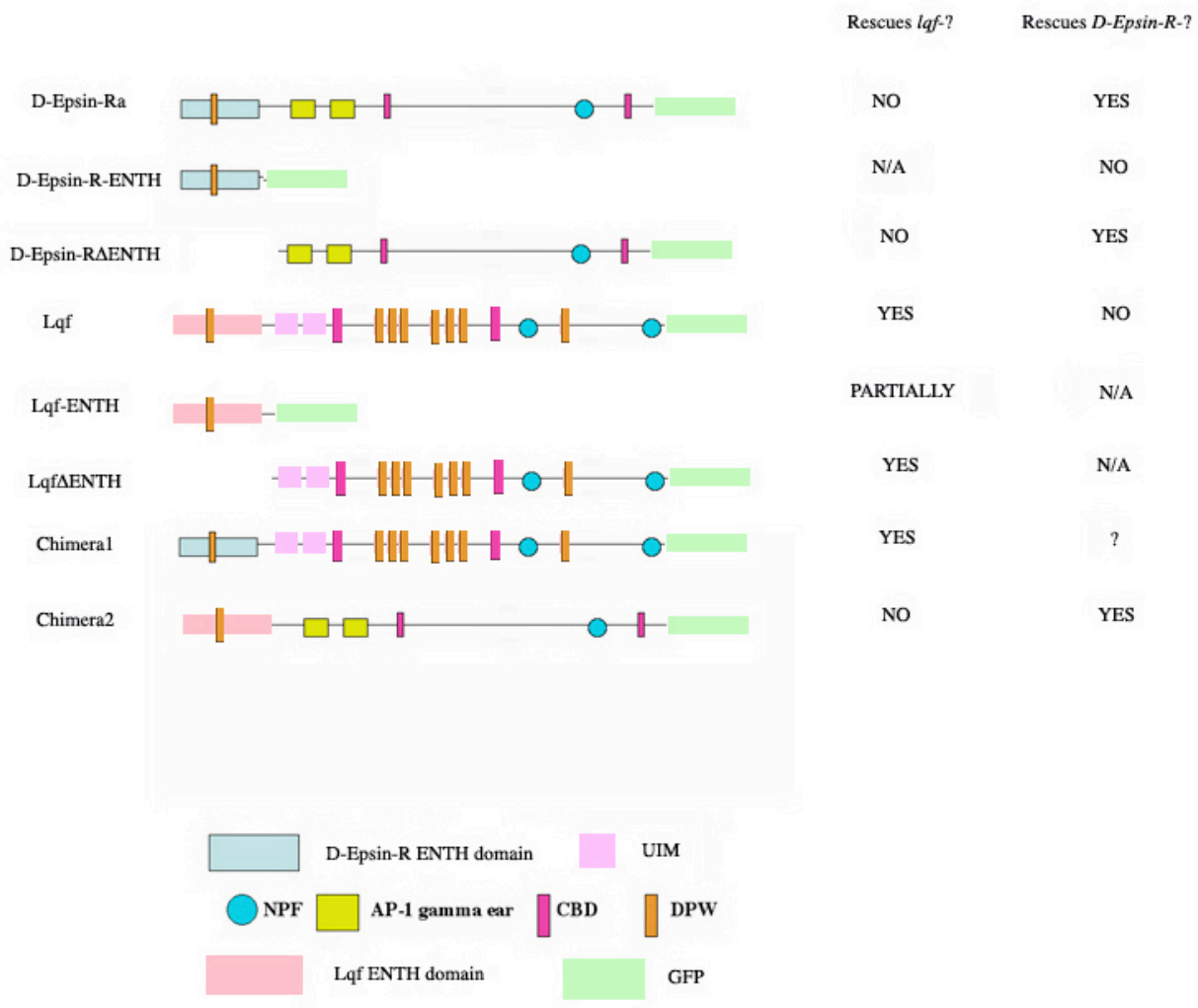

Fig. 2. D-Epsin-R and Lqf 3'GFP tagged constructs. N/A indicates that an experiment has not been performed. ? indicates that the experiment will be performed in the near future. To the right is indicated whether or not the proteins rescue with the promoters described in the text. N.B. the Lqf-ENTH-GFP rescues partially using 2 copies of the transgene. This is a similar result from the analysis presented in chapter 3 (Overstreet et al 2003). Perhaps this protein is unstable like the ENTH-domain constructs without GFP, even though I can detect a high level of GFP expression. Thus, it is possible that increasing the protein concentration in this background (by increasing transgene number) might increase the degree of rescue.

Currently, I am performing experiments to monitor the subcellular localizations of these chimeras in the developing eye disc. Preliminary results

suggest that the ENTH domain of D-Epsin-R does not re-localize ENTH-less Lqf away from the apical plasma membrane and into Golgi structures. However, the ENTH domain of Lqf might re-localize a portion of D-Epsin-R from the Golgi to the plasma membrane.

ENTH-less Lqf/epsin1 may have a vesicular function

One major conclusion from the structure/function analysis of Lqf (Overstreet et al. 2003) is that the ENTH domain of Lqf and the ENTH-less Lqf protein each have independent functions in endocytosis and can function independently of each other. Originally it was thought that these two pieces might have redundant functions since they both rescue the same phenotype, however this seems unlikely since the two Lqf pieces have completely different structures. Also, as I did not test the Lqf ENTH domain for rescue of *lqf* null phenotypes, it is hard to say whether this domain supplies an essential Lqf function in Delta endocytosis/signaling. It may rescue *lqf* hypomorphs somehow by aiding the endogenous full-length protein present in that lqf^{FDD9} mutant background. Thus, it is more likely, these two pieces have independent functions and that the ENTH-less function is the essential function (see below).

If the two parts of Lqf have independent functions in endocytosis, these two functions might be sequential, at two different steps at the same cellular location. Alternatively, the two parts of Lqf might function at two different locations in the endocytosis pathway. In the first case, both Lqf parts should co-

localize subcellularly to the same place. In the second case, the Lqf parts might localize to different regions of the cell along the endocytic pathway.

To distinguish between these alternatives, I constructed functional 3'GFP-tagged full-length, ENTH and ENTH-less Lqf proteins (Fig. 2). They are functional because they are able to rescue *lqf* mutants when expressed under the control of *RO-HS* promoter as described in Overstreet et al. (2003). I expressed these pieces with several different Gal4 drivers and assessed their subcellular localization in the developing eye disc.

The ENTH domain of Lqf when expressed under the control of the *Actin5C-Gal4* promoter locates to the apical plasma membrane where it co-localizes with actin marked by phalloidin staining (Fig 3A). Some GFP signal is diffuse in the cytoplasm. Similar results were obtained with GMR-gal4 and RO-HS drivers (data not shown), however co-localization of the ENTH-GFP signal at the plasma membrane is easily observable when expressed at the furrow, using the *Actin-5CGal4* driver and not as apparent when expressed in other parts of the disc using other drivers.

A

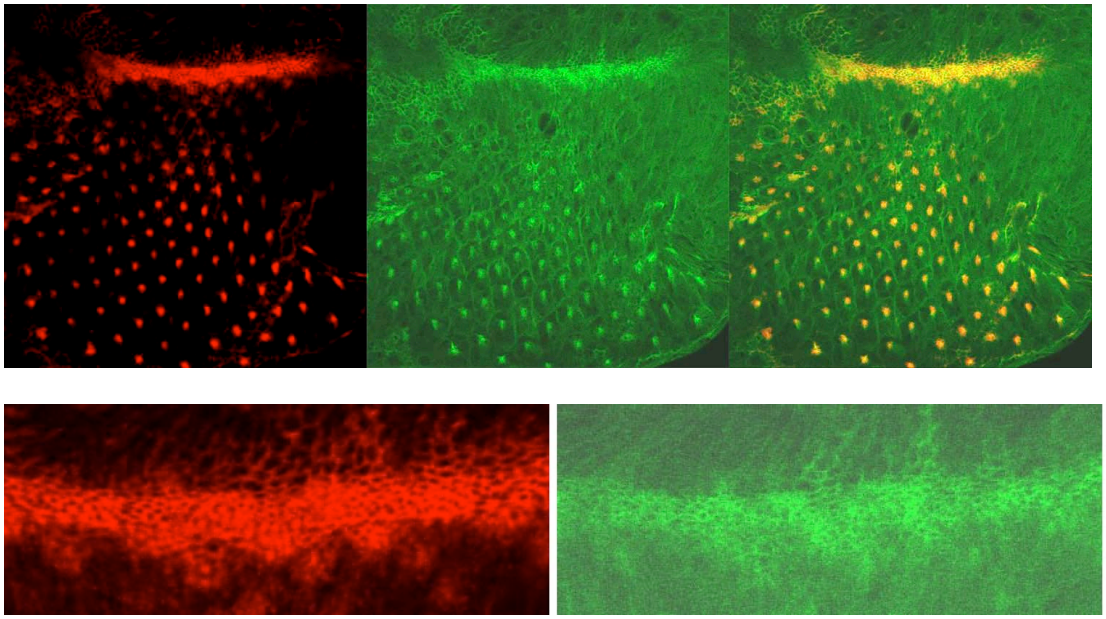

B

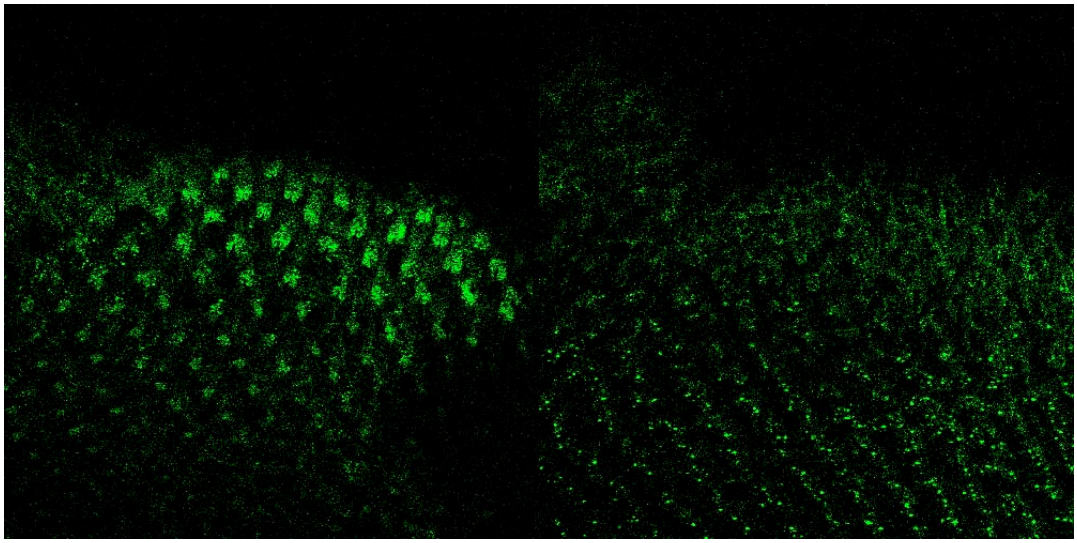

C

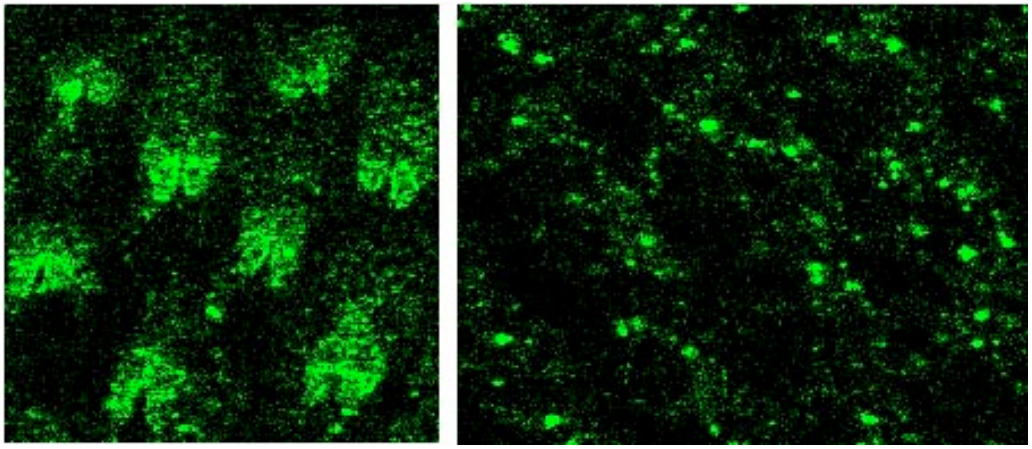

D

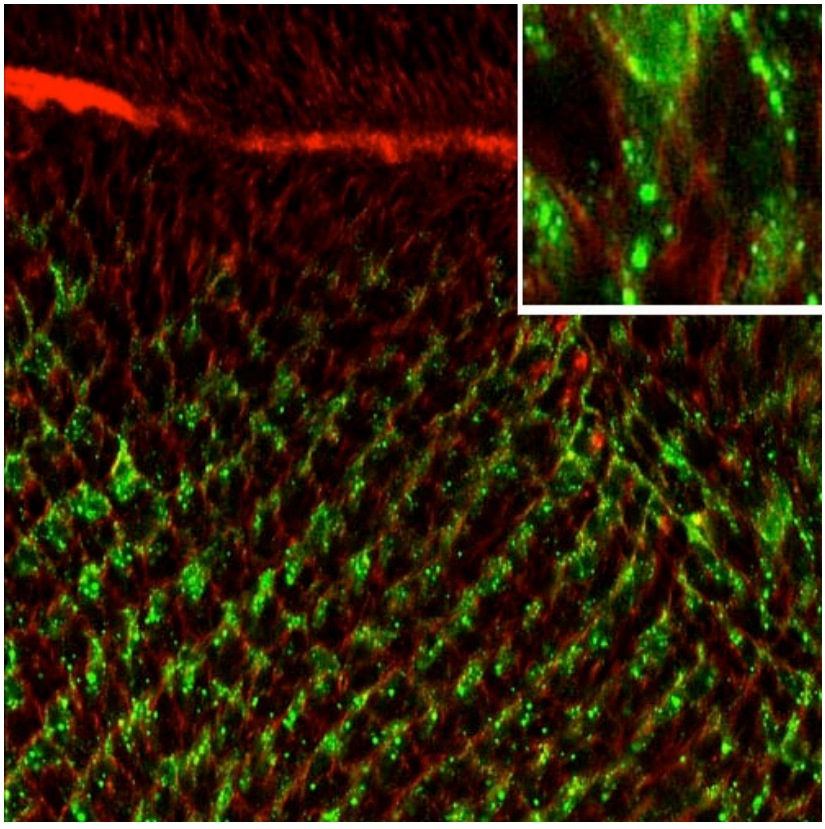

Fig. 3. Localization of GFP-tagged Lqf pieces in the disc proper. Shown are third instar eye discs oriented with anterior side up. (A) Lqf-ENTH-GFP expressed with the *Actin5CGal4* driver (green) co-localizes with actin (red) at the plasma membrane. In the right panel, yellow indicates overlap. Below is a close-up view of the localization at the furrow (B). RO-HS-Lqf-GFP in green. Expression is limited to R-cells 2/3/4/5. In the first panel, this is an apical view near the morphogenetic furrow. The GFP signal weakly outlines the apical membranes of R-cells. GFP also localizes to apical vesicle-like structures. (B). Basal section of the same disc. Larger vesicular structures of Lqf-GFP are seen in the most posterior part of the disc. (C) The first panel is a close up view of the Lqf-GFP signal at the plasma membrane in R-cells 2/3/4/5 from the disc in (B) The second panel is a close up view of the basal Lqf-GFP structures from the disc in (B) (D) LqfΔENTH-GFP expressed with GMR-Gal4 driver in green. Actin is marked by phalloidin in red. Most of the GFP signal is seen in small apical vesicular structures (not shown) and larger basal vesicular structures (shown). Inset is 10X zoom of the basal vesicles in this disc.

The full-length Lqf protein localization differs from the ENTH domain localization. When expressed with the *RO-HS* promoter, this protein does appear to locate weakly to the plasma membrane in R-cells 2/3/4/5 (Fig. 3B). However, it locates mainly to vesicle-like structures. The Lqf-GFP vesicles appear to fall into two different categories. Near the apical membrane of the disc, the Lqf-GFP puncta are small and numerous. In the basal part of the disc, the Lqf-GFP vesicles are larger and fewer in number. The basal vesicles accumulate in the posterior part of the disc after about row 6 or 7 (Fig. 3B). Similar results were obtained with *GMR-Gal4* expression, although the plasma membrane localization was less apparent. Unfortunately, I could not express this construct with *Actin5CGal4* driver because flies carrying both transgenes die.

The ENTH-less Lqf-GFP protein has a similar localization as the full-length protein when expressed with *GMR-Gal4*. The GFP signal accumulates in

small puncta apically near the plasma membrane (data not shown) and in larger puncta basally (Fig. 3D). When expressed with the rough promoter, the ENTH-less-Lqf-GFP protein locates to the plasma membrane in R-cells 2/3/4/5 near the morphogenetic furrow. It also locates to vesicular structures. Thus, the ENTH-less protein can localize to the plasma membrane independently of the ENTH domain (data not shown).

Using this assay, I have observed two distinct subcellular localizations, an apical plasma membrane location and a vesicular location. As the ENTH domain localizes prominently to the plasma membrane, it seems likely that it has a function there. However, as the full-length and ENTH-less versions locate to vesicles, it is possible Lqf has a distinct function at this site. Thus, using this analysis, I may have spatially identified the two functions of the Lqf pieces: a plasma membrane function and a vesicular function.

These results are very surprising because we have never observed a vesicular distribution for Lqf using the anti-Lqf antibody (Chen et al. 2002), even though others have seen epsin in vesicles (see below). Why does the Lqf-GFP localization differ from the Lqf antibody staining pattern? One possibility is that Lqf is normally in vesicles at a low level that escapes detection by the antibody and tagging Lqf with GFP may stabilize Lqf in vesicles. Another possibility is that the Lqf-GFP structures represent an artifact caused by the GFP tag. Sometimes GFP tags induce oligomerization that can result in cytoplasmic accumulation and mislocalization of proteins (Zacharias 2002). Therefore, the

GFP tag could destabilize the ENTH domain association with the membrane and force the protein into vesicles where it wouldn't normally be found. However, the GFP tagged Lqf proteins rescue the mutants when expressed with *RO-HS* promoter, indicating that they are functional, so at least some of the protein must be properly localized.

Others have reported a vesicular localization for epsins. These reports indicate that epsin vesicles are early endosomes or forming clathrin coated pits (CCPs) at the plasma membrane (Ford et al. 2002). Perhaps the smaller Lqf-GFP vesicles near the apical membrane are early endosome or nascent CCPs. The larger Lqf-GFP vesicles appear to be distinct from this class of epsin vesicles because they are located much more basally in the eye disc than early endosomes would be.

The basal Lqf-GFP vesicles may represent a late endocytic compartment, perhaps after the early endosomes have fused. If this is the case, then the fact that Lqf-GFP resides in these vesicles might indicate Lqf has a function there. To date, no one has described a function for epsins post-internalization or away from the plasma membrane. Thus, I want to investigate this possibility further.

If the basal Lqf-GFP vesicles represent a legitimate endocytic compartment, as opposed to cytoplasmic protein aggregation, then they would localize subcellularly with endocytic markers. As Lqf is implicated in Delta endocytosis, I first tested if these vesicles co-localize with Delta endosomes, the multivesicular bodies (MVBs) where Delta is seen in the eye disc. Delta MVBs,

which are located near the apical plasma membrane above the photoreceptor nuclei, are readily detected by staining with an antibody against the extracellular domain of Delta. Most of the large Lqf-GFP vesicles localize closer to the nuclei, slightly more basal than Delta MVBs (data not shown). Thus, the basal Lqf-GFP vesicles appear to occupy a separate compartment from the Delta containing MVBs. The small apical Lqf-GFP puncta do not co-localize with Delta positive MVBs either.

In the near future, I will test if the Lqf-GFP vesicles co-localize with other markers that localize to distinct endocytic compartments in the developing eye. Rab proteins are small GTPases that serve various functions along the endocytic pathway. Individual Rab proteins have distinct functions at separate endocytic compartments. As a result, they localize to discrete subcellular regions of the cell that define particular endocytic compartments. Several GFP-tagged Rab proteins are available for marking these compartments: GFP-Rab5 marks early endosomes (Wucherpfennig et al. 2003), GFP-Rab7 (Entchev et al. 2000) marks late endosomes, and GFP-Rab11 marks recycling endosomes (Hickson et al. 2003). Because these markers are tagged with GFP, I constructed an Lqf-RFP protein, enabling me to assess the Lqf-RFP localization relative to the GFP-Rab markers. Thus, I can co-express Lqf-RFP and GFP-tagged Rabs under the control of UASt vector and driven with *GMR-Gal4* promoter.

CONCLUSIONS AND FUTURE DIRECTIONS

The ENTH-less versions of Lqf and D-epsin-Ra can rescue the eye phenotypes (of *lqf* mutants) and the lethality and eye phenotypes (of *D-Epsin-R* mutants), respectively. This result is contrary to the most popular model suggesting that the ENTH domain is needed to localize the host protein to membrane where it can participate actively in membrane invagination and cargo incorporation. How then can these ENTH-less proteins function? One possibility is that the ENTH domain is required for localization and function and the only reason the ENTH-less versions function in these assays is because they are being highly overexpressed. Upon overexpression, enough of the ENTH-less protein arrives at sites of action by diffusion or chance. In support of this idea, when D-Epsin-R is expressed with the *Actin5Cgal4* driver, it accumulates at high levels all over the cells in the eye disc. However, expression of D-Epsin-R with *EyGal4* driver, which expresses at much lower levels, also rescues. Additionally, the GFP-tagged ENTH-less Lqf piece, when expressed with several drivers, does not accumulate non-specifically in all parts of the cell. It retains a discrete localization at the plasma membrane and in vesicular structures, suggesting that it is not randomly diffusing.

Still another possibility is that these pieces retain function because they localize to CCPs at their respective membranes, perhaps by binding to other proteins in the complex. This is indeed a possibility because Lqf and D-Epsin-R

bind to other proteins that have membrane localization domains. Thus, these proteins might localize to sites of CCP formation via multiple independent binding interactions.

This mode of recruitment may be a general strategy for coat complex proteins. In support of this idea, it was recently shown that the ANTH domain protein, Sla2p in yeast, localizes to endocytic sites without its ANTH domain. However, the ANTH-less protein cannot perform its endocytic function. The authors speculate that the ANTH domain is not needed to localize the protein, but is needed to orient the host protein within the complex for proper spatial and functional interactions with its partners (Sun et al. 2005).

If the ENTH domain is not required for localization, then what is its function? One idea is that the ENTH domain normally does function to localize the host protein. But, the C-terminal protein-protein interactions with coating complex helps to ensure proper membrane localization as well. Thus, these proteins have two independent mechanisms by which to localize. Perhaps the ENTH domain increases the efficiency of plasma membrane localization. In support of this idea, the ENTH-less Lqf protein does not rescue *lqf* mutant phenotypes 100%. Maybe this protein doesn't localize to the plasma membrane efficiently without its ENTH domain.

Alternatively, the ENTH domain may have a function independent of host protein localization. Consistent with this idea, the ENTH domains of yeast Ent proteins can support viability of loss-of-function mutants Also, the ENTH

domain of Lqf can partially rescue the *lqf-* hypomorph eye patterning phenotype caused by a failure of Delta endocytosis and/or trafficking. What is the function of the ENTH domain? As discussed above, the function of the ENTH domain may be to tubularize lipids or participate in protein-protein interactions.

In yeast the ENTH domain function is essential for viability, however, this is probably not the case in flies. The ENTH domain of D-Epsin-R is not required for viability as the ENTH-less version rescues completely and the ENTH domain has no rescuing ability. Whether or not the ENTH domain of Lqf is essential for viability has not been tested directly due to technical difficulties. However, the ENTH-less version can support Delta signaling in the eye in the absence of full-length Lqf. As the essential role of Lqf is probably to regulate Delta signaling, it would not be surprising if the ENTH-less protein could support viability (Wang et al. 2004; Tian et al. 2004; Overstreet et al. 2004).

Does Lqf have a function in vesicles downstream of internalization? This remains to be determined. As a first step to addressing this question, I will first try to identify the basal structures as a bona-fide endocytic compartment. The way I am doing this is to see if these structures co-localize with other endocytic markers. If I am successful in identifying the compartment, this will severely narrow down the possible functional roles for Lqf in vesicles, which might be explored in the future using genetics.

Appendices

Appendix I. Miscellaneous experiments

Experiment I: Neuralized functions in the signaling cells

In Overstreet et al. (2004), I stated that Neuralized (Neur), Faf, and Lqf function in the same group of cells in the eye. The reason I speculated this is because in the absence of *neur*, Delta fails to be endocytosed in R-cells 2/3/4/5. However, I did not test directly if Neur function is required in these cells. To test this directly, I expressed *neur* in the cells where Faf and Lqf are required, R-cells 2/3/4/5, using the *RO-HS* promoter. I tested to see if expression of *neur* in these cells could rescue the Delta endocytosis defect in *neur* null clones in the eye disc. I find that expression of *neur* in R-cells 2/3/4/5 rescues the Delta endocytosis defect in *neur-* clones completely. Thus, Neur functions in the same cells as Faf and Lqf and these proteins are likely to work together in Delta signaling.

A

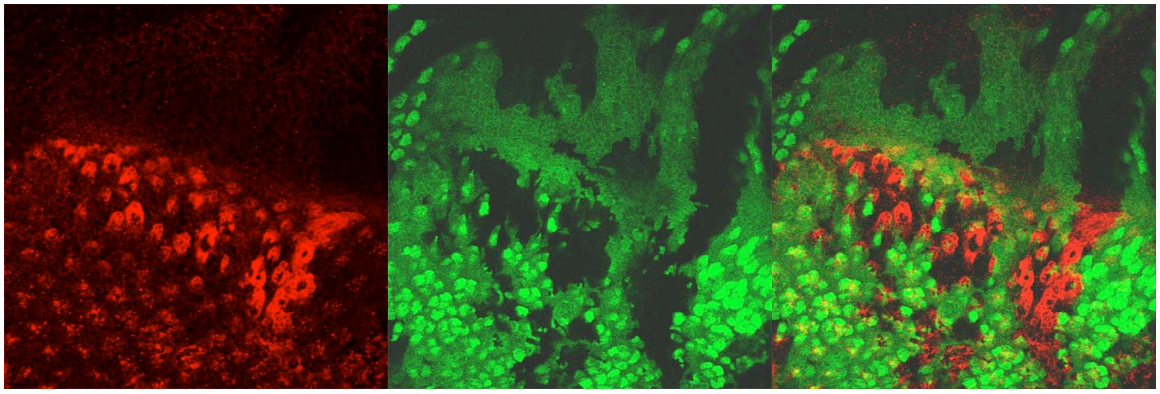

B

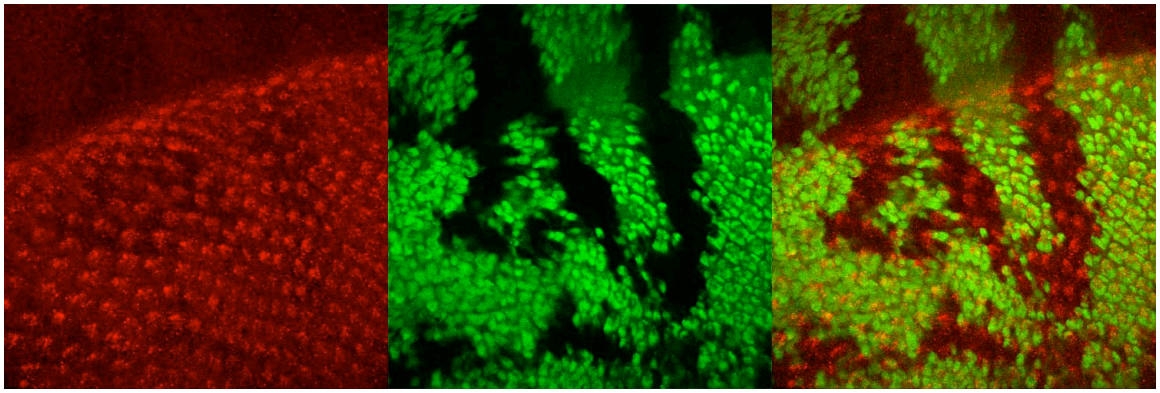

Fig. A1. *RO-HS-Neur* rescues the Delta endocytosis defect of *neur1* mutant in the developing eye disc. (A). *neur1* mutant cells marked by the absence of GFP (green), labeled with anti-delta (red). Delta accumulates on the apical membranes of many cells. Interestingly, very little Delta is seen in vesicles in neur mutant cells. This is unlike *lqf* clones, where Delta is still internalized into vesicles. Perhaps Neur is responsible for the bulk of Delta endocytosis in the eye. (B) neur1 mutant clones again marked by the absence of GFP. These eye discs have one copy of the transgene *RO-HS-neuralized* which expresses in R-cells 2/3/4/5. In this background, Delta (red) is internalized into MVBs. Thus, expression of Neuralized in the same cells where Faf and Lqf function, is sufficient to support Delta endocytosis and probably signaling (although I did not test signaling directly by looking at cell differentiation with markers such as elav).

Experiment II: Major forms of Lqf in eye discs are not ubiquitinated forms

What is the ubiquitination state of Lqf in wild-type discs? Understanding whether or not Lqf is normally present in a ubiquitinated state or not, will help to understand how ubiquitination regulates Lqf activity. Currently, it is not clear if ubiquitination activates or inhibits activity. I expressed the two isoforms of Lqf in bacteria. Western blots of protein extracts from bacteria expressing the Lqf isoforms indicate that these proteins migrate at the same size as the Lqf isofroms detected in extracts from wild-type eye discs. Thus, the major forms of Lqf found in eye discs are not ubiquitinated forms. There may be some ubiquitinated forms that remain undetected. However, this data and others (Chen et al. 2002; Cadavid et al. 2000) suggest that Lqf is active when not ubiquitinated. Ubiquitination of Lqf might act to inhibit its activity.

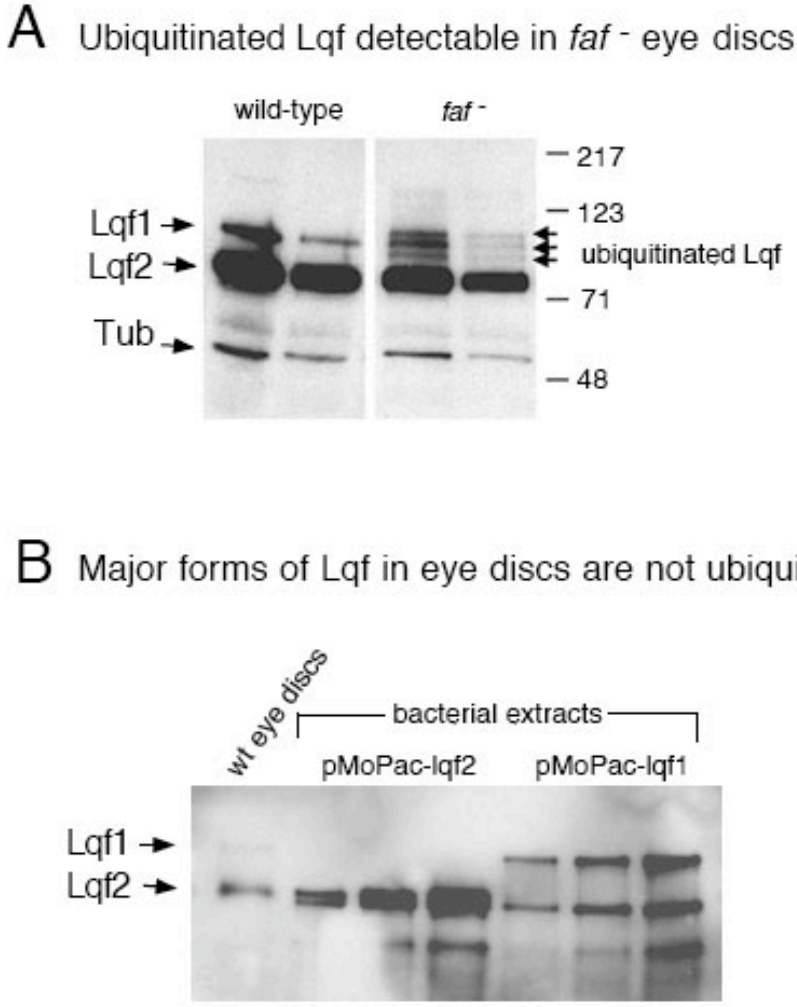

Fig. A2. Major forms of Lqf in eye discs are not ubiquitinated forms. (A). Western blot of eye disc extracts from wild-type and *faf*- eye discs. Blots are stained with anti-Lqf and anti-Tub. In wild-type eye discs, two isoforms of Lqf are detected, Lqf1 and Lqf2. In faf- background, ubiquitinated forms of Lqf are detected which increase in size incrementally by the size of one ubiquitin, 8kDa. Figure from Chen et al. (2002). (B). Western blot of eye disc extracts from wild-type flies and bacterial extracts from bacteria expressing Lqf2 and Lqf1 isoforms (see materials and methods for Appendix I below). The size of Lqf1 and Lqf2 expressed in bacterial cells runs at the same molecular weight as the Lqf isoforms in eye discs. The smaller bands in the bacterial extracts represent degradation products. This experiment provides conclusive evidence that the predominant forms of Lqf in wild-type cells is not ubiquitinated.

Appendix II. Materials and Methods

Chapter 2

Drosophila lines

Our laboratory maintains stocks of *lqf*^{ARI} *FRT80B* (Overstreet et al., 2003), *lqf*^{FDD9} (Cadavid et al., 2000), and *faf*^{FO8} (Fischer-Vize et al., 1992; Chen and Fischer, 2000). *FRT82B Dl*^{rev10} (Baker and Yu, 1996) was obtained from N. Baker. The following lines were obtained from the Bloomington *Drosophila* Stock Center: *neur*^{1} and *neur*^{11} (Lehmann et al., 1993), *Ub-GFP FRT80B* and *FRT82B Ub-GFP* (Flybase, 2003; Xu and Rubin, 1983), *ey-FLP* on X (Newsome et al., 2000), *EGUF; FRT82B GMR-hid l(3)CL-R* (Stowers and Schwarz,1999).

Eye disc clones

lqf^{ARI} eye disc clones were generated in larvae of the following genotypes: *ey-FLP;lqf*^{ARI} *FRT80B/Ub-GFP FRT80B*. *Dl*^{rev10} eye disc clones were generated in larvae of the following genotype: *ey-FLP; FRT82B Dl*^{rev10}*/FRT82B Ub-GFP*. *neur*^{1} eye disc clones were generated in larvae of the following genotype: *ey-FLP; FRT82B neur / FRT82B Ub-GFP*. *neur*^{11} eye discs were generated in larvae of

the following genotype: *EGUF/RO-GFP; FRT82B neur^{11}/ FRT82B GMR-hid l(3)CL-R.*

Analysis of adult eyes

Sectioning, light microscopy, and photography of adult eyes was as described (Huang et al., 1995). Flies with *neur^{11}* eyes were: *EGUF/+ ; FRT82B neur^{11}/FRT82B GMR-hid l(3)CL-R*. The *faf^{FO8}/ faf^{+}* mosaic ommatidia are those described in Fischer-Vize et al. 1992 and they were reanalyzed here using different criteria. The *faf^{BX4}/ faf^{+}* mosaic ommatidia were generated and prepared for microscopy exactly as described in Fischer-Vize et al., 1992.

Immunocytochemistry of eye discs

Primary antibodies used: rabbit polyclonal anti-Ato at 1:2000 (Jarman et al., 1994) from Y. N. Jan; anti-Boss mouse ascites at 1:2000 (Kramer et al., 1991), from H. Kramer; anti-E(spl) mAb323 supernatant at 1:2 (Jennings et al., 1994), from S. Bray; anti-Dl mAb202 supernatant at 1:10 (Parks et al., 1995) from H. Kramer; rat monoclonal anti-Elav supernatant at 1:9 (O'Neill et al., 1994) from the Developmental Studies Hybridoma Bank. Secondary antibodies (Molecular Probes) were Alexa^{633}-anti-mouse, Alexa^{568}-anti-mouse, Alexa^{633}-anti-rat, Alexa^{633}-anti-rabbit, all used at 1:500. Also, Alexa^{568}- and Alexa^{633}-phalloidin

were used as described (Chen et al., 2002). Eye discs immunostaining and confocal microscopy were as described (Chen et al., 2002).

Plasmid constructions for this chapter are described in Appendix IV.

Chapter 3

Drosophila genetics

Flies were reared on standard media at 25°C or 18°C, as indicated. The *lqf* alleles used are described in Cadavid et al., 2000, except for 20.53, L895, L71, and L140, which were gifts from G. Struhl (unpublished). Clones of lqf^{ARI} homozygous cells were induced in eyes of lqf^{ARI}/lqf^{+} flies using chromosomes containing P{ry^{+}; *hs-neo*; *FRT*}80B (Xu and Rubin 1993), P{w^{+}; *Ubi-GFP(S65T)nls*} (Flybase 2000), and P{ry^{+}; *ey-FLP.D*}2 (Newsome et al. 2000). Eye discs with clones were from female third instar larve of the genotype w, P{ry^{+}; *ey-FLP.D*}2/ +; lqf^{ARI} P{ry^{+}; *hs-neo*; *FRT*}80B/ P{w^{+}; *Ubi-GFP(S65T)nls*} P{ry^{+}; *hs-neo*; *FRT*}80B.

Molecular analysis of mutant lqf alleles

Standard molecular biology procedures were followed. DNA of each mutant *lqf* allele was amplified by PCR using as a template either *lqf*$^{-}$ homozygous (for FDD9 and bE428), *lqf*$^{-}$*/Df(3L)pbl-X1* (see Cadavid et al. 2000; for L71, 20.53, and BT), or *lqf*$^{-}$*/TM6B* genomic DNA (for L140 and L895). Genomic DNA was prepared from third instar larvae or adults as follows: ~10 second instar larvae or 1 adult fly were homogenized with a pipet tip in a microfuge tube containing 50 ul of buffer (10 mM Tris pH 8.2, 1 mM EDTA, 25 mM NaCl) and 1ul proteinase K (20 mg/ml). After incubation at 37°C for 30 min. and 100°C for 2 min., 4 ul aliquots were used for a PCR reaction. Four primer pairs were used, each of which generated a PCR product 700-1200 bp long. For all alleles except L140 and L895, the sequences of the PCR products, including all introns except for 1 and 8, and including all exon/intron borders, were determined directly by automated fluorimetric methods. To distinguish artifacts from genomic DNA mutations, PCR products with non-wild-type sequences were reamplified and their sequences determined again. For L140 and L895, each of the four PCR products was subcloned into a plasmid and the DNA sequence of 6 subclones of each were determined. For FDD9, the mRNA produced was also analyzed by RT-PCR as follows. RNA was isolated from adult flies using TriReagent (Molecular Research Center), reverse transcribed using oligo-dT primers and Superscript II (Invitrogen), and then *lqf* cDNA amplified by PCR in two pieces using Supermix (Invitrogen).

Construction of P element plasmids and transformation

The LqfD constructs were generated from the Flag-tagged full-length *lqf1* cDNA construct used to generate the *RO-lqf* transgene described previously (Cadavid et al. 2000). The rat (Chen et al. 1998), human (Rosenthal et al. 1999), and yeast (Wendland et al. 1999) epsin constructs were generated from plasmid clones. Standard molecular biology procedures were used in their construction; for complete details see below. All of the constructs were ligated as *AscI* fragments into the *AscI* site of the P element transformation vector pRO (Huang and Fischer-Vize 1996). P element transformation of w^{1118} flies was performed as described previously (Cadavid et al. 2000). To identify the best rescuing transformant lines, at least three independent lines of each construct were tested for rescue of lqf^{FDD9}eyes.

Western analysis of eye disc proteins

Eye disc protein extracts were generated and analyzed on protein blots, and Lqf was quantified as described in Chen et al. 2002. Expression of Lqf by the *RO-lqf* transgenes was detected using anti-FlagM2 (Sigma) at 1:200 and HRP-conjugated anti-mouse (Santa Cruz Biochemicals) at 1:500. Expression of Lqf by lqf^{FDD9}, lqf^{bE428}, and lqf^{BT} was detected with guinea pig anti-Lqf (Chen et al. 2002) at 1:4000 and HRP-conjugated anti-guinea pig (Jackson) at 1:20,000.

Analysis of eyes

The wild-type strain used was w^{1118}. Third instar larval eye discs were immunostained essentially as described previously, using PEMS fixation and PBST wash and antibody incubation solutions (Fischer-Vize et al. 1992a, b). Primary antibodies used were guinea pig anti-Lqf at 1:1000 (Chen et al. 2002), anti-Dl mAb202 at 1:9 (Parks et al. 1995), anti-Elav mAb9F8A9 at 1:9 (DSHB). Secondary antibodies (Molecular Probes) were Texas Red anti-guinea pig at 1:400, $Alexa^{488}$-anti-mouse at 1:600, and $Alexa^{633}$-anti-mouse at 1:300. After antibody treatment, eye discs were incubated for 20 min. in $Alexa^{568}$-phalloidin (Molecular Probes), which had been dried and resuspended in 200 ul PBST (0.1 unit/ul), and then washed twice in PBST. Eye discs were mounted in VectaShield (Vector Laboratories). Images were produced with a Leica TCS SP2 confocal microscope. Specimens were scanned sequentially to eliminate bleed-through. Images were processed using Adobe Photoshop software. Scanning electron micrographs and tangential sections of adult eyes were produced as described previously (Huang et al. 1995).

Complementation of yeast ent mutants by lqf

The yeast strain BWY1168 (*MATa leu2 ura3 trp1 his3 lys2 ent1::HIS3 ent2::HIS3 + pENT2::URA3*) was transformed with *TRP1*-selectable yeast expression plasmids encoding *ent1* or *ent2* (positive controls), pMET25.424 (negative control), or Flag-tagged *lqf* constructs expressed from a methionine-regulated promoter in both single copy and high copy plasmids. Transformed cells were streaked onto medium containing 5-fluoro-orotic acid to force eviction of the wild-type pENT2::URA3 plasmid; those that are viable under this condition were confirmed to have lost expression of Ent2 by Western blotting of cell extracts with anti-Ent1/2 polyclonal antiserum (Watson et al. 2001). Expression of the Flag-tagged *lqf* constructs under inducing conditions (0 mM methionine) was confirmed in cells containing the high copy vectors by Western blotting with anti-FlagM2 (Sigma). Western blots of yeast extracts were performed as described in Watson et al. 2001.

Plasmid constructions for this chapter are described in Appedix IV.

Chapter 4

Plasmid Rescue

Genomic DNA from *ry[506] P{ry[+t7.2]=PZ}l(3)03685[03685]/TM3, ry[RK] Sb[1] Ser[1]* flies **w**as extracted, cut with *Xba*I, ligated and transformed

into HB101 *E. coli* cells. A plasmid *Drosophila* genomic DNA flanking P{ry+} 03635 was obtained. This plasmid was sequenced with the following primers to obtain the sequence of flanking genomic DNA: Plac4 actgtgcgttaggtcctgttcattgtt and Plac1 cacccaaggctctgctcccacaat. The primer sequences were suggested from the following website: http://www.fruitfly.org/about/methods/inverse.pcr.html.

Preparation of Epsin-2 antibody

Cloned the 5' piece of D-Epsin-R into pET-28a (Novagen and see Appendix IV), containing the first 1300 bp of D-Epsin-R. Expressed antigen, called Comm, in *E. coli* Codon-Plus RIL (Stratagene). The protein was purified by binding to Chelating Sepharose Fast Flow (Pharmacia Biotech). Purified Comm was injected into guinea pigs (Pocano Rabbit Farms) to produce reactive serum. Western blots of protein extracts prepared from eye disc extracts or third instar larvae showed only two bands which correspond to the expected sizes of D-Epsin-Ra and D-Epsin-Rb. Labeling with preimmune serum resulted in no signal on Western blots of protein extracts from eye discs or larvae.

Generation of D-Epsin-R mutants

All fly stocks were maintained at room temperature on standard cornmeal agar media. Mobilization of the P{PZ} 03635 transposable P-element insertion in

ry[506] P{ry[+t7.2]=PZ}l(3)03685[03685]/TM3, ry[RK] Sb[1] Ser[1] (BL-11605) flies was used to generate imprecise excision alleles *D-Epsin-R* $^{\Delta 117}$,*D-Epsin-R* $^{\cdot 116}$. Both allels are ethal over the original insertion and lethal over Df(3R)hh (BL-2252).

For polymerase chain reactions (PCR), genomic DNA was prepared using the single fly PCR protocol (Overstreet et al. 2003). The molecular breakpoints for all deletions were determined using PCR with primers designed to *D-Epsin-R* or its two flanking genes, CG13850 and *Nop56*.

Adult eye clones

D-Epsin-R^{P} *or D-Epsin-R*$^{\Delta 117}$ eye disc clones were generated in larvae of the following genotypes: *ey-FLP/+;D-Epsin-R*^{117} *FRT82B/Ub-GFP FRT82B* or eyFLP/+;*D-Epsin-R*^{P} *FRT82B/Ub-GFP FRT82B*. Eyes completely mutant were generated in larvae of the following genotypes: EGUF/+; *;D-Epsin-R*^{117} *FRT82B/GMR-hid, cl, FRT82B or EGUF/+; D-Epsin-R*^{P} *FRT82B/ GMR-hid, cl, FRT82B* (Stowers and Schwarz 1999; Overstreet et al. 2004). Our laboratory maintains stocks of Actin5Cgal4.

Sectioning, light microscopy, and photography of adult eyes was as described (Huang et al., 1995).

RT-PCR

Total RNA was extracted using TriReagent protocol from Molecular Reseach. RT reaction performed using oligo-dT reverse primer and RT from Invitrogen using the protocol provided. Using 2μL of the RT reaction, PCR was performed using PCR Supermix from Invitrogen and specific primers – described in Appendix 4.

Immunocytochemistry of eye discs

Primary antibodies used: rabbit polyclonal anti-lava 1:2000 (Sisson et al. 2000); mouse monoclonal anti p120 1:200 (CalBioChem); rat monoclonal anti-Elav supernatant at 1:9 (O'Neill et al., 1994) from the Developmental Studies Hybridoma Bank. Secondary antibodies (Molecular Probes) were Alexa^{633}-anti-mouse, Alexa^{568}-anti-mouse, Alexa^{633}-anti-rat, Alexa^{633}-anti-rabbit, all used at 1:500. Also, Alexa^{568}- and Alexa^{633}-phalloidin were used as described (Chen et al., 2002). Eye discs immunostaining and confocal microscopy were as described (Chen et al., 2002).

Western Blots

Eye disc protein extracts were generated and analyzed on protein blots, as described in Chen et al. (2002). Blots of extracts of eye discs or third instar larvae were probed with guinea pig anti-D-Epsin-RComm at 1:1000 and mouse anti-

TubE7 at1:100 (DSHB). These were probed with secondaries HRP-conjugated anti-guinea pig (Jackson) at 1:20,000 and HRP-conjugated anti-mouse (Santa Cruz Biochemicals) at 1:500.

Plasmid constructions for this chapter are described in Appendix IV.

Chapter 5

Drosophila lines

Our laboratory maintains stocks of *lqf*^{ARI} *FRT80B* (Overstreet et al., 2003), *lqf*^{FDD9} (Cadavid et al., 2000), The following lines were obtained from the Bloomington *Drosophila* Stock Center: *Ub-GFP FRT80B* and *FRT82B Ub-GFP* (Flybase, 2003; Xu and Rubin, 1983), *ey-FLP* on X (Newsome et al., 2000), *EGUF; FRT82B GMR-hid l(3)CL-R* (Stowers and Schwarz,1999), UASt-GFP-Rab11, Actin5C-Gal4, and GMR-Gal4. *D-Epsin-R*$^{\Delta 117}$ allele is as described in chapter 4. UASt-GFP-Rab5 and UASt-GFP-Rab7 were obtained from Marcos Gonzalez-Gaitan.

Immunocytochemistry of eye discs

Primary antibodies used: anti-Dl mAb202 supernatant at 1:10 (Parks et al., 1995) from H. Kramer; rat monoclonal anti-Elav supernatant at 1:9 (O'Neill et al., 1994) from the Developmental Studies Hybridoma Bank. Secondary antibodies (Molecular Probes) were Alexa^{633}-anti-mouse, Alexa^{568}-anti-mouse, Alexa^{633}-anti-rat, Alexa^{633}-anti-rabbit, all used at 1:500. Also, Alexa^{568}- and Alexa^{633}-phalloidin were used as described (Chen et al., 2002). Eye discs immunostaining and confocal microscopy were as described (Chen et al., 2002).

Plasmid constructions for this chapter are described in Appendix IV.

Materials and Methods for Appendix I

Drosophila lines

The chromosomes used were the same as those used in Overstreet et al. (2004). I generated *neur*^{1} mutant clones in larvae of the following genotype: *EyFlp/+;FRT82B neu*^{r1}*/FRT82B UbiGFP*

Western analysis of eye disc proteins and immunohistochemistry

Expression of Lqf was detected with guinea pig anti-Lqf (Chen et al. 2002) at 1:4000 and HRP-conjugated anti-guinea pig (Jackson) at 1:20,000. Analysis of eye discs were exactly as described in Overstreet et al. (2004) and the

antibodies were mouse anti-Delta from DSHB and anti-mouse^{488} from Molecular probes.

Generation of Lqf proteins in bacteria

Full-length cDNAs corresponding to *lqf1* and *lqf2* were generated as *NdeI* - *AscI* fragments using plasmids containing *lqf* cDNA-3 and cDNA-2 (Cadavid et al. 2000) and standard molecular methods (complete details furnished upon request.) pMoPac plasmid DNA (A. Hayhurst, unpublished) was restricted with *NdeI* and *AscI* to eliminate the epitope tags and tet^R gene, and each *lqf* cDNA was ligated into the plasmid to generate pMoPac-lqf1 and pMoPac-lqf2. To express the Lqf proteins, *E. coli* strain ABLE C was transformed with each plasmid and overnight cultures grown at 37°C in LB with 30 ug/ul chloramphenicol. Cultures were diluted 1:100, and grown to an OD_{600} of 0.6 (~3 hours), IPTG added to 0.1 mM, and grown for another 3 hrs. Samples of 1, 2.5 and 5 ul were used for Western analysis.

Immunocytochemistry of eye discs

Primary antibodies used: rabbit polyclonal anti-lava 1:2000 (Sisson et al. 2000); mouse monoclonal anti p120 1:200 (CalBioChem); rat monoclonal anti-Elav supernatant at 1:9 (O'Neill et al., 1994) and anti-Delta from the Developmental Studies Hybridoma Bank. Secondary antibodies (Molecular

Probes) were Alexa^{633}-anti-mouse, Alexa^{568}-anti-mouse, Alexa^{633}-anti-rat, Alexa^{633}-anti-rabbit, all used at 1:500. Also, Alexa^{568}- and Alexa^{633}-phalloidin were used as described (Chen et al., 2002). Eye discs immunostaining and confocal microscopy were as described (Chen et al., 2002).

Drosophila lines

Our laboratory maintains stocks of *FRT82B, neur1* (Overstreet et al., 2004), *lqf^{FDD9}* (Cadavid et al., 2000), and *faf^{FO8}* (Fischer-Vize et al., 1992; Chen and Fischer, 2000), *D-Epsin-R$^{\Delta 117}$* (Chapter 4), GMR-Gal4 and Actin5C-Gal4.

Plasmids constructed for Experiment I is described in Appendix IV in the chapter II section. Plasmids constructed for Experiment II are described its own section in Appendix IV.

Appendix III: Fly Stocks

Chapter 2

B43. *w;RO-HS-ShiDN-Line1;lqf^{FDD9}/TM6B*

B2. *w;RO-HS-ShiDN-Line2*

B3. *w;RO-HS-ShiDN-Line1*

B4. *w;RO-HS-GFP on 2*

B5. *w;RO-HS-GFP Line1 on 3*

B6. *w;RO-HS-GFP/Cyo;faf^{BX4}/TM6B*

B7. *w;RO-HS-GFP/Cyo;faf$^{(BX4)(FO8)}$/TM6B*

B8. *w;RO-HS-GFP-Lqf Line1/+;lqf^{FDD9}/TM6B*

B9. *w;RO-HS-GFP-Lqf Line1*

B10. *w;RO-HS-GFP-Lqf Line3 on 2*

B11. *w;RO-HS-GFP-Lqf Line1/Cyo;FRT82B, neur^{11}/TM6B*

B12. *w;RO-HS-DlDN Line1*

B13. *w;RO-HS-DlDN Line2*

B14. *w;RO-HS-DlDN Line3*

B15. *neur^{1},efaf^{FO8}/TM6B*

B16. *e,neur^{1},lqf^{FDD9}/TM6B*

B17. *e,neur^{1},lqf^{FDD9}/TM6,Hu*

B18. *neur^{11},faf^{FO8}/TM3*

B19. *neur^{11},faf^{FO8}/TM6B*

B20. *neur^{11},lqf^{FDD9}/TM3*

B21. *neur^{11},lqf^{FDD9}/TM6B*

B22. *FRT82B,neur^{1}/TM6B*

B23. *FRT82B,neur^{11}/TM6*

B24. *FRT82B,neur^{1},efaf^{FO8}/TM6B LineH*

B25. *FRT82B,neur^{1},efaf^{FO8}/TM6B Line8*

B26. *FRT82B,neur^{1},efaf^{FO8}/TM6B Line7*

B27. *Neur-Gal4/TM6B*

B28. *E,Dl^{9P},faf^{FO8}/TM6B*

B29. *FRT82B,faf^{FO8}/TM6B Line6* *RIP*

B30. *FRT82B,faf^{FO8}/TM6B Line11*

B31. *FRT82B,faf^{FO8}/TM6B Line1*

B32. *lqf^{FDD9},FRT80B/TM6B Line1*

B33. *lqf^{FDD9},FRT80B/TM6B Line2*

B34. *lqf^{L71},FRT80B/TM6B*

B35. *FRT82B,Dl^{Rev}/TM6B*

B36. *FRT82B,Ser,Dl^{Rev}/TM6B*

B37. *EyFlp;GFP, FRT80B/TM6B*

B38. *w;Cyo/Sco; lqf^{FDD9}/TM6B*

B39. *EyFlp; lqf^{FDD9}/TM6B*

B40. *w;Cyo/Sco;faf^{BX4}/TM6B*

B41. *e,lap^{1}, lqf^{FDD9}/TM6B Line1*

B42. *e,lap^{1}, lqf^{FDD9}/TM6B Line2*

B43. *w;RO-HS-Neur Line1/TM6B*

B44. *w;RO-HS-Neur Hop1, FRT82B, neur^{1}/TM6B*

B45. *w;FRT82B, neu^{r1} Line 7/TM6B*

B46. *w; RoNeur Hop1/Cyo; FRT82B, neu^{r1} Line 7/TM6B*

Chapter 3

A1. *w;RO-HS-FLAG-Lqf-ΔENTHUIM-Line4/Cyo;faf^{BX4}/TM6B*

A2. *w;RO-HS-FLAG-Lqf-ΔENTHUIM-Line3;efaf^{FO8}/TM6B*

A3. *w;RO-HS-FLAG-Lqf-ΔENTHUIM-Line6A;faf^{BX4}/TM6B*

Expresses at Lower levels

A4. *w;RO-HS-FLAG-Lqf-ΔENTHUIM-Line9;faf^{FO8}/TM6B*

Expresses at Lower levels

A5. *w;RO-HS-FLAG-Lqf-ΔENTHUIM-Line6B;faf^{BX4}/TM6B*

A6. *w;RO-HS-FLAG-Lqf-ΔENTHUIM-Line4;lqf^{FDD9}/TM6B*

A7. *w;RO-HS-FLAG-Lqf-ΔENTHUIM-Line3; lqf^{FDD9}/TM6B*

A8. *w;RO-HS-FLAG-Lqf-ΔENTHUIM-Line6A;lqf^{FDD9}/TM6B*

Expresses at Lower levels

A9. *w'RO-HS-FLAG-Lqf-ΔENTHUIM-Line9;lqf^{FDD9}/TM6B*

Expresses at Lower levels

A10. *w;RO-HS-FLAG-Lqf-ΔENTHUIM-Line6B;lqf^{FDD9}/TM6B*

A11. *w;RO-HS-FLAG-Lqf-ΔENTHUIM-Line8;lqf^{FDD9}/TM6B*

A12. *w;RO-HS-FLAG-Lqf-ENTHUIM-LineBH5;efaf^{FO8}/TM6B*

Best Rescuer

A13. *w;RO-HS-FLAG-Lqf-ENTHUIM-LineBH5;faf^{BX4}/TM6B*

Best Rescuer

A14. *w;RO-HS-FLAG-Lqf-ENTHUIM-LineBH4;efaf^{FO8}/TM6B*

A15. *w;RO-HS-FLAG-Lqf-ENTHUIM-LineBH4;faf^{BX4}/TM6B*

A16. *w;RO-HS-FLAG-Lqf-ENTHUIM-LineBH5;lqf^{FDD9}/TM6B*

A17. *w;RO-HS-FLAG-Lqf-ENTHUIM-LineBH4;lqf^{FDD9}/TM6B*

A18. *w;RO-HS-FLAG-Lqf-ENTHUIM-LineBH3;lqf^{FDD9}/TM6B*

A19. *w;3XRO-HS-FLAG-Lqf-ENTH;faf^{BX4}/TM6B*

A20. *w;4XRO-HS-FLAG-Lqf-ENTH;lqf^{FDD9}/TM6B*

Best Rescuer

A21. *w;RO-HS-FLAG-Lqf-ENTH;lqf^{FDD9}/TM6B*

A22. *w;RO-HS-FLAG-Lqf-ENTH-Hop1;efaf^{FO8}/TM6B*

A23. *w;RO-HS-FLAG-Lqf-ENTH-Hop1;faf^{BX4}/TM6B*

A24. *w;RO-HS-FLAG-Lqf-ENTH-Hop1;lqf^{FDD9}/TM6B*

A25. *w;RO-HS-FLAG-Lqf-DPWCBD2;efaf^{FO8}/TM6B*

Best Rescuer

A26. *w;RO-HS-FLAG-Lqf-DPWCBD2-Hop2;faf^{BX4}/TM6B*

Best Rescuer

A27. *w;RO-HS-FLAG-Lqf-DPWCBD2-Hop1;efaf^{FO8}/TM6B*

A28. *w;RO-HS-FLAG-Lqf-DPWCBD2-3;lqf^{FDD9}/TM6B*

A29. *w;RO-HS-FLAG-Lqf-DPWCBD2-Hop2;lqf^{FDD9}/TM6B*

Best Rescuer

A30. *w;RO-HS-FLAG-Lqf-DPWCBD2-Hop1;lqf^{FDD9}/TM6B*

A31. *w;RO-HS-FLAG-Lqf-DPWCBD2-Hop1*

A32. *w;RO-HS-FLAG-Lqf-DPWCBDB1-Hop3;faf^{BX4}/TM6B*

A33. *w;RO-HS-FLAG-Lqf-DPWCBDB1-Hop1;faf^{BX4}/TM6B*

A34. *w;RO-HS-FLAG-Lqf-DPWCBDB1-Hop1;efaf^{FO8}/TM6B*

A35. *w;RO-HS-FLAG-Lqf-DPWCBDB1-Hop1;lqf^{FDD9}/TM6B*

A36. *w;RO-HS-FLAG-Lqf-DPWCBDB1-Line1;lqf^{FDD9}/TM6B*

A37. *w;RO-HS-FLAG-Lqf-DPWCBDB1-Line3;lqf^{FDD9}/TM6B*

A38. *w;RO-HS-FLAG-Lqf-ΔENTH-Hop4;efaf^{FO8}/TM6B*

A39. *w;RO-HS-FLAG-Lqf-ΔENTH-Hop1;faf^{BX4}/TM6B*

A40. *w;RO-HS-FLAG-Lqf-ΔENTH(Sco)(Cyo);lqf^{FDD9}/TM6B*

A41. *w;RO-HS-FLAG-Lqf-ΔENTH-Line2;lqf^{FDD9}/TM3*

A42. *w;RO-HS-FLAG-Lqf-ΔENTH-Hop2 on 2*

A43. *w;RO-HS-FLAG-Lqf-ΔENTH-Hop3 on 2*

A44. *w;RO-HS-FLAG-Lqf-ΔENTH-Line1*

A45. *w;RO-HS-FLAG-Lqf-ΔCBD;faf^{BX4}/TM6B*

A46. *w;RO-HS-FLAG-Lqf-ΔCBD-Line3;lqf^{FDD9}/TM6B*

A47. *w;RO-HS-FLAG-Lqf-ΔCBD-Line2*

A48. *w;RO-HS-FLAG-Lqf-ΔDPW3-Line5;faf^{BX4}/TM6B*

A49. *w;RO-HS-FLAG-Lqf-ΔDPW3-Line4;efaf^{FO8}/TM6B*

A50. *w;RO-HS-FLAG-Lqf-ΔDPW3-Line4;lqf^{FDD9}/TM6B*

A52. *w,RO-HS-FLAG-Lqf-ENTH-Line3;faf^{BX4}/TM3*

A53. *w,RO-HS-FLAG-Lqf-ENTH-Line2;faf^{BX4}/TM3*

A54. *w;RO-HS-FLAG-LqfΔENTH/Cyo;GFP, FRT80B/TM6B*

A55. *w;RO-HS-FLAG-LqfΔENTH/Cyo;faf^{BX4}/TM6B*

A56. *w;RO-HS-Ent1 Hop8/Cyo;efaf^{FO8}/TM6B*

A57. *w;RO-HS-FLAG-Ent2 Line2/Cyo;faf^{BX4}/TM6B*

A56. *w;RO-HS-FLAG-Ent1 Hop1 on 3*

A59. *w;RO-HS-FLAG-LqfENTHUIM Hop1;lqf^{FDD9}/TM6B*

A60. *w;RO-HS-Ent1 Line3;*

A61. *w;RO-HS-Ent1 Line3;efaf^{FO8}/TM6B*

A62. *w;RO-HS-Ent1 Hop8; faf^{BX4}/TM6B*

A63. *w;RO-HS-Rat-epsin-1 Line4; lqf^{FDD9}/TM6B*

A64. *w;RO-HS-Rat-epsin-1ΔENTH Hop1 on X*

A65. *w;RO-HS-Rat-epsin-1ΔENTH Line1 on 3*

A66. *w;RO-HS-Rat-epsin-1ΔENTH Line3 on 3*

A67. *w;RO-HS-Rat-epsin-1ΔENTH Line1, efaf^{FO8}/TM6B*

A68. *w;RO-HS-Rat-epsin-1ΔENTH Line4,lqf^{FDD9}/TM6B*

A69. *w;RO-HS-Rat-epsin-1ΔENTH Line4, efaf^{FO8}/TM6B*

A70. *w;RO-HS-Rat-epsin-1 Hop1 on X; lqf^{FDD9}/TM6B*

A71. *w;RO-HS-Rat-epsin-1 Line3; lqf^{FDD9}/TM6B*

A72. *w;RO-HS-Human-epsin-2-like Line2; efaf^{FO8}/TM6B*

A73. *w;RO-HS-Hu-epsin-2-likeΔENTH Line1/Cyo;st faf^{BX4}/TM6B*

A74. *w;RO-HS-Hu-epsin-2-likeΔENTH Line1/Cyo; lqf^{FDD9} /TM6B*

A75. *w;RO-HS-Hu-epsin-2-likeΔENTH Line1/Cyo;efaf^{FO8} /TM6B*

A76. *w;RO-HS-Hu-epsin-2-likeΔENTH Hop1/Cyo;efaf^{FO8} /TM6B*

A77. *w;RO-HS-Hu-epsin-2-likeΔENTH Hop1/Cyo; lqf^{FDD9} /TM6B*

A78. *w;RO-HS-Hu-epsin-2-likeΔENTH Line4/Cyo;efaf^{FO8} /TM6B*

A79. *w;RO-HS-Hu-epsin-2-likeΔENTH Line4/Cyo; lqf^{FDD9} /TM6B*

A80. *w;RO-HS-Hu-epsin-2-likeΔENTH Line4/Cyo;st faf^{BX4}/TM6B*

A81. *w;RO-HS-Hu-epsin-2-like Line2/Cyo; lqf^{FDD9} /TM6B*

A82. *w;RO-HS-Rat-epsin1 Line3/Cyo; lqf^{FDD9} /TM6B*

A83. *w;RO-HS-Ent2 Line 2 on X; lqf^{FDD9} /TM6B*

A84. *w, RO-HS-FLAG-Ent2 Line1 on X*

A85. *w;RO-HS-Hu-epsin-2-like Line3 on X*

A86. *w;RO-HS-Hu-epsin-2-like Line1/Cyo;st faf^{BX4}/TM6B*

A87. *w,RO-HS-FLAG-LqfΔENTH Line1 on X; st faf^{BX4}/TM6B (not sure if faf is still present)*

A88. *w;RO-HS-FLAG-LqfΔDPW3 Line5; st faf^{BX4}/TM6B*

A89. *w;RO-HS-FLAG-Lqf-DPWCBD1- Hop3/Cyo; st faf^{BX4}/TM6B*

Chapter 4

C1. *ry, P(ry+) D-Epsin-R^{03685}/TM2,Ubx*

C2. *ry, P(ry+) D-Epsin-R^{03685}/TM6B*

C3. *w; (hs-neo) FRT82B, P(ry+) D-Epsin-R^{03685}/TM6B*

C4. *ry, D-Epsin-R$^{\Delta 117}$/TM2,Ubx*

C5. *ry, D-Epsin-R$^{\Delta 117}$/TM6B*

C6. *(w); (hs-neo) FRT82B, P(ry+) D-Epsin-R$^{\Delta 117}$/TM6B*

C7. *ry, D-Epsin-R$^{\Delta 116}$/TM2,Ubx*

C8. *ry, D-Epsin-R$^{\Delta 116}$/TM6B*

C9. *ry, D-Epsin-R$^{\Delta 23}$/TM2,Ubx*

C10. *ry, D-Epsin-R$^{\Delta 23}$/TM6B*

C11. *ry, D-Epsin-R$^{\Delta 182}$/TM2,Ubx*

C12. *ry, D-Epsin-R$^{\Delta 101}$/TM2,Ubx*

C13. *ry, D-Epsin-R$^{\Delta 193}$/TM2,Ubx*

C14. *ry, D-Epsin-R$^{\Delta 152}$/TM2,Ubx*

C15. *ry, D-Epsin-R$^{\Delta 72}$/TM2,Ubx*

C16. *ry, D-Epsin-R$^{\Delta 130}$/TM2,Ubx*

C17. *ry, D-Epsin-R$^{\Delta 130}$/TM6B*

C18. *ry, D-Epsin-R$^{\Delta 115}$/TM2,Ubx*

C19. *ry, D-Epsin-R$^{\Delta 115}$/TM6B*

C20. *lqf^{FDD9},P(ry+) D-Epsin-R^{03685}/TM6B (Line1)*

C22. *lqf^{FDD9},P(ry+) D-Epsin-R^{03685}/TM6B (Line2)* *RIP*

C23. *lqf^{FDD9}, P(ry+) D-Epsin-R$^{\Delta 116}$/TM6B*

C24. *lqf^{FDD9},P(ry+) D-Epsin-R$^{\Delta 123}$ /TM6B*

C25. *lqf^{L71},P(ry+) D-Epsin-R^{03685}/TM6B (Line2)*

C26. *w; UAS-CycE, P(ry+) D-Epsin-R^{03685}/TM6B*

C27. *w; UAS-myc-Fng(17)/Cyo; P(ry+) D-Epsin-R^{03685}/TM6B*

C28. *w; hrs/Cyo; P(ry+) D-Epsin-R^{03685}/TM6B*

C29. *w; chico^{1}/Cyo; P(ry+) D-Epsin-R^{03685}/TM6B*

C30. *w;Tor$^{Delta\ P}$/Cyo; P(ry+) D-Epsin-R^{03685}/TM6B*

C31. *w;aux^{e727},P(ry+) D-Epsin-R^{03685}/TM6B (Line1)*

C32. *aux^{e727},P(ry+) D-Epsin-R^{03685}/TM6B (Line2)*

C33. *aux^{ed136},P(ry+) D-Epsin-R^{03685}/TM6B (Line1)*

C34. *vn^{G115},P(ry+) D-Epsin-R^{03685}/TM6B (Line1)*

C35. *vn^{11749},P(ry+) D-Epsin-R^{03685}/TM6B (Line1)*

C36. *w;UASt-D-Epsin-Ra-GFP on 2*

C37. *P(ry+) D-Epsin-R^{03685},hh^{rJ413}/TM6B*

C38. *P(ry+) D-Epsin-R^{03685},hh^{AC}/TM6B*

C39. *fng, P(ry+) D-Epsin-R^{03685}/TM6B*

C40. *syx5^{AR113}/Cyo; P(ry+) D-Epsin-R^{03685}/TM6B*

C41. *w;UASt-(GFP?)D-Epsin-RaLine2, P(ry+) D-Epsin-R^{03685}/TM6B*

C42. *w;UASt-D-Epsin-RaLine4, P(ry+) D-Epsin-R^{03685}/TM6B*

C43. *w;UASt-D-Epsin-RaLine10, P(ry+) D-Epsin-R^{03685}/TM6B*

C44. *w;UASt-D-Epsin-RaLine4, D-Epsin-R^{116}/TM6B*

C45. *w;UASt-D-Epsin-RaLine9, D-Epsin-R^{116}/TM6B*

C46. *w;RO-HS-D-Epsin-Ra Line1,lqf^{FDD9}/TM6B*

C47. *w;RO-HS-D-Epsin-Ra Hop2,lqf^{FDD9}/TM6B*

C48. *w;pCasper4-genomic-D-Epsin-R Line3/TM6B*

C49. *w;pCasper4-genomic-D-Epsin-R Line1/TM6B*

C50. *w;UASt-D-Epsin-RaLine9*

C51. *w;UASt-D-Epsin-RaLine2*

C52. *w;UASt-D-Epsin-RaLine3 on 3*

C53. *w;UASt-D-Epsin-RaLine8 on X*

C54. *w;UASt-D-Epsin-RaLine2/Cyo; UASt-D-Epsin-RaLine10*

C55. *w;UASt-GFP-D-Epsin-RaLine3*

C56. *w;UASt-D-Epsin-RbLine2B on 2*

C57. *w;UASt-D-Epsin-RB-GFP Line1A on 2*

C58. *w;UASt-D-Epsin-RbLine2B/+; P(ry+) D-Epsin-R^{03685}/TM6B*

C59. *w;WgLz/Cyo; P(ry+) D-Epsin-R^{03685}/TM6B*

C60. *w;UASt-D-Epsin-RaLine10 on 3*

C61. *Ras ^{e1b}, P(ry+) D-Epsin-R^{03685}/TM6B Line2*

C62. *Ras ^{e1b}, P(ry+) D-Epsin-R^{03685}/TM6B Line1*

C63. *w;UASt-GFP-D-Epsin-RaLine2/Cyo*

C64. *wgI^{-17}/Cyo; P(ry+) D-Epsin-R^{03685}/TM6B*

C65. *w;UASt-D-Epsin-Ra-GFP Line1; D-Epsin-R^{117} FRT82B/TM6B*

C67. *dpp^{s-11}/Cyo; P(ry+) D-Epsin-R^{03685}/TM6B*

C68. *P(ry+)InR ^{05545},P(ry+) D-Epsin-R^{03685}/TM6B RIP*

C69. *w P(w+) genomic epsin-2 Line2*

C70. *w P(w+) genomic epsin-2 Line1/Cyo; D-Epsin-R^{117} FRT82B/TM6B*

C71. *gig^{109}, P(ry+) D-Epsin-R^{03685}/TM6B Line1*

C72. *gig^{109}, P(ry+) D-Epsin-R^{03685}/TM6B Line2*

C73. *$syx1A^{\Delta 229}$, P(ry+) D-Epsin-R^{03685}/TM6B Line1*

C74. *$syx1A^{\Delta 229}$, P(ry+) D-Epsin-R^{03685}/TM6B Line2*

C75. *$Egfr^{tsla}$/Cyo; P(ry+) D-Epsin-R^{0368}/TM6B*

C76. *$Egfr^{tsla}$/Cyo;MKRS/TM6B*

C77. *w;UASt-D-Epsin-Ra Line 5*

C78. *w;Sco/Cyo; P(ry+) D-Epsin-R^{0368}/TM6B*

C79. *w; UASt-FLP/Cyo;C311-Gal4, D-Epsin-R^{117} FRT82B Line1/TM6B*

C80. *w; UASt-FLP/Cyo;C311-Gal4, D-Epsin-R^{117} FRT82BL4?/TM6B*

C81. *w; P(ry+) D-Epsin-R^{0368}/TM6B*

C82. *w;C311-Gal4, D-Epsin-R^{117} FRT82B Line2/TM6B*

C83. *w;C311-Gal4, D-Epsin-R^{117} FRT82B Line3/TM6B*

C84. *w;C311-Gal4, D-Epsin-R^{117} FRT82B Line1/TM6B*

C85. *w; p^{riso}/Cyo; P(ry+)^{iso} D-Epsin-R^{0368} FRT82B/TM6B Line4*

C86. *w; p^{riso}/Cyo; P(ry+)^{iso} D-Epsin-R^{0368} FRT82B/TM6B Line 3*

C87. *w; p^{riso}/Cyo; P(ry+)^{iso} D-Epsin-R^{0368} FRT82B/TM6B Line1*

C88. *w; p^{riso}/Cyo; P(ry+)^{iso} D-Epsin-R^{0368} FRT82B/TM6B Line2*

C89. ***w;*** *D-Epsin-R^{117} FRT82B/TM6B*

Stocks for chapter 5 and miscellaneous experiments

Relative eye roughness with over-

		expression with GMR-Gal4
D1.	*w;RO-HS-DNDER-Line2B*	
D2.	*w;RO-HS-DNDER-Line2A on 3*	
D3.	*w;RO-HS-DNDER-Line1 on 3*	*RIP*
D4.	*w;RO-HS-DNDER-Line3 on X*	
D5.	*w;RO-HS-DNDER-Line4 on 2*	
D6.	*w;4XUASt-FLAG-Lqf-ENTH*	
D7.	*w;UASt-FLAG-Lqf-ENTH-Line1*	
D8.	*w;UASt-FLAG-Lqf-ENTHB-Line2*	
D9.	*w;UASt-FLAG-Lqf-ENTHB-Hop9*	
D10.	*w;UASt-FLAG-Lqf-ENTHB-Line3*	
D11.	*w;UASt-FLAG-Lqf-ΔENTH-Hop8*	
D12.	*w;UASt-FLAG-Lqf-ΔENTH-Hop11*	+++++
D13.	*w;UASt-FLAG-Lqf-ΔENTH-Hop6*	++++
D14.	*w;UASt-FLAG-Lqf-ΔENTH-Hop10*	+++
D15.	*w;UASt-FLAG-Lqf-ΔENTH-Line3*	
D16.	*w;UASt-FLAG-Lqf-ΔDPW3-Hop9*	++
D17.	*w;UASt-FLAG-Lqf-ΔDPW3-Line1*	
D18.	*w;UASt-FLAG-Lqf-ΔDPW3-Hop7*	+++

D19.	*w;UASt-FLAG-Lqf-ΔDPW3-Hop10*	+++
D20.	*w;UASt-FLAG-Lqf-DPWCBD1-Hop16*	+++
D21.	*w;UASt-FLAG-Lqf-DPWCBD1-Line2*	
D22.	*w;UASt-FLAG-Lqf-DPWCBD1-Hop10*	
D23	*w;UASt-FLAG-Lqf-DPWCBD1-Line2*	
D24.	*w;UASt-FLAG-Lqf-DPWCBD1-Hop9*	++
D25.	*w;UASt-FLAG-Lqf-DPWCBDB1-Line3*	
D26.	*w;UASt-FLAG-Lqf-DPWCBDB1-Line4*	
D28.	*w;UASt-FLAG-Lqf-ΔNPF1-Hop12*	+++
D29.	*w;UASt-FLAG-Lqf-ΔNPF1-Hop3/TM6B*	+
D30.	*w;UASt-FLAG-Lqf-ΔNPF1-Line3*	
D31.	*w;UASt-FLAG-Lqf-ΔNPF1/TM6B*	
D32.	*w;UASt-FLAG-Lqf-ΔCBD-Hop7*	
D33.	*w;UASt-FLAG-Lqf-ΔCBD-Hop2/TM6B*	++++
D34.	*w;UASt-FLAG-Lqf-ΔCBD-Hop9/TM6B*	++
D35.	*w;UASt-FLAG-Lqf-ΔCBD-Line1/TM6B*	
D36.	*w;UASt-FLAG-Lqf-ENTHUIMB-Line1/TM6B*	
D37.	*w;UASt-FLAG-Lqf-ENTHUIMB-Line3/TM6B*	
D38.	*w;UASt-FLAG-Lqf-ENTHUIMB-Line2/Cyo*	
D39.	*w;UASt-FLAG-Lqf-Hop52/TM6B*	
D41.	*w;glrs-FLAG-Lqf-ENTH on 2 Ori*	

F1. *w;UASt-SV40-Lqf Line1A*

F2. *w;UASt-SV40-Lqf Line2*

F3. *w;UASt-SV40-Lqf Line6*

F4. *w;glrs-D-Epsin-Rb-SV40-Gal4VP16*

F5. *w;glrs-Lqf-Gal4VP16*

F6. *w;glrs-Lqf-Gal4VP16 Hop1*

F7. *w;glrs-Lqf-SV40-Gal4VP16 Line1*

F8. *w;glrs-Lqf-SV40-Gal4VP16 Line2*

F9. *w;glrs-Lqf-SV40-Gal4VP16 Line3*

F10. *w;UASt-GFP-Lqf Line1B/TM6B*

F11. *w;UASt-Lqf-GFP Line1*

F12. *w;UASt-Lqf-ENTH-GFP Line3*

F13. *w;UASt-Lqf-ENTH-GFP Line4*

F14. *w;UASt-Lqf-ENTH-GFP Line5*

F15. *w;UASt-Lqf-ENTH-GFP Line6*

F16. *w;UASt-Lqf-ENTH-GFP Line7*

F17. *w;UASt-Lqf-ΔENTH-GFP*

F18. *w;UASt-GFP-D-Epsin-Ra Line4 on 2*

F19. *w;UASt-GFP-D-Epsin-Ra Line3*

F20. *w;UASt-Chimera1 Line1*

F21. *w;UASt-Chimera1 Line4*

F22. *w;UASt-Chimera1 Line5*

F23. *w;RO-HS-Chimera1 Line1 on 3*

F25. *w;UASt-SV40-Lqf Line1*

F26. *w;RO-HS-SV40-Lqf Hop1*

F27. *w;RO-HS-GFP-Lqf Line3 on 2* *RIP*

F28. *w;RO-HS-Lqf-ΔENTH-GFP Line1 on 2*

F29. *w;RO-HS-SV40-Lqf Line2/TM6B*

F30. *w;UASt-Chimera1 Line? on TM6B*

F31. *w;RO-HS-FLAG-Lqf-ΔENTH-GFP Line2 on MKRS*

F32. *w;GLRS-LacZ-Gal4-VP16 Line3 on TM6B*

F33. *w;GLRS-Adh- Gal4-VP16 Line1 on TM6B (goes to nucleus)*

F34. *w;GLRS-LacZ-Gal4-VP16 Line2 on 2*

F35. *w;GLRS-LacZ-Gal4-VP16 Line1*

F36. *w;GLRS-Adh- Gal4-VP16 Line2 on 2*

F37. *w;GLRS-Adh- Gal4-VP16 Line3 on 2*

F38. *w;GLRS-Adh- Gal4-VP16 Line4 on 2*

F39. *w;RO-HS-DlEC-GFP-Ub(K48R) Line3;(e)(st)lqf^{FDD9}/TM6B*

F40. *w;RO-HS-DlEC-GFP-Ub(K48R) Line4;(e)(st)lqf^{FDD9}/TM6B*

F41. *w;RO-HS-DlEC-GFP-Ub(K48R) Line5;(e)(st)lqf^{FDD9}/TM6B*

F42. *w;RO-HS-DlEC-GFP-Ub(K48R) Line8;(e)(st)lqf^{FDD9}/TM6B*

F43. *w;RO-HS-DlEC-GFP-Ub(K48R) Line10;(e)(st)lqf^{FDD9}/TM6B*

F44. *w;RO-HS-DlEC-GFP-Ub(K48R) Line3;(e)(st)faf^{FO8}/TM6B*

F45. *w,RO-HS-DlEC-GFP-Ub(K48R)Line4;(efaf^{FO8})(st faf^{BX4})/TM6B*

F46. *w;RO-HS-DlEC-GFP-Ub(K48R)Line8;(efaf^{FO8})(st faf^{BX4})/TM6B*

F47. *w;RO-HS-DlEC-GFP-Ub(K48R)Line10;(efaf^{FO8})(st faf^{BX4})/TM6B*

F48. *w;RO-HS-DlEC-GFP-Ub(K48R) Line14;(e)(st)faf^{FO8}/TM6B*

F49. *w;RO-HS-DlEC-GFP-Ub(K48R) Line12;(e)(st)lqf^{FDD9}/TM6B*

F50. *w;RO-HS-DlEC-GFP-Ub Line2;st lqf^{FDD9}/TM6B*

F51. *w;RO-HS-DlEC-GFP-Ub Line4;(e)(st) lqf^{FDD9}/TM6B*

F52. *w;RO-HS-DlEC-GFP-Ub Line5;(e)(st) lqf^{FDD9}/TM6B*

F53. *w;RO-HS-DlEC-GFP-Ub Line9;st lqf^{FDD9}/TM6B*

F54. *w;RO-HS-DlEC-GFP-Ub Line11;(e)(st) lqf^{FDD9}/TM6B*

F55. *w;RO-HS-DlEC-GFP-Ub Line2;st faf^{FO8}/TM6B*

F56. *w;RO-HS-DlEC-GFP-Ub Line3;(e)(st)faf^{FO8}/TM6B*

F57. *w;RO-HS-DlEC-GFP-Ub Line4;efaf^{FO8}/TM6B*

F58. *w;RO-HS-DlEC-GFP-Ub Line5;(e)(st)faf^{FO8}/TM6B*

F59. *w,RO-HS-DlEC-GFP-Ub Line9 on X;(e)(st)faf^{FO8}/TM6B*

F60. *w;RO-HS-DlEC-GFP-Ub Line11;(e)(st)faf^{FO8}/TM6B*

F61. *w;RO-HS-DlEC-GFP Line5 (Sb/TM6B) Chrom?*

F62. *w;RO-HS-DlEC-GFP Line4 (Sb/TM6B) Chrom?*

F63. *w;RO-HS-DlEC-GFP Line3 (Sb/TM6B) Chrom?*

F64. *w;RO-HS-Chimera1 Line3 on 3*

F65. *w;RO-HS-Chimera1 Line6 on TM6B*

F66. *w;RO-HS-Chimera1 Line2 on 3*

F67. *w;RO-HS-Lqf-ENTH-GFP Line1D on 3*

F68. *w;RO-HS-Chimera1 Line5 on TM6B*

F69. *w;RO-HS-Lqf-ENTH-GFP Line2 on 2*

F70. *w;RO-HS-Lqf-ENTH-GFP Line1L on3*

F71. *w;RO-HS-Chimera1 Line4 inserts on X and 2*

F72. *w;RO-HS-Chimera2 Line1 on 2*

F72. *w;UASt-D-Epsin-RENTH-GFP Line4;MKRS/TM6B*

F73. *w;UASt-D-Epsin-RENTH-GFP Line1;MKRS/TM6B*

F74. *w;UASt-D-Epsin-RENTH-GFP Line2;MKRS/TM6B*

F75. *w;UASt-D-Epsin-RENTH-GFP Line1; D-Epsin-R^{117}FRT82B/TM6B*

F76. *w;UASt-D-Epsin-RENTH-GFP Line2; D-Epsin-R^{117}FRT82B/TM6B*

F77. *w;RO-HS-FLAG-Lqf-GFP Line1B*

F78. *w;UASt-Chimera1 Line2;MKRS/TM6B*

F79. *w;UASt-Chimera1 Line2; D-Epsin-R^{117} FRT82B/TM6B*

F80. *w;UASt-Chimera2 Line1; D-Epsin-R^{117} FRT82B/TM6B*

F81. *w;UASt-Lqf-ENTH-GFP Line1;MKRS/TM6B*

F82. *w;RO-HS-FLAG-Lqf-ΔENTH-GFP/Cyo;MKRS/TM6B*

F83. *w;UASt-Chimera2 Line1; MKRS/TM6B*

F84. *w;RO-HS-FLAG-Lqf-GFP;FRT82B, $neur^{1}$/TM6B*

F85. *w;RO-HS-FLAG-Lqf-GFP(Sco)/Cyo;MKRS/TM6B*

F86. *w;UASt-LqfENTH-GFP Line2; MKRS/TM6B*

F87. *w;RO-HS-DlEC-GFP-UbK48RΔGG Line12;MKRS/TM6B*

From stock center and other labs

E1.	*Dl^{RF}/TM6C,Sb*	
E2.	*Dl^{ts5605}*	
E3.	*eDl^{9P}/TM3,Sb*	
E4.	*HS-Dl*	
E5.	*N^{ts1}*	*RIP*
E6.	*$N^{fa\text{-}G62}$*	
E7.	*$N^{fa\text{-}swb}$*	
E8.	*HS-N*	
E9.	*shi^{ts1}*	*RIP*
E10.	*shi^{ts2}*	
E11.	*cn,$EGFR^{tsla}$,bw/Cyo-TM6B*	
E12.	*$EGFR^{E1}$*	
E13.	*hh^{MIR}/TM6B*	
E14.	*hh^{2}/TM6B*	
E15.	*ry,hh^{rJ413}/TM3*	
E16.	*w;UAS-Hh on 2*	
E17.	*dpp^{S11}/Cyo*	
E18.	*dpp^{e87}/Cyo*	
E19.	*w;UAS-Dpp-GFP(E)*	

E20. *w;UAS-Dpp-GFP(H)*

E21. *w;UAS-Dpp-GFP (K2H2) on 2 and 3*

E22. *w;UAS-Dpp-GFP(L)/TM3*

E23. *w;Dpp-Gal4/TM3*

E24. *w;UAS-Wg*

E25. *Syx-5^{AR113}/Cyo*

E26. *GammaCOP^{KG06383}/TM3*

E27. *Boca^{1}/Cyo*

E28. *w;UAS-GFP^{565C}-alpha-tub84B on 3*

E29. *w;UAS-CycE on 3*

E30. *MF917*

E31. *MF919*

E32. *MF914*

E33. *MF923*

E34. *MF920*

E35. *G122wgLac-Z/Cyo*

E36. *w;UAS-GFP-Wg*

E37. *w;UAS-myr-mRFP*

E38. *Lsi,ry*

E39. *w;UAS-GFP^{536B}-alpha-tub840/TM3,Sb*

E40. *lap^{KG067}/TM3*

E41. *ek^{D}/TM2*

E42. wg^{l-17}/*Cyo*

E43. wg^{l2}/*Cyo*

E44. wg^{l-8}/*Cyo*

E45. fng^{rG554}/*TM3,Sb*

E46. *fngDf/TM3*

E47. $Tor^{Delta\ P}$, *hs-neo, FRT40A/Cyo*

E48. Tor^{k17004}/*Cyo*

E49. Hrs^{D28}/*Gla,wg*

E50. *sev,*$Ras85D^{e2f}$/*TM3,Sb*

E51. $chico^{1}$/*Cyo*

E52. $dmyc^{2}$ *FRT18D/FM7*

E53. $dmyc^{P645}$ *FRT18D/FM7*

E54. $dmyc^{1}$ *FRT18D/FM7*

E55. chc^{3}/*FM7*

E56. chc^{4}/*FM7*

E57. *Pr,* Ser^{Bd-3}/*TM6B*

E58. Ser^{1}/*e*

E59. *w;FRT82B, Ubi-GFP, Min/TM6B*

E60. *w;FRT82B, Sb, (y+)/TM6B*

E61. *w;FRT82B, Min/TM6B*

E62. *w, Ey-Flp;pConD, FRT80B/TM6B*

E63. *w;gmr-ShiDN/TM6B*

E64. *w;UAS-hid/TM6B*

E65. *w;UAS-tau-mGFP6 on 2*

E66. *w;UAS-rab11GFP on 2*

E67. *w;UAS-rab4mRFP on 2*

E68. *y,w,Δ2-3(piggybac)*

E69. *hs-GFP FRT18D*

E70. *Ser-Gal4*

E71. *y;C311-Gal4*

E72. *sev;Ras85D e1B/Bal*

E73. *dpp ^{d5}/Cyo*

E74. *mwh,jv,red,ro,gigas^{109}/TM3,Ser*

E75. *Egfr ^{tsla}/Cyo*

E76. *GMR-hid, cl, FRT82B/TM6B*

E77. *UAS-dpp-GFP(L)/TM3*

E78. *EyFlp;boss-HRP;FRT-82B, Arm-LacZ*

E79. *ry,InR (Pry+) 05545/TM3*

E80. *w; UASt-Rab7-GFP/Cyo*

E81. *w; UASt-GFP-Rab5 /TM3*

E82. *w; Cyo/Sp;UASt-GFP-Rab5/TM6*

E83. *w;UASt-GFP-Rab7/TM3*

E84. *w; Cyo/Sp;UASt-GFP-myc-2XFYVE/TM6*

E85. *w; Cyo/Sp;UASt-GFP-Rab7/TM6B*

E86. *w;UASt-GFP-myc-2XFYVE/TM3, Sb*

E87. *Dl-lacZ (may be ry+ or Pw+)/TM3, Ser*

E88. *w;UASt-myc-neurΔRF Line2/TM6B*

E89. *w;UASt-myc-neurΔRF/TM6B*

E90. *w;UASt-myc-neur*

Misc Stocks

G1. w;Actin5C-Gal4/Cyo; MKRS/TM6B

G2. *w;UASt-FLP;MKRS/TM6B*

G3. *w;UAS-gapGFP, FRT80B Line 9-9/TM6B*

G4. *w;UAS-gapGFP, FRT80B Line 6-1/TM6B*

G5. *w;UAS-gapGFP, FRT80B Line 6-6/TM6B*

G6. *w,RO-HS-Gal4 on X*

Appendix IV: Plasmids –Arranged in the order they are found in my plasmid box – (see plasmid list)

Most of the following constructs were generated using the following vectors pBSKAscI (Huang and Fischer-Vize, 1996) – Derived from pBSKII from Stratagene

RO-HS (Huang and Fischer-Vize, 1996)

UAStAscI (Huang et al. 1996)

GLRS (Mosely et al 1997)

Chapter 3

RO-HS-FLAG-Lqf-ENTH and UASt-FLAG-Lqf-ENTH and GLRS- FLAG-Lqf-ENTH

PCR and site-directed mutagenesis was used to amplify the ENTH domain from pBSKII-FLAG-Lqf (Cadavid et al. 2000) while introducing a stop codon and an *Asc*I site after the last codon in the the ENTH domain. The following primers were used: 5' primer: 5'-TTGGCGCGCCCAACATGGGATCCG-3' and 3' primer: 5'- GGCGCGCCTTAGTTCTGGGCGAATCTCTCCT-3'. The resulting ~500 bp fragment was subcloned into the *Eco*RV site of pBSKIIII (pBluescript II Stratagene) and sequenced. The resulting *Asc*I fragment was cloned in to the *Asc*I site of RO-HS, UASt and GLRS. Checked for proper orientation by restriction digestion.

RO-HS-FLAG-Lqf-ΔENTH and UASt- FLAG-Lqf-ΔENTH

PCR and site directed mutagenesis was used in the following way. A 5' fragment was generated with an in-frame *Not*I site instead of a *Bam*HI site at the 3' end of the FLAG tag. The 5' primer used for RO-HS-FLAG-Lqf-ENTH was used with this 3' primer: 5'-GCGGCCGCCTTGTCATCGTCGTCCTTGT-3'. The template was pBSKII-FLAG-Lqf. The resulting ~50 bp fragment was subcloned into the *Eco*RV site of pBSKIIII and sequenced. Using PCR, a central fragment was generated containing sequences starting just downstream of the ENTH domain with a 5' *Not*I site and ending at the 3' *Bgl*II site. The following primers were used: 5' primer: 5'-GCGGCCGCTCCGAGTGGGTTCGGCAGCGA-3' and the 3' primer: 5'-CCCCCAGAAATATCCAGC-3'. The resulting ~300 bp fragment was subcloned into the *Eco*RV site of pBSKIIII and sequenced. A 3' fragment was isolated from pBSKII-FLAG-Lqf restricted with *Bgl*II and*Asc*I. The resulting 5' *Asc*I-*Not*I, central *Not*I-*Bgl*II, and 3' *Bgl*II-*Asc*I were simultaneously ligated into the *Asc*I site in pB*Asc*I. This *Asc*I fragment was cloned into the *Asc*I site of RO-HS and UASt. Checked for proper orientation by restriction digestion.

RO-HS-FLAG-Lqf-ΔENTHUIM

PCR and site directed mutagenesis was in the following way. Using pBSKII-FLAG-Lqf as a template, a 5' fragment was generated containing sequences 3' to the UIM to the *AlwN*I site while incorporating a new ATG and a

*Pml*I site immediately after the ATG. The following primers were used: 5' primer: 5'- GGCGCGCCATGCACGTGTTGCTAGATCTGCTGGATATT-3' and the 3' primer: 5'- GTACATGTAGGTATCATCAG-3'. A FLAG tag was introduced into the *Pml*I site just 3' to the ATG using the following 2 annealed primers: 5'- GACTACAAGGACGACGATGACAAG -3' and 5'- CTTGTCATCGTCGTCCTTGTAGTC -3'. The resulting ~1200 bp fragment was subcloned into the *Eco*RV site pBSKIIII and sequenced. A 3' fragment was isolated from pBSKII-FLAG-Lqf restricted with *Alw*NI and*Asc*I. The 5' *Asc*I-*Alw*NI and 3' *Alw*NI-*Asc*I were ligated into *Asc*I site of pB*Asc*I. The junction was sequenced to make sure insert was heterologous. The *Asc*I fragment was ligated into the *Asc*I site of RO-HS.

RO-HS-FLAG-Lqf-ENTHUIM and UASt-FLAG-Lqf-ENTHUIM

PCR and site-directed mutagenesis was used to amplify the region containing the ENTH domain, UIM, and the first CBD while introducing a stop codon and an *Asc*I site. The 5' primer used for FLAG-Lqf- ENTH was used with this 3' primer: 5'-GGCGCGCCTTAGACAACAGCCGTGGGGG-3'. The template was full pBSKII-FLAG-Lqf. The resulting ~750 bp fragment was subcloned into the *Eco*RV site pBSKIIII and sequenced. The *Asc*I fragment was ligated into the *Asc*I site of RO-HS and UASt. Checked for proper orientation by restriction digestion.

RO-HS-FLAG-Lqf-ΔCBD and UASt-FLAG-Lqf-ΔCBD

PCR and site directed mutagenesis was in the following way. A 5' fragment was isolated from pBSKII-FLAG-Lqf restricted with *Asc*I and *Sal*I. Using PCR, a central fragment was generated containing sequences immediately following the *Pvu*II site to the *AlwN*I site. Using site-directed mutagenesis, the *Pvu*II site was changed to a *Sal*I site with the following primers: 5' primer: 5'-GTCGACTAAACAACAGGCCCCGTTTTC-3' and the 3' primer: 5'-GTACATGTAGGTATCATCAG-3'. The resulting ~295 bp fragment was subcloned into the *Eco*RV site pBSKIIII and sequenced. A 3' fragment was isolated from pBSKII-FLAG-Lqf restricted with *Alw*NI and*Asc*I. The resulting 5' *Asc*I-*Sal*I, central *Sal*I-*Alw*NI, and 3' *Alw*NI-*Asc*I were simultaneously ligated into the *Asc*I site in pB*Asc*I. The *Asc*I fragment was cloned into the *Asc*I site of RO-HS and UASt. Checked for proper orientation by restriction digestion.

RO-HS-FLAG-Lqf-ΔDPW3 and UASt-FLAG-Lqf-ΔDPW3

PCR and site directed mutagenesis was in the following way. A 5' fragment was isolated from pBSKII-FLAG-Lqf restricted with *Asc*I and *EcoN*I. Using PCR, a central fragment was generated containing sequences immediately following the *Sal*I site after the 6th DPW to the *Alw*NI site. Using site-directed

mutagenesis, the *Sal*I site was changed in-frame to a *Eco*NI site with the following primers: 5' primer: 5'- CCTGCTGAAGGGGGGGCCACGGCAAAG-3' and the 3' primer: 5'- GTACATGTAGGTATCATCAG-3'. The resulting ~510 bp fragment was subcloned into the *Eco*RV site pBSKIIII and sequenced. A 3' fragment was isolated from pBSKII-FLAG-Lqf restricted with *Alw*NI and*Asc*I. The resulting 5' *Asc*I-*Eco*NI, central *Eco*NI-*Alw*NI, and 3' *Alw*NI-*Asc*I were simultaneously ligated into the *Asc*I site in pB*Asc*I. The *Asc*I fragment was ligated into the *Asc*I site of RO-HS and UASt. Checked for proper orientation by restriction digestion.

RO-HS-FLAG-Lqf-DPWCBD-1 and UASt-FLAG-Lqf-DPWCBD-1

PCR and site directed mutagenesis was in the following way. A 5' fragment was isolated from FLAG-Lqf-ΔENTH restricted with *Asc*I and *Alw*NI. Using PCR, a 3' fragment was generated containing sequences 3' to *Alw*NI site and incorporating a stop codon and *Asc*I site 5' to the last NPF motif. The following primers were used: 5' primer: 5'-TCCTTACTATAATAGTCCAA-3' and the 3' primer: 5'-GGCGCGCCTTAGTTGCTGCTTCCGGCTTG -3'. The template was pBSKII-FLAG-Lqf. The resulting ~280 bp fragment was subcloned into the *Eco*RV site pBSKIIII and sequenced. The 5' *Asc*I-*Alw*NI and 3' *Alw*NI-*Asc*I were ligated into *Asc*I site of pB*Asc*I. The junction was sequenced to make

sure insert was heterologous. The *Asc*I fragment was ligated into the *Asc*I site of RO-HS and UASt. Checked for proper orientation by restriction digestion.

RO-HS-FLAG-Lqf-DPWCBD-2

PCR and site directed mutagenesis was in the following way. A 5' fragment was isolated from FLAG-Lqf-DPWCBD-1 restricted with *Asc*I and *Fse*I. Using PCR, a 3' fragment was generated containing sequences 3' to *Fse*I site and incorporating a stop codon and *Asc*I site 5' to the first NPF motif. The following primers were used: 5' primer: 5'-ACGTGGAGCCACTCCG-3' and the 3' primer: 5'-GGCGCGCCTTAGTACGCCGGCTGATTACC -3'. The resulting ~550 bp fragment was subcloned into the *Eco*RV site pBSKIIII and sequenced. The 5' *Asc*I-*Fse*I and 3' *Fse*I-*Asc*I were ligated into *Asc*I site of pB*Asc*I. The junction was sequenced to make sure insert was heterologous. The *Asc*I fragement was ligated into the *Asc*I site of RO-HS.

pMet414*Asc*I, 414-FLAG-Lqf, 414-FLAG-LqfENTH, and 414-FLAG-Lqf-ENTHUIM

Restricted pMet414 (From Beverly Wendlend) with *Hinc*II and inserted a blunted *Asc*I linker. This plasmid is called pMet414*Asc*I. Used *Asc*I fragments:

FLAG-Lqf-ENTH, FLAG-Lqf, FLAG-Lqf-ENTHUIM and ligated individually into pMet414*Asc*I. Chose plasmids with insert in the correct orientation.

pMet424*Asc*I, 424-FLAG-Lqf, 424-FLAG-LqfENTH, and 424-FLAG-Lqf-ENTHUIM

Cut pMet424 (From Beverly Wendlend) with *Sma*I and inserted a blunted *Asc*I linker. This plasmid is called pMet424*Asc*I. Used *Asc*I fragments: FLAG-Lqf-ENTH, FLAG-Lqf, FLAG-Lqf-ENTHUIM and ligated individually into pMet424*Asc*I. Chose plasmids with insert in the correct orientation.

GLRS-FLAG-Lqf

Chapter 2

Restricted pBSKII-FLAG-Lqf with *Asc*I and ligated the resulting 3400bp fragment into the *Asc*I site of GLRS vector. Checked for correct orientation.

RO-HS-Dl^{DN}

A DNA fragment of *Delta* lacking the cytoplasmic domain and flanked by *Asc*I sites was generated by PCR, using as a template pG1C (Fehon et al., 1990;

obtained from M. Muskavitch) which contains a complete *Delta* cDNA and the following primers, which also inserted a stop codon: 5'GGCGCGCCCACACACACACACAGCCCTG3', 5'GGCGCGCCTTACACCGCATTCTGTTC3'. The PCR product was ligated into pGEM-T-Easy (Promega) to generate pGEM-Dl^{DN}. An *AscI* fragment containing the truncated *Delta* gene was purified from pGEM-Dl^{DN} and ligated into RO-HS. A plasmid, RO-HS-Dl^{DN}, with the *Asc*I fragment in the appropriate orientation was isolated.

RO-HS-Shi^{DN}

An *Spe*I – *Sal*I fragment of pTM1 containing *shi^{K44A}* (Moline et al., 1999; obtained from A. Bejsovec), was ligated into pBSKII restricted with *SpeI* and *SalI* to generate pBSKII-shi^{DN}. *AscI* sites flanking the *shi^{K44A}* gene were added as follows: pBSKII-shi^{DN} was restricted with *Spe*I, treated with Klenow fragment, and an *Asc*I linker ligated in. A second *Asc*I linker was ligated similarly into the *Sal*I site. The resulting *Asc*I fragment of *shi^{K44A}* was purified and ligated into RO-HS. A plasmid, RO-HS-Shi^{DN}, with the *Asc*I fragment in the appropriate orientation, was isolated.

RO-HS-GFP

A DNA fragment containing *GFP* flanked by *Asc*I sites was generated by PCR, using a GFP-containing plasmid (Siemering et al., 1996) as a template and the following primers: 5'GGCGCGCCATGAGTAAAGGAGAAGAAC3', 5'GGCGCGCCTTATTTGTATAGTTCATCCC3'. The PCR product was ligated into pGEM-T-Easy (Promega) to generate pGEM-GFP. The *GFP* DNA sequence in pGEM-GFP was determined, and the *AscI* fragment containing *GFP* was isolated and ligated into the *AscI* site of RO-HS. A plasmid, RO-HS-GFP, with the *AscI* fragment in the appropriate orientation was isolated.

RO-HS-GFP-Lqf and UASt-GFP-Lqf

An *AscI – NdeI* DNA fragment containing *GFP* was generated by PCR using a GFP-containing plasmid (Siemering et al., 1996) as a template and the following primers: 5'CAGATGGGCGCGCCATGAGTAAAGGAGAAC3', 5'CATATGTTTGTATAGTTCATCC3'. The PCR product was ligated into pGEM-T-Easy to generate pGEM-GFP-AN. The *GFP* DNA sequence in pGEM-GFP-AN was determined and the ~700 bp *AscI – NdeI GFP* fragment was isolated and ligated into a plasmid containing the *lqf* cDNA called pMoPac-lqf-cDNA3. pMoPac-lqf-cDNA3 was constructed as follows: The *lqf* cDNA was generated in two parts by PCR using as a template pBSKII-FLAG-Lqf. The 5' part of *lqf* was generated as an *NdeI – HpaI* fragment using the primers 5 ' A T G C A G G T C A A T G T C G C T G G 3 ' a n d

5’CGGTTTGATCAGATTGTCTAGG. The PCR product was ligated into pGEM-T-Easy to generate pGEM-Lqf5’ and the *lqf* DNA sequence in the plasmid was determined. The 3’ part of *lqf* was generated as an *Hpa*I – *Asc*I fragment using the primers 5’TTTCCTCGGCGAGAACTC3’ and 5’TTACGACAAAAACGGATTTGTTG3’. The PCR product was ligated into pGEM-T-Easy to generate pGEM-cDNA3-3’ and the *lqf* DNA sequence in the plasmid was determined. An ~1650 bp *NdeI – HpaI* fragment of pGEM-Lqf5’ and and ~800 bp *Nde*I – *Asc*I fragment of pGEM-cDNA3-3’ were isolated and ligated into pMoPac (Hayhurst et al., 2003) restricted with *Nde*I and *Asc*I. Ligated into the *Asc*I site of RO-HS and UASt.

RO-HS-Lqf-GFP and UASt-Lqf-GFP

PCR’d 3’ fragment of Lqf from *AlwN*I site to last amino acid and inserted an in-frame *Mlu*I site. Used pBSKII-FLAG-Lqf for template. Cloned PCR product into PGEM-TEasy. Obtained plasmid with correct sequence and restricted with *AlwN*I and *Not*I and isolated 300bp band. Cut pBSKII-FLAG-Lqf with *Asc*I and *AlwN*I and *Ahd*I and isolated the 2100 bp band. Ligated these 2 fragments into pBSKII cut with *Not*I and *Asc*I. This plasmid, pBSKII-FLAG-Lqf-Mlu is cut with *Mlu*I and *Not*I. I cut this plasmid with *Mlu*I and *Not*I. Cut the plasmid pGEM-3’GFP with *Mlu*I and *Not*I and ligated this 750 bp fragment into it. This new plasmid is pBSKII-FLAG-Lqf-GFP. This plasmid was restricted with

*BssH*II and this fragment (about 3200 bps) ligated into the *Asc*I site of RO-HS and UASt. A plasmid with the correct orientation was chosen. Used the following primers: For 5'cagcacctgctgatgatgatacctacatgt3' Rev 5'cgcgtcgacaaaaacggatttgt3'

RO-HS-Neuralized

Obtained pBSKII-Neur from Eric Lai. Restricted this plasmid with *BssH*II and isolated a 3Kb fragment. Ligated this fragment in to RO-HS cut with *Asc*I. Selected a plasmid with neur in the correct orientation.

PGEM-3'GFP

PCR'd from p8036 as *Mlu*I-*Asc*I fragment. Inserted a stop before *Asc*I site. Cloned this fragment into pGEM-TEasy. Sequenced and chose one with correct sequence. Used the following primers:For 5'acgcgtagtaaaggagaag3'Rev 5'ggcgcgccttatttgtatagttcatcc3'

Chapter 4

pCasper4-Epsin-2-genomic region (without CG13850)

Obtained Bac clone (30J14) from BacPac resources. Using the protocol they supplied, I made a BAC DNA prep. I cut the DNA with *BssH*II which conveniently surrounds the epsin-2 gene. I ligated the library of *BssH*II fragments into pBSKII cut with *Asc*I. I isolated a plasmid containing an 12Kb fragment and sequenced one end. This plasmid is pBSKII-GenBssHII. This plasmid contains 270bp CG13850, all epsin-2 coding sequence, and the entire 5' gene, Nop56. To eliminate CG13850 sequences, I used this plasmid as template to PCR exactly 663 bp 5' from where Epsin-2 Pry+ P element is inserted. I inserted a *Not*I site and PCR'd to a *Aat*II site. I cloned this PCR product into PGEM and sequenced. Obtained plasmid with correct sequence called PGEM 5'gE2. Cut this plasmid with *Not*I and *Aat*III and obtained fragment about 1100 bp. I cut pBSKII-GenBssHII with *Aat*II and *Hind*III and isolated a 9Kb fragment. Ligate these fragments into pBSKII cut with *Not*I and *Hind*III. This plasmidis pBSKII-gE2. Cut this plasmid with *Not*I and *Kpn*I to isolate a 10KB fragment. I cut pCas4 with *Not*I and *Kpn*I. These fragments were ligated together to obtain the final plasmid. Primers used for PCR:For 5'gcggccgcccacacgctgcaagagaccac3' Rev 5'aaacttggggcgtggg3'.

RO-HS-D-Epsin-Ra and UASt-D-Epsin-Ra

Because I couldn't RT-PCR up the large exon6 (the last exon in D-Epsin-Ra), I chose to amplify it from genomic DNA. There is a conveniently located SAPI site right on the splice junction between exon5 and exon6 that I took advantage of.

Step1. PCR up 5'end of exon6 with following primers: For: ttgctgaagactgccacgc and Rev: cgaagatgtgccaatgaaaatgtatc to obtain a 1850 bp fragment. PCR'd up the 3'end of the exon with For: cctttgtgggaatcttgtaatg and Rev: atacctggaatacaatggcttc to obtain about a 1900 bp fragment. Both of these were cloned in to PGEM and sequenced. Plasmids were designated PGEM-Exon6A and PGEM-Exon6B.

I PCR'd the 3'end of exon5 from pBSKII-D-Epsin-R-I to insert an in-frame *SAP*I site. I used the following primers: For: gacttcaatccgcgtgccagc and Rev: atgccaactgctcttcaacagccatgggcatgctttgg to obtain a product of 355bp. This was cloned into PGEM and sequenced. The plasmid named PGEM-E2SAP.

Cut PGEM-E2SAP with *EcoR*I and SAP to drop out 350 bp fragment. Cut PGEM-Exon6A with *SAP*I and *BamH*I to get a 900 bp fragment. Cut pBSKII with *EcoR*I and *BamH*I and ligated all 3 together to make pBSKII-Exon6RIBam. Cut PGEM-Exon6A with *BamH*I and *Bts*I to get 400 bp fragment. Cut PGEM-Exon6B with *Bts*I and *Xho*I to get 1350 bp fragment. Cut pBSKII cut with

*BamH*I and *Xho*I and ligated all 3 together to make pBSKII-Exon6BamXho. Cut pBSKII with *Asc*I and *Xho*I (3KB). Cut pBSKII-D-Epsin-R-I with *Asc*I and *EcoR*I (1400). Cut pBSKII-Exon6RIBam with *EcoR*I and *BamH*I (1250). Cut pBSKII-Exon6BamXho with *BamH*I and *Xho*I(1750) Ligate all 4 together-insert=4400. This is called pBSKII-D-Epsin-Ra

To make RO-HS and UASt versions, I cut pBSKII-D-Epsin-Ra with *BssH*II and ligated into the *Asc*I sites of each of these vectors and checked for proper orientation.

UASt-GFP-D-Epsin-Ra

Using p8036 as template, I PCR'd GFP inserting in-frame flanking PmlI sites. Used the following primers: For: cacgtgagtaaaggagaag Rev: cacgtgtttgtatagttcatcc. Cloned 750bp fragment in to PGEM and sequenced. This plasmid is called PGEM-PmlGFP. Cut pBSK-D-Epsin-R-I with PmlI and treated with shrimp alkaline phosphatase. Partially digested PGEM-PmlGFP with PmlI and isolated the 750 bp fragment. Ligated the Pml-GFP fragment into D-Epsin-R-I cut with PmlI. Obtained plasmid with GFP in the correct orientation. This plasmid is called pBSK-GFP-D-Epsin-R-I. I cut pBSK-GFP-D-Epsin-R-I with AscI and EcoRI and obtained a 2100bp fragment. I cut pBSK D-Epsin-Ra with EcoRI and BssHII to obtain about a 3kB fragment. I ligated these two fragments

into a pBSK cut with AscI. This plasmid is called pBSK-GFP-D-Epsin-Ra. I cut this plasmid with BssHII and isolated the 5100bp fragment. I ligated this into UASt cut with AscI to make UASt-GFP-D-Epsin-Ra. Plasmid was checked for proper orientation.

RO-HS and UASt-D-Epsin-Rb

And the following PCR primers: For: Gcaaaacagtcagaaaacggcac Rev: agccttggaacgccgcaaag Cloned PCR product into PGEM and sequenced. This plasmid is PGEM-Epsin-2-I

To get the 3' end I used 3' RACE kit from Ambion. Internal race primer I used: Ttcgccatcgccgtctacttcc Obtained about a 1500 bp band and cloned into PGEM and sequenced. This plasmid is called PGEM-eps23. It contains coding sequence of D-Epsin-Rb from bp1300 to stop and some 3'UTR. There was only 1 bp change that resulted in an aa difference from published database:P→A494. However, I have since re-RT-PCR'd this change which appears to be a polymorphism, because I have also RT-PCR'd the published aa.

I used mutagenic PCR primer to insert an *Asc*I site before the ATG and a *Pml*I site in-frame immediately after the ATG (I wanted to use this to insert an epitope tag later) The primer I used was: ggcgcgccatgcacgtggtggataaattcatc and a

reverse primer to *BsoB*I site. I cloned this fragment into PGEM and sequenced. This plasmid is called PGEM-E2Epml. I cut PGEM-E2Epml with *Asc*I and *BsoB*I and isolated about a 450 bp fragment. I cut PGEM-D-Epsin-R-I with *BsoB*I and *EcoR*I and isolated about a 900 bp fragment. I cut pBSKII with *Asc*I and *EcoR*I. All 3 fragments were ligated together to produce pBSKII-D-Epsin-R-I.

D-Epsin-R-I is an *Asc*I---*EcoR*I fragment and Eps23 could be cut from PGEMas an *EcoR*I fragment, I could not ligate them together, though I tried and tried. I even tried different variations of this scheme. No success. So I did the following PCR experiment: I cut PGEM-D-Epsin-R-I with *Not*I and *Stu*I and cut PGEM-Eps23 with *Sal*I and *EcoR*I. These 2 fragments overlap in sequence by 125 bp. I put these fragments in a PCR reaction with the primer used above: ggcgcgccatgcacgtggtggataaattcat and with Rev: catatgttatcattgaaacaagtcgaatgc. Obtained a 2 KB fragment and cloned into PGEM –sequenced this is PGEM-D-Epsin-Rb. I cut this plasmid with *Asc*I and *Not*I and ligated to pBSKII cut with *Asc*I and *Not*I. This plasmid is pBSKII-D-Epsin-Rb. Cut this plasmid with *Asc*I and isolated 2KB fragment and cloned into UASt-cut with *Asc*I and SAP treated. Obtained plasmid with correct orientation. This plasmid is called UASt-D-Epsin-Rb.

UASt-D-Epsin-RaGFP

PCR'd 3' fragment of D-Epsin-Ra SnabI to last amino acid and inserted an in-frame MluI site. Used UASt-D-Epsin-Ra. Cloned PCR product into PGEM-TEasy. Obtained plasmid with correct sequence and restricted with *Snab*I and *Not*I (450) Cut UASt-D-Epsin-Ra with *Asc*I and *Snab*I and isolated 3700 bp fragment .Ligated these 2 fragments into pBSKII cut with *Not*I and *Asc*I. This plasmid is PBSKII-D-Epsin-RaMlu is cut with *Mlu*I and *Not*I. Cut the plasmid PGEM-3'GFP with *Mlu*I and *Not*I and ligated this 750 bp fragment into it. This new plasmid is pBSKII-D-Epsin-Ra-GFP. This plasmid was restricted with *BssH*II and this fragment (about 5000) ligated into the *Asc*I site of UASt. A plasmid with the correct orientation was chosen. Used the following primers:For1 tttacgtaaaatacgaaaatatt Rev 2 acgcgtggcagcctgttccatg

Pet28a-Comm

PCR'd from ATG to *EcoR*I site using pBSKII-D-Epsin-Ra-I (from ATG to *EcoR*I). I inserted *Nde*I site just before ATG. I used the following primers: pETCommFor: catatggtgcataaattcatc and Rev: T7 I cloned the PCR product into PGEM. Sequenced and obtain a plasmid PGEM-Comm. Cut this plasmid with *Nde*I and *EcoR*I and isolated 1300 bp fragment. Cut pET28 with *Nde*Iand *EcoR*I and ligated together. Obtained a plasmid with insert and used to make antigen.

Chapter 5

RO-HS and UASt-Chimera1 (D-Epsin-RENTH-Lqf3'-GFP)

PCR the ENTH domain of D-Epsin-R using UASt-D-Epsin-Ra as template. Insert *Asc*I site immediately 5' to ATG and *Nde*I site in-frame after ENTH domain. PCR a central fragment of Lqf using Angelica's plasmid 5 as template. Make fragment starting from end of ENTH domain to *Bgl*II site; insert an in-frame *Nde*I site at the very beginning of this fragment. Clone both PCRs into PGEM and sequence. Obtain plasmids of correct sequence called PGEM-1 and PGEM-2 respectively. Cut PGEM-1 with *Asc*I and *Nde*I and isolate fragment 500bp. Cut PGEM-2 with *Nde*I and *Bgl*II and get fragment 350bp. Cut Ro-Lqf-GFP with *Bgl*II and *Asc*I and isolate fragment 2300bp. Ligate all into pBSKII cut with *Asc*I, pBSKII-Chimera-1. Restrict this with *BssH*II and get fragment (3200bp) and ligate in to RO-HS and UASt cut with *Asc*I. Check for orientation. Following primers were used: 25'ENTH for: ggcgcgccatggtggataaattcatcagc 23'ENTH rev: catatggtccttgttcttcttcgcc 25'ENTH for: ggcgcgccatggtggataaattcatcagc 23'ENTH rev: catatggtccttgttcttcttcgcc

RO-HS and UASt-Chimera2 (5' Lqf and 3'D-Epsin-Ra)

PCR the ENTH domain of Lqf using Angelica's plasmid number 5 as template. Insert *Asc*I site immediately 5' to ATG and *Nde*I site in-frame after ENTH domain. PCR a central fragment of D-Epsin-Ra using UASt-D-Epsin-Ra as template. Make fragment starting from end of ENTH domain to *Bgl*II site; insert an in-frame *Nde*I site at the very beginning of this fragment. Clone both PCRs into PGEM and sequence. Obtain plasmids of correct sequence called PGEM-3 and PGEM-4 respectively. Cut PGEM-3 with *Asc*I and *Nde*I and isolate fragment 500bp. Cut PGEM-4 with *Nde*I and *EcoR*I and get fragment 550bp. Cut Ro-D-Epsin-Ra-GFP with *EcoR*I and *BssH*II and isolate fragment 4200bp. Ligate all into pBSKII cut with *Asc*I, pBSKII-Chimera-2. Restrict this with *BssH*II and get fragment about 5100bp and ligate in to UASt cut with *Asc*I. Check for orientation. Following primers were used: Q5'ENTH for: ggcgcgccatggtggataaattcatcagc Q5'ENTH rev: catatggtccttgttcttcttcgccc 2Ndefor: catatgaagtacatcggcatgagcag 2BglIIrev:agatctgtagccgttgtggctgc

UASt-D-Epsin-R-ENTH-GFP

PCR from UASt-D-Epsin-Ra inserting an *Asc*I site before ATG to end of ENTH domain and then inserting 5 alanines and an *Mlu*I site in-frame. Use the following primers: For: ggcgcgccatggtggataaattcatc and Rev: acgcgtggcggcggcggcggcgtccttgttcttcttcgc. Clone into PGEM and sequence.

Obtain correct plasmid called PGEM-lqfENTH. Cut this plasmid with *EcoR*I and *Mlu*I to obtain a 500 bp fragment. Cut PGEM-3'GFP with *Mlu*I and *Not*I to obtain a 750 bp fragment. Cut pBSKII with *EcoR*I and *Not*I. Ligate all 3. This plasmid is called pD-Epsin-R-ENTH-GFP. This can now be cut with *Asc*I and a 1250 bp fragment isolated and ligated to UASt cut with *Asc*I. A plasmid of the correct orientation was obtained.

UASt-D-Epsin-R-ΔENTH-GFP

Cut PGEM-4 (from chimera2) with *EcoR*1 and *Nhe*I to obtain a 900bp fragment. Cut UASt-D-Epsin-Ra-GFP with *Nhe*I and *Asc*I to get a 4200 bp fragment. Ligated these 2 fragments into pBSKII cut with *EcoR*I and *Asc*I to obtain a plasmid pBSKII-E2aΔENTH-GFP. Restricted this fragment with *Asc*I to obtain a 4700 bp fragment and ligated into UASt cut with *Asc*I. Obtained plasmid with correct orientation.

RO-HS and UASt-Lqf-ENTH-GFP

PCR from Angelica's plasmid 5 inserting an *Asc*I site before ATG to end of ENTH domain and then inserting 5 alanines and an *Mlu*I site in-frame. Use the following primers: For: ggcgcgccatgcaggtcaatgtcgct and Rev: acgcgtggcggcggcggcggcgaacccactcgggttctg. Clone into PGEM and sequence.

Obtain correct plasmid called PGEM-lqfENTH. Cut this plasmid with *EcoR*I and *Mlu*I to obtain a 500 bp fragment. Cut PGEM-3'GFP with *Mlu*I and *Not*I to obtain a 750 bp fragment. Cut pBSKII with *EcoR*I and *Not*I. Ligate all 3. This plasmid is called pLqfENTH-GFP. This can now be cut with *Asc*I and a 1250bp fragment isolated and ligated to RoHS and UASt cut with *Asc*I. A plasmid of the correct orientation was obtained.

RO-HS and UASt-FLAG-Lqf-ΔENTH-GFP

I cut Ro-FLAG-LqfΔENTH with *Asc*I and *Bgl*II to obtain a 350bp fragment. I cut Ro-Lqf-GFP with *Bgl*II and *Asc*I to obtain a 23050bp fragment. These 2 were ligated into RoHS and UASt cut with *Asc*I. Checked for orientation.

RO-HS-Lqf-ENTH-UIM

PCR'd 5' Lqf containing ENTH and UIM with the following primers: Rev: acgcgtttcctccttcttgggcgc For: primer used for Chimera2. Inserted an *Mlu*I site 3' to UIM. Cloned this 750 bp fragment into PGEM and sequenced. Cut this plasmid with *EcoR*I and *Mlu*I and isolated 750 bp fragment. Cut PGEM-3'GFP plasmid with *Mlu*I and *Not*I. Ligated these two fragments into pBSK cut with

*EcoR*I and *Not*I. Cut this plasmid with *Asc*I and ligated into RO-HS cut with *Asc*I. Isolated plasmid with correct orientation..

RO-HS-LqfΔENTHUIM-GFP and UASt-LqfΔENTHUIM-GFP

PCR'd Lqf immediately 3'to UIM (inserting a 5' *Nde*I and ATG site) to *EcoN*I site. **Primers?** Cloned this into PGEM and sequenced. Cut this plasmid with *Apa*I and *EcoN*I and isolated 500bp fragment. Cut pLqfGFP with *Apa*I and *EcoN*I and isolated 5KB fragment containing pBSK. Ligated these two fragments together and this plasmid is called pΔEUGI. Cut this plasmid with NotI and ligated into pBSK cut with *Not*I. Finally, cut this plasmid with *BssH*II and *Pvu*I and isolate the 2600bp fragment. This fragment was ligated into UASt and RO-HS cut with *Asc*I. Plasmids with the correct orientation were obtained.

RO-HS-FLAG-Lqf-RFP and UASt-FLAG-Lqf-RFP

Obtained pRedHStinger from Posakony lab. PCR'd RFP with following primers: For acgcgtatggcctcctccg and Rev ggcgcgccttatacaggaacaggtg. Inserted Stop and *Asc*I at 3' end and in-frame *Mlu*I site at 5' end. Cloned this 700 bp fragment into PGEM and sequenced. Cut this plasmid with *Mlu*I and *Not*I and isolated 700 bp fragment. Cut pLqf-GFP with *Mlu*I and *Not*I and isolated 6KB fragment. Ligated these two fragments together. This plasmid is pLqfRFP. Cut

this plasmid with *Asc*I and ligated into UASt and RO-HS cut with *Asc*I. Isolated plasmids with correct orientation.

Chapter 2 addendum

RO-HS-Dl-LDL (DA-18)

Obtained pUASt-myc-Dl-LDL from Gary Struhl. Cut with *Xba*I and *Nhe*I. Cloned into pBSK cut with *Xba*I. Cut this plasmid with *BssH*II and *Ahd*I and isolated 2.4kB fragment. Cloned this fragment into RO-HS cut with *Asc*I. Isolated plasmid with correct orientation.

Miscellaneous experiments

RO-HS-Dl(EC)-GFP-Ub(WT)

PCR'd from DlDN a 3' fragment from *Bsa*I to end of TM domain. With reverse primer, inserted 2 alanines and *Hind*III site in-frame. Cloned product into PGEM and sequenced to obtain plasmid PGEM-Dl3'. PCR'd GFP from p8036 and engineered a 5' *Hind*III site followed by 3 alanines. 3' I added 3 more alanines followed by *Sma*I site in-frame. Cloned this fragment to make a plasmid PGEM-GFPAla. PCR'd WT Ubiquitin from Ru's pBSKII-Ubiquitin. I

engineered a 5' SmaI site followed by 3 alanines and at the 3' end I incorporated a stop codon followed by an *Asc*I site. I cloned this into PGEM to make PGEM-Ub. Cut PGEM-Dl3' with *Bsa*I and *Hind*III and isolated 500 bp fragment. Cut PGEM-GFPAla with *Hind*III and *Sma*I and isolated a 750 bp fragment. I cut PGEM-Ub with *Sma*I and *Asc*I and isolated 250 bp fragment. I cut Ro-DlDN with *Asc*I and *Bsa*I and isolated 1500 bp 5' fragment. I ligated all these into pBSKII cut with *Asc*I. I obtained a plasmid called pDlGFPUb. I restricted this plasmid wth *Asc*I and isolated a 3100 bp fragment and ligated into RoHS Check orientation. Use the following primers: For1 (3'Dl) ctggacaactgcagtccg

Rev (3'Dl) aagcttggcggcggccaccgcattctgttcgttc

For2 (GFPAla) aagcttgccgccgccatgagtaaaggagaagaac

Rev2 (GFPAla) cccgggggcggcggctttgtatagttcatcc

For3 (UbWT)cccggggccgccgccatgcagatcttcgtgaag

Rev3 (UbWT) ggcgcgccttaaccaccacggagacg

RO-HS-Dl(EC)-GFP-Ub(K48RΔG76)

PCR'd K48R Ubiquitin from Ru's pBSKII-Ubiquitin(K48R). I engineered a 5' *Sma*I site followed by 3 alanines and at the 3' end I deleted the last G and incorporated a stop codon followed by an *Asc*I site cloned this into PGEM to make PGEM-Ub(K48R). This plasmid is called PGEM-Ub K48R. Cut this plasmid with *Sma*I and *Asc*I and isolated the 250bp fragment. Cut

pDlGFPUbWT with *Asc*I and *Sma*I and isolated the 2800 bp band. These 2 fragments were ligated into RoHS Check orientation. Use the following primers: For3 (UbWT) cccggggccgccgccatgcagatcttcgtgaag Rev3 (UbK48R) ggcgcgccttaacggagacgaagaac

RO-HS-Dl(EC)-GFP

Cut Ro-Dl GFPUbWT with *Asc*I and *Nde*I to isolate 2.3 Kb 5' fragment. Cut Ro-Lqf-GFP with *Nde*I and *Asc*I to isolate 500bp 3' fragment. I ligated these 2 fragments into the *Asc*I site of the RoHS vector. Checked for plasmid with appropriate orientation. Insert size about 2800.

RO-HS-Dl(FL)-GFP-Ub(K48R, GΔ76)

PCR'd the 3' end of Delta from full-length Delta template (see DlDN construct). Using mutagenesis, the Stop codon was eliminated and *Hind*III site was inserted follwed by 3 alanines. The following primers were used: For tgtcgtgcgggatttac and Rev aagcttggcggcggccatatgcggagtgccgccgc. Cloned this 1KB fragment in to PGEM and sequeced. Cut this plasmid with *Sal*I and and *Hind*III. Cut pDl(EC)GFP-Ub(K48RGΔ76) with *Sal*I and *Hind*III and isolated 3'fragment containing pBSK. I ligated these two fragments together and call this plasmid p3'DlGU. I cut this plasmid with *Tth*III and *Asc*I and isolated 2KB

fragment. I cut RoDlDN with *Not*I and *Tth*III and isolated 2KB fragment. I ligated these two fragments together into pBSK cut with *Asc*I and *Not*I. Cut this plasmid with *Asc*I and *Pvu*I and isolated 2.6KB *Asc*I fragment. Ligated this into RO-HS and isolated plasmid with correct orientation.

UASt-FLAG-Lqf-ΔNPF-1

Cut pBSK-FLAG-Lqf (Angelica's plasmid 5) with *Asc*I and *EcoN*I and isolated the 1200bp 5' fragment. Cut pFLAG-Lqf-DPWCBD-1 with *EcoN*I and *Asc*I and isolated the 1200bp 3'fragment. Ligated these two together into pBSK cut with *Asc*I. Cut this plasmid with *Asc*I and isolated 2400 bp fragment, which was ligated into UASt cut with *Asc*I. Aplasmid with the correct orientation was isolated.

UASt-D-Epsin-Rb-GFP

PCR'd 3' fragment of D-Epsin-Rb from *Ahd*I site to last amino acid and inserted an in-frame *Mlu*I site. Used UASt-D-Epsin-Rb for template. Cloned PCR product into PGEM-TEasy. This plasmid is called PGEM-D-Epsin-Rb 3'. Obtained plasmid with correct sequence and restricted with *Ahd*I and *Not*I (200), Cut UASt-D-Epsin-Rb with *Asc*I and *Ahd*I and isolated the 5' 1800bp fragment.

Ligated these two fragments into pBSK cut with *Not*I and *Asc*I. This plasmid is PBSK-D-Epsin-Rb-Mlu is cut with *Mlu*I and *Not*I. Cut the plasmid PGEM-3'GFP with *Mlu*I and *Not*I and ligated this 750 bp fragment into it. This new plasmid is pBSK-D-Epsin-Rb-GFP. This plasmid was restricted with *BssH*II and this fragment (about 2750) ligated into the *Asc*I site of UASt. A plasmid with the correct orientation was chosen. Used the following primers for PCR: For1 gaagaccaacagtccggc Rev 2 acgcgtttgaaacaagtcgaa

pET28a-Lqf

I cut pMoPac-Lqf-cDNA-3 with *Nde*I and *Bgl*II to obtain a 5' 800kb fragment. I cut Angelica's plasmid 5 with *Bgl*II and *Hind*III to get the 3' 1900bp frag. I cut pET28a with *Nde*I and *Hind*III. All three fragments were ligated together to make the final plasmid

GLRS-LacZ-Gal4VP16

PCR'd Gal4VP16 as *Not*I-*Asc*I fragment using plasmid from K. Moses. Inserted a stop before *Asc*I site. Cloned this fragment into pGEM-TEasy. Sequenced and chose one with correct sequence. (PGEM-G4VPNot)PCR'd LacZ from JAF's faf-lacZ inserting an *Asc*I site before the ATG and a *Not*I site in-frame

and eliminating the stop codon. Cloned into PGEM and sequenced (PGEM-lacZ) Cut PGEM-G4VPNot with *Asc*I and *Not*I (800) and cut PGEM-lacZ with *Asc*I and *Not*I(3150) Ligated these 2 fragments into pBSK cut with *Asc*I. Cut this plasmid with *Asc*I and ligated into GLRS cut with *Asc*I. Isolated plasmid with the correct orientation. Primers used for LacZFor: ggcgcgccatgaccatgattacggattcaRev: gcgccgctttttttgacaccagacc Used the following primers for Gal4VP16 For1 gcggccgccgccgccgaagcttctgtcttctRev 2 ggcgcgccttaaccgtactcgtcaattcc

GLRS-Adh-Gal4VP16

Obtained clone from Open Biosystems (GH01616). PCR'd Adh, inserting an *Bgl*II site before the ATG and an *Mlu*I site after the last amino acid. Used the following primers For: agatctatgtcgtttactttgacc Rev: acgcgtgatgccggagtcccagtg. Cloned this fragment (1Kb) into PGEM and sequenced to make PGEM-Adh. Cut PGEM-Adh with *EcoR*I and *Mlu*I to isolate 1Kb fragment. Cut PGEM-3'Gal4VP16 with *Mlu*I and *Not*I (800) and ligated these 2 into pBSK cut with *EcoR*I and *Not*I. This plasmid, pBSK-Adh-Gal4VP16 was restricted with *BssH*II and an 1800 bp band isolated and ligated in to GLRS cut with *Asc*I. A plasmid of the correct orientation was obtained.

GLRS-FLAG-Lqf-SV40-Gal4VP16

PCR'd 3' fragment of Lqf from *AlwN*I site to last amino acid and inserted an in-frame SV40 nuclear localization signal and *Mlu*I site. Used Angelica's plasmid 5 for template. Cloned PCR product into PGEM-TEasy. Obtained plasmid with correct sequence and restricted with *AlwN*I and NotI (350). Cut Angelica's plasmid 5 with *Asc*I and *AlwN*I and *Ahd*I and isolated the 2100 bp *Asc*I-*AlwN*I 5'fragment. Ligated these 2 fragments into pBSK cut with *Not*I and *Asc*I. This plasmid is PBSK-FLAG-Lqf-SV40-Mlu is cut with *Mlu*I and *Not*I. Cut the plasmid PGEM-3'Gal4VP16 with *Mlu*I and *Not*I and ligated this 750 bp fragment into it. This new plasmid is pBSK-FLAG -Lqf- SV40-Gal4VP16. This plasmid was restricted with *BssH*II and this fragment (about 3300) ligated into the *Asc*I site of GLRS. A plasmid with the correct orientation was chosen. Used the following primers:For1 cagcacctgctgatgatgatacctacatgt Rev 2 acgcgtcttcgccttcttcttgggcgacaaaaacggatttgt

GLRS-Lqf-Gal4VP16

PCR'd 3' fragment of Lqf from *AlwN*I site to last amino acid and inserted an in-frame *Mlu*I site. Used Angelica's plasmid 5 for template. Cloned PCR product into PGEM-TEasy. Obtained plasmid with correct sequence and restricted with *AlwN*I and *Not*I (300) Cut Angelica's plasmid 5 with *Asc*I and *AlwN*I and AhdI and isolated the 2100 bp *Asc*I-*AlwN*I frag. Ligated these 2 fragments into pBSK cut with *Not*I and *Asc*I. This plasmid is PBSK-FLAG-Lqf -Mlu is cut with

*Mlu*I and *Not*I. Cut the plasmid PGEM-3'Gal4VP16 with *Mlu*I and *Not*I and ligated this 750 bp fragment into it. This new plasmid is pBSK-FLAG-Lqf- -Gal4VP16. This plasmid was restricted with *BssH*II and this fragment (about 3300) ligated into the *Asc*I site of GLRS. A plasmid with the correct orientation was chosen.Used the following primers: For1 cagcacctgctgatgatgatacctacatgt Rev 2 acgcgtcgacaaaaacggatttgt

RO-HS-SV40-Lqf and UASt-SV40-Lqf

PCR'd a 5' fragment of Lqf to an internal *BstX*I site. The For primer was used to mutangenically insert an *Asc*I site before the ATG and SV40 nuclear localization signal afer ATG (see below) Template was pMoPac-Lqf-cDNA-3. Cloned this PCR product into PGEM T-Easy and sequenced the insert. A plasmid with the correct sequence was chosen and cut with *Asc*I and *BstX*I. (500 bp) PMoPac-Lqf-cDNA-3 was cut with *BstX*I and *EcoR*V (2KB 3'end). These 2 fragments were ligated into pBSK cut with *EcoR*V and *Asc*I. This is now an *Asc*I fragment (see cloning scheme for PmocDNA3) because there is a 3'*Asc*I site. Cut with *Asc*I and cloned into UASt and RO-HS. Check orientation. Used the following primers:For1 ggcgcgccatgcccaagaagaagcggaaggtgcata (SV40For/pmo1) Rev 2 catatgcaggtcaatgtcgctgg (pmo2)

RO-HS-DNDER

Jaf got DNDER from some lab in a vector. Restricted this vector with *Xho* and *EcoR*I and ligated to pBSK restricted with same. Inserted *Asc*I linkers on both sides. Then cut with *Asc*I and cloned into RoHs *Asc*I site. Checked orientation.

RO-HS-Gal4

PCR'd Gal4 from genomic DNA from GMR-Gal4 flies inserting an *Asc*I site before the ATG and after the stop. This 2.7kb fragment was cloned into the PGEM vector and sequenced. PGEM-Gal4 was then cut with *Asc*I and the 2700bp fragment was ligated to RoHS cut with *Asc*I. Orientation was checked. Used the following primers: For1 ggcgcgccatgaagctactgtcttctatcg Rev 2 ggcgcgccttactctttttttgggtttgg

More Chapter 3 plasmids

RO-HS-FLAG-Ent1

Cut pBSK-Ent1-AscI-B with *BamH*I and insert FLAG-tag oligo with sticky ends. This plasmid is cut with *Asc*I and a 2700 bp fragment is isolated and ligated into RO-HS cut with *Asc*I and checked for proper orientation.

RO-HS-Ent1

PCR'd from pEnt1.414 plasmid sent by Beverly Wendland. Used primers to insert *Asc*I and an in-frame BamHI site after the start codon. Jay Hook designed the primers (I don't know where they are). Reverse primer lay down in coding sequence just 3' to *Nde*I site. The PCR product of about 400bp was cloned into TOPO TA cloning vector from Invitrogen. This plasmid is TA-Ent1PCR. Next, cut out *Sal*I-*BamH*I fragment (2700 bp) from pEnt1-414 and clone into pBSK cut with same. This plasmid is pBSK-Ent1. Cut this plasmid with *Xho*I and blunt and insert an *Asc*I linker. Next cut this plasmid with *BamH*I and blunt and re-ligate to destroy this site. Finally, cut this plasmid with *Asc*I and *Nde*I and isolate 5300 bp fragment containing 3' end of Ent1 and pBSK. Cut TA-Ent1-PCR with *Asc*I and *Nde*I and isolate 400bp fragment. Ligate these two together to make pEnt1-AscI-A. Cut this plasmid with *Not*I, blunt with Klenow and insert *Asc*I linker. This plasmid pEnt1-AscI-B is cut with *Asc*I and a 2700bp fragment is isolated and ligated into RO-HS cut with *Asc*I and checked for correct orientation.

RO-HS-Ent2

PCR'd from Beverly Wendland's pEnt2.414 plasmid. Inserted *Asc*I site at 5' and 3' ends with mutagenic primers. Cloned this into PGEM and sequenced. Cut the *Asc*I fragment out (2700bp) and cloned into RO-HS cut with *Asc*I. Isolated plasmid with correct orientation.

RO-HS-Rat-Epsin1-ΔENTH

PCR'd from RO-HS-Rat-Epsin1 made by Angelica. Inserted *Asc*I site and ATG immediately following the ENTH domain and inserted an *Asc*I site after the stop. Used the following primers: For ggcgcgccatgcaggtggccacggcttcctcaagca and Rev: ggcgcgccttataggaggaaggggtt. Cloned the 1.3KB fragment into PGEM and sequenced. Cut this plasmid with *Asc*I and cloned into RO-HS cut with *Asc*I. Chose plasmid with correct orientation.

RO-HS-Human-epsin-2-likeΔENTH

PCR'd from RO-HS-Human-D-Epsin-R-like made by Jay Hook ?. Inserted *Asc*I site and ATG immediately following the ENTH domain and inserted an *Asc*I site after the stop. Used the following primers: For ggcgcgccatgcaggtggccactggtgtgggc and Rev: ggcgcgccctagagaaggaaagggtt. Cloned the 1.5KB fragment into PGEM and sequenced. Cut this plasmid with

*Asc*I and cloned into RO-HS cut with *Asc*I. Chose plasmid with correct orientation.

Appendix I

PMoPac-Lqf-cDNA-2

PCR'd from 5' end,inserting an *Nde*I site immediately before ATG, to *Hpa*I site. Used primers pmo1 and pmo2. PCR'd 5' end from *Hpa*I site to TAA, inserting an *Asc*I site immediately after, with primers pmo3 and pmo4. Cloned both of these fragments into PGEM TEasy and sequenced. They are called PGEM-Lqf5' and PGEM-cDNA-2-3' respectively. Template for 3' end was Angelica's plasmid 13. I cut PGEM-Lqf5' with *Nde*I and *Hpa*I and isolated a 1650 bp fragment. I cut PGEM-LqfcDNA-2-3' with *Hpa*I and *Asc*I and isolated 400bp fragment. I cut pMoPac (about 6Kb) with *Nde*I and *Asc*I and ligated these 2 fragments in. Pmo1 atgcaggtcaatgtcgctgg Pmo2 cggtttgatcagattgtctagg Pmo3 tttcctcggcgagaactc Pmo4 ttacgacaaaaacggatttgttg

PMoPac-Lqf-cDNA-3

PCR'd from 5' end,inserting an *Nde*I site immediately before ATG, to *Hpa*I site. Used primers pmo1 and pmo2. PCR'd 5' end from *Hpa*I site to TAA, inserting an AscI site immediately after, with primers pmo3 and pmo4. Template was

Angelica's plasmid 3. Cloned both of these fragments into PGEM TEasy and sequenced. They are called PGEM-Lqf5' and PGEM-cDNA-3-3' respectively. I cut PGEM-Lqf5' with *Nde*I and *Hpa*I and isolated a 1650 bp fragment. I cut PGEM-LqfcDNA-3-3' with *Hpa*I and *Asc*I and isolated 800bp fragment. I cut pMoPac (about 6Kb) with *Nde*I and *Asc*I and ligated these 2 fragments in. Pmo1 atgcaggtcaatgtcgctgg Pmo2 cggtttgatcagattgtctagg Pmo3 tttcctcggcgagaactc Pmo4 ttacgacaaaaacggatttgttg

References

Artavanis-Tsakonas, S., Rand, M. D. and Lake, R. J. 1999. Notch signaling: cell fate control and signal integration in development. *Science* 284, 770-776.

Aguilar, R.C., H.A. Watson, and B. Wendland. 2003. The yeast Epsin Ent1 is recruited to membranes through multiple independent interactions. *J Biol Chem* 278: 10737-43.

Alberts, B., Johnson, A., Lewis, J., Raff, M., Roberts, K., Walter, P. 2002. Molecular Biology of the Cell. ISBN 0815340729.

Amerik, A.Y., J. Nowak, S. Swaminathan, and M. Hochstrasser. 2000. The Doa4 deubiquitinating enzyme is functionally linked to the vacuolar protein-sorting and endocytic pathways. *Mol Biol Cell* 11: 3365-80.

Amerik, A.Y. and M. Hochstrasser. 2004. Mechanism and function of deubiquitinating enzymes. B*iochim Biophys Acta* 1695: 189-207.

Baeg, G.H., E.M. Selva, R.M. Goodman, R. Dasgupta, and N. Perrimon. 2004. The Wingless morphogen gradient is established by the cooperative action of Frizzled and Heparan Sulfate Proteoglycan receptors. *Dev Biol* 276: 89-100.

Baker, N. E. 2002. NOTCH and the patterning of ommatidial founder cells in the developing *Drosophila* eye in *Drosophila*. In *Drosophila* Eye Development, (ed. K. Moses), pp. 5-20. Berlin, Springer-Verlag.

Baker, N. E. and Yu, S.-Y. 1996. Proneural function of neurogenic genes in the developing *Drosophila* eye. *Curr. Biol.* 7, 122-132.

Baker, N. E., Yu, S. and Han, D. 1996. Evolution of proneural Atonal expression during distinct regulatory phases in the developing *Drosophila* eye. *Curr. Biol.* 6, 1290-1301.

Baker, N. E. and Yu, S.-Y. 1998. The R8-photoreceptor equivalence group in *Drosophila*: fate choice precedes regulated *Delta* transcription and is independent of *Notch* gene dose. *Mech. Dev.* 74, 3-14.

Baker, N. E. 2002. Notch and the patterning of ommatidial founder cells in the developing *Drosophila* eye. In *Drosophila Eye Development* (ed. K. Moses), pp. 35-58. Berlin: Springer-Verlag.

Bardin, A.J., R. Le Borgne, and F. Schweisguth. 2004. Asymmetric localization and function of cell-fate determinants: a fly's view. *Curr Opin Neurobiol* 14: 6-14.

Bardot, B., L.P. Mok, T. Thayer, F. Ahimou, and C. Wesley. 2005. The Notch amino terminus regulates protein levels and Delta-induced clustering of *Drosophila* Notch receptors. *Exp Cell Res* 304: 202-23.

Baron, M. 2003. An overview of the Notch signaling pathway. *Sem. Cell Dev. Biol.* 14, 113-119.

Bejsovec, A. and E. Wieschaus. 1995. Signaling activities of the *Drosophila* wingless gene are separately mutable and appear to be transduced at the cell surface. *Genetics* 139: 309-20.

Belenkaya, T.Y., C. Han, D. Yan, R.J. Opoka, M. Khodoun, H. Liu, and X. Lin. 2004. *Drosophila* Dpp morphogen movement is independent of dynamin-mediated endocytosis but regulated by the glypican members of heparan sulfate proteoglycans. *Cell* 119: 231-44.

Ben-Yaacov, S., R. Le Borgne, I. Abramson, F. Schweisguth, and E.D. Schejter. 2001. Wasp, the *Drosophila* Wiskott-Aldrich syndrome gene homologue, is required for cell fate decisions mediated by Notch signaling. *J Cell Biol* 152: 1-13.

Berdnik, D., Torok, T., Gonzalez-Gaitan, M. and Knoblich, J. A. 2002. The endocytic protein a-Adaptin is required for Numb-mediated asymmetric cell division in *Drosophila. Dev. Cell* 3,. 221-231.

Boehm, M. and J.S. Bonifacino. 2001. Adaptins: the final recount. *Mol Biol Cell* 12: 2907-20.

-. 2002. Genetic analyses of adaptin function from yeast to mammals. *Gene* 286: 175-86.

Brodsky, F.M., C.Y. Chen, C. Knuehl, M.C. Towler, and D.E. Wakeham. 2001. Biological basket weaving: formation and function of clathrin-coated vesicles. *Annu Rev Cell Dev Biol* 17: 517-68.

Bryant, D.M. and J.L. Stow. 2004. The ins and outs of E-cadherin trafficking. *Trends Cell Biol* 14: 427-34.

Cadavid, A. L. M., Ginzel, A. and Fischer, J. A. 2000. The function of the *Drosophila* Fat facets deubiquitinating enzyme in limiting phtoreceptor cell number is intimately associated with endocytosis. *Development* 127, 1727-1736.

Campbell, W. G. 1990. Form and Style in Thesis Writing, a Manual of Style. Chicago: The University of Chicago Press.

Chandrasekharappa, and A.B. Chitnis. 2003. Mind bomb is a ubiquitin ligase that is essential for efficient activation of Notch signaling by Delta. *Dev Cell* 4: 67-82.

Chang, H.C., S.L. Newmyer, M.J. Hull, M. Ebersold, S.L. Schmid, and I. Mellman. 2002. Hsc70 is required for endocytosis and clathrin function in *Drosophila*. *J Cell Biol* 159: 477-87.

Chen, H. and P. De Camilli. 2005. From the Cover: The association of epsin with ubiquitinated cargo along the endocytic pathway is negatively regulated by its interaction with clathrin. *Proc Natl Acad Sci* U S A 102: 2766-71.

Chen, H., Fre, S., Slepnev, V.I., Capua, M.R., Takei, K., Butler, M.H., Di Fiore P.P., and De Camilli P. 1998. Epsin is an EH-domain-binding protein implicated in clathrin-mediated endocytosis. *Nature* 394, 793-797.

Chen, H., S. Polo, P.P. Di Fiore, and P.V. De Camilli. 2003. Rapid Ca2+-dependent decrease of protein ubiquitination at synapses. *Proc Natl Acad Sci* U S A 100: 14908-13.

Chen, H., V.I. Slepnev, P.P. Di Fiore, and P. De Camilli. 1999. The interaction of epsin and Eps15 with the clathrin adaptor AP-2 is inhibited by mitotic phosphorylation and enhanced by stimulation-dependent dephosphorylation in nerve terminals. *J Biol Chem* 274: 3257-60.

Chen, M. S., Obar, R. A., Schroeder, C. C., Austin, T. W., Poodry, C. A., Wadsworth, S. C. and Vallee, R. B. 1991. Multiple forms of dynamin are encoded by *shibire*, a *Drosophila* gene involved in endocytosis. *Nature* 351, 583-586.

Chen, W. and D. Casey Corliss. 2004. Three modules of zebrafish Mind bomb work cooperatively to promote Delta ubiquitination and endocytosis. *Dev Biol* 267: 361-73.

Chen, X. and Fischer, J. A. 2000. *In vivo* structure/function analysis of the *Drosophila fat facets* deubiquitinating enzyme gene. *Genetics* 156,1829-1836.

Chen, X., E. Overstreet, S.A. Wood, and J.A. Fischer. 2000. On the conservation of function of the *Drosophila* Fat facets deubiquitinating enzyme and Fam, its mouse homolog. *Dev Genes Evol* 210: 603-10.

Chen, X., Q. Li, and J.A. Fischer. 2000. Genetic analysis of the *Drosophila* DNAprim gene. The function of the 60-kd primase subunit of DNA polymerase opposes the fat facets signaling pathway in the developing eye. *Genetics* 156: 1787-95.

Chen, X., Zhang, B. and Fischer, J. A. 2002. A specific protein substrate for a deubiquitinating enzyme: Liquid facets is the substrate of Fat facets. *Genes Dev.* 16, 289-294.

Chidambaram, S., N. Mullers, K. Wiederhold, V. Haucke, and G.F. von Mollard. 2004. Specific interaction between SNAREs and epsin N-terminal homology (ENTH) domains of D-Epsin-Related proteins in trans-Golgi network to endosome transport. *J Biol Chem* 279: 4175-9.

Cho, K.O. and K.W. Choi. 1998. Fringe is essential for mirror symmetry and morphogenesis in the *Drosophila* eye. Nature 396: 272-6.

Cho, K.O., J. Chern, S. Izaddoost, and K.W. Choi. 2000. Novel signaling from the peripodial membrane is essential for eye disc patterning in *Drosophila*. *Cell* 103: 331-42.

Collins, B.M., A.J. McCoy, H.M. Kent, P.R. Evans, and D.J. Owen. 2002. Molecular architecture and functional model of the endocytic AP2 complex. *Cell* 109: 523-35.

Confalonieri, S., Salcini, A. E., Puri, C., Tacchetti, C. and Di Fiore, P. P. 2000. Tyrosine phosphorylation of Eps15 is required for ligand-regulated, but not constitutive, endocytosis. *J. Cell Biol.* 150, 905-912.

Cooper, M. T. D. and Bray, S. J. 1999. Frizzled regulation of Notch signaling polarizes cell fate in the *Drosophila* eye. *Nature* 397, 526-530.

Cooper, J.A. and B.W. Howell. 1999. Lipoprotein receptors: signaling functions in the brain? *Cell* 97: 671-4.

De Camilli, P., Chen, H., Hyman, J., Panepucci, E., Bateman, A. and Brunger, A. T. 2001. The ENTH domain. *FEBS Lett.* 25686, 1-8.

De Joussineau ,C., Soule, J., Martin, M., Anguille, C., Montcourrier, P., and Alexandre, D. 2003. Delta-promoted filopodia mediate long-range lateral inhibition in *Drosophila*. *Nature* 426, 503-504.

Deblandre, G. A., Lai, E. C. and Kintner, C. (2001). *Xenopus* Neuralized is a ubiquitin ligase that interacts with Xdelta1 and regulates Notch signaling. *Dev. Cell* 1, 795-806.

Denef, N., D. Neubuser, L. Perez, and S.M. Cohen. 2000. Hedgehog induces opposite changes in turnover and subcellular localization of patched and smoothened. *Cell* 102: 521-31.

DiAntonio, A., A.P. Haghighi, S.L. Portman, J.D. Lee, A.M. Amaranto, and C.S. Goodman. 2001. Ubiquitination-dependent mechanisms regulate synaptic growth and function. *Nature* 412: 449-52.

Dudu, V., P. Pantazis, and M. Gonzalez-Gaitan. 2004. Membrane traffic during embryonic development: epithelial formation, cell fate decisions and differentiation. *Curr Opin Cell Biol* 16: 407-14.

Dumstrei, K., F. Wang, C. Nassif, and V. Hartenstein. 2003. Early development of the *Drosophila* brain: V. Pattern of postembryonic neuronal lineages expressing DE-cadherin. *J Comp Neurol* 455: 451-62.

Duncan, M.C., G. Costaguta, and G.S. Payne. 2003. Yeast D-Epsin-Related proteins required for Golgi-endosome traffic define a gamma-adaptin ear-binding motif. *Nat Cell Biol* 5: 77-81.

Entchev, E.V., A. Schwabedissen, and M. Gonzalez-Gaitan. 2000. Gradient formation of the TGF-beta homolog Dpp. *Cell* 103: 981-91.

Ergito. 2005. Virtual text. Available from http://www.ergito.com.

Eugster, A., E.I. Pecheur, F. Michel, B. Winsor, F. Letourneur, and S. Friant. 2004. Ent5p is required with Ent3p and Vps27p for ubiquitin-dependent protein sorting into the multivesicular body. *Mol Biol Cell* 15: 3031-41.

Fanto, M. and Mlodzik, M. 1999. Asymmetric Notch activation specifies photoreceptors R3 and R4 and planar polarity in the *Drosophila* eye. *Nature* 397, 523-526.

Fehon, R.G., Kooh, P.J., Rebay, I., Regan, C.L., Xu, T., Muskavitch, M.A.T. and Artavanis-Tsakonas, S. 1990. Molecular interactions between the protein products of the neurogenic loci *Notch* and *Delta*, two EGF homologous genes in *Drosophila*. *Cell* 61, 523-534.

Fischer, J. A., Leavell, S. and Li, Q. 1997. Mutagenesis screens for interacting genes reveal three roles for *fat facets* during *Drosophila* eye development. *Dev. Gen.* 21, 167-174.

Fischer, J.A., Overstreet, E. 2002. Fat facests does a Highwire act at the synapse. *Bioessays* 24, 13-16.

Fischer-Vize, J.A., Vize, P.D., and Rubin, G.M. 1992. A unique mutation in the *Enhancer of split* gene complex affects the fates of the mystery cells in the developing *Drosophila* eye. *Development* 115, 89-101.

Fischer-Vize, J. A., Rubin, G. M. and Lehmann, R. 1992. The *fat facets* gene is required for *Drosophila* eye and embryo development. *Development* 116, 985-1000.

Fitzgerald, K. and I. Greenwald. 1995. Interchangeability of *Caenorhabditis elegans* DSL proteins and intrinsic signalling activity of their extracellular domains in vivo. *Development* 121: 4275-82.

Flybase. 2003. The FlyBase database of the *Drosophila* genome projects and community literature. Available from http://flybase.bio.indiana.edu/. *Nucl. Acids Res.* 31, 172-175.

Ford, M.G.J., Mills, I.G., Peter, B.J., Vallis, Y., Praefcke, G.J.K., Evans, P.R., and McMahon, H.T. 2002. Curvature of clathrin-coated pits driven by epsin. *Nature* 419, 361-366.

Friant, S., E.I. Pecheur, A. Eugster, F. Michel, Y. Lefkir, D. Nourrisson, and F. Letourneur. 2003. Ent3p Is a PtdIns(3,5)P2 effector required for protein sorting to the multivesicular body. *Dev Cell* 5: 499-511.

Gibson, M.C. and G. Schubiger. 2000. Peripodial cells regulate proliferation and patterning of *Drosophil*a imaginal discs. *Cel*l 103: 343-50.

Giraldez, A.J., R.R. Copley, and S.M. Cohen. 2002. HSPG modification by the secreted enzyme Notum shapes the Wingless morphogen gradient. Dev Cell 2: 667-76.

Goffeau, A., Barrell, B.G., Bussey, H., Davis, R.W., Dujon, B., Feldmann, H., Galibert, F., Hoheisel, J.D., Jacq, C., Johnston, M., Louis, E.J., Mewes, H.W., Murakami, Y., Philippsen, P., Tettelin, H., and Oliver, S.G. 1996. Life with 6000 genes. *Science* 274, 563-567

Gonzalez-Gaitan, M. and Stenmark, H. 2003. Endocytosis and signaling: a relationship under development. *Cell* 115, 513-521.

Gonzalez-Gaitan, M. 2003. Signal dispersal and transduction through the endocytic pathway. *Nat Rev Mol Cell Biol* 4: 213-24.
-. 2003. Endocytic trafficking during *Drosophila* development. *Mech Dev* 120: 1265-82.

Greenwood, S. and G. Struhl. 1999. Progression of the morphogenetic furrow in the *Drosophila* eye: the roles of Hedgehog, Decapentaplegic and the Raf pathway. *Development* 126: 5795-808.

Gupta-Rossi, N., E. Six, O. LeBail, F. Logeat, P. Chastagner, A. Olry, A. Israel, and C. Brou. 2004. Monoubiquitination and endocytosis direct gamma-secretase cleavage of activated Notch receptor. *J Cell Biol* 166: 73-83.

Han, C., D. Yan, T.Y. Belenkaya, and X. Lin. 2005. *Drosophila* glypicans Dally and Dally-like shape the extracellular Wingless morphogen gradient in the wing disc. *Development* 132: 667-79.

Henderson, S.T., D. Gao, S. Christensen, and J. Kimble. 1997. Functional domains of LAG-2, a putative signaling ligand for LIN-12 and GLP-1 receptors in Caenorhabditis elegans. *Mol Biol Cell* 8: 1751-62.

Henderson, S.T., D. Gao, E.J. Lambie, and J. Kimble. 1994. lag-2 may encode a signaling ligand for the GLP-1 and LIN-12 receptors of C. elegans. *Development* 120: 2913-24.

Herz, J. and H.H. Bock. 2002. Lipoprotein receptors in the nervous system. *Annu Rev Biochem* 71: 405-34.

Hicke, L. 2001. Protein regulation by monoubiquitin. *Nat Rev Mol Cell Biol* 2: 195-201.

Hicke, L. 2003. PtdIns(3,5)P2 finds a partner. *Dev Cell* 5: 363-4.

Hicke, L. and R. Dunn. 2003. Regulation of membrane protein transport by ubiquitin and ubiquitin-binding proteins. *Annu Rev Cell Dev Biol* 19: 141-72.

Hickson, G.R., J. Matheson, B. Riggs, V.H. Maier, A.B. Fielding, R. Prekeris, W. Sullivan, F.A. Barr, and G.W. Gould. 2003. Arfophilins are dual Arf/Rab 11 binding proteins that regulate recycling endosome distribution and are related to *Drosophila* nuclear fallout. *Mol Biol Cell* 14: 2908-20.

Hiesberger, T., M. Trommsdorff, B.W. Howell, A. Goffinet, M.C. Mumby, J.A. Cooper, and J. Herz. 1999. Direct binding of Reelin to VLDL receptor and ApoE receptor

2 induces tyrosine phosphorylation of disabled-1 and modulates tau phosphorylation. *Neuron* 24: 481-9.

Hirst, J., S.E. Miller, M.J. Taylor, G.F. von Mollard, and M.S. Robinson. 2004. D-Epsin-R is an adaptor for the SNARE protein Vti1b. *Mol Biol Cell* 15: 5593-602.

Hofmann, K., and Falquet, L. 2001. A ubiquitin-interacting motif conserved in components of the proteasomal and lysosomal protein degradation systems. *Trends Biochem. Sci.* 26, 347-350.

Hori, K., M. Fostier, M. Ito, T.J. Fuwa, M.J. Go, H. Okano, M. Baron, and K. Matsuno. 2004. *Drosophila* deltex mediates suppressor of Hairless-independent and late-endosomal activation of Notch signaling. *Development* 131: 5527-37.

Howell, B.W., L.M. Lanier, R. Frank, F.B. Gertler, and J.A. Cooper. 1999. The disabled 1 phosphotyrosine-binding domain binds to the internalization signals of transmembrane glycoproteins and to phospholipids. *Mol Cell Biol* 19: 5179-88.

Howell, B.W. and J. Herz. 2001. The LDL receptor gene family: signaling functions during development. *Curr Opin Neurobiol* 11: 74-81.

Huang, K.M., D'Hondt, K., Riezman, H., and Lemmon, S.K. 1999. Clathrin function in the absence of heterotetrameric adaptors and AP180-related proteins in yeast. *EMBO J.* 18, 3897-3908.

Huang, Y., Baker, R. T. and Fischer-Vize, J. A. 1995. Control of cell fate by a deubiquitinating enzyme encoded by the *fat facets* gene. *Science* 270, 1828-1831.

Huang, Y. and Fischer-Vize, J. A. 1996. Undifferentiated cells in the developing *Drosophila* eye influence facet assembly and require the Fat facets ubiquitin-specific protease. *Development* 122, 3207-3216.

Hurley, J.H. and B. Wendland. 2002. Endocytosis: driving membranes around the bend. *Cell* 111: 143-6.

Hussain, N.K., M. Yamabhai, A.L. Bhakar, M. Metzler, S.S. Ferguson, M.R. Hayden, P.S. McPherson, and B.K. Kay. 2003. A role for epsin N-terminal homology/AP180 N-terminal homology (ENTH/ANTH) domains in tubulin binding. *J Biol Chem* 278: 28823-30.

Incardona, J.P., J. Gruenberg, and H. Roelink. 2002. Sonic hedgehog induces the segregation of patched and smoothened in endosomes. *Curr Biol* 12: 983-95.

Itoh, T., Koshiba, S., Kigawa, T., Kikuchi, A., Yokoyama, S., and Takenawa, T. 2001. Role of the ENTH domain in phosphatidylinositol-4,5-bisphosphate binding and endocytosis. *Science* 291, 1047-1051.

Itoh, M., Kim, C. H., Palardy, G., Oda, T., Jiang, Y. J., Maust, D., Yeo, S. Y., Lorick, K., Wright, G. J., Ariza-McNaughton, L., Weissman, A. M., Lewis, J., Chandrasekharappa, S. C. and Chitnis, A. B. 2003. Mind bomb is a ubiquitin ligase that is essential for efficient activation of Notch signaling by Delta. *Dev. Cell* 4, 67-82.

Jahn, R. and H. Grubmuller. 2002. Membrane fusion. *Curr Opin Cell Biol* 14: 488-95.

Jahn, R., T. Lang, and T.C. Sudhof. 2003. Membrane fusion. *Cell* 112: 519-33.

Jahn, R. 2004. Principles of exocytosis and membrane fusion. *Ann N Y Acad Sci* 1014: 170-8.

Jarman, A. P., Sun, Y., Jan, L. Y. and Jan, Y. N. 1995. Role of the proneural gene, *atonal*, in formation of *Drosophila* chordotonal organs and photoreceptors. *Development* 121, 2019-2030.

Jarman, A.P., Grell, E. H., Ackerman, L., Jan, L.Y. and Jan, Y.N. 1994. *atonal* is the proneural gene for *Drosophila* photoreceptors. *Nature* 369, 398-400.

Jennings, B., Preiss, A., Delidakis, C. and Bray, S. 1994. The Notch signaling pathway is required for Enhancer of split protein expression during neurogenesis in the *Drosophila* embryo. *Development* 120, 3537-3548.

Kalthoff, C., S. Groos, R. Kohl, S. Mahrhold, and E.J. Ungewickell. 2002. Clint: a novel clathrin-binding ENTH-domain protein at the Golgi. *Mol Biol Cell* 13: 4060-73.

Kalthoff, C., J. Alves, C. Urbanke, R. Knorr, and E.J. Ungewickell. 2002. Unusual structural organization of the endocytic proteins AP180 and epsin 1. *J Biol Chem* 277: 8209-16.

Kato, M., K. Miyazawa, and N. Kitamura. 2000. A deubiquitinating enzyme UBPY interacts with the Src homology 3 domain of Hrs-binding protein via a novel binding motif PX(V/I)(D/N)RXXKP. *J Biol Chem* 275: 37481-7.

Katzmann, D.J., C.J. Stefan, M. Babst, and S.D. Emr. 2003. Vps27 recruits ESCRT machinery to endosomes during MVB sorting. *J Cell Biol* 162: 413-23.

Kay, B. K., Yamabhai, M. Wendland, B. and Emr, S. D. 1998. Identification of a novel domain shared by putative components of the endocytic and cytoskeletal machinery. *Protein Sci.* 8, 435-438.

Keleman, K., S. Rajagopalan, D. Cleppien, D. Teis, K. Paiha, L.A. Huber, G.M. Technau, and B.J. Dickson. 2002. Comm sorts robo to control axon guidance at the *Drosophila* midline. *Cell* 110: 415-27.

Keleman, K., C. Ribeiro, and B.J. Dickson. 2005. Comm function in commissural axon guidance: cell-autonomous sorting of Robo in vivo. *Nat Neurosci* 8: 156-63.

Kirkpatrick, C.A., B.D. Dimitroff, J.M. Rawson, and S.B. Selleck. 2004. Spatial regulation of Wingless morphogen distribution and signaling by Dally-like protein. *Dev Cell* 7: 513-23.

Kowanetz, K., J. Terzic, and I. Dikic. 2003. Dab2 links CIN85 with clathrin-mediated receptor internalization. *FEBS Lett* 554: 81-7.

Kramer, H. 2001. Neuralized: regulating notch by putting away delta. *Dev Cell* 1: 725-6.

Kramer, H., Cagan, R.L. and Zipursky, S.L. 1991. Interaction of Bride of Sevenless membrane-bound ligand and the Sevenless tyrosine kinase. *Nature* 352, 207-212.

Kreuger, J., L. Perez, A.J. Giraldez, and S.M. Cohen. 2004. Opposing activities of Dally-like glypican at high and low levels of Wingless morphogen activity. *Dev Cell* 7: 503-12.

Kumar, J. 2002. The epidermal growth factor receptor in *Drosophila* eye development. In *Drosophila Eye Development* (ed. K. Moses), pp. 59-71. Berlin: Springer-Verlag.

Lai, E. C., Deblandre, G. A., Kintner, C. and Rubin, G.M. 2001 *Drosophila* Neuralized is a ubiquitin ligase that promotes the internalization and degradation of Delta. *Dev. Cell.* 1, 783-794.

Lai, E. C. and Rubin, G. M. 2001. *neuralized* functions cell-autonomously to regulate a subset of Notch-dependent processes during adult *Drosophila* development. *Dev. Biol.* 231, 217-233.

Lai, E. C. and Rubin, G. M. 2001. *neuralized* is essential for a subset of Notch pathway-dependent cell fate decisions during *Drosophila* eye development. *Proc. Natl. Acad. Sci.* 98, 5637-5642.

Lai, E. C. 2002. Protein degradation: Four E3s for the Notch pathway. *Curr. Biol.* 12, R74-R78.

Le Borgne, R., Y. Bellaiche, and F. Schweisguth. 2002. *Drosophila* E-cadherin regulates the orientation of asymmetric cell division in the sensory organ lineage. *Curr Biol* 12: 95-104.

Le Borgne, R. and Schweisguth, F. 2003. Unequal segregation of Neuralized biases Notch activation during asymmetric cell division. *Dev. Cell.* 5, 139-148.

Le Borgne, R., S. Remaud, S. Hamel, and F. Schweisguth. 2005. Two Distinct E3 Ubiquitin Ligases Have Complementary Functions in the Regulation of Delta and Serrate Signaling in *Drosophila*. *PLoS Biol* 3: e96.

Le Borgne, R., Bardin, A., Schweisguth F. 2005. The roles of receptor and ligand endocytosis in regulating Notch. *Developmen*t 132: 1751-1762.

Lecuit, T. 2004. Junctions and vesicular trafficking during *Drosophila* cellularization. *J Cell Sci* 117: 3427-33.

Lee, J. D. and Treisman, J. E. 2000. *Regulators of the morphogenetic furrow. In Drosophila Eye Development*, (ed. K. Moses), pp.21-33. Berlin, Springer-Verlag.

Legendre-Guillemin, V., S. Wasiak, N.K. Hussain, A. Angers, and P.S. McPherson. 2004. ENTH/ANTH proteins and clathrin-mediated membrane budding. *J Cell Sci* 117: 9-18.

Lehmann, R., Dietrich, U., Jimenez, F. and Campos-Ortega, J. A. 1981. Mutations of early neurogenesis in *Drosophila. Wilhelm Roux's Arch. Dev. Biol.* 190, 226-229.

Lehmann, R., Jimenez, F., Dietrich, U. and Campos-Ortega, J. A. 1983. On the phenotype and development of mutants of early neurogenesis in *Drosophila melanogaster*. *Wilhelm Roux's Arch. Dev. Biol.* 192, 62-74.

Lemmon, S.K. 2001. Clathrin uncoating: Auxilin comes to life. *Curr Biol* 11: R49-52.

Li, Y. and Baker, N. E. 2001. Proneural enhancement by Notch overcomes Suppressor-of-hairless repressor function in the developing *Drosophila* eye. *Curr. Biol.* 11, 330-338.

Li, Y. and Baker, N. E. 2004. The roles of *cis*-inactivation by Notch ligands and of *neuralized* during eye and bristle patterning in *Drosophila*. *BMC Dev. Biol.* 4, 5-15.

Lieber, T., S. Kidd, and M.W. Young. 2002. kuzbanian-mediated cleavage of *Drosophila* Notch. *Genes Dev* 16: 209-21.

Liu, N., D.A. Dansereau, and P. Lasko. 2003. Fat facets interacts with vasa in the *Drosophila* pole plasm and protects it from degradation. *Curr Biol* 13: 1905-9.

Lloyd, T.E., R. Atkinson, M.N. Wu, Y. Zhou, G. Pennetta, and H.J. Bellen. 2002. Hrs regulates endosome membrane invagination and tyrosine kinase receptor signaling in *Drosophila*. *Cell* 108: 261-9.

Lloyd, T.E., Verstreken, P., Ostrin, E.J., Phillippe A., Lichtarge, O., and Bellen, H.J. 2000. A genome-wide search for synaptic vesicle cycle proteins in *Drosophila*. Neuron *26*, 45-50.

Lloyd, V., M. Ramaswami, and H. Kramer. 1998. Not just pretty eyes: *Drosophila* eye-colour mutations and lysosomal delivery. *Trends Cell Biol* 8: 257-9.

Lohi, O., A. Poussu, Y. Mao, F. Quiocho, and V.P. Lehto. 2002. VHS domain -- a longshoreman of vesicle lines. *FEBS Lett* 513: 19-23.

Lu, B., Rothenberg, M., Jan, L.Y. and Jan, Y. N. 1998. Partner of Numb colocalizes with Numb during mitosis and directs Numb asymmetrical localization in *Drosophila* neural and muscle progenitors. *Cell* 95, 225-235.

Mattera, R., B. Ritter, S.S. Sidhu, P.S. McPherson, and J.S. Bonifacino. 2004. Definition of the consensus motif recognized by gamma-adaptin ear domains. *J Biol Chem* 279: 8018-28.

Martin, N.P., R.J. Lefkowitz, and S.K. Shenoy. 2003. Regulation of V2 vasopressin receptor degradation by agonist-promoted ubiquitination. *J Biol Chem* 278: 45954-9.

McMahon, H.T. and I.G. Mills. 2004. COP and clathrin-coated vesicle budding: different pathways, common approaches. *Curr Opin Cell Biol* 16: 379-91.

Miller, S.L., E. Malotky, and J.P. O'Bryan. 2004. Analysis of the role of ubiquitin-interacting motifs in ubiquitin binding and ubiquitylation. *J Biol Chem* 279: 33528-37.

Mills, I.G., G.J. Praefcke, Y. Vallis, B.J. Peter, L.E. Olesen, J.L. Gallop, P.J. Butler, P.R. Evans, and H.T. McMahon. 2003. D-Epsin-R: an AP1/clathrin interacting protein involved in vesicle trafficking. *J Cell Biol* 160: 213-22.

Mishra, S.K., P.A. Keyel, M.J. Hawryluk, N.R. Agostinelli, S.C. Watkins, and L.M. Traub. 2002. Disabled-2 exhibits the properties of a cargo-selective endocytic clathrin adaptor. *EMBO J* 21: 4915-26.

Mlodzik, M. 2002. Tissue polarity in the retina. In *Drosophila Eye Development* (ed. K. Moses), pp. 89-106. Berlin: Springer-Verlag.

Moline, M. M., Southern, C. and Bejsovec, A. 1999. Directionality of Wingless protein transport influences epidermal patterning in the *Drosophila* embryo. *Development* 126, 4375-4384.

Motley, A., N.A. Bright, M.N. Seaman, and M.S. Robinson. 2003. Clathrin-mediated endocytosis in AP-2-depleted cells. *J Cell Biol* 162: 909-18.

Mousavi, S.A., L. Malerod, T. Berg, and R. Kjeken. 2004. Clathrin-dependent endocytosis. *Biochem J* 377: 1-16.

Murray, R.Z., L.A. Jolly, and S.A. Wood. 2004. The FAM deubiquitylating enzyme localizes to multiple points of protein trafficking in epithelia, where it associates with E-cadherin and beta-catenin. *Mol Biol Cell* 15: 1591-9.

Myat, A., P. Henry, V. McCabe, L. Flintoft, D. Rotin, and G. Tear. 2002. *Drosophila* Nedd4, a ubiquitin ligase, is recruited by Commissureless to control cell surface levels of the roundabout receptor. *Neuron* 35: 447-59.

Nagaraj, R., Canon, J. and Banerjee, U. 2002. Cell fate specification in the *Drosophila* eye. In *Drosophila Eye Development* (ed. K. Moses), pp.73-88. Berlin: Springer-Verlag.

Nakashima, S., Morinaka, K., Koyama, S., Ikeda, M., Kishida, M., Okawa, K., Iwamatsu, A., Kishida, S., and Kikuchi, A. 1999. Small G protein Ral and its downstream molecules regulate endocytosis of EGF and insulin receptors. *EMBO J.* 18, 3629-3642.

Nossal, R. and J. Zimmerberg. 2002. Endocytosis: curvature to the ENTH degree. *Curr Biol* 12: R770-2.

Newsome, T. P., Asling, B. and Dickson, B. J. 2000. Analysis of *Drosophila* photoreceptor axon guidance in eye-specific mosaics. *Development* 4, 851-860.

Nie, J., McGill, M., Dermer, M., Dho, S., Wolting, C. and McGlade, C. J. 2002. LNX functions as a RING type E3 ubiquitin ligase that targets the cell fate determinant Numb for ubiquitin dependent degradation. *EMBO J.* 21, 93-102.

Odorizzi, G., C.R. Cowles, and S.D. Emr. 1998. The AP-3 complex: a coat of many colours. *Trends Cell Biol* 8: 282-8.

O'Neill, E. M., Rebay, I., Tjian, R. and Rubin, G. M. 1994. The activities of two Ets-related transcription factors required for *Drosophila* eye development are modulated by the Ras/MAPK pathway. *Cell* 78, 137-147.

Oldham, C. E., Mohoney, R. P., Miller, S. L., Hanes, R. N. and O'Bryan, J. P. (2002). The ubiquitin-interacting motifs target the endocytic adaptor protein epsin for ubiquitination. *Curr. Biol.* 12*,* 1112-1116.

Oldham, S. and E. Hafen. 2003. Insulin/IGF and target of rapamycin signaling: a TOR de force in growth control. *Trends Cell Biol* 13: 79-85.

Overstreet, E., Chen, X., Wendland, B. and Fischer, J. A. 2003. Either part of a *Drosophila* epsin protein, divided after the ENTH domain, functions in endocytosis of Delta in the developing eye. *Curr. Biol.* 13, 854-860.

Overstreet, E., E. Fitch, and J.A. Fischer. 2004. Fat facets and Liquid facets promote Delta endocytosis and Delta signaling in the signaling cells. *Development* 131: 5355-66.

Owen, D.J., B.M. Collins, and P.R. Evans. 2004. Adaptors for clathrin coats: structure and function. *Annu Rev Cell Dev Biol* 20: 153-91.

Owen, D. J., Vallis, Y., Noble, M.E.N., Hunter, J.B., Dafforn, T.R., Evans, P.R., and McMahon, H.T. 1999. A structural explanation for the binding of multiple ligands by the a-adaptin appendage domain. *Cell* 97, 805-815.

Paoluzi, S., Castagnoli, L., Lauro, I., Salcini, A.E., Coda, L., Fre, S., Confalonieri, S., Pelicci, P. G., DiFiore, P.P., and Cesareni, G. 1998. Recognition specificity of individual EH domains of mammals and yeast. *EMBO J.* 17, 6541-6550.

Pappu, K., Mardon, G. 2002. Retinal Specification and Determination in *Drosophila*. In *Drosophila Eye Development*, (ed. K. Moses), pp. 5-20. Berlin, Springer-Verlag.

Parks, A. L., Klueg, K. M., Stout, J. R. and Muskavitch, M. A. T. 2000. Ligand endocytosis drives receptor dissociation and activation in the Notch pathway. *Development* 127, 1373-1385.

Parks, A. L., Turner, F. R. and Muskavitch, M. A. T. 1995. Relationships between complex Delta expression and the specification of retinal cell fates during *Drosophila* eye development. *Mech. Dev.* 50, 201-216.

Pavlopoulos, E., Pitsouli, C., Klueg, K. M., Muskavitch, M. A. T., Moschonas, N. K. and Delidakis, C. 2001. *neuralized* encodes a peripheral membrane protein involved in Delta signaling and endocytosis. *Dev. Cell* 1, 807-816.

Pfeiffer, S., C. Alexandre, M. Calleja, and J.P. Vincent. 2000. The progeny of wingless-expressing cells deliver the signal at a distance in *Drosophila* embryos. *Curr Biol* 10: 321-4.

Pfeiffer, S., S. Ricardo, J.B. Manneville, C. Alexandre, and J.P. Vincent. 2002. Producing cells retain and recycle Wingless in *Drosophila* embryos. *Curr Biol* 12: 957-62.

Polo S., Sigismund, S., Faretta, M., Guidi, M., Capua, M. R., Bossi, G., Chen, H., De Camilli, P., and Di Fiore, P. P. 2002. A single motif responsible for ubiquitin recognition and monoubiquitination in endocytic proteins. *Nature* 416, 381-383.

Poodry, C. A. 1990. *shibire*, a neurogenic mutant of *Drosophila*. *Dev. Biol*. 138, 464-472.

Reutens, A.T. and C.G. Begley. 2002. Endophilin-1: a multifunctional protein. *Int J Biochem Cell Biol* 34: 1173-7.

Rhyu, M. S. Y. and Jan, Y. N. 1994. Asymmetric distribution of Numb protein during division of the sensory organ precursor cell confers distinct fates to daughter cells. *Cell* 76, 477-491.

Robinow, S., and White, K. 1991. Characterization and spatial distribution of of the ELAV protein during *Drosophila melanogaster* development. *J. Neurobiol. 22*, 443-461.

Robinson, M.S. 2004. Adaptable adaptors for coated vesicles. *Trends Cell Biol* 14: 167-74.

Rosenthal, J.A., Chen, H., Slepnev, V.I., Pellegrini, L., Salcini, A.E., Di Fiore, P.P., and De Camilli, P. 1999. The epsins define a family of proteins that interact with components of the clathrin coat and contain a new protein module. *J. Biol. Chem.* 274, 33959-33965.

Saint-Pol, A., B. Yelamos, M. Amessou, I.G. Mills, M. Dugast, D. Tenza, P. Schu, C. Antony, H.T. McMahon, C. Lamaze, and L. Johannes. 2004. Clathrin adaptor D-Epsin-R is required for retrograde sorting on early endosomal membranes. *Dev Cell* 6: 525-38.

Sakata, T., H. Sakaguchi, L. Tsuda, A. Higashitani, T. Aigaki, K. Matsuno, and S. Hayashi. 2004. *Drosophila* Nedd4 regulates endocytosis of notch and suppresses its ligand-independent activation. *Curr Biol* 14: 2228-36.

Salcini, A.E., Confalonieri, S., Doria, M., Santolini, E., Tassi, E., Minenkova, O., Cesareni, G., Pelicci, P.G., and Di Fiore, P.P. 1997. Binding specificity and *in*

vivo targets of the EH domain, a novel protein-protein interaction module. *Genes Dev*. 11, 2239-2249.

Salcini, A.E., H. Chen, G. Iannolo, P. De Camilli, and P.P. Di Fiore. 1999. Epidermal growth factor pathway substrate 15, Eps15. *Int J Biochem Cell Biol* 31: 805-9.

Santolini, E., Puri, C., Salcini, A. E., Gagliani, M. C., Pelicci, P. G., Tacchetti, C. and Di Fiore, P. P. 2000. Numb is an endocytic protein. *J. Cell Biol.* 151, 1345-1352.

Sapir, A., E. Assa-Kunik, R. Tsruya, E. Schejter, and B.Z. Shilo. 2005. Unidirectional Notch signaling depends on continuous cleavage of Delta. *Development* 132: 123-32.

Schmidt, A.A. 2002. Membrane transport: the making of a vesicle. *Nature* 419: 347-9.

Schmitz, C., A. Kinner, and R. Kolling. 2005. The Deubiquitinating Enzyme Ubp1 Affects Sorting of the ATP-binding Cassette-Transporter Ste6 in the Endocytic Pathway. *Mol Biol Cell* 16: 1319-29.

Schnell, J.D. and L. Hicke. 2003. Non-traditional functions of ubiquitin and ubiquitin-binding proteins. *J Biol Chem* 278: 35857-60.

Schweisguth, F. 2004. Notch signaling activity. *Curr Biol* 14: R129-38.

Seabra, M.C. and C. Wasmeier. 2004. Controlling the location and activation of Rab GTPases. *Curr Opin Cell Biol* 16: 451-7.

Seto, E. S., Bellen, H. J. and Lloyd, T. E. 2002. When cell biology meets development: endocytic regulation of signaling pathways. *Genes Dev.* 16, 1314-1336.

Seugnet, L., Simpson, P. and Haenlin, M. 1997. Requirement for Dynamin during Notch signaling in *Drosophila* neurogenesis. *Dev. Biol.* 192, 585-598.

Shenoy, S.K. and R.J. Lefkowitz. 2003. Multifaceted roles of beta-arrestins in the regulation of seven-membrane-spanning receptor trafficking and signalling. *Biochem J* 375: 503-15.

Shenoy, S. K. 2003. Trafficking patterns of beta-arrestin and G protein-coupled receptors determined by the kinetics of beta-arrestin deubiquitination. *J Biol Chem* 278: 14498-506.

Shih, S. C., Katzmann, D. J., Schnell, J. D., Sutanto, M., Emr, S. D., and Hicke, L. 2002. Epsins and Vps27p/Hrs contain ubiquitin-binding domains that function in receptor endocytosis. *Nat. Cell Biol*. 4, 389-393.

Siemering, K.R., Golbik, R., Sever, R. and Haseloff, J. 1996. Mutations that suppress the thermosensitivity of green fluorescent protein. *Curr. Biol.* 6, 1653-1663.

Sigismund, S., T. Woelk, C. Puri, E. Maspero, C. Tacchetti, P. Transidico, P.P. Di Fiore, and S. Polo. 2005. From the Cover: Clathrin-independent endocytosis of ubiquitinated cargos. *Proc Natl Acad Sci* U S A 102: 2760-5.

Sisson, J.C., C. Field, R. Ventura, A. Royou, and W. Sullivan. 2000. Lava lamp, a novel peripheral golgi protein, is required for *Drosophila* melanogaster cellularization. *J Cell Biol* 151: 905-18.

Stahelin, R.V., F. Long, B.J. Peter, D. Murray, P. De Camilli, H.T. McMahon, and W. Cho. 2003. Contrasting membrane interaction mechanisms of AP180 N-terminal homology (ANTH) and epsin N-terminal homology (ENTH) domains. *J Biol Chem* 278: 28993-9.

Stowers, R. S. and Schwarz, T. L. 1999. Genetic method for generating *Drosophila* eye composed exclusively of mitotic clones of a single genotype. *Genetics* 152, 1631-1639.

Sun, X. and Artavanis-Tsakonas, S. 1996. The intracellular deletion of Delta and Serrate define dominant negative forms of the *Drosphila* Notch ligands. *Development* 122, 2465-2474.

Szymkiewicz, I., O. Shupliakov, and I. Dikic. 2004. Cargo- and compartment-selective endocytic scaffold proteins. *Biochem J* 383: 1-11.

Tian, X., D. Hansen, T. Schedl, and J.B. Skeath. 2004. Epsin potentiates Notch pathway activity in *Drosophila* and C. elegans. *Development* 131: 5807-15.

Thomas, C. and P.W. Ingham. 2003. Hedgehog signaling in the *Drosophila* eye and head: an analysis of the effects of different patched trans-heterozygotes. *Genetics* 165: 1915-28.

Traub, L.M. 2003. Sorting it out: AP-2 and alternate clathrin adaptors in endocytic cargo selection. *J Cell Biol* 163: 203-8.

Tomlinson, A. and Struhl, G. 1999. Decoding vectorial information from a gradient: sequential roles of the receptors Frizzled and Notch in establishing planar polarity in the *Drosophila* eye. *Development* 126, 5725-5738.

Tomlinson, A. and Struhl, G. 2001. Delta/Notch and Boss/Sevenless signals act combinatorially to specify the *Drosophila* R7 photoreceptor. *Mol. Cell* 7, 487-495.

Tulipano, G., R. Stumm, M. Pfeiffer, H.J. Kreienkamp, V. Hollt, and S. Schulz. 2004. Differential beta-arrestin trafficking and endosomal sorting of somatostatin receptor subtypes. *J Biol Chem* 279: 21374-82.

Turabian, K. L. 1987. A Manual for Writers of Term Papers, Theses, and Dissertations. 5th ed. Chicago: The University of Chicago Press.

Vieira, A.V., C. Lamaze, and S.L. Schmid. 1996. Control of EGF receptor signaling by clathrin-mediated endocytosis. *Science* 274: 2086-9.

Wang, F., K. Dumstrei, T. Haag, and V. Hartenstein. 2004. The role of DE-cadherin during cellularization, germ layer formation and early neurogenesis in the *Drosophila* embryo. *Dev Biol* 270: 350-63.

Wang, W. and G. Struhl. 2004. *Drosophila* Epsin mediates a select endocytic pathway that DSL ligands must enter to activate Notch. *Development* 131: 5367-80.

Wasiak, S., A.Y. Denisov, Z. Han, P.A. Leventis, E. de Heuvel, G.L. Boulianne, B.K. Kay, K. Gehring, and P.S. McPherson. 2003. Characterization of a gamma-adaptin ear-binding motif in enthoprotin. *FEBS Lett* 555: 437-42.

Wasiak, S., A.Y. Denisov, Z. Han, P.A. Leventis, E. de Heuvel, G.L. Boulianne, B.K. Kay, K. Gehring, and P.S. McPherson. 2003. Characterization of a gamma-adaptin ear-binding motif in enthoprotin. FEBS Lett 555: 437-42.

Weber, U., C. Eroglu, and M. Mlodzik. 2003. Phospholipid membrane composition affects EGF receptor and Notch signaling through effects on endocytosis during *Drosophila* development. *Dev Cell* 5: 559-70.

Wendland, B. 2002. Epsins: adaptors in endocytosis? *Nat Rev Mol Cell Biol* 3: 971-7.

Wendland, B., Steece, K.E., and Emr, S.D. 1999. Yeast epsins contain an essential N-terminal ENTH domain, bind clathrin and are required for endocytosis. *EMBO J* 18, 4384-4393.

Wendler, F. and S. Tooze. 2001. Syntaxin 6: the promiscuous behaviour of a SNARE protein. *Traffic* 2: 606-11.

Wilkin, M.B., A.M. Carbery, M. Fostier, H. Aslam, S.L. Mazaleyrat, J. Higgs, A. Myat, D.A. Evans, M. Cornell, and M. Baron. 2004. Regulation of notch endosomal

sorting and signaling by *Drosophila* Nedd4 family proteins. *Curr Biol* 14: 2237-44.

Wolff, T. and Ready, D. F. 1993. Pattern formation in the *Drosophila* retina. In *The Development of Drosophila melanogaster*, *Vol.II* (eds. M. Bate and A. Martinez Arias), pp.1277-1325. Cold Spring Harbor: Cold Spring Harbor Laboratory Press.

Wu, Z., Li, Q., Fortini, M. and Fischer, J. A. 1999. Genetic analysis of the role of the *Drosophila fat facets* gene in the ubiquitin pathway. *Dev. Genet.* 25, 312-320.

Wucherpfennig, T., M. Wilsch-Brauninger, and M. Gonzalez-Gaitan. 2003. Role of *Drosophila* Rab5 during endosomal trafficking at the synapse and evoked neurotransmitter release. *J Cell Bio*l 161: 609-24.

Xu, T. and Rubin, G. M. 1993. Analysis of genetic mosaics in developing and adult *Drosophila* tissues. *Development* 117, 1223-1237.

Yeh, E., Dermer, M., Commisso, C., Zhou., L., McGlade, C. J. and Boulianne, G. L. 2001. Neuralized functions as an E3 ubiquitin ligase during *Drosophila* development. *Curr. Biol.* 11, 1675-1679.

Yeh, E., Zhou, L., Rudzik, N. and Boulianne, G. L. 2000. Neuralized functions cell autonomously to regulate *Drosophila* sense organ development. *EMBO J.* 19, 4827-4837.

Zacharias, D.A. 2002. Sticky caveats in an otherwise glowing report: oligomerizing fluorescent proteins and their use in cell biology. *Sci STKE* 2002: PE23.

Zhang, B., Koh Y.H., Beckstead, R.B., Budnik, V., Ganetzky, B., and Bellen, H.J. (1998). Synaptic vesicle size and number are regulated by a clathrin adaptor protein required for endocytosis. *Neuron 21*, 1465-1475.

Vita

Erin Camille Overstreet is the daughter of Michael and Valerie Overstreet. She was born on June 15, 1976 in San Antonio, Texas. She graduated from the University of Texas at Austin with a B.S. in microbiology in December, 1998. She began her graduate education in molecular biology in September 1999 at the Institute of Molecular Biology at the University of Texas at Austin. She joined Dr. Fischer's laboratory in the Spring of 2000. She has been awarded several fellowships during her graduate career including the prestigious University Continuing Fellowship from University of Texas at Austin. She has published papers in renowned journals such as *Current Biology* and *Development*. Her graduate training has allowed her to make important scientific contributions to understanding the roles of vesicle trafficking and epsin proteins in important developmental processes. She was awarded degree of Doctor of Philosophy in May, 2005.

Permanent address: 307 Laramie, San Antonio, TX. 78209

This dissertation was typed by Erin Camille Overstreet.